

Reduction of Network Models with a Large Number of Sources

Von der Fakultät für Elektrotechnik und Informatik
der Gottfried Wilhelm Leibniz Universität Hannover
zur Erlangung des akademischen Grades

Doktor-Ingenieur

genehmigte Dissertation

von

Dipl.-Ing. Stefan Ludwig
geboren am 13. Oktober 1981
in Mühlhausen / Germany

2010

Referent: Prof. Dr.-Ing. Wolfgang Mathis
Koreferentin: Prof. Orla Feely, Ph.D.
Vorsitzender: Prof. Dr.-Ing. Bernd Ponick

Tag der Promotion: 07. September 2010

Acknowledgements

I would like to thank Prof. Wolfgang Mathis for supervising this work, his invaluable support and the permanent encouragement during my work. Thanks to Dr. Werner John for many useful discussions and for giving me the opportunity to be part of the research project PARACHUTE. I also want to thank Prof. Orla Feely for many useful comments on this work and Prof. Bernd Ponick for being the chair of the examining committee.

I want to thank my family, my mother Dagmar Ludwig, my father Rainer Ludwig, and my brothers Thomas Ludwig and Mario Ludwig for giving me the necessary backing. Special thanks goes to Beatrice Adolph for supporting me everytime.

I would like to thank every one of the research teams at Fraunhofer Institute of Integrated Circuits, Dresden, Fraunhofer Institute for Reliability and Microintegration, Paderborn and Institute of Electromagnetic Theory at the University of Hannover for providing an pleasant research environment during the last years. Especially I thank Dr.-Ing. Ljubica Radic-Weissenfeld and M.Sc. Reza Kazemzadeh for uncountable fruitful and stimulating discussions. I also want to thank Prof. Bernd Straube for introducing me into the world of science in the time previous to this work and Prof. Albrecht Reibiger for many useful discussions in the beginning of this work.

Abstract

The modeling and simulation of distributed systems is the basis for investigations and optimization of physical systems. For example, distributed systems, such as electromagnetic, thermic or acoustic field distributions are modeled and simulated to improve the properties of electrical and mechanical systems. Due to the high complexity of these distributed systems, investigations are possible only for small sections and with high computational efforts. Behavioral models are necessary to investigate the overall behavior of the distributed systems. These behavioral models have to be a very good approximation to the physical system and small enough for fast and efficient investigations. In this work the focus is on systems where also distributed sources have to be included in the behavioral models. For example, energy sources, thermal sources, sources of noise or other disturbances are incorporated as distributed sources in the behavioral models.

Most widely electrical networks are used for the behavioral modeling of distributed systems and these can be investigated with electrical circuit simulators. Here, the behavioral models of distributed systems are electrical networks with a large number of nodes and have linear resistive, inductive and capacitive elements as well a large number of sources. Typical sizes for such a network are up to millions of linear elements and up to thousands of sources. Due to the high number of electrical elements in the behavioral models of distributed systems, which continue to require high computational efforts in simulations, the practical applicability is limited. Based on the fact that the network is not investigated in all modeled points in space since the behavior at only a few of the nodes of the network is of interest, a motivation for a model reduction is given. As in image processing and audio and video compression, a small model, which has the relevant properties of the original model is sought after. The objective of model reduction is to find a small network model that approximates the behavior at the points of interest of the behavioral model. In simulations the reduced model replaces the large network model, enabling fast simulations with a low computational effort.

The first part of this work deals with the methods for reducing electrical networks in the sense of reducing the number of nodes and elements. The behavior at selected nodes is to be approximated in the reduced network model. Properties of networks which have to be preserved, properties which can be approximated as well as properties which can be neglected in a reduced model are identified. Existing methods for model reduction are examined in a common framework. The applicability for the reduction of electrical networks, such as those used in behavioral modeling, is investigated.

In the second part of this work special attention is paid to distributed systems with a large number of distributed sources. State-of-the-art model reduction methods are able to reduce large linear RLC-networks, but suffer from low efficiency if a network model with an additional large number of sources is to be reduced. Existing model reduction methods approximate the behavior at the nodes of interest of the network within a specified range, for example for all signals in a defined frequency band. For all signals within this range, the behavior at the nodes of interest of the network is to be approximated. A large number of sources requires a

large number of nodes where the behavior of the network is to be approximated. Specifically, in addition to the nodes of interest, the behavior at each node where a source is connected has to be approximated in a reduced model. Several existing approaches dealing with large numbers of nodes where the behavior is to be approximated are presented in this work. Their limitations in applicability and effectiveness for the reduction of networks with distributed sources is emphasized.

Furthermore, in the second part of this work a new method is presented that overcomes some of the drawbacks of the existing methods in the reduction of networks with a large number of distributed sources. Existing model reduction methods do not consider the distributed sources' behavior in the model reduction process. The idea of the presented method takes into account the a priori defined signals at the networks nodes connected with a source. The reducible network model is adapted for an efficient reduction, preserving or approximating the behavior at the network nodes of interest. Thus, the method proposed in this work includes in a preceding step the a priori defined knowledge of the distributed sources' behavior to increase the efficiency of the subsequent model reduction process.

The presented method is divided into two steps. Firstly, the number of nodes where the behavior has to be approximated is reduced. After that the network is more efficiently reduced with model reduction methods. For the first step, based on the functions describing the network models of the distributed sources, a function space is spanned. Due to the large number of distributed sources in the network models, the dimension of the function space is typically very large. With the help of approximation methods a lower dimension function space is found, which describes the distributed sources' behavior. The distributed sources in the network model are replaced by models of the decreased dimension function space. The number of nodes at which the behavior has to be approximated in a reduced model is thereby lowered. In the second part of this work it is shown that a network model is thus generated, which can be more efficiently reduced with model reduction methods.

Illustrative as well as industrial examples with distributed sources are reduced in order to validate the proposed method and to show the higher efficiency in model reduction.

Keywords: Modeling, Model Order Reduction, Linear Networks

Zusammenfassung

Die Modellierung und Simulation von verteilten Systemen ist die Basis für Untersuchungen und die Optimierung von physikalischen Systemen. Beispielsweise werden zur Verbesserung der Eigenschaften von elektrischen und mechanischen Systemen verteilte Systeme, wie elektromagnetische, thermische und akustische Feldverteilungen, modelliert und simuliert. Auf Grund der hohen Komplexität dieser verteilten Systeme sind Untersuchungen nur für kleine Ausschnitte und unter hohem Rechenaufwand möglich. Für Untersuchungen des Gesamtverhaltens des verteilten Systems sind Verhaltensmodelle notwendig. Diese Verhaltensmodelle müssen für eine effiziente Simulation sehr klein sein und das physikalische System sehr gut annähern. In dieser Arbeit wird der Schwerpunkt auf Verhaltensmodelle gelegt, in welchen ebenfalls verteilte Quellen berücksichtigt sind. Zum Beispiel müssen Energiequellen, thermische Quellen, Rauschquellen oder andere Störungen in das Verhaltensmodell eingebaut werden.

Sehr oft werden elektrische Netzwerke als Verhaltensmodelle für verteilte Systeme genutzt und diese können mit Schaltkreissimulatoren untersucht werden. Die in dieser Arbeit betrachteten elektrischen Netzwerke bestehen aus einer hohen Anzahl an Knoten und resistiven, induktiven und kapazitiven Elementen als auch einer hohen Anzahl an Quellen. Typische Größen für ein solches Netzwerkmodell sind bis zu Millionen lineare Elementen und bis zu Tausende von verteilten Quellen. Durch hohe Anzahl an elektrischen Elementen im Verhaltensmodell der verteilten Systeme, welche weiterhin einen hohen Rechenaufwand in Simulationen benötigen, ist die praktische Einsetzbarkeit eingeschränkt. Eine Motivation für eine Modellreduktion ist gegeben, da das Netzwerk nicht in allen modellierten Raumpunkten untersucht werden soll, sondern nur das Verhalten an einigen ausgewählten Knoten im Netzwerk untersucht wird. Wie in der Bildverarbeitung und der Audio- und Videokompression wird ein kleines Modell, welches die relevanten Eigenschaften des Originalmodells besitzt, gesucht. Das Ziel einer Modellreduktion ist das Finden eines kleinen Netzwerkes mit einer geringen Anzahl an Elementen und Knoten, welches das Verhaltensmodell an ausgewählten Knoten nachbildet. In Simulationen wird das große Verhaltensmodell mit dem reduzierten Modell ersetzt und eine schnelle und effiziente Simulation ermöglicht.

Der erste Teil dieser Arbeit beschäftigt sich mit den Methoden der Reduktion der Anzahl der Elemente und Knoten von elektrischen Netzwerken. Das Verhalten in ausgewählten Knoten des Netzwerkes soll dabei erhalten bleiben. Eigenschaften welche im reduzierten Modell erhalten bleiben sollen und Eigenschaften die angenähert oder vernachlässigt werden können, werden identifiziert. Existierende Methoden für die Modellreduktion werden in einem gemeinsamen Rahmen untersucht. Die Anwendbarkeit für die Reduktion von Netzwerken, wie sie in der Verhaltensmodellierung genutzt werden, wird untersucht.

In dieser Arbeit wird im zweiten Teil besondere Aufmerksamkeit auf verteilte Systeme mit einer hohen Anzahl an verteilten Quellen gelegt. Existierende Modellreduktionen sind geeignet für die Reduktion von großen RLC-Netzwerken, allerdings ist die Effektivität in der Reduktion von Netzwerken mit einer hohen Anzahl an Quellen gering. Die Modellreduktionsverfahren basieren auf der Approximation des Verhaltens in bestimmten Knoten des Netzwerkes. Für

alle Signale in einem bestimmten Bereich, wie beispielsweise in einem Frequenzband, wird das Verhalten angenähert. Eine hohe Anzahl an verteilten Quellen im Netzwerk benötigt eine hohe Anzahl an Knoten, an denen das Verhalten in einem reduzierten Modell approximiert werden muss. Zusätzlich zu den gewählten Knoten muss an jedem Knoten im Netzwerk, an den eine Quelle angeschlossen ist, ebenfalls das Verhalten angenähert werden. Einige existierende Ansätze für die Reduktion von Netzwerken, mit vielen Knoten an denen das Verhalten approximiert wird, werden in dieser Arbeit vorgestellt. Ihre Anwendbarkeit und Effektivität für die Reduktion von Netzwerken mit verteilten Quellen wird herausgestellt.

Weiterhin wird im zweiten Teil dieser Arbeit eine neue Methode vorgestellt, welche einige der Nachteile existierender Methoden in der Reduktion von Netzwerken mit vielen verteilten Quellen beseitigt. Existierende Modellreduktionsverfahren berücksichtigen nicht das Verhalten der verteilten Quellen in der Modellreduktion. Die in dieser Arbeit vorgestellte Methode nutzt das Wissen über das definierte Verhalten der verteilten Quellen, um eine höhere Modellreduktion zu erreichen. Das zu reduzierende Netzwerkmodell wird verändert, wobei das Verhalten an den ausgewählten Knoten erhalten oder angenähert wird. Damit wird, basierend auf dem definierten Verhalten der verteilten Quellen, in einem vorangehenden Schritt ein Netzwerkmodell erzeugt, welches sich nachfolgend mit Modellreduktionsverfahren effektiver reduzieren lässt.

Die präsentierte Methode kann in zwei Schritte unterteilt werden. Zuerst wird die Anzahl der Knoten in denen das Verhalten in einem reduzierten Modell angenähert werden muss verringert. Danach wird das Netzwerk mit Modellreduktionsverfahren effektiver reduziert. Für den ersten Schritt wird, basierend auf den Funktionen die das Verhalten der verteilten Quellen beschreiben, ein Signalraum aufgespannt. Auf Grund der hohen Anzahl an verteilten Quellen in den Netzwerkmodellen ist die Dimension des Signalraumes typischerweise sehr groß. Mit Hilfe von Approximationsverfahren wird ein Signalraum mit einer geringeren Dimension gefunden, welcher das Verhalten der verteilten Quellen beschreibt. Die verteilten Quellen im Netzwerkmodell werden ersetzt mit Modellen die den in der Dimension verringerten Signalraum beschreiben. Die Anzahl der Knoten, an denen das Verhalten in einem reduzierten Modell approximiert wird, verringert sich dadurch. Im zweiten Teil dieser Arbeit wird gezeigt, dass dadurch ein Netzwerkmodell erzeugt wird, welches sich effektiver mit Methoden der Modellreduktion reduzieren lässt.

Illustrierende und industrielle Beispielnetzwerke mit verteilten Quellen werden reduziert, um die vorgestellte Methode zu validieren und die höhere Effektivität der Modellreduktion zu zeigen.

Schlagnworte: Modellierung, Modellordnungsreduktion, Lineare Netzwerke

Contents

| | |
|---|------------|
| Acknowledgements | III |
| Abstract | IV |
| Zusammenfassung | VI |
| List of Figures | X |
| List of Tables | XIV |
| List of Symbols | 1 |
| 1 Introduction | 2 |
| 1.1 Motivation | 2 |
| 1.2 Objectives of this Work | 5 |
| 2 Description of Networks | 8 |
| 2.1 System Description | 8 |
| 2.2 Transfer Function | 13 |
| 2.3 System and Network Properties | 15 |
| 2.3.1 Properties of the System Matrices | 15 |
| 2.3.2 Properties of the Transfer Function | 16 |
| 2.3.3 Properties of the Network | 17 |
| 2.4 Illustrative Numerical Example | 20 |
| 3 Model Reduction of Linear Networks | 22 |
| 3.1 Order Reduction | 22 |
| 3.1.1 Circuit Theory Methods | 24 |
| 3.1.2 Gaussian Elimination Methods | 25 |
| 3.1.3 Modal Approximation Methods | 29 |
| 3.1.4 Moment Matching Methods | 31 |
| 3.1.5 Gramian-based Methods | 36 |
| 3.1.6 Interpolation Methods | 40 |
| 3.1.7 Comparison | 42 |
| 3.1.8 Illustrative Numerical Example | 44 |
| 3.2 Network Synthesis | 47 |
| 3.2.1 Transfer Function Synthesis | 47 |
| 3.2.2 System Equations Synthesis | 53 |
| 3.2.3 Further Methods | 60 |
| 3.2.4 Comparison of Synthesis Methods | 60 |
| 3.2.5 Illustrative Numerical Example | 62 |

| | | |
|----------|--|------------|
| 4 | Model Reduction of Networks with Sources | 65 |
| 4.1 | Problem Statement | 65 |
| 4.1.1 | Extraction of Sources | 66 |
| 4.1.2 | Reduction of Systems with Many Ports | 67 |
| 4.2 | State-of-the-Art Reduction of Ports | 78 |
| 4.2.1 | Partitioning | 78 |
| 4.2.2 | Port Correlation | 82 |
| 4.2.3 | Connected Models and Input Signals | 84 |
| 4.3 | Port Reduction Method | 87 |
| 4.3.1 | Reduction of the Dimension of the Function Space | 88 |
| 4.3.2 | Embedding of Reduced Function Space into the Network | 110 |
| 4.3.3 | Implementation of Port Reduction | 119 |
| 4.3.4 | Reduction Efficiency | 124 |
| 4.4 | Comparison and Classification | 133 |
| 5 | Examples | 136 |
| 5.1 | RC-Grid with Independent Sources | 136 |
| 5.1.1 | Port Reduction | 137 |
| 5.1.2 | Model Reduction | 138 |
| 5.1.3 | Simulation Results | 146 |
| 5.1.4 | Conclusion of RC-Grid Reduction | 147 |
| 5.2 | RC-Grid with Nonlinear Controlled Sources | 148 |
| 5.3 | Emission Model of an IC | 154 |
| 5.3.1 | Supply Voltage Domain Related Model | 155 |
| 5.3.2 | Supply Voltage Pin Related Model | 160 |
| 5.3.3 | Conclusion of ICEM Reduction | 163 |
| 6 | Conclusions and Future Work | 164 |
| 6.1 | Conclusion | 164 |
| 6.2 | Future Work | 165 |
| | Bibliography | 166 |

List of Figures

| | | |
|------|---|----|
| 1.1 | Discretization of the space of a distributed system and behavioral modeling with an electric network | 2 |
| 1.2 | Modeling of a finite element model with Dirichlet boundary conditions as network with distributed sources | 3 |
| 1.3 | Modeling of a transmission line with defined input signals as network with distributed sources | 4 |
| 1.4 | Modeling of a distributed system with distributed sources as electrical network with sources | 4 |
| 1.5 | Modeling of a distributed system with distributed nonlinear controlled sources as electrical network with nonlinear controlled sources | 5 |
| 1.6 | Illustration of the generation of a reduced model by using model reduction methods and approximating the behavior of specified nodes | 5 |
| 1.7 | Flow for the reduction of the number of ports by reducing the dimension of the function space of the distributed sources as preceding step of a model reduction | 7 |
| 2.1 | Schematic of a system with inputs \mathbf{u} , internal system variables \mathbf{x} and outputs \mathbf{y} | 13 |
| 2.2 | Illustrative example network | 20 |
| 3.1 | Classification of model reduction methods | 22 |
| 3.2 | Illustrative example transfer function $Z_{1,1}$ of the original and the moment matching reduced models | 46 |
| 3.3 | Relative approximation error of the transfer function $Z_{1,1}$ of the moment matching reduced models | 47 |
| 3.4 | Synthesized network using the Cauey-synthesis for impedances | 48 |
| 3.5 | Synthesized network using the Cauey-synthesis for admittances | 48 |
| 3.6 | Synthesized network using the Foster-synthesis for impedances | 49 |
| 3.7 | Synthesized network using the Foster-synthesis for admittances | 49 |
| 3.8 | Synthesized network using the enhanced Foster-synthesis for admittances | 50 |
| 3.9 | Synthesized network using the enhanced Foster-synthesis for impedances | 50 |
| 3.10 | π -structure of a synthesized network with two ports | 52 |
| 3.11 | T-structure of a synthesized network with two ports | 53 |
| 3.12 | π -structure of a synthesized network with four ports | 53 |
| 3.13 | Network with controlled sources and dynamic elements created by direct stamping. All system variables are interpreted as voltages. | 55 |
| 3.14 | Network with controlled sources and without dynamic elements created by direct stamping. All system variables are interpreted as voltages. | 56 |
| 3.15 | Network with controlled sources and dynamic elements created with direct stamping. All system variables are interpreted as currents. | 57 |
| 3.16 | Network with controlled sources and without dynamic elements created with direct stamping. All system variables are interpreted as currents. | 58 |

| | | |
|------|--|----|
| 3.17 | Synthesized network using GC-synthesis | 59 |
| 3.18 | Synthesized network of the reduced illustrative example using the enhanced Foster-synthesis for impedances | 63 |
| 3.19 | Synthesized network of the reduced illustrative example using GC-synthesis | 63 |
| 3.20 | Illustrative example voltage behavior at the pin of the original and the reduced network | 64 |
| | | |
| 4.1 | Extraction of distributed sources from the reducible network part and connection with the network by ports | 66 |
| 4.2 | Illustrative example network with sources | 69 |
| 4.3 | HSV and the approximated HSV for the illustrative network with sources | 70 |
| 4.4 | Illustrative example transfer function $Z_{1,1}$ of the original and the reduced models with extracted sources | 72 |
| 4.5 | Relative approximation error of the illustrative example transfer function $Z_{1,1}$ of the reduced models with extracted sources | 73 |
| 4.6 | Illustrative example transfer function $Z_{3,1}$ of the original and the reduced models with extracted sources | 73 |
| 4.7 | Relative approximation error of the illustrative example transfer function $Z_{3,1}$ of the reduced models with extracted sources | 74 |
| 4.8 | Section of the RCI-grid with independent current sources | 75 |
| 4.9 | HSV and approximated HSV for the $d = 20$ RCI-grid with $q = 20$ extracted sources and a varying number e of expansion points | 76 |
| 4.10 | HSV and approximated HSV for the $d = 10$ RCI-grid with a varying number q of extracted sources | 76 |
| 4.11 | HSV of the $d = 30$ RCI-grid networks with a varying number q of extracted sources | 77 |
| 4.12 | HSV of the $d = 100$ RCI-grid networks with a varying number q of extracted sources | 77 |
| 4.13 | Model reduction of systems with a large number of ports by partitioning into subsystems with a smaller number of ports and reduction of the subsystems | 79 |
| 4.14 | Partitioning into MIMO-subsystems with a smaller number of ports | 79 |
| 4.15 | Partitioning into SIMO-subsystems with a smaller number of ports | 80 |
| 4.16 | Partitioning into SISO-subsystems with a smaller number of ports | 80 |
| 4.17 | Partitioning into MISO-subsystems with a smaller number of ports | 81 |
| 4.18 | Model reduction of systems with a large number of ports by taking into account port correlations | 82 |
| 4.19 | Schematic flow of port reduction as preceding step of the model reduction | 88 |
| 4.20 | Grouping distributed sources' functions into functions equal or proportional to a basis function | 91 |
| 4.21 | Piece-wise constant representation functions of the example data and two sets of basis functions | 93 |
| 4.22 | Piece-wise linear representation functions of the example data and three sets of basis functions | 97 |

| | | |
|------|--|-----|
| 4.23 | Piece-wise linear representation functions with jump discontinuities of the example data and a canonical set of basis functions | 98 |
| 4.24 | Periodic functions of the example data and a set of periodic basis functions . . . | 100 |
| 4.25 | Regions for the PWL-functions of the example data | 102 |
| 4.26 | Schematic of a feed forward neural network with inputs \mathbf{x} and outputs $\mathbf{f}(\mathbf{x})$ with linear input and output layers and one nonlinear hidden layer | 107 |
| 4.27 | Illustration of the realization of the reduced dimension function space into the network model by replacing of the distributed sources | 110 |
| 4.28 | Realization of the reduced dimension function space into the illustrative example network by replacing of the two independent sources | 117 |
| 4.29 | Synthesized network using GC-synthesis and a large number of controlled sources | 123 |
| 4.30 | Synthesized network using GC-synthesis and a reduced number of controlled sources | 124 |
| 4.31 | HSV for the system of the illustrative network with extracted and with replaced sources | 125 |
| 4.32 | Illustrative example transfer function $Z_{1,1}$ of the original and the reduced models with replaced sources | 127 |
| 4.33 | Relative approximation error of the illustrative example transfer function $Z_{1,1}$ of the reduced models with replaced sources | 128 |
| 4.34 | Illustrative example transfer function $Z_{2,1}$ of the original and the reduced models with replaced sources | 128 |
| 4.35 | Relative approximation error of the illustrative example transfer function $Z_{2,1}$ of the reduced models with replaced sources | 129 |
| 4.36 | HSV for the $d = 30$ RCI-grid networks with $q = 200$ extracted sources and replaced sources with a varying dimension r of the approximating function space | 130 |
| 4.37 | HSV for the $d = 100$ RCI-grid networks with $q = 250$ extracted sources and replaced sources with a varying dimension r of the approximating function space | 131 |
| 4.38 | HSV for the $d = 30$ RCI-grid networks with a varying number of extracted sources q and replaced sources with a dimension of $r = 3$ of the approximating function space | 132 |
| 4.39 | HSV for the $d = 100$ RCI-grid networks with a varying number of extracted sources q and replaced sources with a dimension of $r = 10$ of the approximating function space | 132 |
| 5.1 | Example waveforms of the independent current sources in the RCI-grid | 136 |
| 5.2 | Ramp basis functions for the independent current sources in the RCI-grid . . . | 138 |
| 5.3 | Another set of basis functions for the independent current sources in the RCI-grid | 138 |
| 5.4 | RCI-grid transfer function $Z_{1,1}$ of the original and the moment matching reduced models with comparable approximation error | 139 |
| 5.5 | Relative error of the RCI-grid transfer function $Z_{1,1}$ of the moment matching reduced models with comparable approximation error | 140 |
| 5.6 | RCI-grid transfer function $Z_{1,1}$ of the original and the moment matching reduced models with comparable size | 140 |

| | | |
|------|--|-----|
| 5.7 | Relative approximation error of the RCI-grid transfer function $Z_{1,1}$ of the moment matching reduced models with comparable size | 141 |
| 5.8 | HSV of the RCI-grid networks with extracted and replaced sources | 141 |
| 5.9 | RCI-grid transfer function $Z_{1,1}$ of the original and the Gramian-based reduced models with comparable approximation error | 142 |
| 5.10 | Relative approximation error of the RCI-grid transfer function $Z_{1,1}$ of the Gramian-based reduced models with comparable approximation error | 143 |
| 5.11 | RCI-grid transfer function $Z_{1,1}$ of the original and the Gramian-based reduced models of the same size | 143 |
| 5.12 | Relative approximation error of the RCI-grid transfer function $Z_{1,1}$ of the Gramian-based reduced models of the same size | 144 |
| 5.13 | RCI-grid voltage fluctuation at pin1 of the original and the Gramian-based reduced model with replaced sources | 147 |
| 5.14 | RCI-grid current flow at pin1 of the original and the Gramian-based reduced model with replaced sources | 148 |
| 5.15 | Section of the RCNL-grid with nonlinear elements modeling distributed sources | 149 |
| 5.16 | HSV of the RCNL-grid networks with extracted and replaced sources | 150 |
| 5.17 | RCNL-grid transfer function $Z_{1,1}$ of the original and the Gramian-based reduced models | 151 |
| 5.18 | Relative approximation error of the RCNL-grid transfer function $Z_{1,1}$ of the Gramian-based reduced models | 151 |
| 5.19 | RCNL-grid voltage fluctuation at pin1 of the original and the Gramian-based reduced models | 152 |
| 5.20 | Relative approximation error of the RCNL-grid voltage fluctuation at pin1 for the Gramian-based reduced models | 152 |
| 5.21 | Further RCNL-grid voltage fluctuation at pin1 of the original and the Gramian-based reduced models | 154 |
| 5.22 | Section of the network of the ICEM | 155 |
| 5.23 | ICEM transfer function $Z_{1,1}$ of the original and the reduced model | 158 |
| 5.24 | Relative approximation error of the ICEM transfer function $Z_{1,1}$ of the reduced model | 158 |
| 5.25 | ICEM voltage fluctuation at pin1 of the original and the reduced model | 159 |
| 5.26 | ICEM current flow at pin1 of the original and the reduced model | 159 |
| 5.27 | HSV of the ICEM networks with extracted and replaced sources | 161 |
| 5.28 | ICEM transfer function $Z_{3,3}$ of the original and the reduced models | 162 |
| 5.29 | Relative approximation error of the ICEM transfer function $Z_{3,3}$ of the reduced models | 162 |

List of Tables

- 3.1 Comparison of network synthesis methods for reduced order models 61
- 4.1 Example data for the PWL representation 92
- 4.2 Example data for the PWL representation with finite jump discontinuities . . . 99
- 5.1 Comparison of order reduction results for the RCI-grid network 145
- 5.2 Comparison of model reduction results for the RCI-grid network 146
- 5.3 Comparison of model reduction results of the voltage-domain-related ICEM network 157
- 5.4 Comparison of model reduction results of the supply-pin-related ICEM network 160

List of Symbols

| | |
|----------------------|--|
| A | Matrix |
| a | Vector or Submatrix |
| \mathbf{A}^T | Transpose of A |
| \mathbf{A}^{-1} | Inverse of A |
| \mathbf{A}^h | Hermitian of A |
| \mathbf{A}^* | Complex conjugate of A |
| $\tilde{\mathbf{A}}$ | Matrix of an order reduced system |
| I | Identity matrix |
| s | Laplace variable |
| $\mathbf{H}(s)$ | Matrix transfer function |
| $\mathbf{Z}(s)$ | Matrix transfer impedance |
| $\mathbf{Y}(s)$ | Matrix transfer admittance |
| M | Moment of a transfer function |
| C | System matrix with capacitive and inductive coefficients |
| G | System matrix with resistive and conductive coefficients |
| B | System matrix for inputs |
| L | System matrix for outputs |
| x | Vector of system variables |
| u | Vector of system inputs |
| y | Vector of system outputs |
| P | Controllability Gramian |
| Q | Observability Gramian |
| T | Transformation or projection matrix |
| λ | Eigenvalue |
| Λ | Diagonal matrix containing Eigenvalues |
| S | Matrix containing Eigenvectors |
| σ | Singular value |
| Σ | Diagonal matrix containing singular values |
| U, V | Matrices containing singular vectors |
| p | Number of pins or ports |
| N | Order |
| n | Reduced order |
| q | Number of distributed sources |
| r | Number of basis function sources |
| $f(\mathbf{x}, t)$ | Function describing a distributed source |
| $g(\mathbf{x}, t)$ | Basis function describing distributed sources |
| W, w, w | Weights of linear combination |

1 Introduction

1.1 Motivation

The modeling and simulation of distributed systems is the basis for investigation and optimization of physical systems. Distributed systems are for example electromagnetic, thermic or acoustic field distributions. Due to the high complexity of the physical systems, investigations of the field distributions are only possible for small sections and require a high computational effort. For investigations of the overall behavior of the distributed system behavioral models are necessary. These behavioral models have to be a very good approximation to the physical system and have to be small for fast and efficient investigations. For the investigation of distributed systems electrical networks are thus used as a behavioral model, and can be simulated in circuit simulation environments. One method to obtain a behavioral model of a distributed system is based on the partial differential equations describing a field distribution. The differential equations describing the distributed system are divided into discrete sections in space, and each section is represented as an electrical network (Fig. 1.1). Typical elements of the electrical networks are linear resistors, inductors and capacitors. If the discrete section is smaller, the number of electric elements in the model is higher, and the model is more exact. For an infinitely fine grid the electric network model would be indistinguishable to the real distributed system. For a sufficiently good approximation of a distributed system a fine grid is necessary. Therefore a highly complex electrical network model, in the sense of a large number of network elements and nodes, is necessary for the behavioral model. Another method for modeling a distributed system is based on macromodeling with basis blocks. The distributed system is again divided in sections, and each section is modeled with an electrical basis block (Fig. 1.1). A basis block contains linear electric elements whose values are based on physical properties or on measurements. The basis blocks are interconnected, which results in the overall behavioral model. Independently on the method of building the behavioral model the result is an electrical network with linear resistive, inductive and capacitive elements.

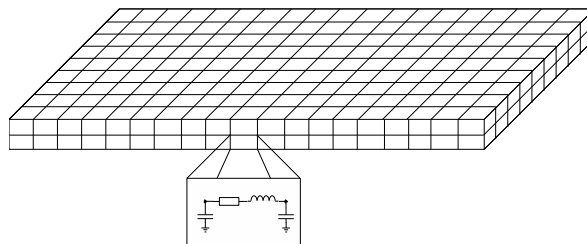


Figure 1.1: Discretization of the space of a distributed system and behavioral modeling with an electric network

Several distributed systems contain distributed sources. For example, energy sources, thermal sources, noise sources and other disturbances have to be included in their behavioral model.

These distributed sources are modeled as current or voltage sources. Several examples of distributed systems with distributed sources are illustrated in the following paragraphs.

In the simulation of distributed systems typically large passive networks, composed of only RLC-elements, are used in the region where the distributed system is to be investigated. The space is discretized in this region using for example finite element methods (FEM) [1–3] or partial element equivalent circuits (PEEC) [4]. Every section is modeled with an electrical network. For Dirichlet-problems, the boundary conditions of the volume under investigation are given. Realizing the boundary conditions in the network model leads to additional independent sources in the network model of the field distribution (Fig. 1.2). If for example a Dirichlet-problem is given, where the boundary conditions are constant over time, at the boundary nodes of the network model DC-sources are connected. In the more complex case, with time variant boundary conditions, independent sources with a time varying waveform are used. In both cases the electrical model used for the simulation of the field distribution contains independent sources, next to the passive RLC-elements.

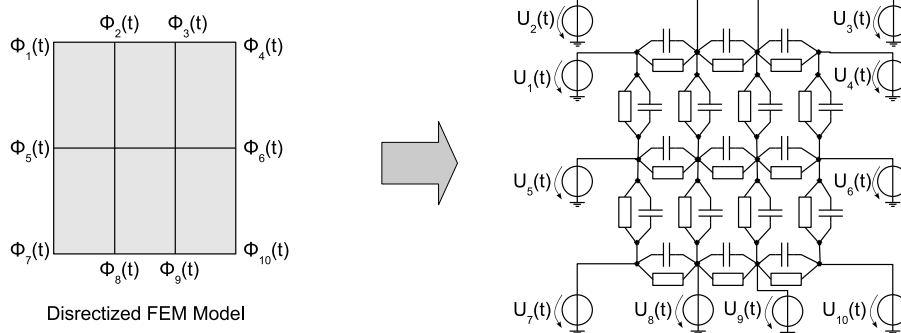


Figure 1.2: Modeling of a finite element model with Dirichlet boundary conditions as network with distributed sources

The modeling of physical devices, where several of the input signals are known a priori, is similar to the modeling of systems with predefined boundary conditions. For example, in the modeling of coupled transmission lines [4–6], where up to hundreds of lines are modeled, not all inputs are undetermined in the modeling process. The determined input signals at the transmission lines are realized as independent sources and connected as input sources with the modeled structure (Fig. 1.3).

Another area, where electrical networks are used as behavioral models in simulations, is the macromodeling of systems with internal distributed sources. Behavioral models are used in the electrical engineering for the investigation of parasitic effects in the design phase of ICs and sensors [7, 8]. Also in other fields, as for example in mechanics, macromodels are used [2] for simulations. Several of the underlying physical models contain internal distributed sources. These distributed sources are modeled in the electrical network model with the help of independent sources (Fig. 1.4). For example, in the simulation of thermal processes the heat distribution is modeled with RLC-networks and the heating sources inside the structure are modeled with independent sources [8, 9]. In the field of construction engineering the structures

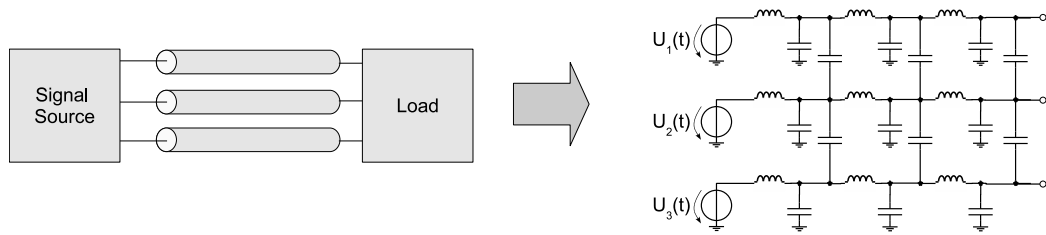


Figure 1.3: Modeling of a transmission line with defined input signals as network with distributed sources

are modeled with networks and the vibrations due to humans inside a building or cars crossing a bridge can be modeled with the help of independent sources. In the IC design the electromagnetic field distribution is modeled with RLC-networks, and the current floating inside the IC, due to the switching of the transistors, is modeled by independent sources [7, 10, 11]. Typically, this modeling of distributed systems with distributed sources is done in a two step algorithm. The parameters of the RLC-elements modeling the underlying structure are determined independently of the distributed sources' behavior. Either by measurements or by performing simulations in a well-defined environment the behavior of the distributed sources is determined. These functions, describing the behavior of the sources, are used as waveforms of the independent sources modeling the distributed sources. A combination of the model of the structure with the model of the distributed sources gives the overall model (Fig. 1.4). The resulting networks contains linear RLC-elements as well as independent sources.

Notably, the former method is only valid if the behavior of the sources changes only slightly if the environment is changed. The effect of the environment on the distributed sources is neglected when using the former modeling steps. If the models of the distributed sources cannot be modeled by independent sources, because the effect of the environment on the sources' behavior cannot be neglected, a source including nonlinear dependencies on other variables can be used. The network element representing this behavior is a nonlinear controlled source. For this modeling method the resulting network contains nonlinear elements in addition to the

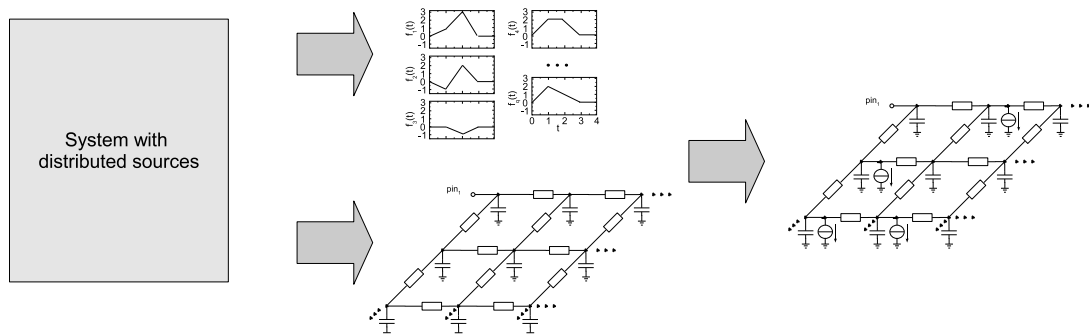


Figure 1.4: Modeling of a distributed system with distributed sources as electrical network with sources

linear passive RLC-elements (Fig. 1.5).

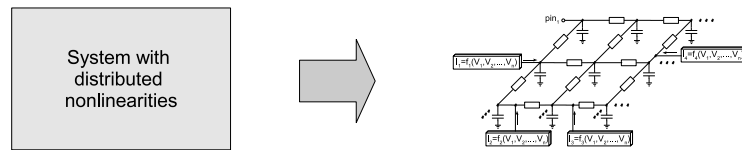


Figure 1.5: Modeling of a distributed system with distributed nonlinear controlled sources as electrical network with nonlinear controlled sources

The presented modeling procedures result in a network containing linear elements and sources. In practical behavioral models the number of linear elements is typically in the range of up to millions, while the number of distributed sources is in the range of thousands. The number of electric elements used for the behavioral modeling of distributed systems is quite large, and the behavioral models require a still high effort in simulations. The high simulation effort limits the practical usage of the created behavioral models. Based on the fact that the network model is not investigated in all modeled points in space, since the behavior at only some of nodes of the network is of interest, a motivation for a model reduction is given. As in image processing and in audio and video compression, a small model is desired, which engulfs the main properties of the original model. The objective of model reduction is to find such a small network model, with a low number of elements and nodes, which approximates the behavior at the points of interest of the behavioral model. The reduced network model replaces the large network model in simulations. Thus the reduced network can be simulated with a lower computational effort and thereby the distributed systems behavior can be more efficiently investigated.

1.2 Objectives of this Work

In this work the methods of reducing an electrical network, in the sense of reducing the number of nodes and elements, are considered. A model, which approximates the behavior at specified nodes in the network is searched for and can be obtained with model reduction, as illustrated in Fig. 1.6.

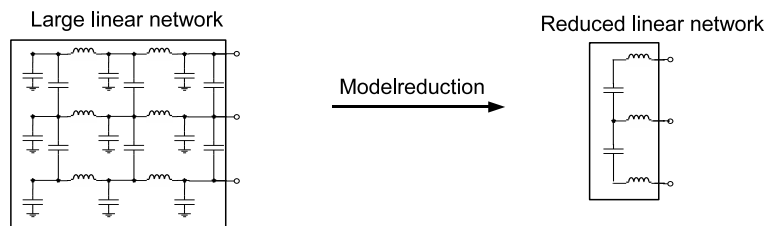


Figure 1.6: Illustration of the generation of a reduced model by using model reduction methods and approximating the behavior of specified nodes

In the first part of this work well-known reduction methods are investigated. Properties of the

network that have to be preserved in a reduced model, properties that can be approximated as well as properties that can be lost in a reduced model are identified in Sec. 2.

Several methods of reducing linear electrical networks exist. Several methods based on circuit theory directly reduce the network. Other methods reduce a mathematical description of the network. Important existing methods for reducing models are investigated in a common framework in Sec. 3. Their applicability for the reduction of electrical networks is examined. After reduction of a mathematical model, methods for synthesizing a reduced mathematical model as an electrical network become necessary to allow for simulations with circuit simulators. State-of-the-art synthesis methods are compared in this work. In addition, a synthesis method which overcomes a major drawback of existing methods and is based on preserved matrix properties of the reduced system, is presented in Sec. 3.

In this work special attention is paid to distributed systems with distributed sources. State-of-the-art model reduction methods suffer from low efficiency if a network model with a large number of sources is to be reduced. For reduction of the network the distributed sources are extracted from the linear network part. The sources and the linear network part are connected by ports. The linear network part can subsequently be reduced with model reduction techniques, approximating or preserving the behavior at the ports of the linear network part. Due to the large number of ports for a large number of sources, the efficiency of the model reduction is low, as illustrated in the upper part of Fig. 1.7. The reason for the lower efficiency is in the larger number of nodes, namely each node connected with a port, where the behavior is to be approximated in a reduced model. The background and details about this will be given in Sec. 4.1. Several model reduction approaches exist that deal with a large number of ports, generated by the extraction of a large number of sources. These methods require several conditions, which are only fulfilled for special examples. Most methods do not take into account the knowledge of the distributed sources' behavior in the model reduction process. In the model reduction process a wide range of signals is allowed at the ports, which limits the efficiency, as an a priori defined signal is present at the ports for the sources. The existing methods for the reduction of networks with a large number of ports, with their advantages and limitations, are presented in Sec. 4.2.

A new method, dealing with the reduction of networks with a large number of distributed sources, is presented in this work in Sec. 4.3. The proposed method includes the knowledge of the distributed sources' behavior in the model reduction process. The method is based on the a priori defined behavior of the distributed sources. The basic steps of the proposed method are shown in the lower part of Fig. 1.7. The reducible network model is adapted for an efficient reduction, preserving or approximating the behavior at the nodes of interest. Based on the functions that describe the models of the distributed sources, a function space is spanned. The dimension of the function space is typically very large, as the number of distributed sources is large. Based on approximation methods a lower dimension function space is found, and methods for this will be presented in Sec. 4.3. All distributed sources' functions can be obtained by linear combination of the basis functions of this lower dimension function space. Replacing the models of the distributed sources by models of the lower dimension function space in the network leads to a network model with a lower number of ports (Sec. 4.3). This preceding step allows for a higher efficiency of a model reduction.

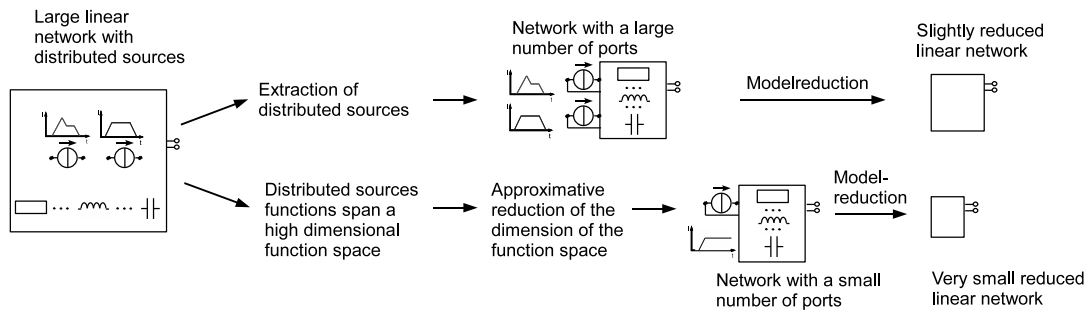


Figure 1.7: Flow for the reduction of the number of ports by reducing the dimension of the function space of the distributed sources as preceding step of a model reduction

Examples illustrating the model reduction method for networks with a large number of distributed sources, as well as industrial examples with distributed sources, are presented in Sec. 5. The higher efficiency of the model reduction, by using the proposed preceding step, is shown, and the presented method is validated. A conclusion and an outlook on further developments of the presented methods are given in at the end of this work in Sec. 6.

2 Description of Networks

In this chapter electrical networks used for the behavioral modeling of distributed systems are described. Their mathematical description in system form with the corresponding transfer function is given in the first and second sections. In the third section important properties of systems and transfer functions describing electrical networks are identified. The importance of the preservation of these properties in a reduced model is highlighted. In the last section of this chapter a small network example and its mathematical description is introduced. In the following chapters the presented methods will be illustrated with this example network.

2.1 System Description

In this section a description of electrical networks as systems of differential equations is presented.

An electrical network is a system composed of a finite number of interconnected elements [12]. Typical elements are resistors, capacitors, inductors and sources. These elements are idealizations of the electrical behavior of physical elements and follow the rules of the electromagnetic theory [12]. With the help of these elements the relation between physical time-dependent scalars like current, voltage and energy is described. The interconnection of these elements follows the rules of the Kirchhoff laws.

Electrical networks can be divided up into subnetworks [12]. As the current flowing into an isolated electrical system is zero, a subnetwork has to contain at least two terminals. The current is flowing into one terminal and leaving the subnetwork through another. The description of a subnetwork with two terminals contains one current through the subnetwork and one voltage across the terminals. For subnetworks with more than two terminals this situation is more complex. If a subnetwork contains k terminals, it is described by $k - 1$ independent currents and $\frac{1}{2}k(k - 1)$ definable voltages. This complex situation can be simplified if the terminals are concentrated into pairs. One pair of terminals is called a port if it is uniquely described by one current and one voltage. A subnetwork which only contains a number of n ports and no further terminals as connections to other subnetworks is called n-port [12]. Voltages across terminals, which do not belong to the same port, are not considered in n-port subnetworks.

If the allowed signals at a port or terminal and in the network span a linear space, the network is linear. Networks where the signals do not span a linear space are nonlinear.

Networks with elements whose physical parameters are independent of time are called time-invariant networks [12]. However, subnetworks whose elements are time-variant, but the behavior at the ports is time-invariant, are called time-invariant.

In the following we will concentrate on networks composed of only linear time-invariant elements, sources and ports.

Network elements used in the modeling of distributed systems with distributed sources con-

sidered in this work are resistors, capacitors, inductors and independent as well as controlled sources. Linear time-invariant resistors with a resistance R or conductance G respectively, are described with the branch constitutive relation (BCR), defining the dependence on the current i through and the voltage u at the element

$$u = R \cdot i \quad \text{or} \quad i = G \cdot u. \quad (2.1)$$

Linear time-invariant capacitors with a capacitance C are described by the initial voltage u_0

$$u(t = 0) = u_0 \quad (2.2)$$

and with the BCR in time-domain

$$i = C \cdot \frac{du}{dt} \quad \text{or} \quad u = \frac{1}{C} \cdot \int i dt \quad (2.3)$$

and in frequency-domain

$$i = sC \cdot u \quad \text{or} \quad u = \frac{1}{sC} \cdot i. \quad (2.4)$$

with the Laplace variable s . Linear time-invariant inductors with an inductance L are described by the initial current i_0

$$i(t = 0) = i_0 \quad (2.5)$$

and with the BCR in time-domain

$$u = L \cdot \frac{di}{dt} \quad \text{or} \quad i = \frac{1}{L} \cdot \int u dt \quad (2.6)$$

and in frequency-domain

$$u = sL \cdot i \quad \text{or} \quad i = \frac{1}{sL} \cdot u. \quad (2.7)$$

Voltage sources are described with

$$u = u_q, \quad i = \text{arbitrary} \quad (2.8)$$

where the voltage u_q is $u_q = f(t)$ in time-domain and $u_q = f(s)$ in frequency domain for independent voltage sources. In the case of nonlinear controlled voltage sources the condition $u_q = f(u_1, u_2, \dots, i_1, i_2, \dots)$ holds, as the voltage is controlled by several voltages and currents in the network $(u_1, u_2, \dots, i_1, i_2, \dots)$ with a nonlinear function f . Current sources are described with

$$i = i_q, \quad u = \text{arbitrary} \quad (2.9)$$

where the current $i_q = f(t)$ is in time-domain and $i_q = f(s)$ in frequency domain for independent current sources. In the case of nonlinear controlled current sources the condition

$i_q = f(u_1, u_2, \dots, i_1, i_2, \dots)$ holds. In addition ports for the connection with other networks are included. For the description of a port the current into the port can be used as input and the voltage at the port is used as output. In this case the port is called impedance port in the following. The notation admittance port is used if the definition is dual.

For the mathematical description of electrical networks, methods such as modified nodal analysis (MNA), mesh analysis and sparse matrix tableau exist [13–17]. The MNA is used in most circuit simulators as it is relatively easy to implement in computer programs [15, 16]. In the following, the MNA for linear RLC-networks with sources and ports is presented.

Basis of the network description are the incidence matrices \mathbf{K} and Kirchoff's Current Law (KCL) in the form [16]

$$\mathbf{K}\mathbf{i} = \mathbf{0}. \quad (2.10)$$

For the considered elements, the incidence matrix as well as the branch currents can be split up according to the type of elements resulting in

$$\left(\mathbf{K}_R \quad \mathbf{K}_C \quad \mathbf{K}_L \quad \mathbf{K}_{VS} \quad \mathbf{K}_{CS} \right) \begin{pmatrix} \mathbf{i}_R \\ \mathbf{i}_C \\ \mathbf{i}_L \\ \mathbf{i}_{VS} \\ \mathbf{i}_{CS} \end{pmatrix} = \mathbf{0}. \quad (2.11)$$

where $\mathbf{i}_R, \mathbf{i}_C, \mathbf{i}_L$ are the currents through the RLC-elements, respectively. The currents \mathbf{i}_{VS} denote all currents through the voltage sources and the currents at the admittance ports. The currents \mathbf{i}_{CS} denote all currents of the current sources and the currents at the impedance ports. The incidence matrices $\mathbf{K}_R, \mathbf{K}_C, \mathbf{K}_L, \mathbf{K}_{VS}, \mathbf{K}_{CS}$ denote the incidence matrices of the resistors, capacitors, inductors, voltage sources as well as admittance ports and current sources as well as impedance ports, respectively. The definition of voltages is given by the following equations

$$\begin{pmatrix} \mathbf{u}_R \\ \mathbf{u}_C \\ \mathbf{u}_L \\ \mathbf{u}_{VS} \end{pmatrix} = \begin{pmatrix} \mathbf{K}_R^T \\ \mathbf{K}_C^T \\ \mathbf{K}_L^T \\ \mathbf{K}_{VS}^T \end{pmatrix} \mathbf{u}^\phi \quad (2.12)$$

where \mathbf{u}^ϕ denotes all nodes potentials, $\mathbf{u}_R, \mathbf{u}_C, \mathbf{u}_L$ are the voltages across the RLC-elements and \mathbf{u}_{VS} are the voltages of the voltage sources and at the admittance ports. The BCR of the elements in frequency domain are given by

$$\begin{aligned} \mathbf{i}_R &= \hat{\mathbf{G}}\mathbf{u}_R \\ \mathbf{i}_C &= s\hat{\mathbf{C}}\mathbf{u}_C \\ \mathbf{u}_L &= s\hat{\mathbf{L}}\mathbf{i}_L \end{aligned} \quad (2.13)$$

with the diagonal matrices $\hat{\mathbf{G}}, \hat{\mathbf{C}}, \hat{\mathbf{L}}$ containing as diagonal entries the element values of the resistors, capacitors and inductors, respectively.

By inserting Eqn. 2.12 and Eqn. 2.13 in Eqn. 2.11 the KCL can be written as

$$\begin{aligned} \mathbf{K}_R \hat{\mathbf{G}} \mathbf{K}_R^T \mathbf{u}^\phi + \mathbf{K}_{Cs} \hat{\mathbf{C}} \mathbf{K}_C^T \mathbf{u}^\phi + \mathbf{K}_L \mathbf{i}_L + \mathbf{K}_{VS} \mathbf{i}_{VS} + \mathbf{K}_{CS} \mathbf{i}_{CS} &= \mathbf{0} \\ s \hat{\mathbf{L}} \mathbf{i}_L - \mathbf{K}_L^T \mathbf{u}^\phi &= \mathbf{0} \\ -\mathbf{K}_{VS}^T \mathbf{u}^\phi &= \mathbf{u}_{VS}. \end{aligned} \quad (2.14)$$

In matrix-form the MNA-description of the network is given with

$$\begin{pmatrix} \mathbf{K}_R \hat{\mathbf{G}} \mathbf{K}_R^T + \mathbf{K}_{Cs} \hat{\mathbf{C}} \mathbf{K}_C^T & \mathbf{K}_L & \mathbf{K}_{VS} \\ -\mathbf{K}_L^T & s \hat{\mathbf{L}} & \mathbf{0} \\ -\mathbf{K}_{VS}^T & \mathbf{0} & \mathbf{0} \end{pmatrix} \begin{pmatrix} \mathbf{u}^\phi \\ \mathbf{i}_L \\ \mathbf{i}_{VS} \end{pmatrix} = \begin{pmatrix} -\mathbf{K}_{CS} & \mathbf{0} \\ \mathbf{0} & \mathbf{0} \\ \mathbf{0} & \mathbf{I} \end{pmatrix} \begin{pmatrix} \mathbf{i}_{CS} \\ \mathbf{u}_{VS} \end{pmatrix}. \quad (2.15)$$

The resulting system of equations can be split up into a frequency dependent and an frequency independent part. This results in a first order differential algebraic system in the form

$$\left[s \begin{pmatrix} \mathbf{c} & \mathbf{0} & \mathbf{0} \\ \mathbf{0} & \mathbf{1} & \mathbf{0} \\ \mathbf{0} & \mathbf{0} & \mathbf{0} \end{pmatrix} + \begin{pmatrix} \mathbf{g} & \mathbf{p} & \mathbf{e} \\ -\mathbf{p}^T & \mathbf{0} & \mathbf{0} \\ -\mathbf{e}^T & \mathbf{0} & \mathbf{0} \end{pmatrix} \right] \cdot \begin{pmatrix} \mathbf{u}^\phi \\ \mathbf{i}_L \\ \mathbf{i}_{VS} \end{pmatrix} = \begin{pmatrix} \mathbf{b1} \\ \mathbf{0} \\ \mathbf{b2} \end{pmatrix} \cdot \begin{pmatrix} \mathbf{i}_{CS} \\ \mathbf{u}_{VS} \end{pmatrix} \quad (2.16)$$

where \mathbf{C}_{def} contains the frequency dependent part and \mathbf{G}_{def} contains the frequency independent part. The sub-blocks of the system matrices are defined with

$$\begin{aligned} \mathbf{g} &= \mathbf{K}_R \hat{\mathbf{G}} \mathbf{K}_R^T \\ \mathbf{c} &= \mathbf{K}_C \hat{\mathbf{C}} \mathbf{K}_C^T \\ \mathbf{p} &= \mathbf{K}_L \\ \mathbf{e} &= \mathbf{K}_{VS} \\ \mathbf{l} &= \hat{\mathbf{L}} \\ \mathbf{b}_1 &= -\mathbf{K}_{CS} \\ \mathbf{b}_2 &= \mathbf{I}. \end{aligned} \quad (2.17)$$

For networks composed of only passive RLC-elements the system matrices $\mathbf{C}_{def}, \mathbf{G}_{def}$ of Eqn. 2.16 are positive semi-definite

$$\mathbf{C}_{def}, \mathbf{G}_{def} \geq 0. \quad (2.18)$$

For the system matrix $\mathbf{C}_{def} = \mathbf{C}_{def}^T$ holds, but \mathbf{G}_{def} is not symmetric $\mathbf{G}_{def} \neq \mathbf{G}_{def}^T$. Indeed both system matrices are J-symmetric

$$\begin{aligned} \mathbf{J} \mathbf{C}_{def} \mathbf{J} &= \mathbf{C}_{def}^T \\ \mathbf{J} \mathbf{G}_{def} \mathbf{J} &= \mathbf{G}_{def}^T \end{aligned} \quad (2.19)$$

for

$$\mathbf{J} = \begin{pmatrix} \mathbf{I} & \mathbf{0} & \mathbf{0} \\ \mathbf{0} & -\mathbf{I} & \mathbf{0} \\ \mathbf{0} & \mathbf{0} & -\mathbf{I} \end{pmatrix} \quad (2.20)$$

with block sizes corresponding to the sub-blocks of the system in Eqn. 2.16. A multiplication of the right and left hand side of the system with \mathbf{J} leads to the system form

$$\left[\begin{array}{c} \overbrace{\begin{pmatrix} \mathbf{c} & \mathbf{0} & \mathbf{0} \\ \mathbf{0} & -\mathbf{1} & \mathbf{0} \\ \mathbf{0} & \mathbf{0} & \mathbf{0} \end{pmatrix}}^{\mathbf{C}_{sym}} + \overbrace{\begin{pmatrix} \mathbf{g} & \mathbf{p} & \mathbf{e} \\ \mathbf{p}^T & \mathbf{0} & \mathbf{0} \\ \mathbf{e}^T & \mathbf{0} & \mathbf{0} \end{pmatrix}}^{\mathbf{C}_{sym}} \end{array} \right] \cdot \begin{pmatrix} \mathbf{u}^\phi \\ \mathbf{i}_L \\ \mathbf{i}_{VS} \end{pmatrix} = \begin{pmatrix} \mathbf{b1} \\ \mathbf{0} \\ -\mathbf{b2} \end{pmatrix} \cdot \begin{pmatrix} \mathbf{i}_{CS} \\ \mathbf{u}_{VS} \end{pmatrix}. \quad (2.21)$$

The system matrices \mathbf{C}_{sym} , \mathbf{G}_{sym} of Eqn. 2.1 are now symmetric

$$\begin{aligned} \mathbf{C}_{sym} &= \mathbf{C}_{sym}^T \\ \mathbf{G}_{sym} &= \mathbf{G}_{sym}^T. \end{aligned} \quad (2.22)$$

Indeed the advantage of symmetry of \mathbf{C}_{sym} , \mathbf{G}_{sym} is accompanied by the disadvantage that \mathbf{C}_{sym} is not semi-definite anymore $\mathbf{C}_{sym} \not\geq 0$. It is noticeable that the internal systems variables, the solution of the system in symmetric form, are equal to the solution of the system in semi-definite form.

A system vector, containing all node voltages, inductor currents as well as voltage source currents can be defined with \mathbf{x} by

$$\mathbf{x} = \begin{pmatrix} \mathbf{u}^\phi \\ \mathbf{i}_L \\ \mathbf{i}_{VS} \end{pmatrix}. \quad (2.23)$$

The input vector \mathbf{u} contains the prescribed electrical values of the current and voltage sources and the input variables at the ports

$$\mathbf{u} = \begin{pmatrix} \mathbf{i}_{CS} \\ \mathbf{u}_{VS} \end{pmatrix}. \quad (2.24)$$

The dual electrical values of the inputs \mathbf{u} , namely the voltages \mathbf{u}_{CS} across the current sources and at the impedance ports as well as the currents \mathbf{i}_{VS} through the voltage sources and the admittance ports, are defined as output vector \mathbf{y} of the system. The description is

$$\begin{aligned} \mathbf{y} = \begin{pmatrix} \mathbf{u}_{CS} \\ \mathbf{i}_{VS} \end{pmatrix} &= \begin{pmatrix} -\mathbf{K}_{CS}^T & \mathbf{0} & \mathbf{0} \\ \mathbf{0} & \mathbf{0} & \mathbf{I} \end{pmatrix} \begin{pmatrix} \mathbf{u}^\phi \\ \mathbf{i}_L \\ \mathbf{i}_{VS} \end{pmatrix} \\ &= \begin{pmatrix} \mathbf{1}_1^T & \mathbf{0} & \mathbf{1}_2^T \end{pmatrix} \begin{pmatrix} \mathbf{u}^\phi \\ \mathbf{i}_L \\ \mathbf{i}_{VS} \end{pmatrix} \\ &= \mathbf{L}^T \mathbf{x}. \end{aligned} \quad (2.25)$$

In the general case the inputs, the system variables and the outputs depend on the Laplace variable, $\mathbf{u}(\mathbf{x}, s), \mathbf{x}(s), \mathbf{y}(s)$. For readability these dependencies are not written explicitly in what follows, and only the variables $\mathbf{u}, \mathbf{x}, \mathbf{y}$ are used. In addition, if nonlinear controlled current or voltage sources are used, the dependence of \mathbf{u} on the system variables in \mathbf{x} is not written explicitly to improve readability.

The system description is now given in short form with

$$\begin{aligned} (s\mathbf{C} + \mathbf{G}) \cdot \mathbf{x} &= \mathbf{B}\mathbf{u} \\ \mathbf{y} &= \mathbf{L}^T \cdot \mathbf{x} \end{aligned} \quad (2.26)$$

where the system matrices of a system of order N with p ports are $\mathbf{C}, \mathbf{G} \in \mathbb{R}^{N \times N}, \mathbf{B}, \mathbf{L} \in \mathbb{R}^{N \times p}$. As typically all dual electrical variables of the inputs are defined as outputs the condition $\mathbf{L} = \mathbf{B}$ for the system with positive (semi-)definite and (J-)symmetric system matrices holds. For the system with symmetric system matrices this condition does not hold.

With the modified nodal analysis a first order differential algebraic system, as schematically shown in Fig. 2.1 is generated. This system describes the behavior of the linear electrical RLC-

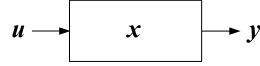


Figure 2.1: Schematic of a system with inputs \mathbf{u} , internal system variables \mathbf{x} and outputs \mathbf{y}

network. The internal system variables \mathbf{x} are composed of node voltages as well as inductor and voltage source currents. The inputs \mathbf{u} of the system are given with sources values as well as port currents or voltages. The outputs \mathbf{y} of the system are the dual electrical values of the inputs.

A description of the network as a second order differential algebraic system is possible too. In this work only the description as first order system is taken into account, as most of the model reduction methods presented in the following chapters deal with first order systems. Nevertheless, an outlook of adapted methods for second order systems is given in the corresponding points in this work.

2.2 Transfer Function

The system of differential equations of the former section describes the electrical network. In this section, the ideas for generating the transfer function $\mathbf{H}(s)$ of a system describing a network are given. The transfer function describes the transfer behavior of the system from its inputs \mathbf{u} to its outputs \mathbf{y} with $\mathbf{y} = \mathbf{H}(s) \cdot \mathbf{u}$

In systems describing electrical networks the matrix pencil (\mathbf{C}, \mathbf{G}) in Eqn. 2.26 is regular [18] for at least one frequency $s_i \in \mathbb{C}$. This means that for at least one $s_i \in \mathbb{C}$ the condition $\det(s_i\mathbf{C} + \mathbf{G}) \neq 0$ holds. This condition allows for writing

$$\begin{aligned} \mathbf{x} &= (s_i\mathbf{C} + \mathbf{G})^{-1}\mathbf{B}\mathbf{u} \\ \mathbf{y} &= \mathbf{L}^T \mathbf{x}, \end{aligned} \quad (2.27)$$

resulting in a transfer behavior, valid for all s where the matrix pencil (\mathbf{C}, \mathbf{G}) is regular. Thus, the transfer behavior is given with

$$\begin{aligned}\mathbf{y} &= \mathbf{L}^T (s\mathbf{C} + \mathbf{G})^{-1} \mathbf{B} \mathbf{u} \\ &= \mathbf{H}(s) \mathbf{u}\end{aligned}\quad (2.28)$$

For sake of simplicity it is assumed that the system matrix \mathbf{G} is nonsingular below. For generating the transfer function $\mathbf{H}(s)$ the system

$$\begin{aligned}(s\mathbf{C} + \mathbf{G}) \mathbf{x} &= \mathbf{B} \mathbf{u} \\ \mathbf{y} &= \mathbf{L}^T \mathbf{x}\end{aligned}\quad (2.29)$$

can be described by left-multiplying with \mathbf{G}^{-1} with

$$\begin{aligned}(s\mathbf{G}^{-1}\mathbf{C} + \mathbf{I}) \mathbf{x} &= \mathbf{G}^{-1}\mathbf{B} \mathbf{u} \\ \mathbf{y} &= \mathbf{L}^T \mathbf{x}\end{aligned}\quad (2.30)$$

With factorization $\mathbf{G}^{-1}\mathbf{C} = \mathbf{S}\mathbf{\Lambda}\mathbf{S}^{-1}$ the matrices $\mathbf{\Lambda}$ and \mathbf{S} are obtained. The matrix $\mathbf{\Lambda}$ contains the eigenvalues of $\mathbf{G}^{-1}\mathbf{C}$ as diagonal entries and \mathbf{S} contains the corresponding eigenvectors as its columns. After left-multiplying with \mathbf{S}^{-1} for nonsingular \mathbf{S} the system is in the form

$$\begin{aligned}(s\mathbf{\Lambda} + \mathbf{I}) \hat{\mathbf{x}} &= \hat{\mathbf{B}} \mathbf{u} \\ \mathbf{y} &= \mathbf{L}^T \mathbf{S} \hat{\mathbf{x}}\end{aligned}\quad (2.31)$$

with

$$\begin{aligned}\hat{\mathbf{B}} &= \mathbf{S}^{-1}\mathbf{G}^{-1}\mathbf{B} \\ \hat{\mathbf{x}} &= \mathbf{S}^{-1}\mathbf{x}\end{aligned}\quad (2.32)$$

For a system with p inputs, the m th row of the system of Eqn. 2.31 can be written

$$(s\Lambda_{m,m} + 1) \hat{x}_m = \sum_{i=1}^p \hat{\mathbf{B}}_{m,i} u_i, \quad (2.33)$$

with the m th eigenvalue $\Lambda_{m,m}$, the m th system variable \hat{x}_m , and the i th input u_i . Inserting x_m into the equation for the j th output in Eqn. 2.31

$$y_j = \mathbf{L}_j^T \mathbf{S} \hat{\mathbf{x}} = \sum_{m=1}^N \mathbf{L}_j^T \mathbf{S}_m \hat{x}_m = \sum_{m=1}^N \sum_{i=1}^p \frac{\mathbf{L}_j^T \mathbf{S}_m \hat{\mathbf{B}}_{m,i} u_i}{s\Lambda_{m,m} + 1} \quad (2.34)$$

The transfer function of the i th input to the j th output, described by the ij th coefficient $H_{i,j}(s)$ in $\mathbf{H}(s)$, is now given with

$$H_{i,j}(s) = \frac{y_j}{u_i} = \sum_{m=1}^N \frac{r_{i,j,m}}{s - p_m} \quad (2.35)$$

with the m th residue of the i to j transfer behavior $r_{i,j,m}$ and the m th pole p_m

$$\begin{aligned} r_{i,j,m} &= \mathbf{L}_j^T \mathbf{S}_m \hat{\mathbf{B}}_{m,i} \mathbf{\Lambda}_{m,m}^{-1} \\ p_m &= -\mathbf{\Lambda}_{m,m}^{-1} \end{aligned} \quad (2.36)$$

can be written.

If the matrix \mathbf{G}^{-1} does not exist, the generalized eigenvalue problem should be solved. A method which allows for the calculation of the poles of large systems with several hundred eigenvalues is described in [19, 20]. Typically for the analysis of even larger networks, only a set of poles is of interest. This results in methods that are capable of finding only the subset of important or dominant poles [21–26].

2.3 System and Network Properties

The networks considered in this work are composed of only real valued elements. The resistive, capacitive and inductive elements are assumed to be passive in the modeling process. In this section important properties of systems describing such linear RLC-networks are identified. Properties of the corresponding transfer functions are described as well. The necessity of the preservation of several of the properties in a reduced model is highlighted.

2.3.1 Properties of the System Matrices

The most important properties of the matrices of the system equations (Eqn. 2.26)

$$\begin{aligned} (s\mathbf{C} + \mathbf{G}) \cdot \mathbf{x} &= \mathbf{B}\mathbf{u} \\ \mathbf{y} &= \mathbf{L}^T \cdot \mathbf{x} \end{aligned} \quad (2.37)$$

are specified in this section.

As all element values are real, the system matrices only contain real coefficients. As each RLC-element is passive, all element values are positive. For the system description this leads to positive (semi-)definite system matrices \mathbf{C} , \mathbf{G} . Another property of the system matrices \mathbf{C} , \mathbf{G} is the J-symmetry for \mathbf{J} given in Eqn. 2.20. By multiplying the system with \mathbf{J} the system matrices are symmetric, as shown in Eqn. 2.1. Nevertheless, by using the system with symmetric system matrices, the system matrices are not (semi-)definite anymore.

The system matrices have a special block structure, where for every type of element a sub-block can be located in the system matrices (Eqn. 2.16). For example, a block containing the resistive elements, a block for the capacitive elements and so on, is defined in the system matrices. This block structure should be preserved in a reduced model, leading to a correlation of matrix blocks to a specific element type.

Another property of the system matrices is, especially for weak coupled networks as often used in modeling, the sparsity of the matrices. The lower the number of elements in comparison to the number of nodes is, the higher is the number of zero coefficients in the system matrices. As

the property of sparse matrices enables more efficient calculations, compared to dense matrices, the sparsity of the system matrices should be preserved in a reduced model.

Typically the system matrix \mathbf{C} is singular, which gives the system as differential algebraic equations (DAE) and the system can thereby not be written as ordinary differential equations (ODE). Only for a few special cases \mathbf{C} is nonsingular and the system can be written in ODE form.

Another property of the system matrices is that the matrix pencil (\mathbf{C}, \mathbf{G}) is regular for at least one frequency $s \in \mathbb{C}$ [18]. This means that for at least one frequency the condition $\det(s\mathbf{C} + \mathbf{G}) \neq 0$ holds.

Concluding this section, relevant system matrices properties are: real coefficients, block structure, sparsity and regularity. If all, or at least most of the properties of the system matrices are preserved in a reduced model, a reinterpretation of the system in the sense of a network model will be eased. Therefore, as many properties of the system matrices as possible should be preserved during model reduction.

2.3.2 Properties of the Transfer Function

For the transfer function, describing the input output behavior of the system of the network (Eqn. 2.28) with

$$\mathbf{H}(s) = \mathbf{L}^T (s\mathbf{C} + \mathbf{G})^{-1} \mathbf{B} \quad (2.38)$$

and its coefficients in poles-residues form (Eqn. 2.35)

$$H_{i,j}(s) = \sum_{m=1}^N \frac{r_{i,j,m}}{s - p_m} \quad (2.39)$$

several properties are defined in this section.

If the transfer function describes a passive system, the function is positive real [27, 28]. The reduced systems transfer function should also be positive real, allowing for an interpretation as a passive network.

Assuming a transfer function given in the poles-residues form, properties of the poles and residues can be defined. For the networks under consideration, all poles have a non-positive real part and thus are located in the open left half-plane of the complex plane. If the real part of the pole equals zero, the pole is in addition simple. All complex poles appear in complex conjugate pairs. The appearance in conjugate complex pairs also holds for the corresponding residues.

Several properties of the transfer behavior can be derived from the transfer functions properties, as shown below. For low frequencies, the poles with a small imaginary part dictate the behavior of the transfer function and vice versa. In a reduced system the most important poles, defined by the frequency range of interest, should be taken into account. In addition, poles with corresponding large residues can be more important than poles with small residues and have to be preserved primarily in a reduced transfer function.

For the transfer function, a series expansion in the form

$$\mathbf{H}(s) \approx \mathbf{M}_0 + \mathbf{M}_1 s + \mathbf{M}_2 s^2 \dots \quad (2.40)$$

approximating the transfer function in a region around $s = 0$, can be defined. The coefficients of this series expansion are called moments in the scalar and block-moments in the matrix transfer function case. The zeroth moment \mathbf{M}_0 is the so-called DC-moment, describing the circuit transfer behavior if all inductors are replaced by short circuits and all capacitors are replaced by open circuits. The first moment \mathbf{M}_1 corresponds to the Elmore-delay [29], describing the response or transfer time from one input to an output. For a reduced model it is preferable to preserve or at least approximate a large number of moments and thereby approximate the transfer behavior.

Properties like positive realness, location of poles and moments of the transfer function should be preserved in the transfer function of reduced models.

2.3.3 Properties of the Network

In this section the physical properties of networks are highlighted and the advantages of the preservation of these properties in a reduced model are shown.

Causality describes the dependence between cause and effect. A system is causal if for all equal input signals (cause) the output signals (effect) are the same. A non-causal system generates for the same input signals different output signals. Reasons for non-causality can be that the system is influenced by future input signals. Furthermore, a system can be non-causal if the output signal is not uniquely defined by the past signals. The property of causality is necessary for models describing physical systems and thus the networks under consideration in this work are causal. A reduced network should be also causal to avoid non-physical behavior of the reduced model.

Structural properties of networks are controllability and observability. A network is controllable if all internal states can be changed to every value in a finite time by applying input signals at the ports. Observability is defined in a dual way. A network is observable if all internal states can be determined by observing the output signals at the ports in a finite time. Observability and controllability can be mathematically described with the help of the Gramians, resulting from the solution of the Lyapunov Equations [30]. If the Gramians have full rank, the system is controllable and observable. A definition for controllability and observability in the field of network theory is given in [31, 32]. The condition is valid for unhinged networks without loops of only voltage sources and capacitors and without cut-sets of only current sources and inductors and is based on the differential equations describing the network. With simple matrix-properties, namely that the matrices connecting inputs and outputs with the state have to be nonzero, the observability and controllability are proven [31, 32]. An extension to networks including mutual inductors is given in [33]. The property of controllability and observability should be preserved in a reduced network, as states not controllable or not observable should be avoided in a reduced model to enable a higher efficiency in simulations.

Another property of networks is stability, which can be defined in several ways. A definition for

stability, oriented on [34], is bounded-input-bounded-output (BIBO) stability. This definition of stability does not need knowledge about the inner part of the circuit and only the behavior at the ports is of interest. A system of a network is BIBO stable if the output signal is bounded for every bounded input signal. A system of a network is short circuit stable if the output current is bounded for all bounded input voltages. A system of a network is open circuit stable if the output voltage is bounded for all bounded input currents. A system of a network that produces unbounded outputs for bounded inputs is unstable. Another definition for stability can be made by including knowledge about the inner part of the system of a network. A system is stable if its transfer function, in the form of Eqn. 2.35, has only stable poles [35]. For stable poles p the following conditions has to hold: for multiple poles the real part is negative $Re(p) < 0$ and for single poles the real part is not positive $Re(p) \leq 0$. This property is fulfilled for the transfer function of the networks under consideration as described in the former section. The property of stability should be preserved in a reduced network to enable stable simulations.

The passivity of a network is defined in the sense that a network cannot deliver energy at any time. A network is strict passive if it dissipates energy. A system is lossless passive if it cannot deliver energy nor dissipates energy. A network which is not passive is active. For the proof of passivity the complex energy w is defined with the currents i and voltages u

$$\begin{aligned} w &= i^h \cdot u \\ w^* &= u^h \cdot i \end{aligned} \quad (2.41)$$

where h denotes the conjugate complex transpose $a^h = (a^*)^T$. The effective energy is the real part of the complex energy

$$2Re(w) = i^h \cdot u + u^h \cdot i. \quad (2.42)$$

In the system of the network (Eqn. 2.26) the input vector \mathbf{u} contains currents or voltages at the ports and sources, and the corresponding output vector \mathbf{y} the dual electrical values. Therewith $\mathbf{u} \cdot \mathbf{y}^*$ is composed of $u_k \cdot i_k^*$ or $i_k \cdot u_k^*$ for the k th input and output of the system. Note that the real part of both descriptions is identical [12], and thereby Eqn. 2.42 can be written as

$$2Re(w) = \mathbf{u}^h \cdot \mathbf{y} + \mathbf{y}^h \cdot \mathbf{u}. \quad (2.43)$$

With the transfer function $\mathbf{y} = \mathbf{H}(s) \cdot \mathbf{u}$ it can be written

$$\begin{aligned} 2Re(w) &= \mathbf{u}^h \cdot \mathbf{H}(s) \cdot \mathbf{u} + \mathbf{u}^h \cdot \mathbf{H}(s)^h \cdot \mathbf{u} \\ &= \mathbf{u}^h (\mathbf{H}(s) + \mathbf{H}(s)^h) \mathbf{u}. \end{aligned} \quad (2.44)$$

For positive real part of the frequency $Re(s) \geq 0$, the effective energy dissipated by the system $Re(w)$ must not be below zero

$$Re(w) \geq 0. \quad (2.45)$$

The system must not produce energy if the system is passive. Therefore, $\mathbf{H}(s) + \mathbf{H}(s)^h$ has to be positive semi-definite for all $Re(s) \geq 0$. A matrix which fulfills this condition is called positive real matrix. Concluding, the necessary and sufficient condition for passivity of a system is a positive real transfer function $\mathbf{H}(s)$ [34]:

1. $\mathbf{H}(s^*) = \mathbf{H}^*(s)$ where $*$ is the conjugate complex operator
2. $\mathbf{H}(s)$ is positive, that means $\mathbf{a}^h (\mathbf{H}(s) + \mathbf{H}(s)^h) \mathbf{a} \geq 0$, with h as Hermitian operator, is satisfied for all complex s with $Re(s) \geq 0$ and for all finite complex vectors \mathbf{a}
3. $\mathbf{H}(s)$ is analytical

For passive systems the transfer function in impedance or admittance form is a positive real matrix. For passive systems

$$\mathbf{u}^h (\mathbf{H}(s) + \mathbf{H}(s)^h) \mathbf{u} \geq 0 \quad (2.46)$$

for strict passive systems

$$\mathbf{u}^h (\mathbf{H}(s) + \mathbf{H}(s)^h) \mathbf{u} > 0 \quad (2.47)$$

and for lossless systems

$$\mathbf{u}^h (\mathbf{H}(s) + \mathbf{H}(s)^h) \mathbf{u} = 0 \quad (2.48)$$

holds for all input signals \mathbf{u} and all frequencies with $Re(s) \geq 0$. Active systems are divided into autonomous-active and non-autonomous-active systems. When an active system is disconnected from the rest of the circuit and a voltage appears at its open terminals, the system is called autonomous-active [36]. If no voltage appears at the open terminals, but the circuit can generate energy by connection with the rest of the circuit, the circuit is called non-autonomous-active [36]. As the reducible part of the network models of the distributed systems is passive, in a reduced network the passivity should be preserved. Passivity is a much stronger condition than stability, as it is guaranteed that the connection of passive system will always lead to a stable system. By preservation of passivity, the simulation of the reduced model connected with other passive models is guaranteed to be stable. Thus, not only stability, but also passivity should be preserved in a reduced model.

Another relevant property is reciprocity. A network is reciprocal if for all port-port-combinations it holds: for all input signals u_k at a port k the output signal y_l at a port l is the same if the input signal u_l at a port l generates the same output signal y_k at a port k . For all input signals

$$u_k = u_l \quad (2.49)$$

it holds

$$y_k|_{u_l} = y_l|_{u_k} \quad (2.50)$$

for all ports k and l . A system where a port-port-combination exists for which this condition is not fulfilled for at least one input signal is non-reciprocal. The transfer function of a reciprocal network is symmetric for the admittance or impedance description and J-symmetric in the hybrid case [12]. Reciprocity is a necessary condition for a matrix transfer function to be realizable as pure RLC-network. The reducible network models are RLC-networks and thus reciprocal, and the property of reciprocity should be preserved in a reduced model. If a reduced model is not reciprocal it cannot be described by RLC-elements. In this case additional non-reciprocal elements, such as controlled sources or gyrators, are necessary for a realization of

the non-reciprocal system as an electrical network. Thus the property of reciprocity should be preserved in a reduced network.

Properties like causality, controllability, observability, stability and passivity of the network modeling a physical distributed system should be preserved in a reduced network to enable efficient and stable simulations.

2.4 Illustrative Numerical Example

In this section a network is introduced. Due to its simplicity, this network will be used for illustration purpose in the following chapters of this work. The presented methods will be illustrated with this network. The network contains resistors and capacitors and is shown in Fig. 2.2. The left node of the network is used for the connection with other networks and thus a port with ground as second terminal is defined. The current at the port is defined as the input of the system describing the network, and the voltage between the port-node and ground is defined as the output. Thus the resulting system describes the impedance of the network.

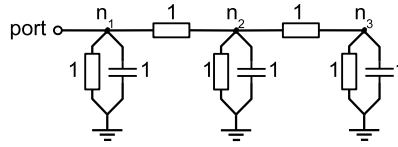


Figure 2.2: Illustrative example network

The network is to be described as a linear system of equations with the help of MNA. The incidence matrices for the resistors, capacitors and the impedance port are given with

$$\mathbf{K}_R = \begin{pmatrix} 1 & 1 & 0 & 0 & 0 \\ 0 & -1 & 1 & 1 & 0 \\ 0 & 0 & 0 & -1 & 1 \end{pmatrix}, \quad \mathbf{K}_C = \begin{pmatrix} 1 & 0 & 0 \\ 0 & 1 & 0 \\ 0 & 0 & 1 \end{pmatrix}, \quad \mathbf{K}_{CS} = \begin{pmatrix} 1 \\ 0 \\ 0 \end{pmatrix}, \quad (2.51)$$

respectively. With the unit valued elements

$$\hat{\mathbf{G}} = \mathbf{I}_{5 \times 5}; \quad \hat{\mathbf{C}} = \mathbf{I}_{3 \times 3} \quad (2.52)$$

the MNA of the network yields the system

$$\left[s \begin{array}{c} \mathbf{C} \\ \left(\begin{array}{ccc} 1 & 0 & 0 \\ 0 & 1 & 0 \\ 0 & 0 & 1 \end{array} \right) \end{array} + \begin{array}{c} \mathbf{G} \\ \left(\begin{array}{ccc} 2 & -1 & 0 \\ -1 & 3 & -1 \\ 0 & -1 & 2 \end{array} \right) \end{array} \right] \underbrace{\begin{pmatrix} \phi_{n1} \\ \phi_{n2} \\ \phi_{n3} \end{pmatrix}}_{\mathbf{x}} = \underbrace{\begin{pmatrix} 1 \\ 0 \\ 0 \end{pmatrix}}_{\mathbf{B}} \underbrace{\begin{pmatrix} u_p \end{pmatrix}}_{\mathbf{u}}$$

$$\underbrace{\begin{pmatrix} u_p \end{pmatrix}}_{\mathbf{y}} = \underbrace{\begin{pmatrix} 1 & 0 & 0 \end{pmatrix}}_{\mathbf{L}^T} \underbrace{\begin{pmatrix} \phi_{n1} \\ \phi_{n2} \\ \phi_{n3} \end{pmatrix}}_{\mathbf{x}} \quad (2.53)$$

of order $N = 3$. The system variable ϕ_j is the corresponding node potential of the node n_j . For this system the system matrices \mathbf{G} , \mathbf{C} are positive (semi-)definite, symmetric and $\mathbf{B} = \mathbf{L}$ holds.

The factorization of $\mathbf{G}^{-1}\mathbf{C} = \mathbf{S}\mathbf{\Lambda}\mathbf{S}^{-1}$ leads to

$$\mathbf{\Lambda} = \text{diag}\left(1, \frac{1}{2}, \frac{1}{4}\right) \quad (2.54)$$

which results in the three simple real poles at $-1, -2, -4$. With the calculations given in Sec. 2.2, the impedance transfer function in pole-residues form is given with

$$Z(s) = \frac{1/3}{s+1} + \frac{1/2}{s+2} + \frac{1/6}{s+4}. \quad (2.55)$$

With the help of the network introduced in this section (Fig. 2.2), the corresponding system equations (Eqn. 2.53) and the transfer function (Eqn. 2.55) the following methods of this work will be illustrated.

3 Model Reduction of Linear Networks

In this chapter, methods for the reduction of large linear networks, as used in the modeling of distributed systems, are presented. The presented approaches can be divided, as shown in Fig. 3.1, into methods based on reducing the network directly, methods reducing the transfer function of the network and methods reducing the system equations describing the network.

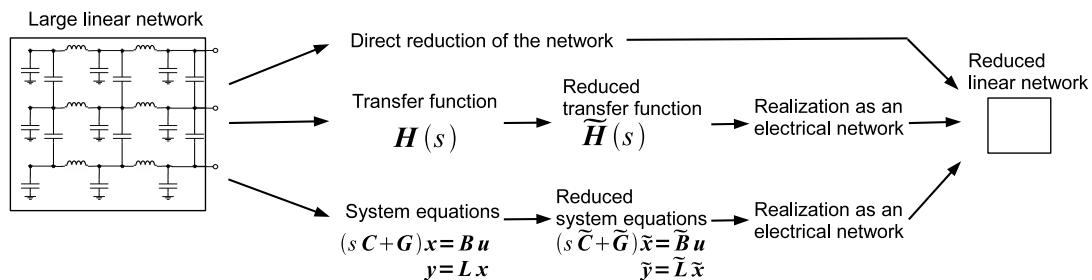


Figure 3.1: Classification of model reduction methods

In the first section of this chapter methods directly reducing the network, based on circuit theory algorithms, are described. Methods ranging from engineering methods to control theory algorithms, based on the reduction of the mathematical description of the network, are presented as well in the first section. A unified framework is used for the model reduction algorithms, which allows for comparing the methods with respect to their applicability of reducing network models. Properties of the network that are preserved using the reduction methods are given. For methods reducing a mathematical description of the network a subsequent realization as electrical network is necessary. The methods for realization of reduced mathematical models as electrical networks are presented in the second section of this chapter. At the end of this chapter the model reduction methods are illustrated by reducing the example network introduced in the former chapter.

3.1 Order Reduction

With the help of order reduction a reduced model is searched for. The order reduction methods can be divided into three different methods, according to the model description where the reduction is applied.

The first method is dealing with the network directly. The order can be defined as the number of nodes or the number of elements of the network. The behavior at several specified nodes, for example the nodes for the connection with other networks, is to be approximated. Order reduction is applied to the network in the sense that the number of nodes or elements is reduced. The reduction should only result in slight changes of the behavior at specified nodes.

For the second and third order reduction method the starting point is a description of the network as linear time-invariant system with p inputs and outputs, and the corresponding $p \times p$ transfer function. The system is described by N equations in the form of Eqn. 2.26 and the transfer function of the system is in the form of Eqn. 2.35 as described in the former chapter.

The second class of order reduction methods is based on the reduction of the transfer function. The order N of the transfer function is defined by the number of poles. With the help of model order reduction a transfer function $\tilde{\mathbf{H}}(s)$ with lower order shall be found, which approximates the original transfer function in magnitude and phase in a confined frequency range $s_{low} \leq s \leq s_{high}$. Thereby the condition

$$\tilde{\mathbf{H}}(s) \approx \mathbf{H}(s) \quad (3.1)$$

has to hold in a range of s defined between s_{low} and s_{high} . Each coefficient of the reduced transfer function describing the i th input to the j th output behavior can be written in polynomial form as

$$\tilde{H}_{i,j}(s) = \sum_{m=1}^n \frac{\tilde{r}_{i,j,m}}{s - \tilde{p}_m} \quad (3.2)$$

with a lower number of poles $n < N$ compared to the original transfer function.

The third order reduction class is based on reducing the number of equations of the system, which describes the network. For the system the order is defined as the number of system variables, which is equal to the number of equations of a well-defined system. A reduced system with a reduced order $n < N$ has to be found with order reduction methods

$$\begin{aligned} (s\tilde{\mathbf{C}} + \tilde{\mathbf{G}}) \tilde{\mathbf{x}} &= \tilde{\mathbf{B}}\mathbf{u} \\ \tilde{\mathbf{y}} &= \tilde{\mathbf{L}}^T \tilde{\mathbf{x}}, \end{aligned} \quad (3.3)$$

which has the form of the unreduced system. The matrices $\tilde{\mathbf{C}}, \tilde{\mathbf{G}} \in \mathbb{R}^{n \times n}$ and $\tilde{\mathbf{B}} \in \mathbb{R}^{n \times p}, \tilde{\mathbf{L}}^T \in \mathbb{R}^{p \times n}$ describe the reduced system. The transfer behavior between input and output of the reduced system has to be similar to the unreduced system. This means that, for the same input \mathbf{u} , the output of the reduced system $\tilde{\mathbf{y}}$ is approximating the magnitude and phase of the output of the unreduced system \mathbf{y}

$$\tilde{\mathbf{y}}(s) \approx \mathbf{y}(s) \quad (3.4)$$

in a frequency range $s_{low} \leq s \leq s_{high}$. For the reduced system there does not need to be a direct correlation between the system variables $\tilde{\mathbf{x}}, \mathbf{x}$ in the reduced and the unreduced system, respectively.

Additionally to the approximation of the input-/output or transfer function behavior, the reduced system shall preserve all, or at least most properties, of the unreduced model presented in the former chapter.

For the generation of a reduced network different approaches exist. The most widely used algorithms are presented below, and are divided into classes having the same or a similar basic idea for the motivation of a reduction. The applicability of the model reduction methods to networks used in behavioral modeling of distributed systems is discussed.

3.1.1 Circuit Theory Methods

The model reduction methods presented in this section are mainly developed in the field of Layout-to-Circuit extraction in the design phase of integrated circuits [10, 37–39]. The presented methods are directly manipulating the network. The methods are based on removing internal nodes or elements and approximating the behavior of the whole circuit at several specified points.

For networks composed of only one type of electrical element, a simple reduction method is given by dissolving series and parallel connections until all internal nodes are eliminated. For networks with more than one type of element this dissolving can be done for series and parallel connections of the same type of element. As in typical modeling procedures the amount of one type of element series or parallel connections is quite low, the reduction is very low with this method.

Another simple reduction technique replaces resistors having a high resistance by an open circuit and resistors with a small resistance by a short circuit. In the system description system variables are either eliminated or coefficients in the matrices are replaced by zero by using this simple replacing method. The strong disadvantage of this method is the heuristical approach. The definition of 'small' or 'large' element values remains open. In addition, an element with a locally negligible influence can have a significant global influence. The error of approximation cannot be controlled with this simplistic method and specific properties cannot be preserved.

Another method of eliminating internal nodes and elements is used for regular structured networks that model physical devices. In the regular structured networks the network size is reduced by using a coarser grid size. This method can only be applied for regular network grids such as networks used to model the power distribution in ICs [10, 39, 40] and is not applicable to irregularly structured networks.

With the former method neither estimation nor control of error is possible. Thereby methods preserving specified properties such as timing-issues or DC-behavior become necessary. The first algorithms as well as their extensions are presented below. One of the earliest methods is presented in [37, 38], where the special structure of electrical interconnect models is used in the reduction process. In the interconnect models only RC-elements connected in the form of an RC-ladder are used. The goal of the method in [37] is to preserve only the nodes for the connection with loads or driver and to eliminate all internal nodes in the network. For this reduction the values of a first order RC-section are calculated, approximating the electrical behavior at the nodes for driver and load. The method preserves the so-called Elmore time constants [29], which allows for a first order approximation of the network behavior.

The advantage of the methods presented in this section is their simplicity, as they are dealing directly with the network. These reduction methods construct a reduced network with the same type of elements as in the original network. The network elements in the reduced network are either purely resistive or resistive and capacitive with only positive real element values, like in the unreduced network. Thus the resulting networks are stable, passive and reciprocal. The disadvantage of these reduction methods is the low efficiency and the limited domain of application. Another disadvantage is that with this method neither error estimation nor control

is possible. Only very limited properties such as DC-behavior or timing delay can be preserved, but higher order effects are not taken into account.

Further methods applied directly to the network are, for example, the star-delta transformation used in [41], with which an internal node can be eliminated. As this transformation is in fact a Gaussian elimination step in the system matrices, it will be presented in the next section.

3.1.2 Gaussian Elimination Methods

A systematic method for the order reduction is based on the elimination of the internal nodes of the network or internal variables of the system, respectively. The method is inspired by Gaussian elimination employing the Schur complement, which is used for solving linear systems of equations. The basic principle of solving a linear system with the Schur complement is that the system of equations is firstly solved for a set of unknowns. With the solutions of the first set the rest of the unknowns is determined. For the order reduction, firstly a set of variables is defined, corresponding to the variables of interest. The reduced system is generated by using a system described only by these variables, as will be shown in this section.

The Schur complement is used to solve a system of equations in the form

$$\begin{pmatrix} \mathbf{A} & \mathbf{B} \\ \mathbf{C} & \mathbf{D} \end{pmatrix} \begin{pmatrix} \mathbf{a}_1 \\ \mathbf{a}_2 \end{pmatrix} = \begin{pmatrix} \mathbf{b}_1 \\ \mathbf{b}_2 \end{pmatrix} \quad (3.5)$$

where $\mathbf{a}_1, \mathbf{a}_2$ are the unknowns. The matrices $\mathbf{A}, \mathbf{B}, \mathbf{C}, \mathbf{D}$ are the coefficients of the equations and $\mathbf{b}_1, \mathbf{b}_2$ are the right hand side of the system of equations. The system of equations has, after a block Gaussian elimination step, a triangular form

$$\begin{pmatrix} \mathbf{A} - \mathbf{B}\mathbf{D}^{-1}\mathbf{C} & \mathbf{0} \\ \mathbf{C} & \mathbf{D} \end{pmatrix} \begin{pmatrix} \mathbf{a}_1 \\ \mathbf{a}_2 \end{pmatrix} = \begin{pmatrix} \mathbf{b}_1 - \mathbf{B}\mathbf{D}^{-1}\mathbf{b}_2 \\ \mathbf{b}_2 \end{pmatrix}. \quad (3.6)$$

The block $\mathbf{A} - \mathbf{B}\mathbf{D}^{-1}\mathbf{C}$ is the so-called Schur complement. The system of equations is now solved for the first set of variables \mathbf{a}_1 . By inserting the solution of \mathbf{a}_1 in the second row, the solution for \mathbf{a}_2 is obtained.

For order reduction this method can be applied to the system description in the form of Eqn. 2.26 as well as to the transfer function in the form of Eqn. 2.35.

For the system description in the form of Eqn. 2.26 the system vector \mathbf{x} is split up into a part \mathbf{x}_{ext} that is connected with the external ports that will be preserved, and an internal part \mathbf{x}_{int} that will be eliminated. According to this splitting, the system can be written for example for purely resistive networks with

$$\begin{pmatrix} \mathbf{G}_{1,1} & \mathbf{G}_{2,1} \\ \mathbf{G}_{2,1} & \mathbf{G}_{2,2} \end{pmatrix} \begin{pmatrix} \mathbf{x}_{ext} \\ \mathbf{x}_{int} \end{pmatrix} = \begin{pmatrix} \mathbf{B}_{ext}\mathbf{u} \\ \mathbf{0} \end{pmatrix}. \quad (3.7)$$

The preserved system variables in \mathbf{x}_{ext} , which are the solution of

$$\left(\mathbf{G}_{1,1} - \mathbf{G}_{1,2}\mathbf{G}_{2,2}^{-1}\mathbf{G}_{2,1} \right) \mathbf{x}_{ext} = \mathbf{B}_{ext}\mathbf{u} \quad (3.8)$$

after applying a block Gaussian elimination step, are used in a reduced system. This system of equations now describes a reduced order model [42, 43]. The order of the system is equal to the number of system variables connected by ports with other systems. For capacitive or inductive networks the reduced system can be defined in the same way, but in addition, the system vector is multiplied with s or $1/s$ respectively.

For the transfer function in the form of Eqn. 2.35 only the impedance or admittance of networks composed of only one type of element is considered. With this the transfer function only contains scalar values and no polynomials. Thus this approach is limited to transfer functions describing resistive, inductive or capacitive networks only. For this reduction method a transfer function is built, describing the transfer behavior from each node to all other nodes. Firstly this transfer function is inverted

$$\mathbf{H}^{-1}\mathbf{y} = \mathbf{u}. \quad (3.9)$$

The inputs are split up into nonzero inputs \mathbf{u}_{nz} and inputs equal zero $\mathbf{u}_z = \mathbf{0}$. By splitting the inverse transfer function accordingly with

$$\mathbf{H}^{-1} = \begin{pmatrix} \mathbf{H}_{1,1}^i & \mathbf{H}_{2,1}^i \\ \mathbf{H}_{2,1}^i & \mathbf{H}_{2,2}^i \end{pmatrix} \quad (3.10)$$

the resulting function is

$$\begin{pmatrix} \mathbf{H}_{1,1}^i & \mathbf{H}_{2,1}^i \\ \mathbf{H}_{2,1}^i & \mathbf{H}_{2,2}^i \end{pmatrix} \begin{pmatrix} \mathbf{y}_{nz} \\ \mathbf{y}_z \end{pmatrix} = \begin{pmatrix} \mathbf{u}_{nz} \\ \mathbf{0} \end{pmatrix}. \quad (3.11)$$

By applying the block Gaussian elimination the reduced function is [41]

$$\left(\mathbf{H}_{1,1}^i - \mathbf{H}_{1,2}^i \mathbf{H}_{2,2}^{i-1} \mathbf{H}_{2,1}^i \right) \mathbf{y}_{nz} = \mathbf{u}_{nz}. \quad (3.12)$$

In the reduced transfer function only nodes connected with a nonzero inputs are taken into account. As only the outputs for the nonzero input nodes are of interest, the reduced transfer function $\tilde{\mathbf{H}}$ is obtained by inversion with

$$\begin{aligned} \mathbf{y}_{nz} &= \left(\mathbf{H}_{1,1}^i - \mathbf{H}_{1,2}^i \mathbf{H}_{2,2}^{i-1} \mathbf{H}_{2,1}^i \right)^{-1} \mathbf{u}_{nz} \\ &= \tilde{\mathbf{H}} \mathbf{u}_{nz} \end{aligned} \quad (3.13)$$

The main difference of this method applied to the transfer function, in comparison with the method applied to the system equations reduction, is the use of the inverse of the Schur complement. The dimension of the reduced transfer function depends on the number of nodes with nonzero inputs.

Both presented methods for the elimination of internal variables are exact, as no approximation is done. Thus properties like stability, passivity and reciprocity are preserved. Nevertheless, due to the necessary inversions, numerical errors are introduced, which are unavoidable using this reduction method. In addition, due to numerically crucial operations, this method is limited to networks with a sufficiently small number of internal nodes.

The presented methods based on the Schur complement are restricted to networks with one type of elements, which limits their applicability. An extension is possible for the reduction of networks with inductors, resistors and capacitors if only a fixed frequency is considered. By using the impedance or admittance values of the elements in the specified frequency, the above algorithms can be used by employing complex arithmetic, as every value is complex and not real anymore. Nevertheless, the resulting system is only valid at the chosen frequency. For other frequencies the reduced system is not valid. Thereby these methods are not useful for approximating a network behavior in a narrow frequency range.

For systems describing networks with more than one type of elements the Schur complement is given with

$$\left[s\mathbf{C}_{1,1} + \mathbf{G}_{1,1} - (s\mathbf{C}_{1,2} + \mathbf{G}_{1,2}) \cdot (s\mathbf{C}_{2,2} + \mathbf{G}_{2,2})^{-1} \cdot (s\mathbf{C}_{2,1} + \mathbf{G}_{2,1}) \right] \mathbf{x}_{ext} = \mathbf{B}_{ext} \mathbf{u} \quad (3.14)$$

valid for all frequencies. The matrix $\mathbf{C}_{i,j}$ denotes the blocks of the matrix \mathbf{C} partitioned as in Eqn. 3.7. For transfer functions describing networks with more than one type of elements the internal nodes can be eliminated by using matrices of rational functions of s . The main hurdle using this reduction method is the complexity of the rational functions, as their order is typically very high. Thus a numerical implementation of this method is quite complicated.

For an applicable method of the reduction of networks with more than one type of element, the basic idea of Gaussian elimination can be used in another way. The method based on Gaussian elimination cannot only be applied to the complete set of internal variables, but also to single variables. This equals the elimination of single nodes in each step, contrary to the elimination of all internal nodes at once. The elimination procedure is then repeated node by node. The method equals a star-delta transformation applied directly to the network. The internal network node of a star-network is eliminated by creating the delta-network, which has the same behavior at the outer nodes as the star-network. This Gaussian elimination or star-delta transformation can be easily applied to network nodes with only one type of elements as shown before. If the reduction is applied to a network node connected with more than one type of element, the delta network element values are polynomials in s . In the general case these polynomials cannot be interpreted as resistive, inductive or capacitive elements directly. Thus this approach cannot be applied directly to networks with more than one type of element. To overcome this problem several solutions exist. The first method deals with the reduction of a class of RC-networks in [44]. The RC-networks contain only resistors connected between different nodes and capacitors connected between a node and ground. If the branch-impedances of the star-network contain more than only one type of elements, the resulting impedances of the delta-network typically are complex. In [44] the branch of the delta network is interpreted as purely resistive or purely capacitive, depending on the larger absolute value of the real or imaginary part of the impedance. Secondly in [45, 46] a method is proposed for RC-networks. In the presented method an internal node that is to be eliminated is selected and the capacitance connected from this node to ground is distributed into capacitances connected between the neighboring nodes and ground. After this step only resistors are connected with the node, and therefore the node can be eliminated by Gaussian elimination. With this method the Elmore time constants as well as the overall sum of all capacitance values is preserved. The network structure which

can be handled is similar to the network structure used in the former paragraph, describing the methods of [37, 38]. All nodes in the network model have to be connected with the neighboring nodes by a resistor and with ground by a capacitor. In addition to the methods of [37, 38], the methods of [45, 46] can also handle resistive loops and coupling capacitances. A third approach, presented in [47, 48], is based on overcoming the problems of the calculation with polynomials by first order approximations. The polynomials in the impedances of the delta-network are approximated by first order polynomials. A new arithmetic is defined, where the higher order polynomials, resulting from the operations of the Gaussian elimination, are neglected. By preserving the first order coefficient of the polynomials, the Elmore time constants are preserved. The disadvantage of truncating the higher order polynomials might cause a loss of stability and passivity. The method in [49, 50] extends these ideas and includes higher order moments for handling RLC-networks. With these methods the reduction of networks with more than one type of element is possible.

A disadvantage of the Schur complement method and the Gaussian elimination of all internal nodes is that the sparsity in the unreduced system is not preserved. The reduced system is smaller in order, but contains typically full matrices, as the Schur complement is typically dense. Thus the number of nonzero elements can be higher, leading to models that need a higher computational effort in simulations. For the reduced network the disadvantage is the typically full-connected network, where the number of nodes is reduced, but the number of elements can be even higher. A method to overcome the disadvantage of dense matrices is a Cholesky or a LU decomposition, which can be used instead of the block Gaussian step [43, 51] for one-element type networks. By using these decompositions the sparsity of the system matrices can be preserved. Other methods for generating sparse reduced models are based on preserving some internal system variables or nodes for generating sparse matrices or networks respectively. In most methods the reduction of single nodes is performed until a specified criterion. The method presented in [52] is based on eliminating single nodes and stopping the algorithm if the number of branches is increasing. Another method, which produces sparse models and does not eliminate all internal nodes, but preserves a few 'important' internal nodes, is presented in [53]. The method is relying on graph and matrix reordering algorithms. The method in [44] is based on iterative reduction of nodes and is suitable for networks with more than one type of elements. The reduction is performed until a given maximum error, calculated as the sum of the errors made by neglecting the imaginary or real part of each branch, is exceeded. As in the former methods, in this reduction method not all internal nodes are eliminated and the algorithm stops at a given maximum error. The idea of eliminating not all internal nodes but preserving important nodes is also used in [54], where for every node an error is calculated if the node is removed. Afterwards only nodes introducing small errors are eliminated. In [55] only adjacent nodes connected by small resistances are eliminated, which defines another criterion. Another method for finding nodes that can be eliminated by Gaussian elimination is described in [56]. For every node a time constant is defined, given by the resistors and capacitors connected to it. Eliminating nodes with large or small time constants with the Gaussian algorithm leads to a reduced network. Thereby a reduction of networks is enabled, where not all internal nodes are eliminated, which can lead to small and sparse networks.

Overall the reduction methods based on Gaussian elimination are successfully used in the field

of layout extraction [44, 54–56]. Reciprocity of the reduced system or network is guaranteed, as only RLC elements, or coefficients representing these elements in the system description, are used. Stability and passivity are preserved in these reduction methods if only positive real valued elements in the network, or coefficients representing these elements in the system description, are used. Nevertheless, the methods based on Gaussian elimination have several disadvantages. Networks with only one type of element are quite successfully reduced, but the methods used therein are not applicable to arbitrary RLC-networks. For networks with more than one type of element an approximation error is introduced, which cannot be estimated nor controlled. Most of the methods for networks with more than one type of element are limited to special structures of the network and to RC-networks used in the layout modeling, and cannot be generalized to the whole class of RLC networks.

3.1.3 Modal Approximation Methods

The order reduction method based on modal approximation is presented in this section. Basically this reduction is developed in the field of control theory. The idea of reduction is based on the approximation of the relevant poles of the transfer function, or the relevant eigenvalues of the system matrices, respectively.

In control theory physical systems are modeled with linear ordinary differential equations

$$\begin{aligned} s\mathbf{x} &= \mathbf{A}\mathbf{x} + \mathbf{B}\mathbf{u} \\ \mathbf{y} &= \mathbf{C}\mathbf{x} \end{aligned} \quad (3.15)$$

with $\mathbf{A} \in \mathbb{R}^{N \times N}$ and $\mathbf{B}, \mathbf{C}^T \in \mathbb{R}^{N \times p}$, which is equal to a system of equations in the form of Eqn. 2.26 where $\mathbf{C} = \mathbf{I}$ holds. This system of equations typically has a large order N in the sense of a large number of equations and states \mathbf{x} . A system with a lower order in the same form

$$\begin{aligned} s\tilde{\mathbf{x}} &= \tilde{\mathbf{A}}\tilde{\mathbf{x}} + \tilde{\mathbf{B}}\mathbf{u} \\ \tilde{\mathbf{y}} &= \tilde{\mathbf{C}}\tilde{\mathbf{x}} \end{aligned} \quad (3.16)$$

with $\tilde{\mathbf{A}} \in \mathbb{R}^{n \times n}$ and $\tilde{\mathbf{B}}, \tilde{\mathbf{C}}^T \in \mathbb{R}^{n \times p}$ is generated by reducing the original system. The reduced system has a lower order n whereas the reduced matrix $\tilde{\mathbf{A}}$ has the same so-called 'dominant' eigenvalues and eigenvectors as the unreduced systems matrix \mathbf{A} [24].

The same method can be applied to the transfer function in the pole-residue form of Eqn. 2.35 with a large number of poles. For approximating the transfer behavior only a small fraction of the poles is necessary.

The main questions for this reduction are how to determine the number of dominant poles or eigenvalues necessary for a good approximation and how to distinguish between dominant and non-dominant poles or eigenvalues. For the first question the reduction is performed iteratively by starting with a low number of poles or eigenvalues and checking the accuracy of the reduced model. By adding more poles or eigenvalues the accuracy is improved. The process is stopped if the desired accuracy is achieved. For the second question, the definition of dominance of

poles or eigenvalues several approaches exist. For example, the distance of a pole of the transfer function, or a eigenvalue of the system matrix, from the origin or the imaginary axis [21] in the complex plane is used as criterion for the dominance. The assumption is that the shorter the distance from the origin the higher the impact on the system behavior. For the poles of the transfer function of the system in [25] for example, the corresponding absolute value of the residue $|r_m|$ of the transfer function is used as measure for the dominance. Another approach combining the values of pole and residue is used in several methods in [22–24], with the weighted absolute value of the residue divided by the (real) part of the pole for defining the dominance of a pole with $|r_m|/|p_m|$ or $|r_m|/|Re(p_m)|$. A graphical approach is based on the examination of the transfer function and definition of the poles near the modes as dominant ones. All approaches suffer from the disadvantage that with these criterions also poles that can have a substantial effect on the transfer behavior are not marked as dominant and therefore are neglected. Most of these methods are not able to detect structural non-minimality as shown in [26]. An improved method is presented in [26] where the Hankel Singular Values are used to distinguish between dominant and non-dominant eigenvalues.

The reduction method can now be formulated as follows. Compute the dominant eigenvalues and corresponding eigenvectors (or dominant poles and corresponding residues) for a given system (or transfer function) and form a reduced system (or transfer function) from this dominant part. Methods for finding this dominant part are called dominant pole algorithms (DPA). The most well-known DPA algorithm [25] calculates iteratively the dominant poles. The basic principle is presented in the following and is oriented on [25, 57]. Starting with a scalar transfer function $H(s)$ and its transpose

$$H(s) = \mathbf{c}^T (s\mathbf{I} - \mathbf{A})^{-1} \mathbf{b} = H^T(s) = \mathbf{b}^T (s\mathbf{I} - \mathbf{A})^{-T} \mathbf{c} \quad (3.17)$$

the system description can be written as

$$\begin{bmatrix} (s\mathbf{I} - \mathbf{A}) & -\mathbf{b} \\ \mathbf{c}^T & 0 \end{bmatrix} \begin{bmatrix} \mathbf{x}(s) \\ u(s) \end{bmatrix} = \begin{bmatrix} (s\mathbf{I} - \mathbf{A})^T & -\mathbf{c} \\ \mathbf{b}^T & 0 \end{bmatrix} \begin{bmatrix} \widehat{\mathbf{x}}(s) \\ u(s) \end{bmatrix} = \begin{bmatrix} \mathbf{0} \\ y(s) \end{bmatrix} \quad (3.18)$$

with the system vectors $\mathbf{x}, \widehat{\mathbf{x}}$ of the original and the transposed system, respectively. For s approaching a pole p_j , $s \rightarrow p_j$, the input tends to zero $u(s) \rightarrow 0$ for any finite value of the output $y(s)$, while the system vectors $\mathbf{x}, \widehat{\mathbf{x}}$ converge to the right and left eigenvectors $\mathbf{X}_r, \mathbf{X}_l$. With that, an iterative method for finding the poles is built. The output of the system is fixed at 1. An initial value s_k is defined, and the iteration process is started by solving the systems

$$\begin{bmatrix} (s_k\mathbf{I} - \mathbf{A}) & -\mathbf{b} \\ \mathbf{c}^T & 0 \end{bmatrix} \begin{bmatrix} \mathbf{x}(s_k) \\ u(s_k) \end{bmatrix} = \begin{bmatrix} \mathbf{0} \\ 1 \end{bmatrix} \quad (3.19)$$

and

$$\begin{bmatrix} (s_k\mathbf{I} - \mathbf{A})^T & -\mathbf{c} \\ \mathbf{b}^T & 0 \end{bmatrix} \begin{bmatrix} \widehat{\mathbf{x}}(s_k) \\ u(s_k) \end{bmatrix} = \begin{bmatrix} \mathbf{0} \\ 1 \end{bmatrix}. \quad (3.20)$$

By computing the new value s_{k+1} with

$$s_{k+1} = s_k + \frac{u(s_k)}{\widehat{\mathbf{x}}^T(s_k)\mathbf{x}(s_k)} \quad (3.21)$$

the systems (Eqn. 3.19 and Eqn. 3.20) are again solved for s_{k+1} . For every iteration step the input $u(s_k)$ converges to zero and the iteration stops if the change of the approximated pole $p_j = s_k$ is smaller than a given convergence tolerance. In addition, the right and left eigenvectors are given with $\mathbf{X}_r, \mathbf{X}_l$, having the eigenvectors $\mathbf{x}, \hat{\mathbf{x}}$ as columns. Extensions to this algorithm are presented in [58] by using multiple s_k as starting vector. For acceleration of the pole calculation subspace algorithms can be used as shown in [57].

If the dominant eigenvalues and eigenvectors are found, the reduced transfer function is built with

$$\tilde{H}(s) = \sum_{j=1}^n \frac{r_j}{s - p_j} \quad (3.22)$$

where the residue r_j is calculated using the eigenvectors with $r_j = (\mathbf{c}\mathbf{X}_r)(\mathbf{X}_l\mathbf{b})$. Similarly a reduced system can be defined with

$$\begin{aligned} s\tilde{\mathbf{x}} &= \mathbf{\Lambda}\tilde{\mathbf{x}} + (\mathbf{X}_l\mathbf{b})u \\ y &= (\mathbf{c}\mathbf{X}_r)\tilde{\mathbf{x}} \end{aligned} \quad (3.23)$$

where the diagonal matrix $\mathbf{\Lambda} = \text{diag}(p_1, \dots, p_n)$ contains the dominant poles [24, 59].

The order of the reduced transfer function, as well as the order of the reduced system, depends on the number of poles marked as dominant. Stability of the reduced system is preserved as long as only stable poles are used. Passivity is not preserved in the general case. For reducing system equations the method is limited to state space systems and cannot directly be used for the generalized state space system used in the network modeling. An extension to generalized state space systems is shown for example in [24], for several algorithms. Using the methods based on the modal approximation, system matrix properties such as (J-)symmetry, (semi-)definiteness, only real coefficients and the equality of the input and output system matrices are not preserved. The previously presented methods are suitable for scalar transfer functions only. In the case of systems with more than one input and output the transfer function is in matrix form. Extensions for a reduction of matrix transfer functions are presented in [60, 61]. Concluding, the methods based on modal approximation, and thereby preserving the dominant poles or eigenvalues of a system, have the advantage of good approximations over a broad frequency range. This, for example, is useful, due to the possible physical interpretation of the reduced model. Nevertheless, for systems or transfer functions of electrical networks most of the typical properties cannot be preserved.

3.1.4 Moment Matching Methods

In this section moment matching methods for model reduction are presented. Order reduction methods based on moment matching rely on the Maclaurin series expansion of a scalar transfer function at a frequency s_p

$$\hat{H}(s) = \sum_{j=0}^{\infty} M_j(s - s_p)^j \quad (3.24)$$

with the moments M_j . The series expansion of the transfer function approximates the original transfer functions magnitude and phase in a region around the expansion point s_p

$$\hat{H}(s) \approx H(s) \quad s_{low} \leq s \leq s_{high}. \quad (3.25)$$

A transfer function $\tilde{H}(s)$, with a reduced order in the sense of a reduced number of poles, is searched for in the model reduction process, fulfilling the requirement: The first moments of the reduced transfer function $\tilde{H}(s)$ should be equal or similar to the first moments of the original transfer function $H(s)$ in a region around s_p . If the first moments of the unreduced and the reduced transfer function are equal, the term 'the moments are matched' is used in the following. The methods can be divided into explicit and implicit moment matching methods and the methods for deriving a reduced model with matched moments are presented below.

The first explicit moment matching method is Asymptotic Waveform Evaluation (AWE) [62]. The AWE algorithm was motivated by the investigation of the timing properties in RC-networks modeling the interconnections in integrated circuits and printed circuit boards. AWE is based on explicit moment matching of a Padé-series expansion of a scalar transfer function. The reduction is done by considering only the first elements of the moment series expansion of Eqn. 3.24. The first n moments \tilde{M}_j of the reduced transfer function are matched with moments of the original transfer function

$$\begin{aligned} H(s) &\approx \tilde{H}(s) \\ M_j &= \tilde{M}_j \quad 0 \leq j \leq n-1. \end{aligned} \quad (3.26)$$

A Padé-Approximation of this finite series consists of the quotient of two polynomials $N(s)$ and $P(s)$

$$\begin{aligned} \tilde{H}(s) &= \frac{N(s)}{P(s)} \\ &= \frac{\sum_{j=0}^k n_j s^j}{1 + \sum_{j=1}^{k+1} p_j s^j} \\ &= \frac{n_p s^k + \dots + n_1 s + n_0}{p_{k+1} s^{k+1} + p_k s^k + \dots + k_1 s + 1} \end{aligned} \quad (3.27)$$

where $N(s)$ contains the zeros n_j and $P(s)$ the poles p_j of the transfer function $\tilde{H}(s)$. The moments of the original transfer function are calculated explicitly up to a specified order $n = 2k + 1$. By setting the Maclaurin series of the first moments equally to the Padé-Approximation the poles of the Padé-Approximation can be calculated directly by solving the system of equations

$$\begin{pmatrix} \mu_0 & \mu_1 & \cdots & \mu_k \\ \mu_1 & \mu_2 & \cdots & \mu_{k+1} \\ \vdots & \vdots & \ddots & \vdots \\ \mu_k & \mu_{k+1} & \cdots & \mu_{2k} \end{pmatrix} \begin{pmatrix} p_{k+1} \\ p_k \\ \vdots \\ p_1 \end{pmatrix} = - \begin{pmatrix} \mu_{k+1} \\ \mu_{k+2} \\ \vdots \\ \mu_{2k+1} \end{pmatrix} \quad (3.28)$$

and the zeros are obtained directly with

$$\begin{pmatrix} n_0 \\ n_1 \\ \vdots \\ n_k \end{pmatrix} = - \begin{pmatrix} \mu_0 & 0 & \cdots & 0 \\ \mu_1 & \mu_0 & \cdots & 0 \\ \vdots & \vdots & \ddots & \vdots \\ \mu_k & \mu_{k-1} & \cdots & \mu_0 \end{pmatrix} \begin{pmatrix} 1 \\ p_1 \\ \vdots \\ p_k \end{pmatrix}. \quad (3.29)$$

This leads to a reduced order transfer function, where the first n moments at a specified frequency are matched. Higher order moments are not matched and thus an approximation error is induced. In the first algorithms the moments are expanded at zero frequency $s_p = 0$. Methods using expansion points different from zero are for example described in [63, 64]. Stability is preserved in a reduced model by using only stable poles. Passivity cannot be preserved by explicit moment matching. The main problem in using explicit moment matching is in the numerical implementation. Typically, for a higher dimension of the matrices, the calculation of the coefficients of the polynomials gets ill conditioned. This results in inaccurate reduced models. Another disadvantage of the presented explicit moment matching is the limited applicability to SISO systems. Necessary extensions to MIMO systems are only possible with a high effort, as shown in [65–67].

Despite the explicit moment matching methods, with open issues in numerical robustness, the implicit moment matching methods arise. The order reduction based on implicit moment matching avoids the direct calculation of the moments. A solution to overcome the numerical ill-conditioned calculations is Padé Via Lanczos (PVL) [67, 68]. PVL is based on AWE but is numerically more stable. The Padé-Approximation is calculated with the help of the Lanczos-Algorithm. A disadvantage of PVL is that the stability of the system is only preserved for symmetric systems. Passivity of the system is not preserved in the general case.

For the further developed class of implicit moment matching the transfer function is written with the system matrices as

$$\begin{aligned} \mathbf{H}(s) &= \mathbf{L}^T (s\mathbf{C} + \mathbf{G})^{-1} \mathbf{B} \\ &= \mathbf{L}^T ((s - s_p)\mathbf{A} + \mathbf{I})^{-1} \mathbf{R} \end{aligned} \quad (3.30)$$

where

$$\mathbf{A} = -(s_p\mathbf{C} + \mathbf{G})^{-1} \mathbf{C} \quad (3.31)$$

$$\mathbf{R} = (s_p\mathbf{C} + \mathbf{G})^{-1} \mathbf{B}. \quad (3.32)$$

The moments of the matrix transfer function in a frequency point s_p are now defined by

$$\begin{aligned} \hat{\mathbf{H}}(s) &= \sum_{j=0}^{\infty} \mathbf{M}_j (s - s_p)^j \\ &= \sum_{j=0}^{\infty} \mathbf{L}^T \mathbf{A}^j \mathbf{R} (s - s_p)^j. \end{aligned} \quad (3.33)$$

The method is based on the Arnoldi algorithm for reducing \mathbf{A} into a small upper Hessenberg matrix \mathbf{H}_q . By generating the orthonormal basis \mathbf{T} of a Krylov subspace $\text{colsp}(\mathbf{T}) = \mathcal{K}_n(\mathbf{R}, \mathbf{A})$ with

$$\begin{aligned} \mathcal{K}_n(\mathbf{R}, \mathbf{A}) &= \mathcal{K}_n((s_p \mathbf{C} + \mathbf{G})^{-1} \mathbf{B}, (s_p \mathbf{C} + \mathbf{G})^{-1} \mathbf{C}) \\ &= (\mathbf{R}, \mathbf{A}\mathbf{R}, \dots, \mathbf{A}^n \mathbf{R}) \\ &= ((s_p \mathbf{C} + \mathbf{G})^{-1} \mathbf{B}, \dots, (-(s_p \mathbf{C} + \mathbf{G})^{-1} \mathbf{C})^n (s_p \mathbf{C} + \mathbf{G})^{-1} \mathbf{B}). \end{aligned} \quad (3.34)$$

the upper Hessenberg matrix $\mathbf{H}_q \in \mathbb{R}^{n \times n}$ is

$$\mathbf{H}_q = \mathbf{T}^T \mathbf{A} \mathbf{T}. \quad (3.35)$$

The system matrices of a reduced system of order n can now be defined with [69, 70]

$$\begin{aligned} \tilde{\mathbf{C}} &= \mathbf{H}_q \\ \tilde{\mathbf{G}} &= \mathbf{1} - s_p \mathbf{H}_q \\ \tilde{\mathbf{B}} &= \mathbf{T}^T \mathbf{B} \\ \tilde{\mathbf{L}} &= \mathbf{T}^T \mathbf{L} \end{aligned} \quad (3.36)$$

The upper Hessenberg matrix \mathbf{H}_q is used as the reduced matrix $\tilde{\mathbf{C}}$. For an expansion point equally zero $s_p = 0$ the reduced matrix $\tilde{\mathbf{G}}$ is equal the identity matrix and for expansion points different from zero the reduced system matrix $\tilde{\mathbf{G}}$ is calculated by the identity matrix shifted by the product of the s_p and \mathbf{H}_q . The reduced matrices $\tilde{\mathbf{B}}$ and $\tilde{\mathbf{L}}$ are generated by projection with \mathbf{T} . Again the first n moments of the reduced transfer function are matched with the original transfer function [70], but the algorithm avoids the direct computation of the moments.

Another variant for generation the reduced system matrices is proposed in [71, 72]. In this method the Arnoldi-algorithm is used to generate the projection matrix \mathbf{T} . In contrast to the generation of the reduced system matrices like in Eqn. 3.36 the matrices of the reduced order system of order n are all generated by projection with \mathbf{T} by

$$\begin{aligned} \tilde{\mathbf{C}} &= \mathbf{T}^T \mathbf{C} \mathbf{T} \\ \tilde{\mathbf{G}} &= \mathbf{T}^T \mathbf{G} \mathbf{T} \\ \tilde{\mathbf{B}} &= \mathbf{T}^T \mathbf{B} \\ \tilde{\mathbf{L}} &= \mathbf{T}^T \mathbf{L}. \end{aligned} \quad (3.37)$$

The (semi-)definiteness of \mathbf{C} , \mathbf{G} is preserved by using this projection. Thus, passivity can be also preserved in the reduced system. At the expansion point the first n moments of the reduced transfer function are matched with the moments of the original transfer function. In the presented methods the expansion point for the moment expansion can be any real or complex frequency. However, for the preservation of passivity only real points are allowed. An investigation of the influence of the choice of the expansion points on the approximation error is given

in [73]. A further extension of the reduction is achieved by using different expansion points. By adjoining the Krylov subspaces

$$\mathcal{K} = [\mathcal{K}_n^1, \mathcal{K}_n^2, \dots, \mathcal{K}_n^k] \quad (3.38)$$

a new basis for the reduction can be generated [74]. The basis \mathcal{K} generated in this way does not span a Krylov subspace anymore, but with an appropriate choice of the expansion points a higher precision of the reduced model can be achieved in a wider frequency range. The moments are not matched but approximated at the chosen frequency points [74].

In [75, 76] an algorithm is proposed, which preserves the block structure of the unreduced system matrices in the reduced system. This is done by splitting the projection matrix \mathbf{T} block diagonally into

$$\hat{\mathbf{T}} = \begin{pmatrix} \mathbf{T}_1 & \mathbf{0} \\ \mathbf{0} & \mathbf{T}_2 \end{pmatrix} \quad (3.39)$$

with block sizes corresponding to the system matrices blocks in Eqn. 2.16. The projection matrix $\hat{\mathbf{T}}$ does not span a Krylov subspace anymore, but contains the subspace [75]

$$\mathcal{K}_N = \text{span}\mathbf{T}_N \subseteq \text{span}\hat{\mathbf{T}}_N. \quad (3.40)$$

The reduced system is generated by projecting all system matrices with $\hat{\mathbf{T}}$ as in Eqn. 3.37. Due to the splitting the order of the reduced system is twice the order of the reduced system without splitting the projection matrix. Nevertheless, as shown in [75], the number of matched moments is doubled, which compensates the disadvantage of higher order.

Furthermore, not only the block structure of the system matrices can be preserved, but also the typical structure of \mathbf{B} , \mathbf{L} , containing only ones, minus ones and zeros, as shown in [77]. The system of equations is reordered in a way that all variables connected with a port are written in the upper part of the system equations. By reordering the columns accordingly, the (J-)symmetry of \mathbf{C} , \mathbf{G} is preserved. In the next step the projection matrix is split into three diagonal blocks

$$\hat{\mathbf{T}} = \begin{pmatrix} \mathbf{I} & \mathbf{0} & \mathbf{0} \\ \mathbf{0} & \mathbf{T}_1 & \mathbf{0} \\ \mathbf{0} & \mathbf{0} & \mathbf{T}_2 \end{pmatrix} \quad (3.41)$$

with the identity matrix having columns as much as the system has ports. With this projection the structure of the incidence matrices \mathbf{B} , \mathbf{L} is preserved at the cost of an higher order of the reduced system.

Methods dealing with the reduction of second order systems by using the basic algorithms of implicit moment matching, Krylov subspaces and the Arnoldi algorithm are presented for example in [78–80].

With implicit moment matching several disadvantages of explicit moment matching vanish. Firstly, the methods are numerically more robust, as, for example, the calculation of the transfer function and the moments is not necessary because the implicit moment matching methods can

work directly on the system matrices. Secondly, the extension to MIMO systems is quite simple.

Most properties of the system matrices can be preserved by using implicit moment matching. For real coefficients in the reduced system matrices, the parameter of the reduction have to be chosen properly by using real expansion points. The typical block structure of the system matrices can be preserved by splitting the projection matrix. This splitting is extended for the preservation of the incidence structure of the input and output system matrices \mathbf{B} , \mathbf{L} . The (J-)Symmetry of the system matrices \mathbf{C} , \mathbf{G} can be preserved by using the projection of each system matrix. With this method, the (semi-)definiteness of the system matrices \mathbf{C} , \mathbf{G} can also be preserved. Preserving J-symmetry and (semi-)definiteness together is more crucial and is only possible by using the split projection matrices and projection of each system matrix. Sparsity of the system matrices is not preserved, as typically the projection matrix \mathbf{T} is dense. Concluding, most of the important properties of the system matrices can be preserved by using adapted methods.

An overview of preservable system properties by using implicit moment matching is given in this paragraph. If the reduction methods are applied to systems or transfer functions of circuits, the stability can be preserved with most of the methods. Passivity is more crucial. Only the algorithms based on the projection of each system matrix can guarantee a passive reduced system for suitably described original systems and reduction parameters. For positive (semi-)definite system matrices of the original system the passivity can be preserved by preserving the positive (semi-)definiteness in the reduced system matrices. In addition a method is presented in [81], where by the use of projection methods, even active or unstable systems can be reduced to stable and passive reduced order systems. The reciprocity of systems with at least two ports cannot be preserved in the general case. One solution is motivated by preserving the (J-)symmetry of the system matrices \mathbf{C} , \mathbf{G} by splitting the projection matrices, which gives a reciprocal system with $\mathbf{B} = \mathbf{L}$. By using the projection with the split matrices, (J-)symmetry of the system matrices and thereby the reciprocity can be preserved. Overall most of the system properties can be preserved in the reduced model by using appropriate implicit moment matching methods.

3.1.5 Gramian-based Methods

Based on the controllability and observability of the states of a system, a group of algorithms for order reduction was developed in the area of control theory [82]. The states of a system in state space form

$$\begin{aligned} \dot{\mathbf{x}} &= \mathbf{A}\mathbf{x} + \mathbf{B}\mathbf{u} \\ \mathbf{y} &= \mathbf{C}\mathbf{x} + \mathbf{D}\mathbf{u}. \end{aligned} \tag{3.42}$$

are divided into high and low controllable and observable states. The high controllable and observable states are the so-called strong system part. States that are either low controllable or observable are called weak system part. The reduction method is based on the truncation of weak system parts. The reduced system contains only the strong system part.

To enable such a truncation the system has to be balanced. For balancing, the generalized state space system (Eqn. 2.26) has to be transformed into the state space form. The most widely

used method for balancing the system is based on the Lyapunov equations. The controllability Gramian

$$\mathbf{P} = \int_0^{\infty} \exp^{\mathbf{A}t} \mathbf{B}\mathbf{B}^* \exp^{\mathbf{A}^*t} dt \quad (3.43)$$

as well as the observability Gramian

$$\mathbf{Q} = \int_0^{\infty} \exp^{\mathbf{A}t} \mathbf{C}\mathbf{C}^* \exp^{\mathbf{A}^*t} dt \quad (3.44)$$

are used for balancing the system. The Gramians are the unique, symmetric and positive (semi-)definite solutions of the Lyapunov equations

$$\begin{aligned} \mathbf{A}\mathbf{P} + \mathbf{P}\mathbf{A}^* &= -\mathbf{B}\mathbf{B}^* \\ \mathbf{A}^*\mathbf{Q} + \mathbf{Q}\mathbf{A} &= -\mathbf{C}^*\mathbf{C}. \end{aligned} \quad (3.45)$$

A system is called balanced if controllability and observability Gramian are equal $\mathbf{P} = \mathbf{Q}$. For balancing the observability Gramian is decomposed with Cholesky-decomposition into

$$\mathbf{P} = \mathbf{R}\mathbf{R}^T, \quad (3.46)$$

$\mathbf{R} \in \mathbb{R}^{N \times N}$, and with singular value decomposition

$$\mathbf{R}\mathbf{Q}\mathbf{R}^T = \mathbf{U}^T \Sigma^2 \mathbf{U} \quad (3.47)$$

the transformation matrix

$$\mathbf{T} = \mathbf{R}^T \mathbf{U}^T \Sigma^{-1/2} \quad (3.48)$$

and its inverse

$$\mathbf{T}^{-1} = \Sigma^{1/2} \mathbf{U} \mathbf{R}^{-1} \quad (3.49)$$

are obtained. With the transformation matrix \mathbf{T} , the Gramians of the balanced system

$$\begin{aligned} \mathbf{P}_{balanced} &= \mathbf{T}^{-1} \mathbf{P} \mathbf{T}^* = \Sigma \\ \mathbf{Q}_{balanced} &= \mathbf{T}^* \mathbf{Q} \mathbf{T} = \Sigma \end{aligned} \quad (3.50)$$

can be calculated. The system associated to the balanced Gramians is built with the projection of the system matrices with \mathbf{T}

$$\begin{aligned} \mathbf{A}_{balanced} &= \mathbf{T}^{-1} \mathbf{A} \mathbf{T} \\ \mathbf{B}_{balanced} &= \mathbf{T}^{-1} \mathbf{B} \\ \mathbf{C}_{balanced} &= \mathbf{C} \mathbf{T} \\ \mathbf{D}_{balanced} &= \mathbf{D}. \end{aligned} \quad (3.51)$$

Note that this system in balanced form is not reduced in order and the input-output behavior is equal to the original unbalanced system. For reduction the weak system part has to be identified. This is done according to the Hankel singular values (HSV) σ on the diagonal of Σ . A large absolute value of a HSV signalizes a strong part of the system. Therefore, the HSV can be divided into two groups, strong and weak HSV, depending on their absolute values

$$\Sigma = \begin{pmatrix} \Sigma_{strong} & 0 \\ 0 & \Sigma_{weak} \end{pmatrix}. \quad (3.52)$$

With the same partitioning the system matrices can be divided into

$$\begin{aligned} \mathbf{A}_{balanced} &= \begin{pmatrix} \mathbf{A}_{strong} & \mathbf{A}_{coupling-ws} \\ \mathbf{A}_{coupling-sw} & \mathbf{A}_{weak} \end{pmatrix} \\ \mathbf{B}_{balanced} &= \begin{pmatrix} \mathbf{B}_{strong} \\ \mathbf{B}_{weak} \end{pmatrix} \\ \mathbf{C}_{balanced} &= (\mathbf{C}_{strong} \quad \mathbf{C}_{weak}) \end{aligned} \quad (3.53)$$

where only the strong part of the system, associated to the large singular values, composes the reduced system

$$\begin{aligned} s\tilde{\mathbf{x}} &= \mathbf{A}_{strong}\tilde{\mathbf{x}} + \mathbf{B}_{strong}\mathbf{u} \\ \tilde{\mathbf{y}} &= \mathbf{C}_{strong}\tilde{\mathbf{x}} + \mathbf{D}\mathbf{u}. \end{aligned} \quad (3.54)$$

The most outstanding advantage of this reduction method is that a global approximation error bound is calculable by the use of the HSV prior to the reduction itself. The maximum approximation error of the transfer function in frequency domain is defined in the \mathbb{H}_∞ norm and obtained by the neglected HSV with [83, 84]

$$\|\tilde{\mathbf{H}} - \mathbf{H}\|_{\mathbb{H}_\infty} \leq 2 \sum_{j=N-n+1}^N \sigma_j. \quad (3.55)$$

By application of the reduction method to several examples it was observed that the approximation error is very low in the high frequency range, but quite high at low frequencies and at DC [84]. The major drawback of the reduction by balancing and truncation is the high computational effort for solving the Lyapunov equations. In addition, the conversion of the generalized state space equations of networks into state space form can be numerically crucial or even impossible. Thus extensions for the basic order reduction method exist. For example, a solution, which allows for the reduction of generalized state space systems, is presented in [85, 86]. A method, which generates iteratively an approximately balanced system, is presented in [87], lowering the computational effort. To overcome the bad approximation at low frequencies, a weighted frequencies method is presented in [84] at the high cost of loss of the calculable error bound. Another method for reducing the approximation error at low frequencies is based on singular perturbation methods on the balanced system [88, 89].

For the preservation of system properties of models describing electrical networks several conclusions are drawn in the following. The system matrices contain only real coefficients by

using the Gramian-based reduction method. Therefore, the property of only real coefficients in the system matrices is preserved. The properties of (J-)symmetry, (semi-)definiteness, sparsity and diagonal dominance of the system matrices are not preserved. In addition, the block structure of the system matrices is lost in the reduced model. Advantageous of this method is that the reduced model is balanced and minimal. Stability of the model is preserved with this reduction method, but passivity is not preserved in the general case. Although, by using adapted methods, the passivity, and also reciprocity, can be preserved [90].

Worth mentioning is the Poor Man's TBR (PMTBR) method [91], which is a model reduction algorithm motivated by a connection between projection methods in implicit moment matching and Gramian-based methods. The PMTBR algorithm is based on the fact that the controllability Gramian

$$\mathbf{P} = \int_{-\infty}^{\infty} (j\omega\mathbf{C} + \mathbf{G})^{-1}\mathbf{B}\mathbf{B}^T(j\omega\mathbf{C} + \mathbf{G})^{-H} d\omega \quad (3.56)$$

under the assumption $\mathbf{B} = \mathbf{L}$ can be approximated by $\hat{\mathbf{P}}$ with

$$\begin{aligned} \hat{\mathbf{P}} &= \sum_k \omega_k \mathbf{z}_k \mathbf{z}_k^H \\ &= \mathbf{Z}\mathbf{W}^2\mathbf{Z}^H \end{aligned} \quad (3.57)$$

by applying numerical quadrature. \mathbf{Z} is a matrix defined with

$$\mathbf{z}_k = (j\omega_k\mathbf{C} + \mathbf{G})^{-1}\mathbf{B} \quad (3.58)$$

and \mathbf{W} is a diagonal matrix with the square root of the weights of the quadrature scheme as diagonal entries. The projection matrix \mathbf{T}_L can be obtained by factorization of the Gramian

$$\mathbf{P} = \mathbf{T}_L \sum \mathbf{T}_L^T. \quad (3.59)$$

If the quadrature rule is accurate $\hat{\mathbf{P}}$ will converge to the Gramian \mathbf{P} . Considering the singular value decomposition of $\mathbf{Z}\mathbf{W}$

$$\mathbf{Z}\mathbf{W} = \mathbf{T}_Z \mathbf{S}_Z \mathbf{U}_Z \quad (3.60)$$

with real diagonal matrix \mathbf{S}_Z and unitary matrices $\mathbf{T}_Z, \mathbf{U}_Z$, which leads to

$$\hat{\mathbf{P}} = \mathbf{T}_Z \mathbf{S}_Z^2 \mathbf{T}_Z^T. \quad (3.61)$$

The singular vectors \mathbf{T}_Z converge to the eigenvectors \mathbf{T}_L and can be used as projection matrix in the model reduction algorithm. Approximations to the Hankel singular values can now be directly obtained from \mathbf{S}_Z . The approximation error can be obtained from the singular values of \mathbf{Z} , in fact the singular value decomposition of \mathbf{Z} leads to the same information as revealed by the Gramian-based methods. In [91] it is shown that even for a small number of expansion points $j\omega_k$ the matrix $\hat{\mathbf{P}}$ will converge to the Gramian \mathbf{P} . With that, a small number of expansion points will lead to singular vectors \mathbf{T}_Z , which can be used as projection matrix

for an order reduction. The singular values \mathbf{S}_Z can be interpreted as gains between the filtered inputs and weighted outputs of the system [91]. The truncated singular values thus provide an approximate error bound of the reduced model. This can be used as a guide for choosing the reduced systems order. Choosing an appropriate estimated error, the matrix \mathbf{T}_Z is subdivided

$$\mathbf{T}_Z = [\mathbf{T}_{Z1} \quad \mathbf{T}_{Z2}] \quad (3.62)$$

according to the magnitude of the singular values. In the next step the projection matrix \mathbf{T}_{Z1} is used for projecting the system matrices for order reduction. The main advantage of this method is the low computational effort for the reduction. If the expansion points are chosen at purely real frequencies, the projection matrix is real and (J-)symmetry and (semi-)definiteness of the system matrices can be preserved during reduction by using the methods of the implicit moment matching reduction. Thus the stability, passivity and reciprocity of the model can be preserved in this Gramian-based reduction by utilizing the extensions used in the implicit moment matching reduction.

3.1.6 Interpolation Methods

A class of methods used for order reduction is based on the modeling process from measured or calculated input/output data. The system behavior is modeled with interpolation methods. In this modeling process the internal variables and underlying physical properties are either unknown or not taken into account, which also leads to the nomenclature of black box modeling. From the observed input/output behavior a model is created, which can be used in simulations for investigations and predictions of the model behavior [92, 93].

Already in the fifties of the last century black box modeling methods are used for simplification of electrical networks. In the field of power flow studies of overhead lines, the highly complex lines, which are impossible to model directly, are modeled by black box methods [94]. By taking measurements at specified nodes, a simplified circuit model is obtained. The measurements are taken at DC and the measured values are satisfying the rough necessary accuracy of the power network model. Nevertheless, this approach was quite ad hoc and more sophisticated methods, modeling a network not only at DC but in a certain frequency range, were developed over the years.

Even if the underlying original model is known in part or completely, the black box methods can be used to describe a high order model by its input/output behavior. This behavior is afterwards described with a low order model. The low order model interpolates the behavior of the high order model in several selected points of the transfer function. Thus these methods can be used as an order reduction algorithm.

One of the most well-known methods of approximating points of data with a continuous function is curve fitting, presented in [92]. The transfer function approximates the given data with a rational transfer function

$$H(s) = \frac{N(s)}{D(s)} \quad (3.63)$$

in a frequency range specified by the measured or simulated data set. The numerator $N(s)$ and the denominator $D(s)$ can be chosen for example as rational fraction [93]

$$N(s) = \sum_{i=0}^n a_i s^i \quad (3.64)$$

$$D(s) = \sum_{i=0}^n b_i s^i \quad (3.65)$$

or as partial fraction function [95]

$$N(s) = \sum_{i=1}^n \frac{r_{n_i}}{s + p_{n_i}} \quad (3.66)$$

$$D(s) = 1 + \sum_{i=1}^n \frac{r_{d_i}}{s + p_{d_i}} \quad (3.67)$$

or any other preferably orthogonal or orthonormal basis function [96–98]. The order n of the transfer function is chosen to be much smaller than the order of the original system to enable an order reduction. The goal of the reduction process is to find the coefficients of the transfer function for which the data set is well approximated. The basic principle for this approximation is based on the non-linear optimization methods [99, 100] or linearization of the problem and optimizing the linear problem [93]. An extension of the curve fitting approach to matrix transfer functions, and hence systems with many inputs and outputs or systems with additional parameters is proposed in [101–104]. The main hurdle is the optimization algorithm for estimation of the coefficients of the transfer function. Much research is still going on in the field of fast, stable and reliable algorithms for optimizing the accuracy of the approximating transfer function, see [105] and references therein. Another drawback is that the created models are not passive in the general case. Post-processing steps with passivation of the system are necessary. Passivation methods are for example presented in [106–109]. Another approach for the generation of a passive system is presented in [110] by creating passive models during optimization. The reciprocity of the generated reduced order model can, for example, be guaranteed during optimization by forcing the transfer function to be (J-)symmetric.

A method overcoming the drawback of the optimization algorithms necessary for curve fitting is the interpolation with the Loewner matrix [105, 111, 112]. Instead of specific input signals, the left and right input directions $\mathbf{d}_l, \mathbf{d}_r$ in a frequency point s_l or s_r defined with

$$\begin{aligned} \mathbf{d}_{l_i}^T \mathbf{H}(s_{l_i}) &= \mathbf{y}_{l_i}^T \\ \mathbf{H}(s_{r_i}) \mathbf{d}_{r_i} &= \mathbf{y}_{r_i} \\ 1 \leq i \leq n \end{aligned} \quad (3.68)$$

are used. The n values $\mathbf{y}_{l_i}^T, \mathbf{y}_{r_i}$ are simulated or measured by using the original model. The system matrices are given directly from these values. The reduced system matrix $\tilde{\mathbf{C}}$ is given by

the Loewner matrix [113]

$$\tilde{\mathbf{C}} = - \begin{pmatrix} \frac{\mathbf{y}_{l_1}^T \mathbf{d}_{r_1} - \mathbf{d}_{l_1}^T \mathbf{y}_{r_1}}{s_{l_1} - s_{r_1}} & \cdots & \frac{\mathbf{y}_{l_1}^T \mathbf{d}_{r_n} - \mathbf{d}_{l_1}^T \mathbf{y}_{r_n}}{s_{l_1} - s_{r_n}} \\ \vdots & \ddots & \vdots \\ \frac{\mathbf{y}_{l_n}^T \mathbf{d}_{r_1} - \mathbf{d}_{l_n}^T \mathbf{y}_{r_1}}{s_{l_n} - s_{r_1}} & \cdots & \frac{\mathbf{y}_{l_n}^T \mathbf{d}_{r_n} - \mathbf{d}_{l_n}^T \mathbf{y}_{r_n}}{s_{l_n} - s_{r_n}} \end{pmatrix}, \quad (3.69)$$

the reduced system matrix $\tilde{\mathbf{G}}$ by the shifted Loewner matrix [114]

$$\tilde{\mathbf{G}} = \begin{pmatrix} \frac{s_{l_1} \mathbf{y}_{l_1}^T \mathbf{d}_{r_1} - s_{r_1} \mathbf{d}_{l_1}^T \mathbf{y}_{r_1}}{s_{l_1} - s_{r_1}} & \cdots & \frac{s_{l_1} \mathbf{y}_{l_1}^T \mathbf{d}_{r_n} - s_{r_n} \mathbf{d}_{l_1}^T \mathbf{y}_{r_n}}{s_{l_1} - s_{r_n}} \\ \vdots & \ddots & \vdots \\ \frac{s_{l_n} \mathbf{y}_{l_n}^T \mathbf{d}_{r_1} - s_{r_1} \mathbf{d}_{l_n}^T \mathbf{y}_{r_1}}{s_{l_n} - s_{r_1}} & \cdots & \frac{s_{l_n} \mathbf{y}_{l_n}^T \mathbf{d}_{r_n} - s_{r_n} \mathbf{d}_{l_n}^T \mathbf{y}_{r_n}}{s_{l_n} - s_{r_n}} \end{pmatrix} \quad (3.70)$$

and the reduced system matrices $\tilde{\mathbf{B}}, \tilde{\mathbf{L}}$ by the measurement or simulation results

$$\tilde{\mathbf{B}} = \begin{pmatrix} \mathbf{y}_{l_1}^T \\ \mathbf{y}_{l_2}^T \\ \vdots \\ \mathbf{y}_{l_n}^T \end{pmatrix} \quad \tilde{\mathbf{L}} = \begin{pmatrix} \mathbf{y}_{r_1} & \mathbf{y}_{r_2} & \cdots & \mathbf{y}_{r_n} \end{pmatrix}. \quad (3.71)$$

The advantage of this method is that no calculations are necessary, and hence neither iterations nor convergence problems can occur. A minimal generalized state space system is derived directly from the measured or simulated data. The order of the generated system depends on the rank of

$$\text{rank}(s\tilde{\mathbf{C}} + \tilde{\mathbf{G}}) = \text{rank}(\tilde{\mathbf{C}}\tilde{\mathbf{G}}) = \text{rank} \begin{pmatrix} \tilde{\mathbf{C}} \\ \tilde{\mathbf{G}} \end{pmatrix} = n \quad (3.72)$$

and equals the number of measured or simulated data values n if the above conditions have full rank. Otherwise a truncated realization by using for example an SVD can be applied. If the knowledge of the original unreduced system is taken into account, with dominant pole algorithms [25] the most dominant poles of the transfer function can be found and used for the measured frequencies s_l, s_r . Thus a higher reduction with improved accuracy can be achieved. A disadvantage of the approach based on the Loewner matrix is that the typical block structure of the system matrices is not existent. In addition the resulting system matrices can contain complex values, which can be avoided by using only real frequency points for the interpolation. Another disadvantage is that the system is neither stable nor passive. By stabilization and passivation of the system using a mirror array as proposed in [105, 112] this issue can be solved.

3.1.7 Comparison

Several methods for the order reduction of networks, systems of networks and transfer functions describing networks were presented in the former sections. The applicability of the methods for networks and the preservation of important properties was investigated. In this section, concluding remarks for the reduction of networks using the presented methods are given.

The methods reducing the network directly are mainly limited to networks where the structure is simple, several series or parallel connections can be merged or networks where very large as well as very small element values are used. Most often the models that are to be reduced are more complex and require more sophisticated methods. The Gaussian elimination in its original form is limited to networks with only one type of element. Extensions to networks with different types of elements are presented, but are still limited to a class of networks with a special structure. Gaussian elimination methods are only used for one type of element networks, built in IC substrate modeling or for networks with special structures built in the IC layout extraction. Nevertheless, the application to more complex networks is still under investigation. Modal approximation, based on algorithms for finding dominant poles of systems, is used if the preservation of some of the poles is necessary. The disadvantage of this method is in losing almost all system properties of the original networks system. More efficient are the methods based on moment matching, because not the location of the poles is approximated, but the complete transfer behavior is taken into account. The moment matching methods are the most widely used methods for the reduction of networks, due to their simplicity, efficiency and adaptability. Their main disadvantage is that neither error estimation nor control is available and the reduction parameters are often chosen manually. Therefore, the Gramian-based methods are of increased interest. Based on control theory methods, their main advantage is the estimation and control of the error of the reduced system. The main disadvantages are a higher necessary effort for the reduction as well as a lower adaptability to systems of electrical networks. These disadvantages are actually under investigation and vanish more and more. The class of interpolation methods, mainly built for systems where the underlying model is unknown, is able to provide an alternative to the reduction methods, based on the knowledge of the internal structure of the model. Nevertheless, these methods suffer from the disadvantage of neglecting knowledge that can be helpful for finding an efficient reduced model.

The preservation of properties of systems and transfer functions of networks in a reduced model is depicted in this paragraph. Concluding for the properties, most order reduction algorithms are able to preserve stability. Passivity is more crucial, but algorithms, based on direct network manipulation and Gaussian elimination, are able to preserve passivity. For the methods based on modal approximation, moment matching and the Gramians, several extensions exist with which passivity can be preserved. Nevertheless, due to numerical issues, the reduced systems can be active, which in this case leads to the necessity of an additional passivation step. For most of the interpolation methods an additional passivation step is necessary after the order reduction, resulting in passive reduced systems. For reduction methods that are capable of reducing systems of networks with more than one port, the reciprocity preservation is of interest. The methods, directly manipulating the network as well as the Gaussian elimination, preserve reciprocity by construction. By using adapted methods, the preservation of reciprocity is also possible in the moment matching as well as the Gramian-based methods. For the modal approximation as well as the interpolation methods boundary conditions for the generation of the reduced model are necessary for generating a reciprocal reduced model.

The preservation of typical properties of system matrices describing a network, as well as their transfer functions, are investigated in this paragraph. Firstly, the reduction of differential algebraic equations of generalized state space systems instead of ordinary differential equations

of state space system is possible with almost all methods. The moment matching methods are explicitly suitable for DAE systems, while for the modal approximation and the Gramian-based methods several extensions exist to incorporate DAE's. For the interpolation methods the structure of the original system is not of interest, as they are based on simulated or measured input-output relations. Secondly, the use of only real coefficients is preserved in the system matrices by using direct network manipulations, Gaussian elimination and Gramian-based methods. By a proper choice of reduction parameters in the moment matching and interpolation methods the real coefficients can be as well preserved. For the modal approximation, complex coefficients in the reduced models system equations can occur, due to complex poles used as coefficients. Definiteness of the system matrices is preserved by construction in direct network manipulation and Gaussian elimination methods. By using suitable projection methods, the (semi-)definiteness can also be preserved with moment matching methods. More complicated, or even impossible, is the preservation of (semi-)definiteness if reduction methods based on modal approximation, the Gramians and interpolation are used. The J-symmetry, as well as the block structure of the system matrices, can only be preserved by using adapted moment matching methods. Sparsity can be preserved by using Gaussian elimination and a stop criterion for the reduction, if the density of the matrices increases above a given level. The reduced models with modal approximation are sparse, as the system matrix is diagonal, having the poles on the main diagonal. Sparsity is not preserved by using moment matching, Gramian-based methods and interpolation methods.

If methods are used, which generate stable, passive and reciprocal reduced models, the properties of the transfer function are most often preserved in the reduced transfer function. Thus the statements of the former paragraph, regarding the reduction properties of the several algorithms, also apply to the properties of the transfer function.

3.1.8 Illustrative Numerical Example

In this section the network of Sec. 2.4 is reduced for illustration purpose. Reduction methods based on the system equations describing the network are used to obtain a reduced order model. Because of the possible preservation of several properties of systems describing networks, the implicit moment matching, with projection of the system equations, will be illustrated.

The system equations (Eqn. 2.53) of order $N = 3$ of the example network (Fig. 2.2)

$$\left[s \begin{array}{c} \mathbf{C} \\ \left(\begin{array}{ccc} 1 & 0 & 0 \\ 0 & 1 & 0 \\ 0 & 0 & 1 \end{array} \right) + \mathbf{G} \\ \left(\begin{array}{ccc} 2 & -1 & 0 \\ -1 & 3 & -1 \\ 0 & -1 & 2 \end{array} \right) \end{array} \right] \begin{array}{c} \mathbf{x} \\ \left(\begin{array}{c} \phi_{n1} \\ \phi_{n2} \\ \phi_{n3} \end{array} \right) \end{array} = \begin{array}{c} \mathbf{B} \\ \left(\begin{array}{c} 1 \\ 0 \\ 0 \end{array} \right) \end{array} \underbrace{\left(\begin{array}{c} \mathbf{u} \\ i_p \end{array} \right)}_{\mathbf{u}}$$

$$\underbrace{\left(\begin{array}{c} u_p \\ \mathbf{y} \end{array} \right)}_{\mathbf{y}} = \underbrace{\left(\begin{array}{ccc} 1 & 0 & 0 \end{array} \right)}_{\mathbf{L}^T} \underbrace{\left(\begin{array}{c} \phi_{n1} \\ \phi_{n2} \\ \phi_{n3} \end{array} \right)}_{\mathbf{x}} \quad (3.73)$$

are to be reduced with order reduction. From 10^{-5} Hz to 10^5 Hz the transfer behavior at the port is to be approximated by a reduced model. Due to the simplicity of the transfer function only a first order Krylov subspace \mathcal{K} in one real expansion point $s_p = 0.1$ is built, which leads to

$$\mathcal{K} = (s_p \mathbf{C} + \mathbf{G})^{-1} \mathbf{B} \approx \begin{pmatrix} 0.5818 \\ 0.2217 \\ 0.1056 \end{pmatrix} \quad (3.74)$$

for the network. With QR-decomposition an orthogonal projection matrix \mathbf{T} is obtained

$$\mathbf{T} \approx \begin{pmatrix} -0.9213 \\ -0.3511 \\ -0.1672 \end{pmatrix}. \quad (3.75)$$

By projection the reduced system matrices of order $n = 1$ are given

$$\begin{aligned} \tilde{\mathbf{C}} &= \mathbf{T}^T \mathbf{C} \mathbf{T} = 1 \\ \tilde{\mathbf{G}} &= \mathbf{T}^T \mathbf{G} \mathbf{T} \approx 1.3589 \\ \tilde{\mathbf{B}} &= \mathbf{T}^T \mathbf{B} \approx -0.9213 \\ \tilde{\mathbf{L}} &= \mathbf{T}^T \mathbf{L} \approx -0.9213. \end{aligned} \quad (3.76)$$

and the resulting reduced order system is

$$\begin{aligned} \left[s \underbrace{\tilde{\mathbf{C}}}_{(1)} + \underbrace{\tilde{\mathbf{G}}}_{(1.3589)} \right] \underbrace{\tilde{\mathbf{x}}}_{(\tilde{\phi}_{n1})} &= \underbrace{\tilde{\mathbf{B}}}_{(-0.9213)} \underbrace{\mathbf{u}}_{(i_p)} \\ \underbrace{(u_p)}_{\tilde{\mathbf{y}}} &= \underbrace{(-0.9213)}_{\tilde{\mathbf{L}}^T} \underbrace{(\tilde{\phi}_{n1})}_{\tilde{\mathbf{x}}} \end{aligned} \quad (3.77)$$

The reduced order system matrices are still real, as the expansion point in the reduction is chosen as a real frequency point. Also the system matrices $\tilde{\mathbf{C}}$, $\tilde{\mathbf{G}}$ are still positive definite and $\tilde{\mathbf{B}} = \tilde{\mathbf{L}}$ holds as in the unreduced system. The reduced order transfer function is computed with

$$\tilde{Z}_{s_p=0.1}(s) \approx \frac{0.8488}{s + 1.3589}. \quad (3.78)$$

The reduced order system has only one real pole at $p_1 \approx -1.3589$, while the unreduced system is described with three poles.

For comparison, the expansion point is chosen at a higher frequency of $s_p = 10$, and the reduced system is obtained with

$$\begin{aligned} \left[s \underbrace{\tilde{\mathbf{C}}}_{(1)} + \underbrace{\tilde{\mathbf{G}}}_{(1.8511)} \right] \underbrace{\tilde{\mathbf{x}}}_{(\tilde{\phi}_{n1})} &= \underbrace{\tilde{\mathbf{B}}}_{(-0.9970)} \underbrace{\mathbf{u}}_{(i_p)} \\ \underbrace{(u_p)}_{\tilde{\mathbf{y}}} &= \underbrace{(-0.9970)}_{\tilde{\mathbf{L}}^T} \underbrace{(\tilde{\phi}_{n1})}_{\tilde{\mathbf{x}}} \end{aligned} \quad (3.79)$$

and the transfer function is given with one pole at $p_1 \approx -1.8511$

$$\tilde{Z}_{s_p=10}(s) \approx \frac{0.9940}{s + 1.8511}. \quad (3.80)$$

The transfer functions of the unreduced and the reduced systems as well as the approximation errors due to model reduction are shown in Fig. 3.2 and Fig. 3.3. The results validate the good approximation. The reduced system, with an expansion point at $s_p = 0.1$, shows a good accuracy in the low frequency range. The reduced system, with the expansion point at a higher frequency $s_p = 10$, is accurate in the high frequency range, but shows a worse accuracy in the low frequency range. This shows that the accuracy in specific frequency ranges can be adjusted with the choice of the expansion points.

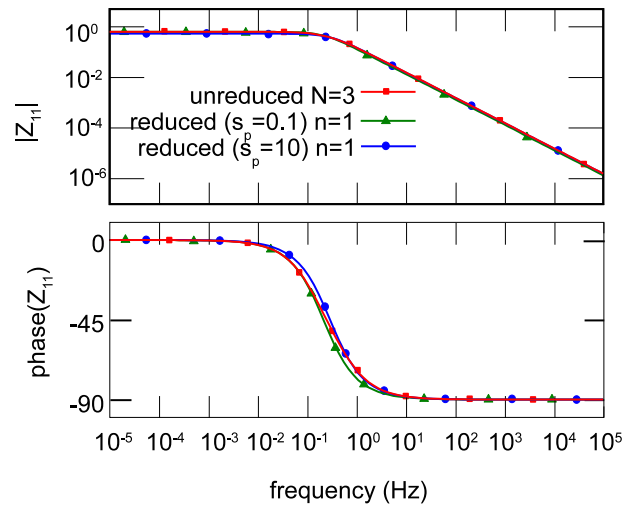


Figure 3.2: Illustrative example transfer function $Z_{1,1}$ of the original and the moment matching reduced models

With this example an order reduction is illustrated. A system description of a network of order $N = 3$ is reduced to an order of $n = 1$, while the behavior at the port of the network is approximated.

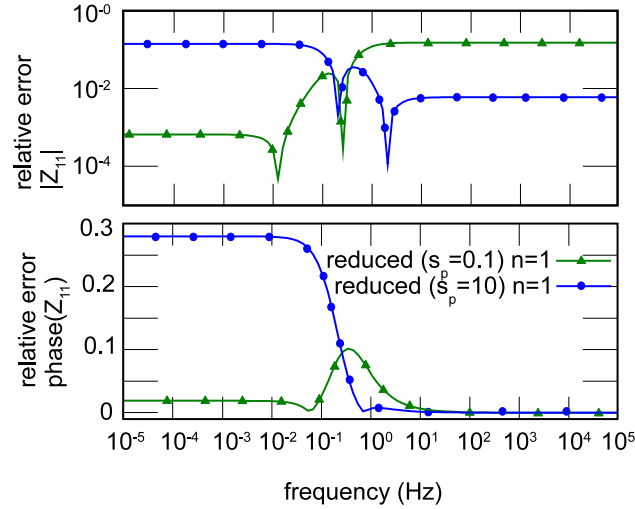


Figure 3.3: Relative approximation error of the transfer function $Z_{1,1}$ of the moment matching reduced models

3.2 Network Synthesis

For the simulation of reduced order models in standard simulation environments electrical networks are preferred. For the reduction algorithms reducing the network directly (Sec. 3.1.1 and several algorithms of Sec. 3.1.2), the resulting reduced model is still an electrical network. For order reduction algorithms dealing with the mathematical description of the network, either in transfer function or in system equations form, a translation of the order reduced model into an electrical network is necessary. This translation from the reduced mathematical description into a network realization is called synthesis in the following. The transfer function is assumed to be reduced in the sense that the number of poles is lowered. If the reduction method is applied on the system description, the number of equations is assumed to be reduced. For both types of order reduced models, network synthesis algorithms are required in the model reduction process and are described in the following sections.

3.2.1 Transfer Function Synthesis

For the generation of an electrical network from a reduced order transfer function several methods are developed in the field of filter synthesis. In filter synthesis an electrical filter is to be built from a transfer function generated from given specifications. This task is inverse to the analysis of electrical networks. Pioneering work in this field is done by Cauer [27] and Foster [115], for two types of elements networks, and by Brune for RLC networks [28]. In the beginning, the filter synthesis methods mainly dealt with nondissipative networks. The main goal of the synthesis methods in the field of filter synthesis is physical realizability. Thus the synthesized network has to be built only from positive real valued elements, has to have a low sensitivity to parameter variations and has to contain only a low number of elements.

For a reduced order transfer function the boundary conditions for the synthesis of an electrical network model are somewhat different. The goal is a fast and efficient simulation of the synthesized network. As long as the complete model is passive, ensuring stable simulations, negative element values are allowed in several simulation environments. In addition, elements like controlled sources can be used. As the simulations are performed for nominal values, the numerical stability during the simulation process is more important than low sensitivity to parameter fluctuations. A low number of elements, as preferred in the filter synthesis, is as well a main goal for the minimal realization, but this condition is supplemented by a low number of nodes of the synthesized reduced model.

Firstly two methods, based on Cauer- and Foster-synthesis for transfer functions with only real poles and residues, are presented. The Cauer-Synthesis is based on a continued fraction expansion of the transfer function. For a one-port reduced model the continued fraction expansion can be calculated to

$$\begin{aligned} \tilde{H}(s) &= \tilde{H}_0 + \frac{1}{a_1/s + \frac{1}{b_1 + \frac{1}{a_2/s + \frac{1}{b_2 + \dots}}}} \\ &= \tilde{H}_0 + \frac{1}{|a_1/s} + \frac{1}{|b_1} + \frac{1}{|a_2/s} + \frac{1}{|b_2} \dots \end{aligned} \quad (3.81)$$

This continued fraction expansion can be realized as an electrical network, in the case of an impedance as an RL-ladder network as shown in Fig. 3.4. In the dual case of an admittance, a GC-ladder network is synthesized as shown in Fig. 3.5. For the impedance case the element

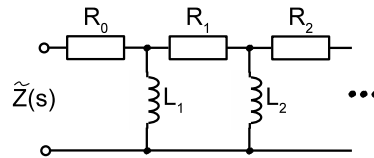


Figure 3.4: Synthesized network using the Cauer-synthesis for impedances

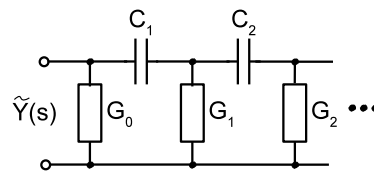


Figure 3.5: Synthesized network using the Cauer-synthesis for admittances

values are obtained directly from the reduced transfer function with

$$\begin{aligned} R_0 &= \tilde{H}_0 \\ R_m &= b_m \quad (1 \leq m \leq n) \\ L_m &= 1/a_m \quad (1 \leq m \leq n) \end{aligned} \quad (3.82)$$

and for the admittance case with

$$\begin{aligned} G_0 &= \tilde{H}_0 \\ G_m &= b_m \quad (1 \leq m \leq n) \\ C_m &= 1/a_m \quad (1 \leq m \leq n) \end{aligned} \quad (3.83)$$

The Foster-Synthesis is based on a partial fraction expansion of the reduced order transfer function. The transfer function of a reduced model of a one-port can be written with

$$\tilde{H}(s) = \tilde{H}_0 + \sum_{m=1}^n \frac{a_m s}{s + b_m}. \quad (3.84)$$

This partial fraction expansion can be realized as an electrical network in the case of an impedance as series connection of RL-parallel connections, as shown in Fig. 3.6. In the dual case of an admittance, the synthesized network is a parallel connection of GC-series connections as shown in Fig. 3.7. For the impedance the element values are obtained from the transfer

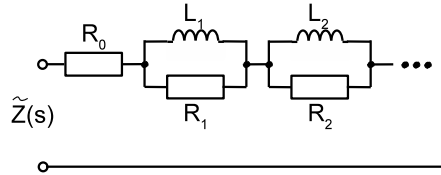


Figure 3.6: Synthesized network using the Foster-synthesis for impedances

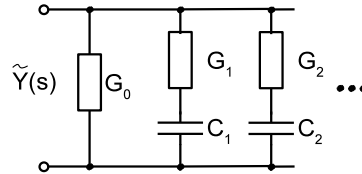


Figure 3.7: Synthesized network using the Foster-synthesis for admittances

function coefficients with

$$\begin{aligned} R_0 &= \tilde{H}_0 \\ R_m &= a_m \quad (1 \leq m \leq n) \\ L_m &= a_m/b_m \quad (1 \leq m \leq n) \end{aligned} \quad (3.85)$$

and for the admittance with

$$\begin{aligned} G_0 &= \tilde{H}_0 \\ G_m &= a_m \quad (1 \leq m \leq n) \\ C_m &= a_m/b_m \quad (1 \leq m \leq n). \end{aligned} \quad (3.86)$$

In both cases the zeroth resistance or conductance can be set to zero if the H_0 term does not exist in the reduced transfer function. For both Cauer- and Foster-synthesis methods the size of the network of the reduced model depends on the number of poles n . The reduced network has around $2n$ elements and contains n nodes.

In the former paragraph only real poles and residues in the reduced order transfer function are considered. After order reduction the poles are typically complex, which leads to enhanced synthesis methods. As an example the enhanced Foster-Synthesis is presented. This method is based on the pole-residues form of the reduced order transfer function for a model of a one-port

$$\tilde{H}(s) = s \cdot \tilde{H}_\infty + \tilde{H}_0 + \sum_{m=1}^{n_r} \frac{r_{r_m}}{s - p_{r_m}} + \sum_{m=1}^{n_c} \left(\frac{r_{c_m}}{s - p_{c_m}} + \frac{r_{c_m}^*}{s - p_{c_m}^*} \right). \quad (3.87)$$

The transfer function contains n_r real poles p_r and their corresponding real residues r_r and n_c conjugate complex poles p_c and residues r_c . This transfer function can be realized as an electrical network in the case of an admittance as shown in Fig. 3.8, or in the case of an impedance as shown in Fig. 3.9. In case of a reduced order admittance the element values of the zero and

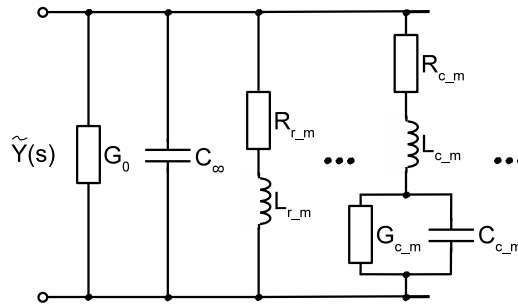


Figure 3.8: Synthesized network using the enhanced Foster-synthesis for admittances

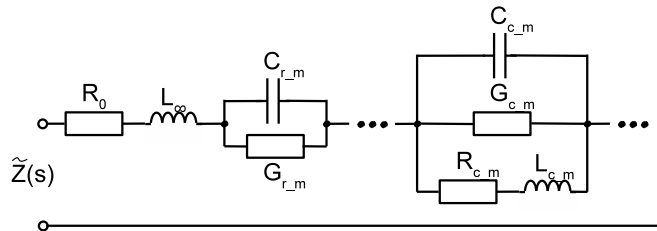


Figure 3.9: Synthesized network using the enhanced Foster-synthesis for impedances

infinity part of the transfer function are given with

$$\begin{aligned} G_0 &= \tilde{H}_0 \\ C_\infty &= \tilde{H}_\infty \end{aligned} \quad (3.88)$$

and for the real poles and residues the synthesized network elements are

$$\begin{aligned} L_{r_m} &= 1/r_{r_m} \\ R_{r_m} &= -p_{r_m}/r_{r_m}. \end{aligned} \quad (3.89)$$

For the conjugate complex poles and residues the reduced order admittance can be written with

$$\begin{aligned} H_{c_m}(s) &= \frac{r_c}{s - p_c} + \frac{r_c^*}{s - p_c^*} \\ &= \frac{s \cdot 2\operatorname{Re}\{r_c\} - 2\operatorname{Re}\{r_c \cdot p_c^*\}}{s^2 - s \cdot 2\operatorname{Re}\{p_c\} + |p_c|^2} \end{aligned} \quad (3.90)$$

where * denotes conjugate complex and $\operatorname{Re}\{a\}$ the real part of a complex number a . The admittance of the network shown in Fig. 3.8 for the complex poles is given with

$$\begin{aligned} Y_{c_m}(s) &= \frac{1}{R_{c_m}} \parallel \frac{1}{s \cdot L_{c_m}} \parallel (s \cdot C_{c_m} + G_{c_m}) \\ &= \frac{s \cdot \frac{1}{L_{c_m}} + \frac{G_{c_m}}{L_{c_m} \cdot C_{c_m}}}{s^2 + s \cdot \left(\frac{R_{c_m}}{L_{c_m}} + \frac{G_{c_m}}{C_{c_m}} \right) + \frac{1 + R_{c_m} \cdot G_{c_m}}{L_{c_m} \cdot C_{c_m}}}. \end{aligned} \quad (3.91)$$

Comparing the coefficients in 3.90 and 3.91 leads to the following element values

$$\begin{aligned} R_{c_m} &= \frac{\operatorname{Re}\{r_c \cdot p_c^*\} - 2 \cdot \operatorname{Re}\{r_c\} \cdot \operatorname{Re}\{p_c\}}{2 \cdot \operatorname{Re}^2\{r_c\}} \\ G_{c_m} &= \frac{-2 \cdot \operatorname{Re}^2\{r_c\} \cdot \operatorname{Re}\{r_c \cdot p_c^*\}}{\operatorname{Re}^2\{r_c \cdot p_c^*\} - 2 \cdot \operatorname{Re}\{r_c\} \cdot \operatorname{Re}\{r_c \cdot p_c^*\} \cdot \operatorname{Re}\{p_c^*\} + \operatorname{Re}^2\{r_c\} \cdot |p_c|^2} \\ C_{c_m} &= \frac{2 \cdot \operatorname{Re}^3\{r_c\}}{\operatorname{Re}^2\{r_c \cdot p_c^*\} - 2 \cdot \operatorname{Re}\{r_c\} \cdot \operatorname{Re}\{r_c \cdot p_c^*\} \cdot \operatorname{Re}\{p_c^*\} + \operatorname{Re}^2\{r_c\} \cdot |p_c|^2} \\ L_{c_m} &= \frac{1}{2 \cdot \operatorname{Re}\{r_c\}}. \end{aligned} \quad (3.92)$$

In the case of an impedance, the network is dual as shown in Fig. 3.9. The element values for this network can be determined in the same way as for the admittance and are given with

$$\begin{aligned} R_0 &= \tilde{H}_0 \\ L_\infty &= \tilde{H}_\infty \\ C_{r_m} &= 1/r_{r_m} \\ G_{r_m} &= -p_{r_m}/r_{r_m} \\ G_{c_m} &= \frac{\operatorname{Re}\{r_c \cdot p_c^*\} - 2 \cdot \operatorname{Re}\{r_c\} \cdot \operatorname{Re}\{p_c\}}{2 \cdot \operatorname{Re}^2\{r_c\}} \\ R_{c_m} &= \frac{-2 \cdot \operatorname{Re}^2\{r_c\} \cdot \operatorname{Re}\{r_c \cdot p_c^*\}}{\operatorname{Re}^2\{r_c \cdot p_c^*\} - 2 \cdot \operatorname{Re}\{r_c\} \cdot \operatorname{Re}\{r_c \cdot p_c^*\} \cdot \operatorname{Re}\{p_c^*\} + \operatorname{Re}^2\{r_c\} \cdot |p_c|^2} \\ L_{c_m} &= \frac{2 \cdot \operatorname{Re}^3\{r_c\}}{\operatorname{Re}^2\{r_c \cdot p_c^*\} - 2 \cdot \operatorname{Re}\{r_c\} \cdot \operatorname{Re}\{r_c \cdot p_c^*\} \cdot \operatorname{Re}\{p_c^*\} + \operatorname{Re}^2\{r_c\} \cdot |p_c|^2} \\ C_{c_m} &= \frac{1}{2 \cdot \operatorname{Re}\{r_c\}}. \end{aligned} \quad (3.93)$$

With this the size of the synthesized network depends on the number of poles n . The number of elements in the synthesized network is around $2n$ and the number of nodes is around n .

In the former paragraphs it was shown how circuits can be generated out of the scalar transfer function of a one port. If a network is to be generated from a reduced order model with more than one port the matrix transfer function

$$\mathbf{H}(s) = \begin{pmatrix} \tilde{H}_{1,1}(s) & \cdots & \tilde{H}_{1,p}(s) \\ \vdots & \ddots & \vdots \\ \tilde{H}_{p,1}(s) & \cdots & \tilde{H}_{p,p}(s) \end{pmatrix} \quad (3.94)$$

has to be taken into account. A demand on the reduced order model, as it is to be synthesized as pure RLC-network with the filter synthesis methods, is the preservation of reciprocity. Necessary extensions to the filter synthesis algorithms for reduced order systems with more than one port will be described below.

Starting with a two-port network, the network synthesized from a reduced model is shown for example as a Π -realization in Fig. 3.10. For this two port the elements are

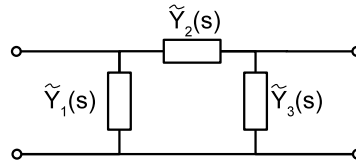


Figure 3.10: π -structure of a synthesized network with two ports

$$\begin{aligned} \tilde{Y}_1(s) &= \tilde{H}_{1,1}(s) + \tilde{H}_{1,2}(s) \\ \tilde{Y}_2(s) &= -\tilde{H}_{1,2}(s) \\ \tilde{Y}_3(s) &= \tilde{H}_{2,2}(s) + \tilde{H}_{1,2}(s) \end{aligned} \quad (3.95)$$

for the admittance case. In case of an impedance description the T -realization shown in Fig. 3.11 is more suitable with the element parameters

$$\begin{aligned} \tilde{Z}_1(s) &= \tilde{H}_{1,1}(s) - \tilde{H}_{1,2}(s) \\ \tilde{Z}_2(s) &= \tilde{H}_{2,2}(s) - \tilde{H}_{1,2}(s) \\ \tilde{Z}_3(s) &= \tilde{H}_{1,2}(s). \end{aligned} \quad (3.96)$$

Nevertheless, Π - and T -realizations are both possible for the two-port synthesis of an admittance and an impedance and calculations of the element functions are similar. The resulting one-port impedances or admittances composing the two-port network can now be synthesized with the one-port synthesis algorithms presented in the former paragraphs.

For systems with more than two ports the synthesis problem is well studied for admittance description. For impedances the synthesis problem is not straightforward as in the admittance

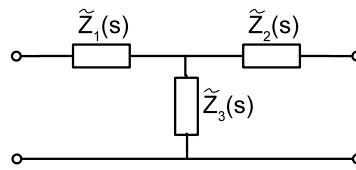
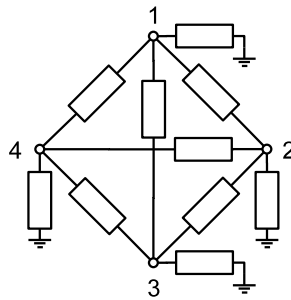


Figure 3.11: T-structure of a synthesized network with two ports

case [116–118] and still faces several open problems. In the following we will concentrate on admittance descriptions for reduced models with p ports. A network can be built, where all ports are connected with each other by a one-port network and every port is connected with the ground by a one-port network. The resulting network is a complete graph where every branch contains a one-port. This leads to an enhanced Π -realization for the p -port. As an example an admittance with four ports is shown in Fig. 3.12. The admittances connecting the


 Figure 3.12: π -structure of a synthesized network with four ports

ports with each other and with ground are synthesized with the one-port algorithms presented in the former paragraphs. Overall the size of the network depends on the number of ports p and the number of poles n . The synthesized Π -network contains $2n \cdot (p^2 + p)/2$ elements and $n \cdot (p^2 + p)/2$ nodes, which shows a strong dependence of the size of the network on the number of ports.

3.2.2 System Equations Synthesis

For reduction algorithms based on the system equations the resulting order reduced model is a system of equations with a lowered number of equations. In this section methods for the synthesis of an electrical network from the reduced order system equations are presented. In the following for the estimation of the size of the reduced network it is assumed that the matrices of the reduced order system are full populated, having almost no zero coefficients.

In the unreduced system every variable in \mathbf{x} corresponds to a node voltage, an inductor current or a voltage source current (Sec. 2.1). After order reduction the mapping of the system variables in $\tilde{\mathbf{x}}$ to currents and voltages is abrogated. For the reduced system variables it can be freely chosen if they are treated as node voltages or as branch currents. If methods capable

of preserving the block structure of the system matrices as presented in Sec. 3.1.4 are used, the mapping of the system variables to currents or voltages is possible in the reduced system variables. Nevertheless, for the synthesis as an electrical network, the system variables of the reduced system can also be chosen to be interpreted as currents or as voltages.

The most straightforward way to synthesize a network out of the reduced system matrices is done by so-called direct stamping methods. For the direct stamping methods the following controlled sources are necessary: current controlled current source (CCCS), voltage controlled current source (VCCS), current controlled voltage source (CCVS) and voltage controlled voltage source (VCVS). For the direct stamping method information about the simulation environment is necessary. In the following the term dynamic element is used for controlled elements defined by a multiplication of the Laplace variable s with the controlling value

$$\begin{aligned} \text{CCCS} : i_{CS} &= s \cdot i_{CC}, & u_{CS} &= \text{arbitrary} \\ \text{VCCS} : i_{CS} &= s \cdot u_{VC}, & u_{CS} &= \text{arbitrary} \\ \text{CCVS} : u_{VS} &= s \cdot i_{CC}, & i_{VS} &= \text{arbitrary} \\ \text{VCVS} : u_{VS} &= s \cdot u_{VC}, & i_{VS} &= \text{arbitrary}. \end{aligned}$$

The term polynomial controlled source is used for controlled sources defined by a sum of first order polynomials

$$\begin{aligned} \text{CCCS} : i_{CS} &= \sum_{j=1}^m w_j \cdot i_j, & u_{CS} &= \text{arbitrary} \\ \text{VCCS} : i_{CS} &= \sum_{j=1}^m w_j \cdot u_j, & u_{CS} &= \text{arbitrary} \\ \text{CCVS} : u_{VS} &= \sum_{j=1}^m w_j \cdot i_j, & i_{VS} &= \text{arbitrary} \\ \text{VCVS} : u_{VS} &= \sum_{j=1}^m w_j \cdot u_j, & i_{VS} &= \text{arbitrary}. \end{aligned}$$

By direct stamping a matrix stamp is realized by finding a network that produces the same stamp in the internal simulator matrices as in the reduced system matrices. With this method the coefficients in the matrices are realized by controlled sources, including resistors, capacitors and inductors as special cases. The direct stamping method can be divided into two essential steps. In the first step the matrices $\tilde{\mathbf{C}}, \tilde{\mathbf{G}}$ are realized as an electrical network. In the second step the connection of this network with the ports, described by $\tilde{\mathbf{B}}, \tilde{\mathbf{L}}$, is realized. In the following the resulting networks, realized by the interpretation of the reduced system variables in $\tilde{\mathbf{x}}$ interpreted as voltages or currents, are presented. The differences in the synthesized networks depending on the capability of the simulation environment, regarding the availability of dynamic elements and polynomial sources, are shown.

If the reduced system variables in $\tilde{\mathbf{x}}$ are interpreted as voltages, every system variable is associated to a node voltage in the synthesized network. Every row in the reduced system description

is thereby treated as Kirchhoff current law, whereas the currents depend on the node voltages. The synthesized network contains as many nodes as there are equations in the reduced system description. At every node controlled current sources are connected. With that synthesis method for every system given in matrix form as in Eqn. 3.3, a network can be generated containing controlled sources and dynamic elements as shown in Fig. 3.13. If for the direct stamp-

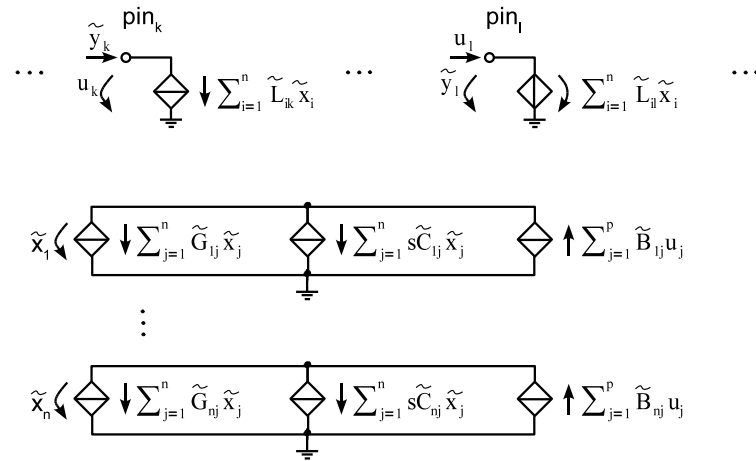


Figure 3.13: Network with controlled sources and dynamic elements created by direct stamping. All system variables are interpreted as voltages.

ing method no polynomial sources are available, the number of synthesized elements equals $2n^2$, which equals the number of coefficients in the matrices $\tilde{\mathbf{C}}$, $\tilde{\mathbf{G}}$. If polynomial sources are available in the simulation environment the number of elements can be reduced. For example, parallel controlled current sources can be combined into one source. With polynomial sources only n elements for the matrix $\tilde{\mathbf{C}}$ and n elements for the matrix $\tilde{\mathbf{G}}$ are necessary, as every row is described by one polynomial source. In the next step the connection of the generated network with the ports is realized. For the connection of the input values at the ports with the system variables the matrix $\tilde{\mathbf{B}}$ is synthesized. Depending on whether the input is a current or a voltage, CCCSs and VCCSs are realized in the network. Without polynomial sources, $n \cdot p$ elements are necessary for the matrix $\tilde{\mathbf{B}}$, as every coefficient is to be realized by one controlled source. Only n elements are necessary if there are polynomial sources available, as every column is realized by a controlled source. The outputs at the ports, which are typically the dual electrical values of the inputs at the port, are described by $\tilde{\mathbf{L}}$. The matrix $\tilde{\mathbf{L}}$ is realized with VCCS and VCVS for currents and voltages as outputs respectively. Without polynomial controlled sources $n \cdot p$ elements are necessary for realizing the matrix $\tilde{\mathbf{L}}$. Only p elements are necessary if there are polynomial sources available. The number of nodes of the network realizing $\tilde{\mathbf{L}}$ differs depending on the type of outputs. For an electrical current as output, the controlled sources realizing the current can be connected in parallel, and thereby only one node for each output is necessary. For the dual case of voltage outputs the controlled voltage sources have to be connected in series, and thereby n nodes between the voltage sources are necessary for each output. This results in $n \cdot p$ nodes for all p outputs. This problem vanishes if polynomial controlled sources

are available, as each output value is generated by one source controlled by all system variables together, and thus only one node per output is necessary. The overall number of elements of the complete synthesized network is equal to the number of coefficients $2n^2 + 2n \cdot p$ in the matrices, if there are no polynomial sources available. If polynomial sources can be used, the overall number of elements reduces to $3n + p$.

The advantage of this method is the low number of nodes that is used in the synthesized network. Only as many nodes as the order n of the system are necessary for the network realizing the matrices $\tilde{\mathbf{C}}, \tilde{\mathbf{G}}$ independently on the availability of polynomial sources. If no polynomial sources are available $n \cdot p$ nodes are necessary for the port connection. With polynomial sources the number of necessary additional nodes is reduced to p . The disadvantage of the synthesis method is that dynamic elements are necessary, which are not always available. Furthermore, the number of elements can be very high, especially in the case if there are no polynomial sources available. An advantage of this method is that no requirements on the structure of the reduced system matrices are necessary, except that the coefficients are real for real controlled sources gains.

In several simulation environments dynamic elements as described in Eqn. 3.97 are not supported. In this case a network containing only static sources is necessary. The direct stamping method can be extended to build a network with only static controlled sources. Therefore, every coefficient in the matrix $\tilde{\mathbf{C}}$ is synthesized with an additional capacitor connected with a VCVS controlled by the voltage corresponding to the column of the coefficient with the gain one. In the synthesized network a CCCS with a gain one, controlled by the current through the additional capacitor, is used instead of dynamic elements. The structure of the resulting small additional networks is shown in Fig. 3.14 at the right side. The behavior of the network at its ports is identical to the behavior of the network with dynamic elements. The advantage of this

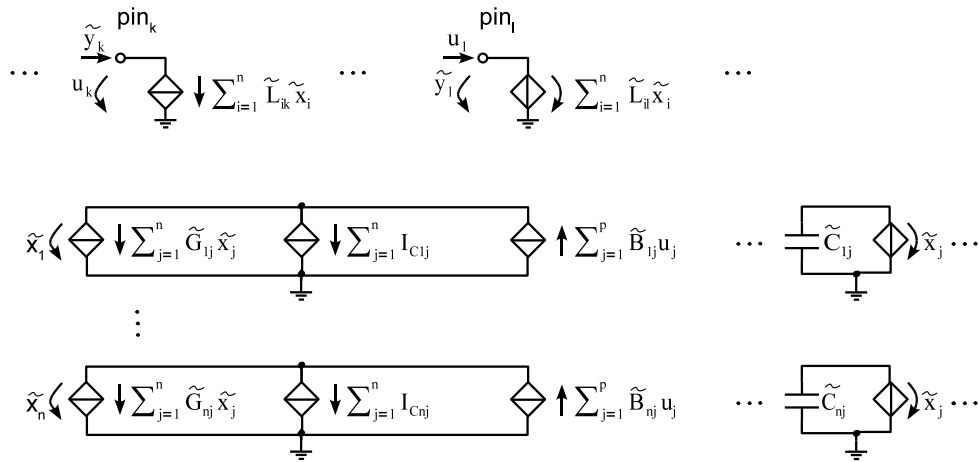


Figure 3.14: Network with controlled sources and without dynamic elements created by direct stamping. All system variables are interpreted as voltages.

method is that only static controlled sources and capacitors are necessary. The number of elements for the matrices $\tilde{\mathbf{G}}, \tilde{\mathbf{B}}, \tilde{\mathbf{L}}$ is equal to the direct stamping methods with available dynamic

elements, as for these matrices only static sources are necessary. For the matrix $\tilde{\mathbf{C}}$ in addition $2n^2$ elements and n^2 nodes are necessary. Therefore the disadvantage of this approach is the larger number of elements compared to the direct stamping method with dynamic elements. The overall number of elements is $4n^2 + 2n \cdot p$ if there are no polynomial sources available in the simulation environment. If polynomial sources can be used, the number of elements reduces to $2n^2 + 3n + p$. A second disadvantage of this method is the high number of nodes that is necessary. As many nodes as the order of the reduced system n plus n^2 are necessary for the network, independently on the availability of polynomial sources. If no polynomial sources are available, $n \cdot p$ nodes are necessary for the port connection. Only p nodes are necessary, if polynomial sources are available. Again, the advantage of this synthesis method is that no requirements on the structure of the reduced system matrices are necessary, except that the coefficients are real for real gains of the controlled sources and real element values.

In the former paragraphs the variables $\tilde{\mathbf{x}}$ in the reduced system are interpreted as voltages for the network synthesis. This leads to an interpretation of the reduced system equations as Kirchhoff current law. If the variables in $\tilde{\mathbf{x}}$ are interpreted as currents, every current is associated to a loop current. This case leads to an interpretation of the reduced system equations as Kirchhoff voltage law. The synthesized network contains as many loops as there are equations in the reduced system description. In every loop controlled voltage sources are used. The networks with controlled voltage sources can be built in a similar way as in the former paragraph by realizing matrix stamps. The resulting network is shown in Fig. 3.15.

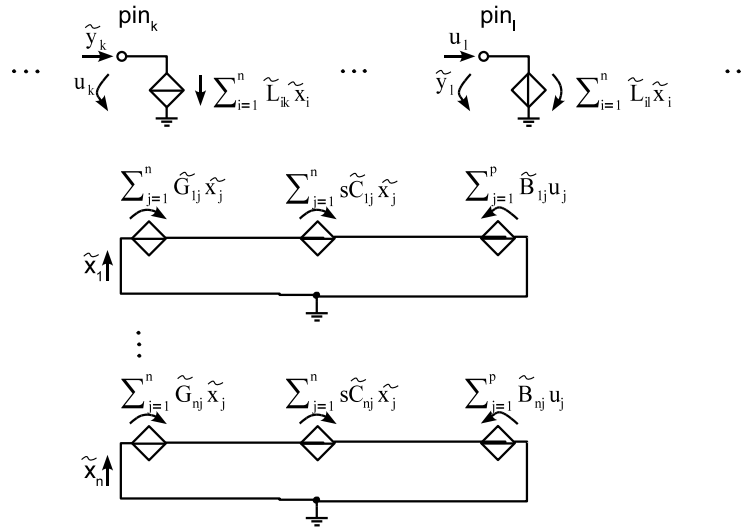


Figure 3.15: Network with controlled sources and dynamic elements created with direct stamping. All system variables are interpreted as currents.

For simulation environments without dynamic elements, in the synthesized network for every coefficient in the matrix $\tilde{\mathbf{C}}$, an inductor connected with a CCCS is added. In the synthesized network a VCVS with a gain one, controlled by the voltage across the inductor, is used instead of dynamic elements. This realizes the behavior of a dynamic element. The resulting network is

shown in Fig. 3.16. Again, an advantage of this direct stamping method is that no requirements

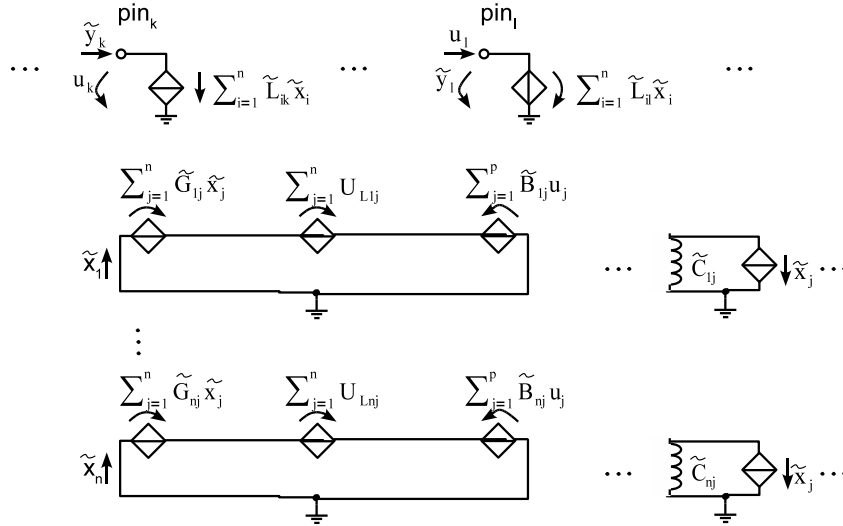


Figure 3.16: Network with controlled sources and without dynamic elements created with direct stamping. All system variables are interpreted as currents.

on the structure of the reduced system matrices are necessary, except that the coefficients in the matrices are real for real controlled sources gains. The overall number of elements is equal to the number of elements in the direct stamping method, with the system variables interpreted as voltages. Again, the availability of dynamic elements and polynomial sources decreases the size of the network. Nevertheless, the main disadvantage of this method is a large number of nodes, which is necessary in comparison to the synthesis method interpreting the system variables as voltages. Thereby this method, relying on loop currents instead of node voltages, should only be used if the reduced system variables need to be interpreted as currents.

As shown in the previous paragraphs, the direct stamping methods have several disadvantages. Mainly the necessity for dynamic elements in the form of Eqn. 3.97 to synthesize networks with a low number of elements and nodes from the reduced system limits their applicability. If only static controlled sources are available, the direct stamping methods generate networks with an increasingly large number of elements and nodes. In this section a synthesis approach based on the reduced system matrices is introduced, which does not need dynamic elements. The so-called GC-network synthesis approach is presented in this work and published in [119]. The synthesized network has a comparable low number of elements and nodes as the direct stamping methods with dynamic elements. For synthesis the variables in $\tilde{\mathbf{x}}$ are considered as node voltages. Therefore a network with as many nodes as variables in $\tilde{\mathbf{x}}$ is generated. As an additional requirement to the direct stamping methods, not only the coefficients in the matrices need to be real, but also the matrices $\tilde{\mathbf{C}}$ and $\tilde{\mathbf{G}}$ need to be (J-)symmetric. The method of generating the network is shown in the following. By utilizing the (J-)symmetry of the reduced system matrices, a network with capacitors and resistors realizing the matrices $\tilde{\mathbf{C}}$ and $\tilde{\mathbf{G}}$ as shown in Fig. 3.17 can be synthesized. Every one of the n nodes is connected with every other

tance or hybrid descriptions by using the appropriate type of controlled sources for the $\tilde{\mathbf{B}}, \tilde{\mathbf{L}}$ matrices. The network realizing the $\tilde{\mathbf{C}}, \tilde{\mathbf{G}}$ matrices remains the same, independently on the sort of port definition.

Further enhancements of the direct stamping and GC-synthesis methods are based on sparsification techniques to reduce the number of elements [77, 120] and regularization techniques to avoid numerical errors due to very small and very large eigenvalues of the reduced systems matrices [77].

3.2.3 Further Methods

Another class of networks synthesized from the reduced system equations is based on numerical integration techniques. The synthesized networks contain time-variant element values [64, 121–124]. Based on internal state variables and port voltages and currents, at each time-point in the simulation the corresponding element values are calculated. The main advantage is the fast simulation of the generated networks. The disadvantage is that the implementation of these networks usually requires specialized simulation environments or additions to existing simulators. As these methods are more situated in the field of numerical integration of the reduced models than in synthesizing in the sense of creating a network from a given function, only a short overview is given in the following. A synthesis method using time-variant elements is proposed in [122], based on backward-Euler integration, which can be extended to other numerical integration methods [121]. A method for avoiding the matrix inversions in [122] is presented in [123]. The simulation environment presented in [64] is also based on simulating reduced order time-variant models. A state variable formulation on which integration methods are applied is presented in [124].

3.2.4 Comparison of Synthesis Methods

In the following, the necessary number of elements and nodes of the presented network synthesis algorithms is compared. Not considered here is the number of loops, as practically all simulators are based on nodal analysis, where the number of nodes, instead of the number of loops, is crucial for the resources in a simulation.

Let p be the number of ports, n be the reduced number of equations in the system description or the reduced number of pole-residues pairs in the rational transfer function form. The number of elements and nodes of the network synthesis algorithms presented in this section is summarized in Tab. 3.1.

As typically complex poles and residues occur in the reduced models, the enhanced Foster-synthesis method is used as representative method for the transfer function synthesis methods. For this filter synthesis method every entry in the matrix transfer function is realized with a one-port network with $2n$ elements and n nodes. For a network with p ports $(p^2 + p)/2$ of these one-port networks are necessary. The size of the resulting network is $n \cdot (p^2 + p)$ for the elements and $n \cdot (p^2 + p)/2$ for the nodes. This shows the dominating dependency of the size of the network on the number of ports. The advantage of the filter synthesis methods is the

Table 3.1: Comparison of network synthesis methods for reduced order models

| Method | dynamic elements | poly sources | Elements | Nodes |
|------------------|------------------|--------------|------------------------|---|
| Direct Stamping | - | - | $4n^2 + 2n \cdot p$ | $n^2 + n + p$ up to $n^2 + n + n \cdot p$ |
| | - | X | $2n^2 + 3n + p$ | $n^2 + n + p$ |
| | X | - | $2n^2 + 2n \cdot p$ | $n + p$ up to $n + n \cdot p$ |
| | X | X | $3n + p$ | $n + p$ |
| GC-synthesis | - | - | $n^2 + n + 2n \cdot p$ | $n + p$ up to $n + n \cdot p$ |
| | - | X | $n^2 + 2n + p$ | $n + p$ |
| Filter-Synthesis | - | - | $n \cdot (p^2 + p)$ | $n \cdot (p^2 + p)/2$ |

realization as pure RLC-network by construction, enabling a robust simulation.

For the networks created from the reduced system equations, the interpretation of the reduced system variables as voltages always leads to a smaller number of nodes, because the resulting equations are based on nodal equations instead of mesh equations. Thus only the methods realizing the variables as voltages are taken into account in the following. With the direct stamping method the number of elements mainly depends on $n^2 + n \cdot p$, except for the case where polynomial controlled sources and dynamic elements are available and the number of elements can be reduced down to $n + p$. The number of nodes is mainly limited by the availability of dynamic elements in the simulation environment. If there are no dynamic elements allowed, the number of nodes mainly depends on $n^2 + p$, which is reduced down to $n + p$ if polynomial controlled sources are available. Overall, the number of elements and nodes is mainly limited by the reduced order and the capabilities of the simulation environment. The disadvantage of the direct stamping methods is the high number of controlled sources possibly affecting the robustness of the simulation.

For the GC-synthesis, which uses static controlled sources, resistors and capacitors and does not need dynamic elements in the form of Eqn. 3.97, the network size mainly depends on n^2 for the number of elements and on $n + p$ for the number of nodes. The number of nodes is as low as possible and equals the number of nodes of the direct stamping method with dynamic elements. The number of elements is higher than in the direct stamping method with dynamic elements, but nevertheless below the number of elements in the direct stamping method with only static controlled sources. For the GC-synthesis the size of the synthesized network mainly depends on the reduced order and less on the simulation environment capabilities. An advantage is the reduced number of necessary controlled sources compared to the direct stamping methods.

A comparison of the sizes of the networks created from the order reduced models leads to the following conclusion. For networks with a comparably high order and a quite high number of ports, a smaller network is synthesized with the system synthesis approaches than by using the transfer function synthesis methods. Transfer function synthesis methods create smaller networks for systems with a quite low number of ports and a comparably low order.

For the transfer function synthesis methods reciprocity is necessary, as the realized networks has to be reciprocal by using only RLC-elements. An advantage of the system synthesis approaches is that reciprocity has not to be preserved. Even non-reciprocal systems can be syn-

thesized with system synthesis approaches due to the use of controlled sources. Nevertheless, reciprocity should be preserved in a reduced model, allowing for accurate investigations.

Regarding network properties such as stability and passivity, the system synthesis and filter synthesis methods both preserve these properties, as the generated network is an exact representation of the reduced model. Despite the fact that the complete network is passive concerning the behavior at the ports, a few internal elements may be active. For example, negative resistors are used in the system synthesis methods for positive off-diagonal coefficients in the reduced system matrices. Also if the reduced system matrices are not positive (semi-)definite, negative element values are necessary. In filter synthesis methods the use of negative valued elements is avoided by construction. Both networks, synthesized with system synthesis and transfer function synthesis, are passive at the ports. Nevertheless, only the transfer function synthesis methods create networks by using only passive elements.

Another fact that should be taken into consideration is that the filter synthesis methods can only be applied to admittance descriptions if the system contains more than two ports. The synthesis methods, based on the reduced state space system, the direct stamping, as well as the GC-synthesis methods, can be applied to admittance, impedance and hybrid descriptions.

For simulation environments, where a direct access to the internal numerical integration algorithms is possible, the implementation of the time-variant networks is a possible choice.

To sum up, there is no optimal synthesis method for all reduced models. Depending on the type of the reduced model, the relation of the reduced order and the number of ports and the possibilities of the simulation environment an appropriate synthesis algorithm has to be chosen.

3.2.5 Illustrative Numerical Example

In this section the example of Sec. 2.4, whose order was reduced in Sec. 3.1.8, is synthesized for illustration purpose. Both transfer function synthesis and system equation synthesis are applied to the reduced models.

Firstly a filter synthesis method, the enhanced Foster-synthesis is used, which is based on the pole-residue form of the transfer function. The reduced impedance transfer function is given in Sec. 3.1.8 with

$$\tilde{Z}(s) \approx \frac{0.8488}{s + 1.3589} \quad (3.97)$$

and by using the enhanced Foster-synthesis procedure a network is generated. The generated network contains two elements: a parallel connection of a capacitor and a conductor. The network is shown in Fig. 3.18.

For the reduced system equations of Sec. 3.1.8

$$\begin{aligned} [s(1) + (1.3589)] \tilde{x}_1 &= (-0.9213) u_p \\ \tilde{y}_p &= (-0.9213) \tilde{x}_1 \end{aligned} \quad (3.98)$$

the GC-synthesis method is applied. The matrices $\tilde{\mathbf{C}} = 1$, $\tilde{\mathbf{G}} = 1.3589$ are synthesized with a capacitor and a conductor. For the connection between the input current and the system vector

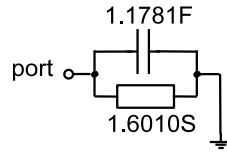


Figure 3.18: Synthesized network of the reduced illustrative example using the enhanced Foster-synthesis for impedances

a CCCS is generated, having the gain of $\tilde{\mathbf{B}} = -0.9213$. Finally, the output voltage is generated by a VCVS at the port, multiplying the internal voltage \tilde{x}_1 by the value of $\tilde{\mathbf{L}} = -0.9213$. The resulting network contains four elements: a capacitor, a conductor and two controlled sources. The network is shown in Fig. 3.19.

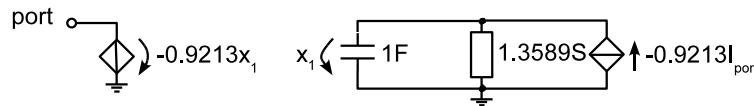


Figure 3.19: Synthesized network of the reduced illustrative example using GC-synthesis

Both synthesized networks are quite small for this illustrative example. Nevertheless, both synthesis methods can be applied to arbitrary large reduced order models.

It is noticeable that, as both the reduced transfer function and the reduced system have the same transfer behavior, both synthesized networks are indistinguishable at the port. Nevertheless, the behavior at the port approximates the behavior of the original network (Fig. 2.2), because the transfer impedance is reduced by order reduction techniques and the behavior is approximated in a narrow frequency band.

The approximation of the frequency domain behavior is already shown in Sec. 3.1.8. Thereby in the following, time-domain simulations are performed in an electrical simulation environment, to show the approximated behavior of the reduced networks compared to the original network. As simulation environment the SPICE simulator LTSPICE is used and the reduced network created with enhanced Foster-synthesis is simulated. At the port a current source with a ramp function is used and the voltage at the port is observed. The reduced network is simulated around 30% faster than the original network and simulation results are shown in Fig. 3.20. As can be seen, the approximation error of the reduced network, due to the model reduction, is quite low. This shows the applicability of the model reduction process.

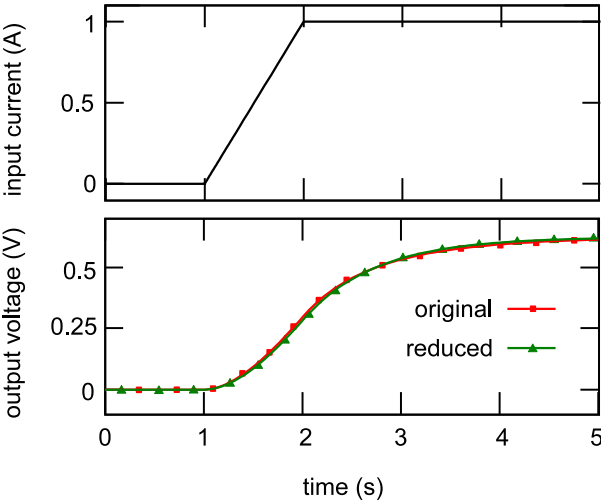


Figure 3.20: Illustrative example voltage behavior at the pin of the original and the reduced network

4 Model Reduction of Networks with Sources

In the former chapter, methods for reducing the RLC-part of a network were presented. In this chapter, the reduction of networks with additionally a large number of distributed sources is presented. In the introduction (Sec. 1.1) a motivation was given, in which applications, besides a large number of linear RLC-elements, also a large number of sources is used. By extracting the models of the distributed sources from the reducible network part, a large number of ports is created for their connection. The problem arising in the reduction of the models with a large number of ports by using the methods of the former chapter, is highlighted in the first section of this chapter (Sec. 4.1). State-of-the-art extensions to model reduction techniques, capable to reduce models with a large number of ports more efficiently, are presented in the second section of this chapter (Sec. 4.2). As will be shown, the existing methods suffer from low efficiency or a limited applicability for the reduction of networks with distributed sources.

Thus, in the third section of this chapter (Sec. 4.3), a new method for the reduction of networks with a large number of sources is presented. The method is applicable to general RLC-networks with distributed sources, where the distributed sources are modeled as independent sources or nonlinear controlled sources. In the modeling process the behavior of the distributed sources is specified, which is taken into account by the proposed reduction method. In state-of-the-art model reduction algorithms the behavior at the ports of a reducible model is not taken into account. The new proposed method includes the knowledge of the behavior of the sources connected with the ports. A preceding step reduces the number of necessary ports, while maintaining the overall influence of the distributed sources. The method is based on approximating the functions of the sources with a lower dimensional function space. The distributed sources' models in the network are replaced by models for the lowered dimensional function space. The number of elements that have to be extracted from the reducible part is lowered. Thereby the number of necessary ports for the distributed sources is reduced. The port reduced model can afterwards be more efficiently reduced with model reduction techniques. The idea of the port reduction is developed in this work and allows for several advantages compared to the existing methods, which will be shown in the fourth section of this chapter (Sec. 4.4).

4.1 Problem Statement

In the modeling of distributed systems with distributed sources network models are built, having a large number of distributed sources in addition to the linear RLC-elements. From a simulation and reduction point of view these models have in common that, after the modeling step, the resulting networks typically have a large number of elements and nodes. The networks are composed of linear passive RLC-elements, ranging from thousands to millions. In addition a large number of independent sources or nonlinear elements, typically ranging from

tens to thousands are used in the network model. The reduction of these models is limited by the large number of models for the distributed sources, as will be shown in this section. The generation of a large number of ports by extracting the distributed sources' models from the reducible network, is shown in Sec. 4.1.1. The reduced efficiency in model reduction of these networks is presented in Sec. 4.1.2.

4.1.1 Extraction of Sources

The model reduction methods, presented in Sec. 3, are based on linear transfer functions or linear time-invariant systems. For the reduction, the network model has to be divided into a reducible part and an irreducible part. In the networks under consideration, the class of elements, which can be included in the model reduction, consists of linear resistors, capacitors and inductors as well as linear time-invariant controlled sources. Elements that cannot be included in the reducible part are time-variant elements, such as independent current or voltage sources and time-varying controlled sources, as well as every kind of nonlinear element, as for example diodes, transistors or nonlinear controlled sources.

All network elements that cannot be included in the reduction process are extracted from the reducible part. The connection of these elements is done with the help of ports. For example, the extraction of sources in the network model and the connection with the help of ports is shown for independent current sources in Fig. 4.1. The resulting passive RLC-network part is to be reduced with model order reduction techniques.

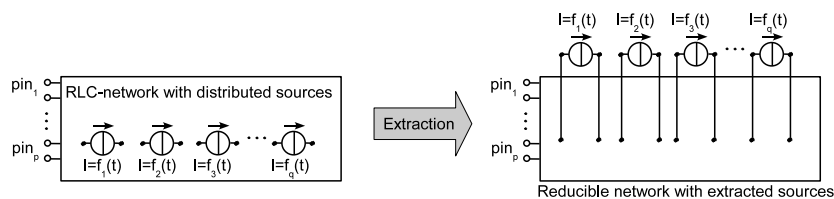


Figure 4.1: Extraction of distributed sources from the reducible network part and connection with the network by ports

The class of extracted elements can be roughly divided into three groups. The first group are independent sources described by a function $f(t)$, where $f(t)$ describes the current or voltage waveform of the distributed sources. For this class, the port definition is done by defining the voltage or current waveform as input at the port and the dual electrical value as output. The input functions are completely determined by the waveform functions of the independent sources. The second group are a special class of nonlinear elements, the nonlinear controlled sources. A nonlinear controlled source is described by a time-variant or time-invariant current or voltage function $f(x, t)$. The current or voltage, generated by the nonlinear controlled source, depends on the electrical values in x of the network with a nonlinear function. To these class of elements belong, as a special case, also two-terminal elements, which are controlled by an electrical value over or through itself. Example are diodes and nonlinear resistors ex-

plicitly described by a current or voltage function. In the port definition the voltage or current generated by the nonlinear controlled source is defined as electrical input value at the port. The dual electrical value is defined as the output. The input waveform is not known a priori, but its dependence on internal electrical values and time is given by $f(\mathbf{x}, t)$. The third group of extracted elements are nonlinear elements, described by implicit functions, or having more than two terminals. For example, transistors having three or more terminals, as well as diodes and nonlinear resistors described by implicit functions, belong to this class. For this class the definitions of the port or terminals are done in a similar way, but no assumptions about the input functions can be made.

The distributed sources in the networks under consideration are modeled by explicit current or voltage functions. Thus in the following only models belonging to the first and second group are taken into consideration for the presented methods.

Overall the reducible network model part contains ports or terminals which number depends on the number of nonlinear or time-variant elements in the model. For a large number of irreducible elements the reducible network part has a large number of ports or terminals. In the following it is not distinguished between a port and a terminal and generally the name port is used. Nevertheless, the presented methods are also valid for the terminal case. The challenges in the reduction of network models with a large number of nonlinear or time-variant elements, which model the distributed sources' behavior, is shown in the following section.

4.1.2 Reduction of Systems with Many Ports

As shown in the former section the reducible part of networks with distributed sources has a large number of ports. The network is divided into a linear time-invariant reducible RLC-part and an irreducible part containing the models of the distributed sources. Both parts of the network are connected by ports, which results in a large number of ports for a large number of distributed sources. To find a smaller network for the reducible part, the model reduction techniques presented in Sec. 3 are used. The different efficiency limitations of the reduction caused by the large number of ports are highlighted in this section.

For the methods reducing directly the network (Sec. 3.1.1) there is no direct dependency of model reduction efficiency on the number of ports. Nevertheless, there is an indirect dependence, as the nodes connected to a port cannot be included in the reduction and have to be preserved. Furthermore, the behavior at all these nodes is to be approximated, limiting the elimination of other nodes.

A direct dependence of the size of the reduced model on the number of ports exists for the Gaussian elimination using the Schur complement presented in Sec. 3.1.2. The number of nodes that has to be preserved is equal to the order to which the system of the network is to be reduced. As all nodes connected to a port have to be preserved, the number of ports equals the reduced order. For methods preserving some internal nodes in the reduced model, the Gaussian elimination behaves similarly as the methods directly reducing the network. The lower limit of the number of preserved nodes is given by the number of ports, but reduction is typically limited earlier due to the large amount of nodes, where the behavior has to be approximated.

Modal approximation (Sec. 3.1.3) is limited by the ports, in the way that the higher the number of input-output relations is, the higher is the number of dominant poles. The algorithm is thereby not directly limited by the number of ports. But as the number of dominant poles is higher, the reduced system will be larger, which shows the indirect dependency.

In the moment matching methods (Sec. 3.1.4) the dependency of the reduction efficiency and the number of ports is more direct. The generated Krylov subspace (Eqn. 3.34), used for the generation of the projection matrix in the implicit moment matching, depends directly on the number of ports. With a larger number of ports, the size of the generated Krylov subspace increases linearly. As the reduced model is generated by projection on this subspace, the size of the reduced model also linearly increases with the number of ports.

In the Gramian-based reduction methods (Sec. 3.1.5) there is no direct dependency of the reduction efficiency on the number of ports. Nevertheless, a high number of ports, and thereby a high number of nodes where the network can be excited and observed, yields a better controllability and observability of the system states. Thus the controllable and observable subspace of the system states is higher. As only the weak controllable and observable states are to be eliminated, the reduced system is bigger for a larger number of ports. In the Gramian-based reduction the dependence of the reducibility on the number of ports can be directly observed during the reduction process. The Hankel Singular Values give an estimation of the approximation error of the reduced model depending on its reduced size. Typically the Hankel singular values decay much slower for a larger number of ports, as will be shown in the next sections. The slower decay shows a higher approximation error for a given reduced order. Or in the other way around, the slower decay shows a higher necessary reduced order for a given approximation error.

The interpolation methods (Sec. 3.1.6) are as well limited by a large number of ports. The larger the number of ports, the higher the simulated or measured input-output relations. As every input-output relation is to be interpolated by the model construction process, a large number of ports results in a large size of the generated reduced model.

Overall, every of the presented model reduction methods is, directly or indirectly, limited by a large number of ports of the reducible system. In the following sections this will be illustrated by example networks. By reducing networks with a large number of ports, the efficiency limitation of model reduction is investigated.

4.1.2.1 Illustrative Numerical Example

In this section the arising difficulty in the model reduction of networks with a large number of sources is shown. With the illustrative example of Sec. 2.4 the lowered efficiency of model reduction of networks with distributed sources is shown.

To generate a network with a large number of sources, two independent sources are added to the illustrating example network (Fig. 2.2). In addition to the passive RC-elements two independent current sources are connected at the middle node and the right node, as shown in Fig. 4.2. The independent current sources cannot be included in the model reduction and are extracted from the reducible network part. The two independent current sources and the

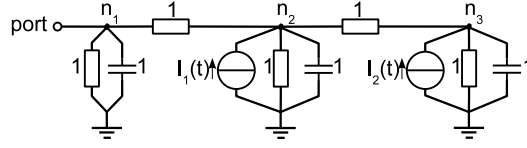


Figure 4.2: Illustrative example network with sources

reducible network part are connected by two ports. The network is described with the help of MNA and the resulting system is given with

$$\begin{aligned}
 \left[s \begin{pmatrix} \mathbf{C} \\ \begin{pmatrix} 1 & 0 & 0 \\ 0 & 1 & 0 \\ 0 & 0 & 1 \end{pmatrix} \end{pmatrix} + \begin{pmatrix} \mathbf{G} \\ \begin{pmatrix} 2 & -1 & 0 \\ -1 & 3 & -1 \\ 0 & -1 & 2 \end{pmatrix} \end{pmatrix} \right] \begin{pmatrix} \mathbf{x} \\ \begin{pmatrix} \phi_{n1} \\ \phi_{n2} \\ \phi_{n3} \end{pmatrix} \end{pmatrix} &= \begin{pmatrix} \mathbf{B} \\ \begin{pmatrix} 1 & 0 & 0 \\ 0 & 1 & 0 \\ 0 & 0 & 1 \end{pmatrix} \end{pmatrix} \begin{pmatrix} \mathbf{u} \\ \begin{pmatrix} i_p \\ I1 \\ I2 \end{pmatrix} \end{pmatrix} \\
 \begin{pmatrix} u_p \\ u_{I1} \\ u_{I2} \end{pmatrix} &= \begin{pmatrix} \mathbf{L}^T \\ \begin{pmatrix} 1 & 0 & 0 \\ 0 & 1 & 0 \\ 0 & 0 & 1 \end{pmatrix} \end{pmatrix} \begin{pmatrix} \mathbf{x} \\ \begin{pmatrix} \phi_{n1} \\ \phi_{n2} \\ \phi_{n3} \end{pmatrix} \end{pmatrix}. \quad (4.1)
 \end{aligned}$$

The system of the network with additional current sources now contains three ports, one port for the pin and two ports for the independent current sources. The current at the pin, as well as the currents of the independent sources, are defined as inputs of the system in \mathbf{u} . The voltage at the pin, as well as the voltages across the independent current sources, are defined as outputs of the system in \mathbf{y} . Note that the system matrices \mathbf{C} , \mathbf{G} are equal to the network without independent current sources (Sec. 2.4). Thus for this network the system matrices are still symmetric and positive (semi-)definite. The symmetric 3-port transfer function of the reciprocal RC-network is given with

$$\begin{aligned}
 \mathbf{Z}(s) &= \begin{pmatrix} 1/3 & -1/3 & -1/3 \\ -1/3 & 1/3 & 1/3 \\ -1/3 & 1/3 & 1/3 \end{pmatrix} \frac{1}{s+1} + \begin{pmatrix} 1/2 & 0 & 1/2 \\ 0 & 0 & 0 \\ 1/2 & 0 & 1/2 \end{pmatrix} \frac{1}{s+2} + \\
 &\quad \begin{pmatrix} 1/6 & 1/3 & -1/6 \\ 1/3 & 2/3 & -1/3 \\ -1/6 & -1/3 & 1/6 \end{pmatrix} \frac{1}{s+4}. \quad (4.2)
 \end{aligned}$$

having the same poles as the transfer function of the network without sources.

For illustration purposes the system of the network is to be reduced with several model reduction algorithms. The frequency range of interest where the transfer behavior is to be approximated is set to from 10^{-5} Hz to 10^5 Hz, as in the reduction of the network without sources (Sec. 3.1.8).

As described in the former section, all reduction algorithms have several disadvantages if the number of ports is large. For example, the methods dealing directly with the network, as well

as the methods based on Gaussian elimination are unable to reduce the network. All nodes need to be preserved, which rules out the use of these methods. The next method is the reduction with moment matching by projection of the system matrices. As the number of ports is three, the smallest possible Krylov-subspace of first order already has three columns. This leads to a projection matrix with three columns as well. A projection, with a projection matrix generated in this way, would result in a reduced order model of order three. Thus no reduction is possible with moment matching. Due to the large number of ports, and in this example the number of ports is equal to the order of the unreduced system, no reduction is possible with moment matching methods. In systems where the number of ports is smaller than the order of the unreduced system a reduction is possible. Even though the reduction efficiency is strongly limited.

Next a reduction method based on the Gramians of the system is used. Due to the possible preservation of properties of a system describing a network, the PMTBR algorithm presented in [91] is used. Gramian-based methods do not directly depend on the number of ports, as stated in Sec. 3.1.5. But, as will be shown with this example, there is an indirect dependency. For estimation of the approximation error, the Hankel Singular Values are used (Sec. 3.1.5). In the PMTBR algorithm only an approximation of the HSV is used. The exact as well as the approximated HSV are calculated for the example network. As can be seen in Fig. 4.3, the exact as well as the approximated HSV of the system decay very slowly. All HSV, both the exact as well as the approximated, have a similar order of magnitude. This shows that this illustrative example is hardly reducible. Despite the bad estimation of the reducibility,

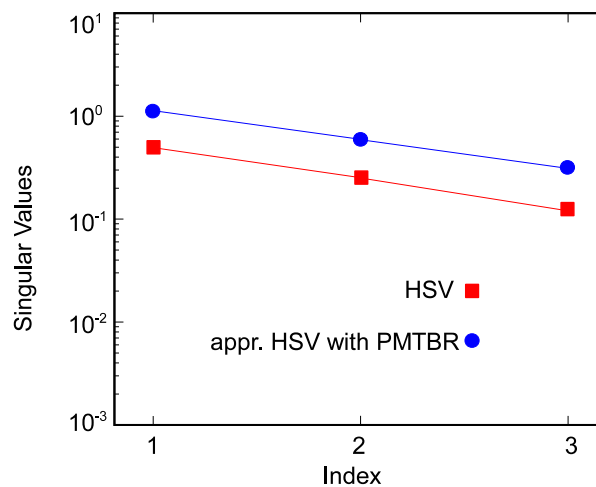


Figure 4.3: HSV and the approximated HSV for the illustrative network with sources

the system is reduced with PMTBR from order $N = 3$ to orders of $n = 2$ and $n = 1$. The resulting reduced systems are given in the following, whereas for readability reasons all values

are rounded. The reduced system of order $n = 2$ is given by

$$\left[s \begin{array}{c} \underbrace{\tilde{\mathbf{C}}}_{\begin{pmatrix} 1 & 0 \\ 0 & 1 \end{pmatrix}} + \underbrace{\tilde{\mathbf{G}}}_{\begin{pmatrix} 1 & 0 \\ 0 & 2 \end{pmatrix}} \end{array} \right] \underbrace{\begin{pmatrix} \tilde{\mathbf{x}} \\ \tilde{\phi}_{n1} \\ \tilde{\phi}_{n2} \end{pmatrix}}_{\tilde{\mathbf{x}}} = \underbrace{\begin{pmatrix} -0.5774 & -0.5774 & -0.5774 \\ 0.7071 & 0 & -0.7071 \end{pmatrix}}_{\tilde{\mathbf{B}}} \underbrace{\begin{pmatrix} i_p \\ I1 \\ I2 \end{pmatrix}}_{\mathbf{u}} \quad (4.3)$$

$$\underbrace{\begin{pmatrix} u_p \\ u_{I1} \\ u_{I2} \end{pmatrix}}_{\tilde{\mathbf{y}}} = \underbrace{\begin{pmatrix} -0.5774 & 0.7071 \\ -0.5774 & 0 \\ -0.5774 & -0.7071 \end{pmatrix}}_{\tilde{\mathbf{L}}^T} \underbrace{\begin{pmatrix} \tilde{\phi}_{n1} \\ \tilde{\phi}_{n2} \end{pmatrix}}_{\tilde{\mathbf{x}}}$$

with the transfer function with two poles

$$\tilde{\mathbf{Z}}_{n=2}(s) \approx \begin{pmatrix} 1/3 & 1/3 & 1/3 \\ 1/3 & 1/3 & 1/3 \\ 1/3 & 1/3 & 1/3 \end{pmatrix} \frac{1}{s+1} + \begin{pmatrix} 1/2 & 0 & -1/2 \\ 0 & 0 & 0 \\ -1/2 & 0 & 1/2 \end{pmatrix} \frac{1}{s+2}. \quad (4.4)$$

The reduced system of order $n = 1$ is

$$\left[s \begin{array}{c} \underbrace{\tilde{\mathbf{C}}}_{(1)} + \underbrace{\tilde{\mathbf{G}}}_{(1)} \end{array} \right] \underbrace{\begin{pmatrix} \tilde{\mathbf{x}} \\ \tilde{\phi}_{n1} \end{pmatrix}}_{\tilde{\mathbf{x}}} = \underbrace{\begin{pmatrix} -0.5774 & -0.5774 & -0.5774 \end{pmatrix}}_{\tilde{\mathbf{B}}} \underbrace{\begin{pmatrix} i_p \\ I1 \\ I2 \end{pmatrix}}_{\mathbf{u}} \quad (4.5)$$

$$\underbrace{\begin{pmatrix} u_p \\ u_{I1} \\ u_{I2} \end{pmatrix}}_{\tilde{\mathbf{y}}} = \underbrace{\begin{pmatrix} -0.5774 \\ -0.5774 \\ -0.5774 \end{pmatrix}}_{\tilde{\mathbf{L}}^T} \underbrace{\begin{pmatrix} \tilde{\phi}_{n1} \end{pmatrix}}_{\tilde{\mathbf{x}}}$$

with the transfer function with one pole

$$\tilde{\mathbf{Z}}_{n=1}(s) \approx \begin{pmatrix} 1/3 & 1/3 & 1/3 \\ 1/3 & 1/3 & 1/3 \\ 1/3 & 1/3 & 1/3 \end{pmatrix} \frac{1}{s+1}. \quad (4.6)$$

The coefficients of $\tilde{\mathbf{B}}$, $\tilde{\mathbf{L}}$ and in the transfer function are not equal and differ in the 10th decimal, which is not shown here due to readability purpose. Also note the fact that the poles of the reduced transfer functions being quite similar to several of the original transfer function poles is a coincidence. The poles differ after several decimals, which is not shown in this work due to readability. For other parameters of the reduction and larger networks the poles will differ more from that of the original transfer function.

The transfer function is calculated in several points in the frequency range of interest. Transfer function plots of the reduced systems can be seen in Figs. 4.4-4.7. For the transfer function $Z_{1,1}$, describing the impedance behavior at the pin, the results for the system with a reduced order of $n = 2$ are quite good (Fig. 4.4). The approximation error of the magnitude and the

phase is below 20% in the whole frequency range of interest (Fig. 4.5). But as can be seen for the transfer function $Z_{3,1}$, describing the transfer impedance between the right current source and the pin, large errors occur in frequencies above 0.1 Hz (Fig. 4.6,4.7). The system with a reduced order of $n = 1$ is not feasible, as all transfer functions have unacceptable errors in almost the whole frequency range of interest (Figs. 4.4-4.7).

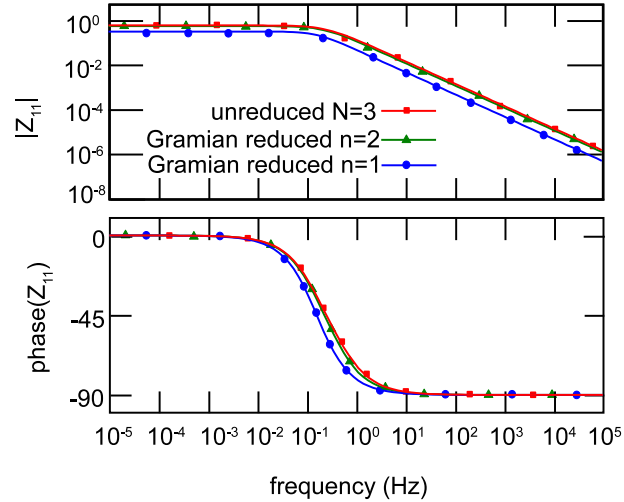


Figure 4.4: Illustrative example transfer function $Z_{1,1}$ of the original and the reduced models with extracted sources

The network without distributed sources was efficiently reduced in Sec. 3.1.8. With the reduction in this section the lowered efficiency with state-of-the-art model reduction methods is shown, if the network contains additional distributed sources. Due to the large number of ports, resulting from the extraction of the sources, with model reduction methods no feasible reduced model can be generated. None of the reduced systems approximate the original system with a tolerable approximation error in the frequency range of interest. With other reduction methods similar characteristics can be expected, due to the dependency of the reduction efficiency on the number of ports as described in Sec. 4.1.2. With this illustrative example it is show that some networks with a large number of sources cannot be reduced efficiently with standard model reduction methods.

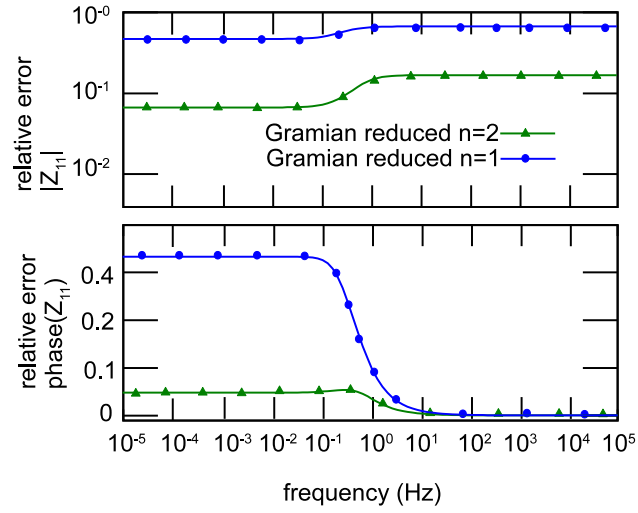


Figure 4.5: Relative approximation error of the illustrative example transfer function $Z_{1,1}$ of the reduced models with extracted sources

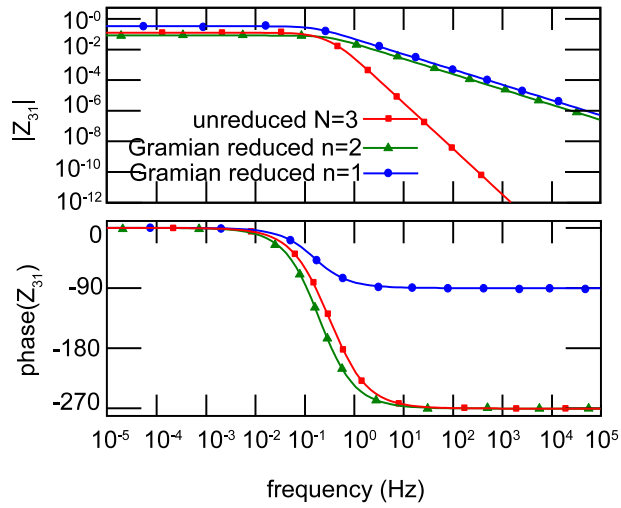


Figure 4.6: Illustrative example transfer function $Z_{3,1}$ of the original and the reduced models with extracted sources

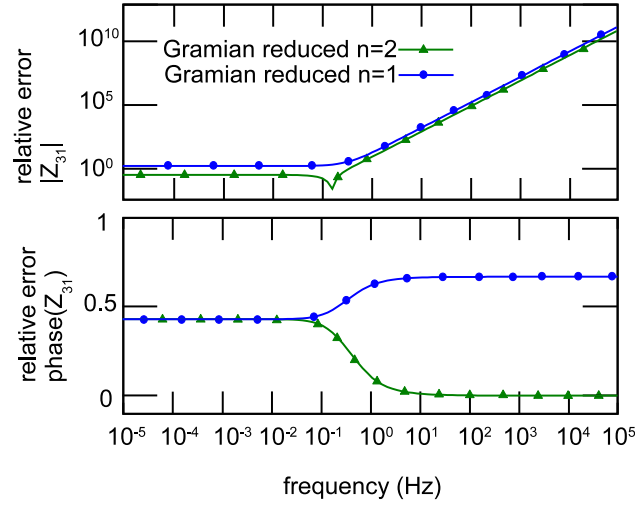


Figure 4.7: Relative approximation error of the illustrative example transfer function $Z_{3,1}$ of the reduced models with extracted sources

4.1.2.2 Illustrative RC-Grid

As a further example for the illustration of the arising problems of the reduction of networks with a large number of ports, an RCI-grid model is used in this section. The RCI-grid contains a $d \times d$ array of nodes, where each node is connected with its direct neighbors and ground by a resistor. In addition, each node is connected by a capacitor to ground. This results in overall d^2 capacitors and around $2d^2$ resistors. The values of the elements are randomly chosen within the range of $1 \pm 0.5\Omega$ and $0.1 \pm 0.05F$ for the resistors and capacitors, respectively. Two pins are located at opposite corners of the array, marking specified nodes, whose behavior is to be approximated in a reduced model. The frequency range of interest, where the transfer behavior is to be approximated, is set from 10^{-5}Hz to 10^5Hz . In addition to the resistive and capacitive elements q independent current sources are connected between arbitrary chosen nodes of the network and ground, modeling distributed sources' behavior. Exemplary, the resulting structure of the network for $d = 3$ and $q = 4$ is shown in Fig. 4.8. This network structure is for example used in the field of modeling of power grids in integrated circuit design [10, 11, 40, 125, 126].

Different networks with varying sizes d and a varying number of sources q will be used to show the trends in the reducibility of networks, depending on the model size and the number of sources. For investigations, the size of the grid is chosen between $d = 10$ and $d = 100$. The number of independent sources q is varied from five to 250. This leads to a range of network sizes between 100 nodes connected by 300 elements and 10000 nodes connected by 30000 elements. For the reduction all independent sources are extracted and connected through ports with the system. The networks are described with the help of MNA as linear systems which leads to systems ranging from order 100 to 10000. The number of ports ranges from 7 to 252, including the two nodes where the behavior of the network is to be approximated in a reduced model.

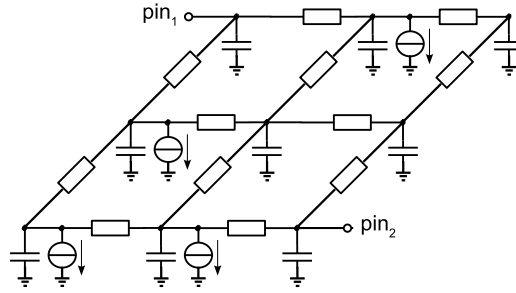


Figure 4.8: Section of the RCI-grid with independent current sources

As reduction method the Gramian-based PMTBR is used [91] (Sec. 3.1.5). Due to the approximation of the HSV during the reduction, a good insight into the reducibility of the models is possible. As with PMTBR only an approximation to the real HSV is calculated, the accuracy of the approximation is compared for several small networks. As first step, the number $1 \leq k \leq e$ of expansion points used in the PMTBR reduction algorithm in Eqn. 3.58 is varied. With a larger number of expansion points, distributed in the frequency range of interest, the approximated HSV converge to the original HSV [91]. In Fig. 4.9 the HSV, as well as the HSV approximated with PMTBR for a different number e of expansion points, for an RCI-grid ($d = 20, q = 20$) are shown. It can be seen that for 15 expansion points the approximated HSV calculated during PMTBR are in good correlation to the HSV. This shows that a sufficient number of expansion points enables a fast approximation of the HSV with PMTBR. Another comparison for the accuracy of the approximated HSV is shown in Fig. 4.10. The HSV of the system of a network with $d = 10, q = 250$ and $d = 10, q = 50$ are compared with the approximated HSV during PMTBR. The decay of the HSV, which is of interest in the reduction process, is well approximated. It is noticeable that the calculation of the HSV for this example is in the range of days on actual computers and thereby only the approximation of the HSV with PMTBR is used in the following. For larger networks the exact HSV cannot be calculated due to the high computational effort. The approximation of the HSV with PMTBR is quite good for showing the trends of reducibility as presented with the following examples.

As the preliminary investigations in this section have shown that the PMTBR algorithm can be used to compute fast approximations to the HSV, this algorithm is used to show the dependency of the reducibility of a network on the number of extracted distributed sources. For a network with $d = 30$ the largest singular values for a varying number of sources q are shown in Fig. 4.11. The resulting system has an order of 900 and the number of ports varies between seven, five for the extracted sources and two for the pins, up to 202, 200 for the extracted sources and two for the pins. It can be seen in Fig. 4.11 that for a larger number ports the approximated HSV decay slower. For comparison, the size of the network is increased and leading with $d = 100$ to a system of an order of 10000. The number of extracted sources is varied from 20 to 250. The resulting approximated HSV are shown in Fig. 4.12 and follow the same trend of slower decay rate for a larger number of ports.

For both networks a similar trend of the decay of the approximated HSV depending on the number of ports is observed. With a larger number of ports the HSV decay slower. The esti-

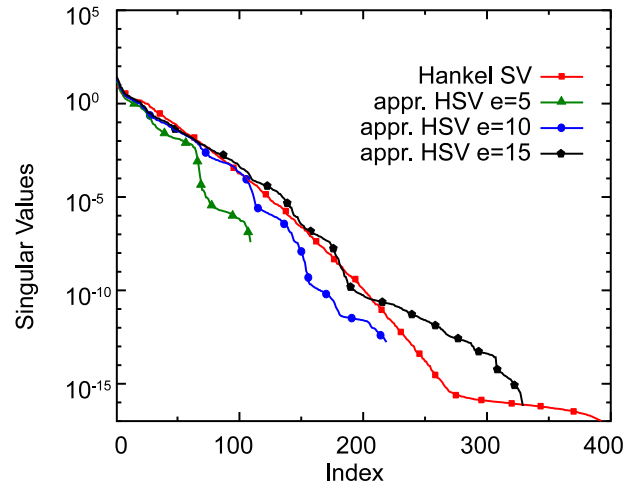


Figure 4.9: HSV and approximated HSV for the $d = 20$ RCI-grid with $q = 20$ extracted sources and a varying number e of expansion points

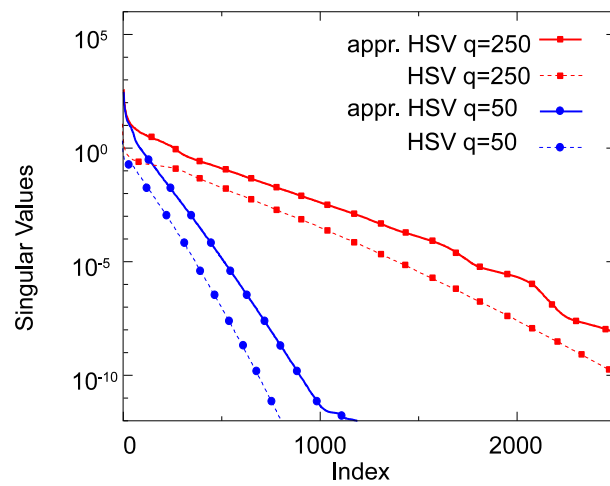


Figure 4.10: HSV and approximated HSV for the $d = 10$ RCI-grid with a varying number q of extracted sources

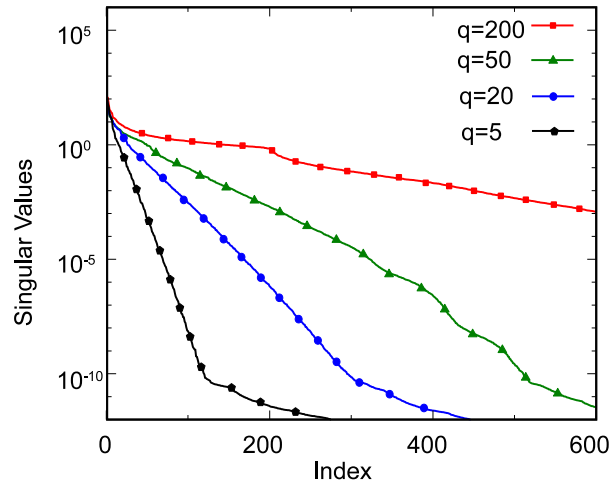


Figure 4.11: HSV of the $d = 30$ RCI-grid networks with a varying number q of extracted sources

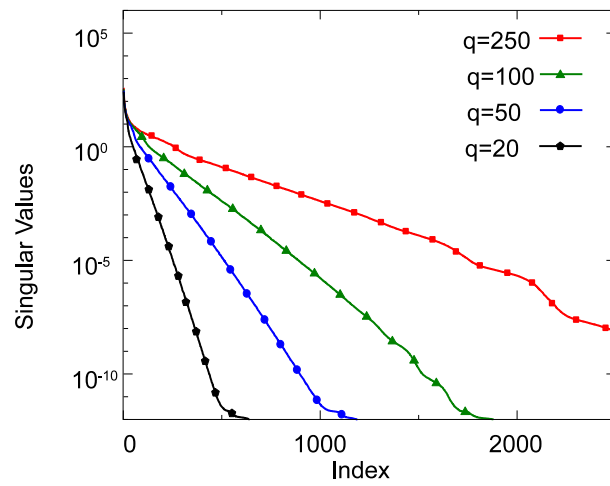


Figure 4.12: HSV of the $d = 100$ RCI-grid networks with a varying number q of extracted sources

mated approximation error of a reduced model is given by the sum of the HSV corresponding to the truncated states. For a system with slower decaying HSV, for a given estimated error of the reduced model the necessary size of the reduced model is larger. This means that for a given approximation error of a reduced model, the networks with a larger number of extracted sources can be less effectively reduced. Vice versa for a given reduced order, the reduced systems are less accurate, if the number of ports is larger. This leads to the conclusion that the reduction efficiency is lower for networks with a larger number of ports. Thus a high number of extracted distributed sources in a network, leading to a large number of ports, limits the reduction efficiency of the network.

Similar results to the observations in this section are presented in [91, 125, 127], where power grids and RC-meshes with a varying number of ports are investigated, which proves the observations in this section.

4.2 State-of-the-Art Reduction of Ports

For dealing with the large number of ports of a reducible network in model reduction, several methods are developed. The methods can be roughly divided into four basic mechanisms. The first group of methods use reduction algorithms, which have a less decreased efficiency for systems with a large numbers of ports. Nevertheless, all reduction algorithms suffer from the direct or indirect dependency of the efficiency on the number of ports. The second group of methods use the partitioning of the networks into several subnetworks or the partitioning of the transfer function. The usage of the correlation of the behavior of several ports is the basis for the third method. The fourth method is based on the limitation of allowed signals and the incorporation of determined input signals in a reduced order simulation process. The main ideas of the last three methods, as well as their advantages and drawbacks are presented in this section.

4.2.1 Partitioning

The basic idea behind the partitioning of systems of networks with a large number of ports is that many systems with a low number of ports can be more efficiently reduced than one system with a large number of ports. Due to the linearity of the reducible networks, the overall behavior can be obtained by superposition of the single subsystem.

The general partitioning flow is shown in Fig. 4.13 for systems with k inputs and l outputs. Note that for systems of electrical networks $k = l$ holds, as one electrical value at the port is the input and the dual electrical value is the output. The network is described as a system with a large number of inputs and outputs. The system is divided into subsystems by partitioning. A subsystem has to have a lower number of ports compared to the complete system. Each subsystem is reduced with model reduction techniques. The resulting overall reduced system is given by assembling the reduced subsystems. The system assembled by the reduced subsystems should be smaller compared to the reduced system with a large number of ports. Several partitioning methods are presented in the following.

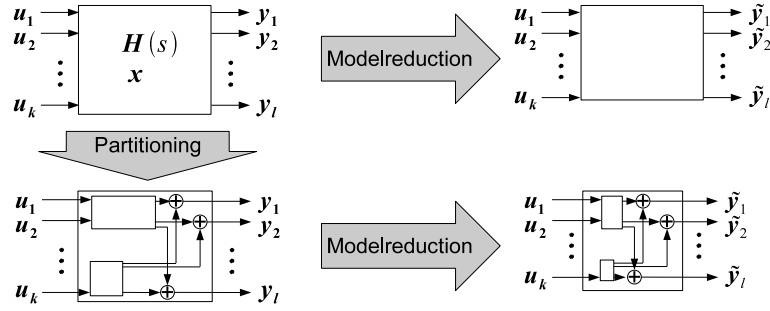


Figure 4.13: Model reduction of systems with a large number of ports by partitioning into subsystems with a smaller number of ports and reduction of the subsystems

4.2.1.1 Partitioning into MIMO-Systems

The first method is the partitioning of a system with a large number of ports into small subsystems with a lower number of ports (Fig. 4.14) as for example used in [128]. The partitioning is

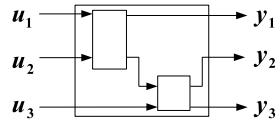


Figure 4.14: Partitioning into MIMO-subsystems with a smaller number of ports

based on block-wise partitioning of the transfer function. Every subsystems contains multiple inputs and multiple outputs (MIMO). This method can be also used for loosely coupled networks, where a partitioning in subnetworks with only a few ports can be found. The method of finding such a partitioning can be based on the knowledge of the internal structure of the model, on heuristic search algorithms [128] or on graph theoretic methods [129, 130].

4.2.1.2 Partitioning into SIMO-Systems

Another method for partitioning is given in [131], where all subsystems contain exactly one input and produce a portion of all outputs (Fig. 4.15). The resulting subsystems are single input multiple output (SIMO) systems. By superposition, the system outputs $y_i(s)$ are calculated from the j th subsystem outputs $y_{i,j}(s)$ with

$$\mathbf{y}_i(s) = \sum_{j=1}^k \mathbf{y}_{i,j}(s) = \sum_{j=1}^k \mathbf{H}_{i,j}(s) u_j(s). \quad (4.7)$$

The partitioning is a column-wise partitioning of the transfer function. The number of subsystems equals the number of inputs. After order reduction the reduced subsystems are given with $\tilde{\mathbf{H}}_i(s)$. The resulting reduced transfer function of the overall system is

$$\mathbf{H}(s) \approx \tilde{\mathbf{H}}(s) = [\tilde{\mathbf{H}}_1(s), \tilde{\mathbf{H}}_2(s), \dots, \tilde{\mathbf{H}}_k(s)]. \quad (4.8)$$

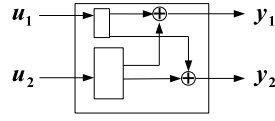


Figure 4.15: Partitioning into SIMO-subsystems with a smaller number of ports

The advantage of this method is that every subsystem has only one input.

4.2.1.3 Partitioning into SISO-Systems

The partitioning into subsystems with one input and one output [132] is another partitioning method (Fig. 4.16). The resulting subsystems are single input single output (SISO) systems.

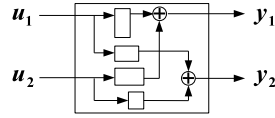


Figure 4.16: Partitioning into SISO-subsystems with a smaller number of ports

The transfer functions of the overall system are given by the subsystems transfer functions $\mathbf{H}_{i,j}(s)$ with

$$\mathbf{H}(s) = \begin{pmatrix} H_{1,1}(s) & \dots & H_{1,l}(s) \\ \vdots & \ddots & \vdots \\ H_{k,1}(s) & \dots & H_{k,l}(s) \end{pmatrix}. \quad (4.9)$$

The partitioning is an element-wise partitioning of the transfer function. The number of subsystems equals the number of input ports multiplied with the number of output ports, and therefore the number of coefficients in the matrix transfer function of the complete system. With order reduction of every element of the matrix transfer function the reduced transfer function is

$$\mathbf{H}(s) \approx \tilde{\mathbf{H}}(s) = \begin{pmatrix} \tilde{H}_{1,1}(s) & \dots & \tilde{H}_{1,l}(s) \\ \vdots & \ddots & \vdots \\ \tilde{H}_{k,1}(s) & \dots & \tilde{H}_{k,l}(s) \end{pmatrix}. \quad (4.10)$$

Advantageous in this method is that every subsystem is a SISO-system and model reduction algorithms, only capable of reducing SISO systems, can now be applied to the subsystems [59, 132].

4.2.1.4 Partitioning into MISO-Systems

Based on methods of process control a partitioning of a system into subsystems with multiple inputs and a single output (MISO) (Fig. 4.17) is presented in [133]. The method is based on

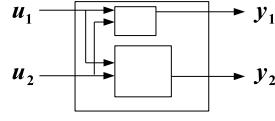


Figure 4.17: Partitioning into MISO-subsystems with a smaller number of ports

row-wise partitioning of the transfer function. This results in as many subsystems as there are outputs of the complete system. Every subsystem is reduced and the approximated outputs are given by the corresponding reduced subsystem transfer function

$$\tilde{\mathbf{y}}_i(s) = \tilde{\mathbf{H}}_i(s)\mathbf{u}. \quad (4.11)$$

For this partitioning method several approximative variants are built, where several inputs can be neglected for some outputs. This reduces the number of inputs of the subsystems. The method is based on the fact that not all inputs are relevant for an output. With the help of a relative gain array, defined with

$$\lambda = \begin{pmatrix} \lambda_{1,1} & \dots & \lambda_{1,k} \\ \vdots & \ddots & \vdots \\ \lambda_{l,1} & \dots & \lambda_{l,k} \end{pmatrix}, \quad (4.12)$$

the interaction of an input and an output can be quantified [134]. Every element of the relative gain array describes the coupling between the input and an output

$$\lambda_{i,j} = \frac{(\Delta y_i / \Delta u_j)|_{u=\text{constant}}}{(\Delta y_i / \Delta u_j)|_{y=\text{constant}}}. \quad (4.13)$$

A subsystem for every output is built and by defining a lower bound of interaction between the inputs and the output, the number of inputs of every subsystem is lowered. With this method the number of ports of the subsystems is also lowered. The subsystems can be even more efficiently reduced with model reduction algorithms. An extension of the method is given in [126], where multiple outputs are allowed in a subsystem and the resulting inputs are the union of the dominant inputs for all outputs. Only the dominant inputs for the given outputs are used in the reducible subsystem. In the approaches of [126, 133] an arbitrary choice of the bound to neglect the interaction is used. The error induced by this step is possibly small, but cannot be controlled. Also generally there is no basis for the assumption that an interaction, as small as it may be, is insignificant in networks.

4.2.1.5 Conclusion

A drawback of all methods based on partitioning is that the arising problems for systems with a large number of ports are shifted to the problem of dealing with a large number of systems describing one model. Instead of one reduced system a large number of reduced systems is generated, which have to be composed into the complete reduced system. This requires a calculation overhead in the simulation of the reduced subsystems, and also an increased number

of elements if the reduced subsystems are synthesized as electrical network. In addition, properties of the complete system, such as passivity and reciprocity, are typically not preserved in the subsystems, and can therefore not be preserved during the model reduction. Also error estimation and control is more complicated. If the reduced subsystems have small tolerable approximation errors the overall reduced system may still have an unacceptable high error.

4.2.2 Port Correlation

The idea that in regularly structured networks the electrical characteristics at the ports show a correlation gives rise to the next port reduction method illustrated in Fig. 4.18. The ports of the reducible part of the network are reduced. For the connection with other networks a coupling network maps the reduced number of ports with the original outer ports.

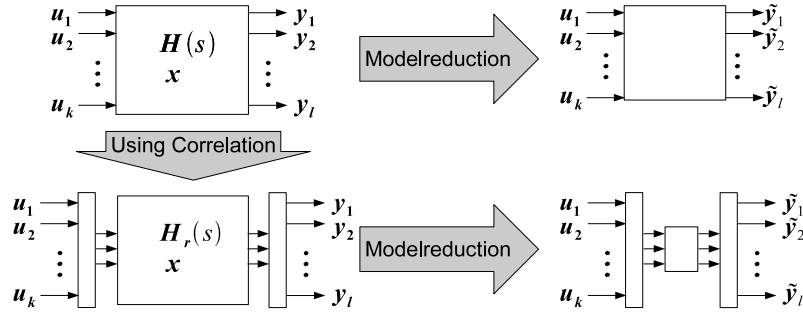


Figure 4.18: Model reduction of systems with a large number of ports by taking into account port correlations

A method based on the port correlation is presented in [135]. If the network is regularly structured, the transfer function of the network can be described with a low rank approximation. The idea is similar to the approximation of matrices by performing a singular value decomposition (SVD) and keeping only the important singular values and singular vectors. A SVD of the transfer function at DC gives

$$\mathbf{H}(s=0) = \mathbf{L}^T \mathbf{G}^{-1} \mathbf{B} = \mathbf{U} \boldsymbol{\Sigma} \mathbf{V}^T \quad (4.14)$$

where $\boldsymbol{\Sigma}$ is a diagonal matrix containing the singular values of $\mathbf{H}(s=0)$. Singular values which are large in magnitude are called dominant. An approximation is obtained by keeping only the r dominant singular values

$$\mathbf{H}(s=0) = \mathbf{U} \boldsymbol{\Sigma} \mathbf{V}^T \approx \mathbf{U}_r \boldsymbol{\Sigma}_r \mathbf{V}_r^T. \quad (4.15)$$

By approximation of \mathbf{L} , \mathbf{B} with

$$\begin{aligned} \mathbf{L} &\approx \mathbf{L}_r \mathbf{U}_r^T \\ \mathbf{B} &\approx \mathbf{B}_r \mathbf{V}_r^T \end{aligned} \quad (4.16)$$

using the Moore-Penrose-Pseudoinverse

$$\begin{aligned}\mathbf{L}_r &= \mathbf{L}\mathbf{U}_r(\mathbf{U}_r^T\mathbf{U}_r)^{-1} \\ \mathbf{B}_r &= \mathbf{B}\mathbf{V}_r(\mathbf{V}_r^T\mathbf{V}_r)^{-1}\end{aligned}\quad (4.17)$$

the transfer function can now be written as

$$\mathbf{H}(s) \approx \mathbf{U}_r \underbrace{\mathbf{L}_r^T(\mathbf{G} + s\mathbf{C})^{-1}\mathbf{B}_r}_{\mathbf{H}_r(s)} \mathbf{V}_r^T. \quad (4.18)$$

Now the transfer function $\mathbf{H}_r(s)$ has a lowered number r of ports and is reduced with model reduction algorithms

$$\tilde{\mathbf{H}}_r(s) \approx \mathbf{H}_r(s). \quad (4.19)$$

The overall reduced transfer function is then given by

$$\tilde{\mathbf{H}}(s) = \mathbf{U}_r \tilde{\mathbf{H}}_r(s) \mathbf{V}_r^T. \quad (4.20)$$

Extensions are presented by using SVD of the transfer function at frequencies different from DC, of the (higher) moments at DC or any other frequency [136] or even multiple frequencies [137]. In addition, methods based on distinguishing between input and output moments [138] and by partitioning of the transfer function and SVD of every partition [136] are presented.

Another approach based on the correlation of the ports is TermMerg [139]. By a clustering algorithm the inputs and outputs are grouped with respect to their timing behavior. For each group of input ports a representative input port is created. A representative output port represents a group of outputs. With this method inputs and outputs are merged into a small number of representative ports.

The main advantage of the methods based on correlation is that the number of ports is reduced while the allowed signals at the ports remain arbitrary. Another advantage is that only one reduced system is generated. Only the knowledge of the inner structure of the network, which is determined before the reduction, is used for the reduction of the number of ports. This advantage entails a major drawback: the correlation of the ports requires the network to have a regular structure. Most examples reduced with these methods contain only RC-elements [135, 136, 138, 139], due to the simple structure and therefore possibly higher correlation. For RLC-networks the necessary correlation is a quite strong limitation. The transfer behavior is much more complicated than in RC-networks due to effects like undershoot, overshoot or ringing, and the correlation of the ports is quite low. In addition for RLC-networks, the correlation of transfer functions at DC or a specific frequency point cannot be easily generalized for predictions in the whole frequency band. Therefore, the frequency points used for the determination of the correlation of the ports have to be chosen carefully.

A major drawback of the methods based on port correlation is that no error estimation or error control exists. The methods are based on arbitrarily chosen limits for separating the singular values into important and negligible. Also as shown in [138], the limits for the SVD have to be

adjusted by manual inspection of the singular values to achieve better results, showing that the whole process is not completely automated at this time.

Passivity preservation is an important factor in model reduction of electrical networks. The SVD-based port reduction algorithm cannot preserve passivity in the general case. The loss of passivity is because the SVD-based port reduction method includes the singular vectors in the model reduction process. The port reduced system is not passive in the general case. For the special case of reciprocal electrical networks, described by an impedance or admittance transfer function, where all ports are defined bidirectional and $\mathbf{B} = \mathbf{L}$ is fulfilled, the transfer function is symmetric leading to $\mathbf{V}_r = \mathbf{U}_r$. For this case the passivity can be preserved using appropriate order reduction algorithms. But with the drawback of low efficiency of the SVD-based methods for systems with bidirectional ports [138], the passivity preservation lowers the efficiency. In the TermMerg method the passive network part is not changed and the ports for the connection with other networks are connected with a coupling network. The coupling network for the connection of the representative ports with the ports for the connection with other networks can be non-passive. Only the passivity of the inner part, excluding the coupling network, can be preserved using appropriate model reduction algorithms [138].

4.2.3 Connected Models and Input Signals

The approaches of port reduction presented in this section rely on the fact that information of the elements connected with a port is known a priori. This information is included in the model reduction to enable a higher reduction efficiency.

4.2.3.1 Correlated Input Signals

An approach based on stochastically distributed input signals is presented in [91, 127]. The approach is inspired by the simulation of parasitic coupling networks for packages or substrates in the modeling of integrated circuits. In these parasitic coupling networks the signals have quite similar characteristics. For the reduction this property is used and it is assumed that on the ports always a correlation of the excitation is present. For example, the input signals can have a typical waveform where a little derivation in phase and magnitude is allowed, which results in a high correlation of the input signals. The method is based on the Gramian-based model reduction algorithms (Sec. 3.1.5), whereas the Controllability Gramian \mathbf{X} needs to be computed with the Lyapunov Equation

$$\mathbf{G}\mathbf{X}\mathbf{C}^T + \mathbf{C}\mathbf{X}\mathbf{G}^T = \mathbf{B}\mathbf{B}^T. \quad (4.21)$$

Assuming a correlation of the input signals u , a correlation matrix \mathbf{K} for k samples of the inputs can be calculated

$$\mathbf{K}_{i,j} = \frac{1}{k} \sum_{l=1}^k u_i^l u_j^l \quad (4.22)$$

and can be included in the Lyapunov equations with

$$\mathbf{G}\mathbf{X}_K\mathbf{C}^T + \mathbf{C}\mathbf{X}_K\mathbf{G}^T = \mathbf{B}\mathbf{K}\mathbf{B}^T \quad (4.23)$$

resulting in a controllability Gramian \mathbf{X}_K , whose eigenvalues decay faster if the correlation described in \mathbf{K} is high [127]. As the decay of the eigenvalues gives an insight of the possible error of the reduced model, a faster decay of the eigenvalues allows for a more efficient model reduction. An advantage of using this method is that the input signals have not to be known a priori; only the correlation of them has to be estimated. The major drawback of this method is that, if the estimation of the waveforms is quite bad, the resulting model is not accurate enough. If only a few of the input waveforms can be estimated before the reduction, the other input signals can remain undetermined, leading to an identity submatrix in \mathbf{K} for the uncorrelated ports. A drawback of this method is the restriction to Gramian-based model reduction algorithms. The preservation of system properties, such as stability, passivity and reciprocity, can be preserved by using appropriate Gramian-based reduction methods. Preservation of system matrix properties like (J-)symmetry, (semi-)definiteness and block structure is more complicated or even impossible for Gramian-based methods as described in Sec. 3.1.5. Thus, the major drawback of the methods based on correlated input signals is the limitation to the Gramian-based model reduction method.

4.2.3.2 Determined Input Signals

A second approach relying on input information is presented in [140–142]. The approach is inspired by the simulation of power grids. A power grid is typically built as an RC-mesh, modeling the parasitic behavior in an integrated circuit. Independent current sources are distributed over the network, modeling the influence of the switching currents. The voltage distribution at the grid nodes is investigated by simulation. In these models all inputs at all ports are determined before the reduction. This a priori given information is used in the reduction process. In standard reduction the inputs \mathbf{u} are undetermined and the matrix \mathbf{B} , connecting the inputs with the system, is used in the reduction. Due to the large number of columns for a large number of ports this limits the efficiency of model reduction methods. In the methods, based on the determined inputs, instead of \mathbf{B} the product $\mathbf{B}\mathbf{u}$ is used in model reduction. This product has only one column, leading to a more efficient reduction. For piece-wise linear waveforms of the inputs $\mathbf{u}(s)$ the method in [140, 141] uses the modeling as weighted delayed ramps in the frequency domain with the moments expansion at $s = 0$

$$\mathbf{u}(s) = \mathbf{u}_0 + \mathbf{u}_1s + \mathbf{u}_2s^2 \dots \quad (4.24)$$

The model reduction process is done accordingly to projection on Krylov subspaces. For the subspace generation

$$\begin{aligned} \mathcal{K}_n(\mathbf{R}, \mathbf{A}) &= (\mathbf{R}, \mathbf{A}\mathbf{R}, \dots, \mathbf{A}^{n-1}\mathbf{R}) \\ \mathbf{A} &= -(s_0\mathbf{C} + \mathbf{G})^{-1}\mathbf{C} \\ \mathbf{R} &= (s_0\mathbf{C} + \mathbf{G})^{-1}\mathbf{B} \end{aligned} \quad (4.25)$$

in Eqn. 3.34 is used in the projection, where the number of columns of the subspace is the order of the subspace multiplied with the number of ports. Instead, the subspace generation of the method in [140, 141] uses

$$\begin{aligned}\mathcal{K}_n(\mathbf{R}, \mathbf{A}) &= (\mathbf{R}_1, \mathbf{A}\mathbf{R}_2, \dots, \mathbf{A}^n\mathbf{R}_n) \\ \mathbf{A} &= -(s_0\mathbf{C} + \mathbf{G})^{-1}\mathbf{C} \\ \mathbf{R}_i &= (s_0\mathbf{C} + \mathbf{G})^{-1}\mathbf{B}\mathbf{u}_i s_0^i,\end{aligned}\tag{4.26}$$

where the number of columns of the subspace is equal to the order of the subspace. The rest of the reduction process is done by implicit moment matching by projection of the system matrices as described in Sec. 3.1.4. This method is strongly correlated with the Krylov-subspace reduction by projection and cannot be used with other order reduction algorithms. Also this method is limited to piece-wise linear waveforms of the inputs. Another algorithm relying on input information, but using the Gramian-based model reduction method, is proposed in [142]. The input signals are represented by fast Fourier transformation. For the reduction the PMTBR algorithm [91], as described in Sec. 3.1.5 is used. The slight change is that instead of using

$$\mathbf{z}_k(s_0) = (s_0\mathbf{C} + \mathbf{G})^{-1}\mathbf{B}\tag{4.27}$$

(Eqn. 3.58), the input information is included by using

$$\mathbf{z}_k(s_0) = (s_0\mathbf{C} + \mathbf{G})^{-1}\mathbf{B}\mathbf{u}_k(s_0)\tag{4.28}$$

in the model reduction. The advantage of this alteration is that the columns of $\mathbf{z}_k(s_0)$ are now equal to one, whereas in the standard approach the size equals the number of input ports. For the rest of the reduction the Gramian-based reduction flow of Sec. 3.1.5 is used.

The main advantage of the methods of [140–142] is the high efficiency. Independently on the number of sources, the reduction is done as if the system has only one port. The drawback is that no undetermined inputs are allowed. The complete network with all excitations has to be given. No other network models can be connected to the reduced model after model reduction. This leads to the conclusion that this reduction method is more into a reduced order simulation than a model reduction.

4.2.3.3 Specified Loads

Another approach for the reduction of networks with a large number of ports is based on information about the connected elements, and is presented in [143]. The method is based on the fact that only predefined elements are connected with a port. This approach is inspired by the simulation of coupled transmission lines. In the simulation of transmission lines the ports are divided into transmitter ports, whereas several drivers are connected, and into receiver ports, where the loads are connected. Following this, the ports are divided into ports with unknown connected driver elements and ports where the kind of load is specified. The loads that can be included are linear resistive, linear capacitive or combined linear capacitive and resistive elements. Also the range of the values of the loads is known before the reduction process.

The loads are incorporated into the system and the element values of the loads are included as parameters in the reducible system matrices

$$[s\mathbf{C}(c_1, c_2, \dots) + \mathbf{G}(g_1, g_2, \dots)] \mathbf{x} = \mathbf{B}\mathbf{u}. \quad (4.29)$$

The order reduction is done with respect to these parameters in addition to the frequency

$$\tilde{\mathbf{H}}(s, c_1, c_2, \dots, g_1, g_2, \dots) \approx \mathbf{H}(s, c_1, c_2, \dots, g_1, g_2, \dots). \quad (4.30)$$

Thus the problem of the reduction of systems with a large number of ports is shifted to the parameterized reduction of systems [144–149], where the system is reduced with respect to more than one parameter. The advantage of this method is the higher efficiency if the range of the allowed parameters of the connected loads is relatively small. But if the range of the allowed element values is broadened, the efficiency is lowered dramatically, which is well-known for the parameterized model reduction algorithms [146].

4.3 Port Reduction Method

As shown in the former sections, the algorithms for the reduction of networks with a large number of ports suffer from several disadvantages. Partitioning methods produce a large number of reducible subsystems describing the complete system. Furthermore, properties of the complete system are not preserved in the subsystems. Methods relying on correlation of ports are limited to networks with regular structures. The methods, incorporating information about the connected networks, require model reduction methods producing parametric reduced models and are thereby limited in efficiency and synthesizability as an electrical network. Other methods, incorporating input signals information, either require knowledge about all system inputs, leading to a simulation method instead of a model reduction method. Or the methods are limited in the model reduction algorithms to Gramian-based reduction which is not capable of preservation of several relevant system and network properties.

In this section a new method dealing with the problem of the model reduction of networks with a large number of distributed sources is presented. The proposed method overcomes most of the disadvantages of the former methods. Nevertheless, the proposed method is limited to networks with distributed sources as used in this work, resulting in a more limited range of application compared to the former methods.

Every element modeling the distributed sources has to be extracted from the linear time-invariant network part and connected by a port. The number of ports is quite large for a large number of distributed sources (Sec. 4.1.1). This large number of ports limits the reduction of the network with model reduction techniques (Sec. 4.1.2). The method presented in this section is based on reducing the number of ports for the network elements modeling the distributed sources. In the port reduction the knowledge of the distributed sources' behavior is taken into account. For the independent sources the waveforms and for the nonlinear elements the describing functions are considered. Based on this knowledge the number of necessary ports for the distributed sources elements is reduced, which will be described in the following sections.

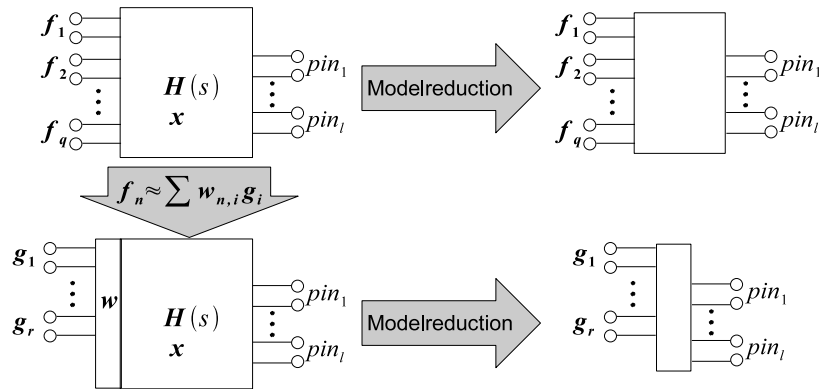


Figure 4.19: Schematic flow of port reduction as preceding step of the model reduction

The overall port reduction flow is shown in Fig. 4.19. The original reducible network (upper left part in Fig. 4.19) has a large number of ports \mathbf{u} for the connection with other network models and $\mathbf{f}(\mathbf{x}, t)$ for the network elements modeling the distributed sources. Due to the large number of ports only a slight reduction is possible (upper right part in Fig. 4.19). With a port reduction method the number of ports for the distributed sources is lowered. The functions of the network elements modeling the distributed sources span a function space. The dimension of this function space equals the number of functions, and thereby the number of distributed sources elements. As the number of the distributed sources elements is typically very high in the models under consideration, the dimension of the function space spanned in this way is also very high. The dimension of the function space of the distributed sources is lowered, resulting in a lower number of basis functions $\mathbf{g}(\mathbf{x}, t)$. Several applicable methods for the reduction of the dimension of the function space of the distributed sources are presented in Sec. 4.3.1. The function space with a reduced dimension is realized in the network, whereas the network elements modeling the distributed sources are replaced. System and network properties of the reducible network part are preserved during this step. This replacement and the preservation of relevant properties is shown in Sec. 4.3.2. Only the functions of the reduced dimension function space have to be extracted from the reducible part (lower left part in Fig. 4.19). The number of extracted elements is lower, and therefore the number of ports of the reducible network part is also lower. The overall number of ports is lowered, as the number of ports is now given by the number of pins for the connection with other networks and the number of elements realizing the basis functions, which is lower than the original number of sources. An efficient implementation of this method in existing model reduction flows is shown in Sec. 4.3.3. The resulting network, having a lower number of ports, can now be more efficiently reduced with model reduction techniques (lower right part in Fig. 4.19). The higher efficiency of the model reduction techniques will be presented in Sec. 4.3.4.

4.3.1 Reduction of the Dimension of the Function Space

For the port reduction method of this work the function space spanned by the distributed sources' models has to be described by a reduced dimension function space. In this section

an overview of methods, which are capable for the reduction of the dimension of the function space, is given.

For the reduction of the dimension of the function space methods of approximation theory, device modeling, function analysis and data processing can be used. In these methods mostly for one function an approximation is searched for. Contrary to this, for reducing the dimension of the function space for several functions, a shared subset of basis functions is searched for.

For every set of functions describing the distributed sources, a reduction of the dimension of the function space is to be found. The functions describing the distributed sources' models are taken into account, independently on the type of distributed sources' model, either nonlinear controlled sources' functions or waveforms of independent sources. For q independent sources the variable is the time, which is starting typically at zero and is continuously increasing. The functional values are currents or voltages and thus the functions describe current- or voltage-waveforms

$$\begin{aligned} U_j &= f_j(t) & \text{or} \\ I_j &= f_j(t) \\ 1 &\leq j \leq q. \end{aligned} \tag{4.31}$$

For q nonlinear controlled sources the variables are currents and voltages and the functional values are also currents or voltages, therefore the functions are U-I curves

$$\begin{aligned} U_j &= f_j(x_1, x_2, \dots, x_m) = f_j(I_1, I_2, \dots, U_1, U_2, \dots) & \text{or} \\ I_j &= f_j(x_1, x_2, \dots, x_m) = f_j(I_1, I_2, \dots, U_1, U_2, \dots) \\ 1 &\leq j \leq q \end{aligned} \tag{4.32}$$

where all functional values depend on m variables. In this section it is not necessary to divide between nonlinear controlled sources and independent sources. The difference between these two kinds of elements lies only in the interpretation of the functions and only the term $f_j(x)$ is used in the following for readability reasons.

The original q -dimensional function space is spanned by the functions $f(x)$. For all functions a decomposition in the form of the weighted linear combination

$$\begin{aligned} f_j(x) &\approx \sum_{i=1}^r w_{j,i} g_i(x) \\ 1 &\leq j \leq q \\ r &< q. \end{aligned} \tag{4.33}$$

with the basis functions $g_i(x)$ and the weights matrix

$$\mathbf{W} = \begin{pmatrix} w_{1,1} & \cdots & w_{1,r} \\ \vdots & \ddots & \vdots \\ w_{q,1} & \cdots & w_{q,r} \end{pmatrix} \tag{4.34}$$

is searched for. A function space is spanned by the r basis functions $g(x)$, having a lower dimension if $r < q$ holds. The reduction of the dimension of the function space is hereby formulated by finding an exact or approximative decomposition in the form of Eqn. 4.33. The functions of the distributed sources $f(x)$ can be approximated with the reduced dimension function space, spanned by $g(x)$, as described in Eqn. 4.33 by linear combination with the weights \mathbf{W} .

The reduction of the dimension of the function space can be divided with respect to several properties. Depending on the type of basis function the decomposition can be locally or globally valid. In the range of validity the decomposition can be exact or approximative. The parameters of the decomposition can be calculated directly or can be estimated by an iterative method. Despite this, the overall result, a reduction of the dimension of the function space in the form of Eqn. 4.33, is the same for all presented methods.

Several methods, which can be used to reduce the dimension of the function space of widely used models for distributed sources, are presented in the following section. Firstly the simplest method for reducing the dimension of the function space is presented in Sec. 4.3.1.1 by grouping functions. For more sophisticated methods, the class of functions used for the modeling of the distributed sources, is taken into account. The first class are piece-wise linear functions, used for independent sources as well as nonlinear controlled sources, which can be decomposed into basis functions as presented in Sec. 4.3.1.2. In the second class models for distributed sources are taken into account, which are valid in a specified range and can therefore be described by a small set of polynomial basis functions using a series expansion in Sec. 4.3.1.3. The third and most general class are general nonlinear functions, where basis functions can be found by using the neural network modeling approach of approximation theory, which is presented in Sec. 4.3.1.4.

4.3.1.1 Grouping into Equal and Proportional Functions

In this section the method of grouping functions, to reduce the dimension of the function space of distributed sources' models in the form of Eqn. 4.33, is presented.

In several behavioral models the distributed sources are modeled in a simple way. In these models only a few functions are used for the behavior of the distributed sources. This behavior is multiplied with a specified gain and the resulting sources' functions are distributed in the model. For example, in the modeling of distributed sources in distributed systems a typical function of the sources is measured or determined by simulation. According to the strength of activity of the source in the distributed system this typical function is amplified or attenuated.

The simplest way of obtaining basis functions of a reduced dimension function space is by grouping the functions again. Every group of functions is represented by a basis function, where all distributed sources' functions are equal to this basis function or can be calculated by a weighting factor multiplied with this basis function. The method is illustrated in Fig. 4.20 for an amount of q distributed sources' functions $f(\mathbf{x})$. All of these functions are grouped into equal or proportional functions, represented by r basis functions $g(\mathbf{x})$.

With every representing basis function a function space can be spanned. The dimension of

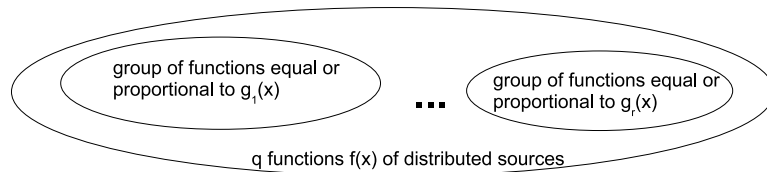


Figure 4.20: Grouping distributed sources' functions into functions equal or proportional to a basis function

this function space is lower if in at least one group at least two functions are joined. The larger the number of functions that can be represented by one basis function is, the lower is the necessary number of basis functions. The lower the number of necessary basis functions, the lower the dimension of the function space that is necessary for modeling the distributed sources' behavior. With grouping, a simple, but yet often applicable, method for the reduction of the dimension of the function space is presented.

4.3.1.2 Piece-Wise Linear Basis Functions

In several modeling aspects the functions describing the distributed sources of the model are given as piece-wise linear (PWL) functions. In several models the PWL-functions are an approximation to much more complicated nonlinear functions. In other models the functions are determined through measurement of a finite number of functional values and the behavior between these functional values is linearly approximated.

For the reduction of the dimension of the function space of the PWL-functions used in these models several conditions are used below. It is assumed that the functions of the q distributed sources are given as tabulated data in k points. Thus the functions are described for k sections. For every j th function ($1 \leq j \leq q$) of the k points, the corresponding l th ($1 \leq l \leq k$) functional value $f_j(x_l)$ of the point x_l is given. It is assumed that for every of the q functions the functional values are given in the same points x_l . If the points for which the functional values are given are different for several functions, the union of all variables have to be used and the missing functional values have to be calculated by interpolation for the presented methods.

For a given set of tabulated data, several PWL approximations can be used. In this section the step-function approximation, an approximation of continuous lines and section-wise PWL-functions with discontinuities are considered. As there is an infinite number of possible representations several straightforward decompositions and the canonical representation of Chua [150] are presented for the reduction of the dimension of the function space. The conditions for the applicability of the methods for the proposed port reduction of this work are given in the following sections.

4.3.1.2.1 Continuous PWL-functions Firstly the reduction of the dimension of the function space spanned by continuous PWL-functions is presented. The class of piece-wise constant as well as piece-wise linear functions is used. For illustration the tabulated data given in Tab. 4.1 is used in the following.

Table 4.1: Example data for the PWL representation

| l | x_l | $f_1(x_l)$ | $f_2(x_l)$ | $f_3(x_l)$ | $f_4(x_l)$ | ... | $f_q(x_l)$ |
|-----|-------|------------|------------|------------|------------|-----|------------|
| 1 | 0 | 0 | 0 | 0 | 0 | ... | 0 |
| 2 | 1 | 1 | -1 | 0 | 2 | ... | 2 |
| 3 | 2 | 3 | 2 | -1 | 2 | ... | 1 |
| 4 | 3 | 0 | 0 | 0 | 0 | ... | 0 |

In the class of piece-wise constant functions the functional value of every given variable is kept constant in a section between several variables as shown in the left part of Fig. 4.21 for the example data of Tab. 4.1. There are several possibilities for decomposing piece-wise constant functions into basis functions. Two different methods, based on signum functions

$$\text{sgn}(x) = \begin{cases} -1, & x < 0 \\ 0, & x = 0 \\ 1, & x > 0 \end{cases} \quad (4.35)$$

are represented.

One set of basis functions is built from shifted signum functions as shown as the first set of basis functions in Fig. 4.21. For piece-wise constant functions with k sections at least $r = k$ basis functions

$$g_i(x) = \frac{1}{2} \left[\text{sgn}(x - x_i + \frac{1}{2}) + 1 \right] \quad (4.36)$$

are necessary. The number of basis functions is less or equal k , and thereby the function space with a reduced dimension has a dimension equal to or lower than the number of sections used in the modeling of the distributed sources. The weights w of the linear combination of Eqn. 4.33 are obtained by the difference between the functional values of adjacent sections with

$$w_{j,i} = f_j(x_i) - f_j(x_{i-1}). \quad (4.37)$$

For the illustrative example data, three basis functions span the reduced dimension function space. The matrix \mathbf{W} containing the weights w for the linear combination of Eqn. 4.33 is calculated to

$$\mathbf{W} = \begin{bmatrix} 1 & 2 & -3 \\ -1 & 3 & -2 \\ 0 & -1 & 1 \\ 2 & 0 & -2 \\ \dots & & \\ 2 & -1 & -1 \end{bmatrix}. \quad (4.38)$$

Another set of basis functions can be obtained by using bars built from two shifted signum functions

$$g_i(x) = \frac{1}{2} \left[\text{sgn}(x - x_i + \frac{1}{2}) - \text{sgn}(x - x_i - \frac{1}{2}) \right] \quad (4.39)$$

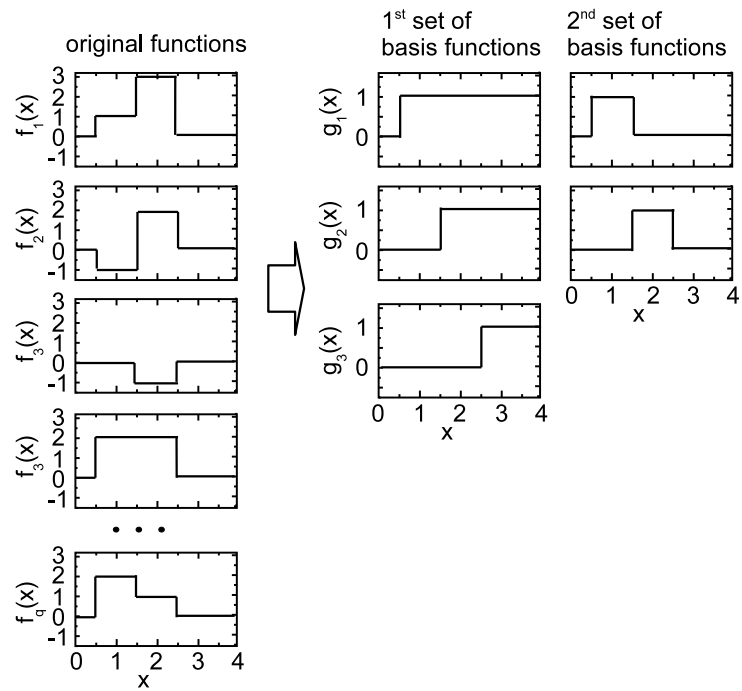


Figure 4.21: Piece-wise constant representation functions of the example data and two sets of basis functions

as shown in Fig. 4.21 with the second set of basis functions. For functional values that are zero for $\pm\infty$ the number of basis functions is less or equal the number of sections k . The weights w of the linear combination of Eqn. 4.33 are given directly by the functional values with

$$w_{j,i} = f_j(x_i). \quad (4.40)$$

For the illustrative example data two basis functions span the reduced dimension function space. The matrix \mathbf{W} containing the weights w for the linear combination of Eqn. 4.33 is calculated to

$$\mathbf{W} = \begin{bmatrix} 1 & 3 \\ -1 & 2 \\ 0 & -1 \\ 2 & 2 \\ \dots & \\ 2 & 1 \end{bmatrix}. \quad (4.41)$$

Another method for decomposition of piecewise constant functions into basis functions is based on wavelet-decomposition using the Haar-wavelet as basis function. This method will be explained as a special case in Sec. 4.3.1.4.

Another class of PWL-functions is constructed by approximating the sections between given values with a continuous linear function with a slope a . For illustration the tabulated data of Tab. 4.1 is used and the corresponding PWL-functions are graphically shown in Fig. 4.22. For this type of PWL-function the corresponding slopes $a_{j,i}$ of each segment of each function can be calculated with

$$a_{j,i} = \frac{f_j(x_{i+1}) - f_j(x_i)}{x_{i+1} - x_i}. \quad (4.42)$$

The decompositions presented are based on ramp functions, which can be defined in several ways with

$$\begin{aligned} \text{rmp}(x) &= \begin{cases} x, & x \geq 0 \\ 0, & x < 0 \end{cases} \\ &= \frac{1}{2} (\text{sgn}(x) + 1) x \\ &= \frac{1}{2} (|x| + x). \end{aligned} \quad (4.43)$$

One set of basis functions is given with shifted ramp functions and graphically shown as the first set in Fig. 4.22 for the illustrative example data. This set of basis functions is defined with

$$g_i(x) = \text{rmp}(x - x_i). \quad (4.44)$$

The number of basis functions, which span the reduced dimension function space, depends on the number of sections k used in the modeling of the distributed sources' behavior. This decomposition can be used if the functional values are bounded and if the functional values

diverge for ∞ , because the basis functions are also diverging. The weights w of the linear combination of Eqn. 4.33 are obtained by the difference of the slope between adjacent sections

$$w_{j,i} = a_{j,i} - a_{j,i-1}. \quad (4.45)$$

For the illustrative example data, four basis functions span the reduced dimension function space. The matrix \mathbf{W} containing the weights w for the linear combination of Eqn. 4.33 is calculated to

$$\mathbf{W} = \begin{bmatrix} 1 & 1 & -5 & 3 \\ -1 & 4 & -5 & 2 \\ 0 & -1 & 2 & -1 \\ 2 & -2 & -2 & 2 \\ \dots & & & \\ 2 & -3 & 0 & 1 \end{bmatrix} \quad (4.46)$$

for the example data.

As another set of basis functions the shifted ramp functions shown as second set in Fig. 4.22 for the illustrative example data. The shifted ramp basis functions are defined by

$$g_i(x) = \text{rmp}(x - x_i) - \text{rmp}(x - x_i - 1). \quad (4.47)$$

For this set of basis functions the weights w of the linear combination of Eqn. 4.33 can be calculated by the slope of each segment

$$w_{j,i} = a_{j,i}. \quad (4.48)$$

The number of necessary basis functions depends on the number of sections k used in the modeling of the distributed sources' behavior. This decomposition is only feasible for bounded functions, as the basis functions are also bounded. For functions diverging for $\pm\infty$ an infinite number of basis functions would be necessary by using this decomposition. For the illustrative example data, three basis functions span the reduced dimension function space. The matrix \mathbf{W} containing the weights w for the linear combination of Eqn. 4.33 is calculated to

$$\mathbf{W} = \begin{bmatrix} 1 & 2 & -3 \\ -1 & 3 & -2 \\ 0 & -1 & 1 \\ 2 & 0 & -2 \\ \dots & & \\ 2 & -1 & -1 \end{bmatrix} \quad (4.49)$$

for the example data.

By using triangular functions another decomposition can be obtained. The resulting basis functions are shown as the third set in Fig. 4.22 for the illustrative example data. Shifted triangular functions

$$\begin{aligned} g_i(x) &= \begin{cases} 1 - |x - x_i|, & |x - x_i| < 1 \\ 0, & \text{otherwise} \end{cases} \\ &= \text{rmp}(x - x_i) - 2\text{rmp}(x - x_i - 1) + \text{rmp}(x - x_i - 2) \end{aligned} \quad (4.50)$$

are used as basis functions. The number of necessary basis functions using the triangular functions is less or equal the number of sections k used in the modeling of the distributed sources' behavior. The weights w of the linear combination of Eqn. 4.33 are calculated with the functional values by

$$w_{j,i} = f_j(x_i). \quad (4.51)$$

For the illustrative example data only two basis functions span the reduced dimension function space. The matrix \mathbf{W} containing the weights w for the linear combination of Eqn. 4.33 are calculated to

$$\mathbf{W} = \begin{bmatrix} 1 & 3 \\ -1 & 2 \\ 0 & -1 \\ 2 & 2 \\ \dots & \\ 2 & 1 \end{bmatrix} \quad (4.52)$$

for the example data.

For the methods of this section it is assumed that for all functions $f(0) = 0$ holds. In distributed sources of models where this condition does not hold an offset basis functions $f(x) = const.$ has to be used, increasing the dimension of the reduced function space by one.

A reduced dimension function space is necessary for the port reduction presented in this work. In this section, for several continuous PWL-functions of one variable, methods are presented which are able to lower the dimension of the function space of models of distributed sources. With illustrative example data it is shown that basis functions spanning the reduced dimension function space can be found. The dimension mostly depends on the number of sections used in the modeling of the distributed sources. By using the presented methods, for a large number of continuous PWL-functions, described by a lower number of PWL sections, the dimension of the function space can be reduced.

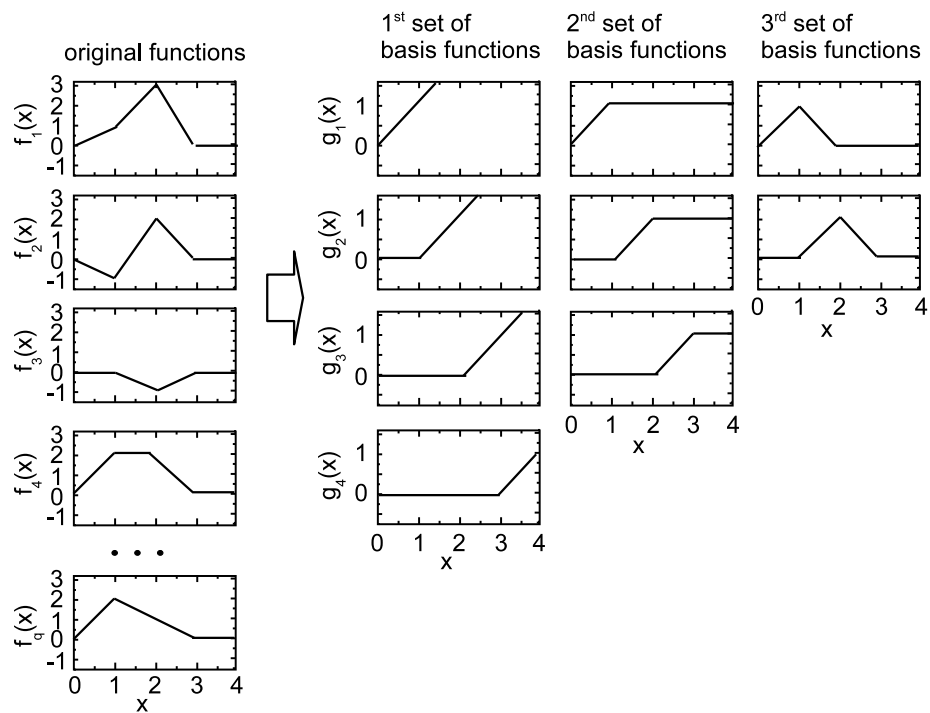


Figure 4.22: Piece-wise linear representation functions of the example data and three sets of basis functions

4.3.1.2.2 PWL-functions with Finite Jump Discontinuities Another class of PWL-functions is section-wise linear with finite jump discontinuities. Example functions are shown in the left part of Fig. 4.23, for illustration purpose. The functions are defined the tabulated

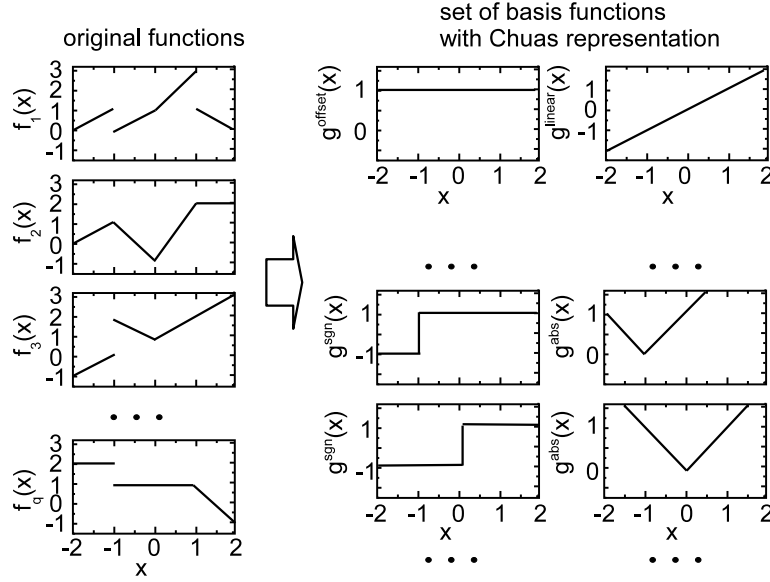


Figure 4.23: Piece-wise linear representation functions with jump discontinuities of the example data and a canonical set of basis functions

data in Tab. 4.2. It is assumed that the slope of the first and last segment continues to $\pm\infty$. For this class of functions a canonical representation

$$f_j(x) = w_j^0 + w_j^{lin}x + \sum_{i=1}^k w_{j,i}^{abs}|x - x_i| + \sum_{i=1}^k w_{j,i}^{sgn}\text{sgn}(x - x_i) \quad (4.53)$$

is proposed by Chua in [150]. The advantage of this representation is the closed analytical form, which allows for analytical studies and the fast computation of the coefficients. The representation can be easily used to determine a decomposition of PWL-functions including discontinuities in the form of Eqn. 4.33. The basis functions that span the reduced dimension function space are defined with

$$\begin{aligned} g^0 &= 1 \\ g^{lin}(x) &= x \\ g_i^{abs}(x) &= |x - x_i|; \quad 1 \leq i \leq k \\ g_i^{sgn}(x) &= \text{sgn}(x - x_i); \quad 1 \leq i \leq k \end{aligned} \quad (4.54)$$

and are graphically shown in the right part of Fig. 4.23. The original functions can be obtained by linear combination of the reduced dimension basis functions where the weights w of

Table 4.2: Example data for the PWL representation with finite jump discontinuities

| l | x_l | $f_1(x_l)$ | $a_{f_1}(x_l)$ | $f_2(x_l)$ | $a_{f_2}(x_l)$ | $f_3(x_l)$ | $a_{f_3}(x_l)$ | ... | $f_q(x_l)$ | $a_{f_q}(x_l)$ |
|-----|-------|------------|----------------|------------|----------------|------------|----------------|-----|------------|----------------|
| 0 | -2 | 0 | 1 | 0 | 1 | -1 | 1 | ... | 2 | 0 |
| 1 | -1 | $1^-/0^+$ | 1 | 1 | -2 | $0^-/2^+$ | -1 | ... | $2^-/1^+$ | 0 |
| 2 | 0 | 1 | 2 | -1 | 3 | 1 | 1 | ... | 1 | 0 |
| 3 | 1 | $3^-/1^+$ | -1 | 2 | 0 | 2 | 1 | ... | 1 | -2 |

Eqn. 4.33 are, according to [150] with the slight correction of [151], defined with

$$\begin{aligned}
 w_j^{lin} &= \frac{1}{2}(a_{j,0} + a_{j,k}) \\
 w_{j,i}^{abs} &= \frac{1}{2}(a_{j,i} - a_{j,i-1}); \quad 1 \leq i \leq k \\
 w_{j,i}^{sgn} &= \begin{cases} 0, & \text{if } f(x_i) \text{ is continuous} \\ \frac{1}{2}[f(x_i^+) - f(x_i^-)] & \text{otherwise} \end{cases} \\
 w_j^0 &= f(0) - \sum_{i=1}^k [w_{j,i}^{abs}|x_i| + w_{j,i}^{sgn} \operatorname{sgn}(-x_i)]. \quad (4.55)
 \end{aligned}$$

The number of necessary basis functions and therefore the dimension of the function space is given by the number of sections used for the modeling of the distributed sources. Overall the number of necessary basis functions is less or equal $2k + 2$ for the representation of the PWL-functions using Chua's representation.

For the illustrative example data eight basis functions span the reduced dimension function space. The matrix \mathbf{W} containing the weights w for the linear combination of Eqn. 4.33 are calculated to

$$\begin{aligned}
 \mathbf{W} &= \begin{bmatrix} w^{lin} & w^0 & w_1^{abs} & w_2^{abs} & w_3^{abs} & w_1^{sgn} & w_2^{sgn} & w_3^{sgn} \end{bmatrix} \\
 &= \begin{bmatrix} 0 & 2 & 0 & 1/2 & -3/2 & -1/2 & 0 & -1 \\ 1/2 & 3/2 & -3/2 & 5/2 & -3/2 & 0 & 0 & 0 \\ 1 & 1 & -1 & 1 & 0 & 1 & 0 & 0 \\ \dots & & & & & & & \\ -1 & 3/2 & 0 & 0 & -1 & -1/2 & 0 & 0 \end{bmatrix} \quad (4.56)
 \end{aligned}$$

for the example data.

The reduced dimension function space, for the port reduction presented in this work, of distributed sources modeled with PWL-functions with finite jump discontinuities can be found by using the presented canonical representation.

4.3.1.2.3 Periodic PWL-functions Periodic functions are used especially in the modeling of PWL-functions describing waveforms of independent sources. For periodic functions the modeled function repeats within a specified period of variables, as for example in a period of

time. The periodicity is graphically shown in Fig. 4.24 for the example data of Tab. 4.1 repeating with a period of four variables. For this case a decomposition into basis functions with the former mentioned methods would lead to an unnecessary large number of basis functions, as the basis functions are non-periodic. A method to decompose the periodic PWL-functions into a smaller subset of basis functions is based on periodic basis functions. The PWL-functions are decomposed for one period. The resulting basis functions are repeated with the same period as the original functions. This is exemplary graphically shown in the basis functions of the right side of Fig. 4.24 for the set of basis functions in Eqn. 4.50 repeated with a period of four variables

$$g_i(x) = \begin{cases} 1 - |x - x_i|, & |x - x_i| < z \cdot T + 1, \\ 0, & \text{otherwise.} \end{cases} \quad z \in \mathbb{Z} \quad (4.57)$$

The number of necessary basis functions is now equal to the number of basis functions for one period, which is less or equal to the number of sections k in one period, as shown in the former paragraphs.

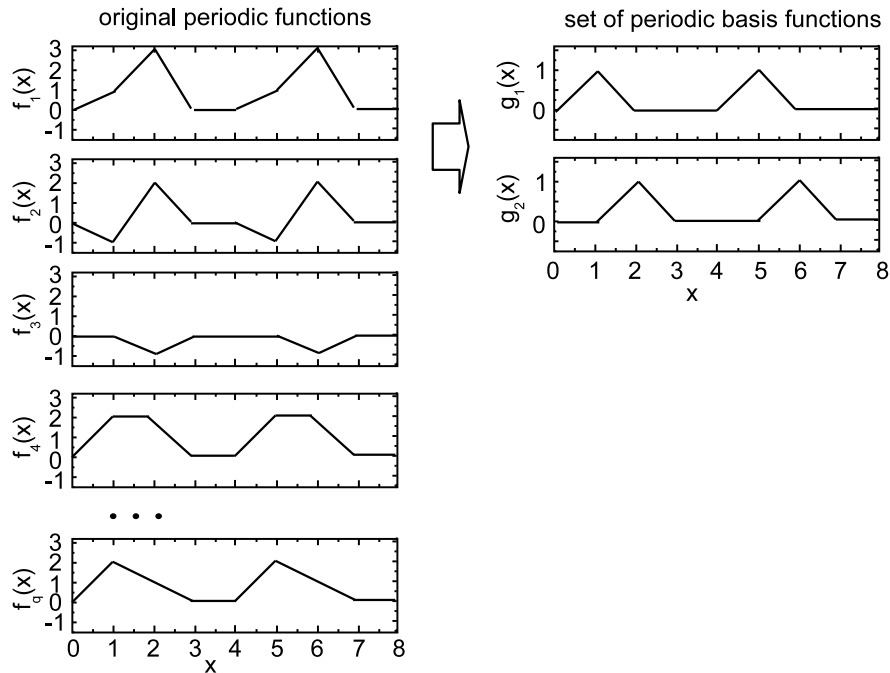


Figure 4.24: Periodic functions of the example data and a set of periodic basis functions

4.3.1.2.4 PWL-functions of Several Variables In the former sections all PWL-functions $f_j(x)$ are considered to depend on the same variable x . This is typical for elements like independent sources where the variable is time and for nonlinear controlled sources where one specified current or voltage controls all sources. In the more general case, functions $f_j(\mathbf{x}) = f_j(x_1, x_2, x_3, \dots, x_m)$ of m variables have to be considered. The class of elements

modeling distributed sources, which can be handled by the port reduction of this work, is extended to nonlinear controlled sources that are controlled by several currents or voltages. The methods presented in this section are based on methods of modeling nonlinear elements with PWL-functions. The main constraint in this area is the storage of the elements functions with a low number of parameters. The adaption of these methods for reducing the dimension of the function space of distributed sources is shown in the following.

The first class of functions considered here are defined according to [150] as continuous PWL over each cross section. This can be proven by freezing all except one variable. For clarity it is assumed that for every variable of every of the q functions the number of given functional values is k . These functions can now be described with

$$f(x_1, x_2, x_3, \dots, x_m) = \sum_{l_1=1}^k \sum_{l_2=1}^k \dots \sum_{l_m=1}^k w(l_1, l_2, \dots, l_m) \cdot \prod_{j=1}^m \phi_{l_j}(x_j) \quad (4.58)$$

with the parameters w and the functions

$$\begin{aligned} \phi_1(x_j) &= 1 \\ \phi_2(x_j) &= x_j \\ \phi_3(x_j) &= |x_j - x_{j1}| \\ &\dots \\ \phi_k(x_j) &= |x_j - x_{jk-2}|. \end{aligned} \quad (4.59)$$

The resulting function involves products of the terms $1, x_1, \dots, x_j, |x_1 - x_{11}|, \dots, |x_j - x_{jk-2}|$. This representation needs only a small amount of coefficients in comparison to the tabulated data representation. Nevertheless, for the representation of the function in the form of Eqn. 4.33 the number of basis functions grows exponentially with the number of sections k , and with the number of variables m , with $O(k^m)$. Every possible product of the terms $\phi(x_j)$ has to be treated as a basis function. This limits the efficiency of the decomposition of PWL-functions of several variables into a small set of basis functions. Thus only if the number of functions of distributed sources is large $q \gg k^m$, the decomposition leads to a significant reduction of the dimension of the function space.

The second class of considered PWL-functions are functions of m variables affine over a finite number of regions and bounded by k linear partitions. The representation for discontinuous functions is [151]

$$f_j(\mathbf{x}) = w_j^0 + \sum_{i=1}^m w_{j,i}^{lin} \mathbf{x}_i + \sum_{i=1}^k w_{j,i}^{abs} |\boldsymbol{\alpha}_{j,i}^T \mathbf{x} - \beta_{j,i}| + \sum_{i=1}^k w_{j,i}^{sgn} \text{sgn}(\boldsymbol{\alpha}_{j,i}^T \mathbf{x} - \beta_{j,i}) \quad (4.60)$$

where $\beta_{j,i}, \boldsymbol{\alpha}_{j,i} \in \mathbb{R}^m$. With this description the number of coefficients is dramatically lowered with $q + q \cdot m + k(q + m + 1)$ compared to tabulated data descriptions and the description of [150]. In the following it is assumed that the q functions of the distributed sources are defined on the same regions with equal partitioning boundaries. If the regions differ, the union of all partitioning boundaries has to be used for all functions. With the same partitioning

boundaries for all functions

$$\begin{aligned}\alpha_{j,i} &= \alpha_i \\ \beta_{j,i} &= \beta_i\end{aligned}\quad (4.61)$$

holds. The basis functions of for the form of Eqn. 4.33 are defined with

$$\begin{aligned}g^0 &= 1 \\ g^{lin}(x) &= x_i; \quad 1 \leq i \leq m \\ g_i^{abs}(x) &= |\alpha_i^T \mathbf{x} - \beta_i|; \quad 1 \leq i \leq k \\ g_i^{sgn}(x) &= \text{sgn}(\alpha_i^T \mathbf{x} - \beta_i); \quad 1 \leq i \leq k.\end{aligned}\quad (4.62)$$

This representation leads for functions of m variables with partitions with k boundaries to $1 + m + k$ basis functions for continuous and to $1 + m + 2k$ for discontinuous functions. Extensions for the representation are given in [152, 153].

The first example in [154] with $m = 2$ variables, $q = 2$ functions defined on regions partitioned by $k = 2$ boundaries is used for illustration purpose. The regions are defined in \mathbb{R}^2 and are shown in Fig. 4.25. The continuous functions defined on the four regions are given with

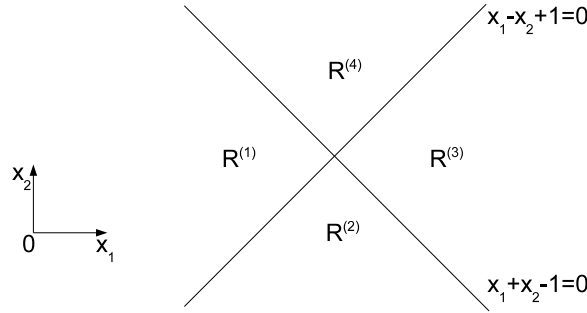


Figure 4.25: Regions for the PWL-functions of the example data

$$\begin{pmatrix} f_1(x_1, x_2) \\ f_2(x_1, x_2) \end{pmatrix} = \begin{pmatrix} -1 & 1 \\ 0 & -1 \end{pmatrix} \begin{pmatrix} x_1 \\ x_2 \end{pmatrix} + \begin{pmatrix} -1 \\ 1 \end{pmatrix}, \quad \text{for } \mathbf{x} \in R^{(1)} \quad (4.63)$$

$$\begin{pmatrix} f_1(x_1, x_2) \\ f_2(x_1, x_2) \end{pmatrix} = \begin{pmatrix} 3 & -3 \\ -2 & 1 \end{pmatrix} \begin{pmatrix} x_1 \\ x_2 \end{pmatrix} + \begin{pmatrix} 3 \\ -1 \end{pmatrix}, \quad \text{for } \mathbf{x} \in R^{(2)} \quad (4.64)$$

$$\begin{pmatrix} f_1(x_1, x_2) \\ f_2(x_1, x_2) \end{pmatrix} = \begin{pmatrix} 3 & -3 \\ 0 & 3 \end{pmatrix} \begin{pmatrix} x_1 \\ x_2 \end{pmatrix} + \begin{pmatrix} 3 \\ -3 \end{pmatrix}, \quad \text{for } \mathbf{x} \in R^{(3)} \quad (4.65)$$

$$\begin{pmatrix} f_1(x_1, x_2) \\ f_2(x_1, x_2) \end{pmatrix} = \begin{pmatrix} -1 & 1 \\ 2 & 1 \end{pmatrix} \begin{pmatrix} x_1 \\ x_2 \end{pmatrix} + \begin{pmatrix} -1 \\ -1 \end{pmatrix}, \quad \text{for } \mathbf{x} \in R^{(4)}. \quad (4.66)$$

The resulting canonical PWL-function is

$$\begin{pmatrix} f_1(x) \\ f_2(x) \end{pmatrix} = \mathbf{w}^0 + \mathbf{w}_1^{lin} x_1 + \mathbf{w}_2^{lin} x_2 + \mathbf{w}_1^{abs} |x_1 + x_2 - 1| + \mathbf{w}_2^{abs} |x_1 - x_2 + 1| \quad (4.67)$$

whereas the weights \mathbf{w} of the linear combination in the form of Eqn. 4.33 are given by

$$\mathbf{W} = [\mathbf{w}^0 \mathbf{w}_1^{lin} \mathbf{w}_2^{lin} \mathbf{w}_1^{abs} \mathbf{w}_2^{abs}]^T \quad (4.68)$$

with

$$\mathbf{w}^0 = \begin{bmatrix} 1 \\ -1 \end{bmatrix}, \mathbf{w}_1^{lin} = \begin{bmatrix} 1 \\ 0 \end{bmatrix}, \mathbf{w}_2^{lin} = \begin{bmatrix} -1 \\ 1 \end{bmatrix}, \mathbf{w}_1^{abs} = \begin{bmatrix} 0 \\ 1 \end{bmatrix}, \mathbf{w}_2^{abs} = \begin{bmatrix} 2 \\ -1 \end{bmatrix} \quad (4.69)$$

for the five basis functions. Note that the decomposition leads to an increase in the dimension of the function space, as the number of basis functions is higher than the number of original functions. Nevertheless, this method can be used for an arbitrarily large number of distributed sources' functions q . For a larger number q of sources, a decrease in the dimension of the function space can be obtained, as the number of basis functions is fixed for fixed boundaries. For the given example boundaries this decomposition can be used for $q > 5$ functions for a reduction of the dimension of the function space.

For an arbitrary number of boundaries the condition $q > 1 + m + k$ for continuous and $q > 1 + m + 2k$ for discontinuous functions has to hold for a reduction of the dimension of the function space. If the number of functions equals the number of variables, as for example used in modeling of semiconductor elements like transistors or diodes [155], the number of basis functions is higher than the number of original functions. Therefore no reduction of the dimension of the function space is possible for these models. The method is thereby only feasible, if the number of functions is higher than the number of variables $q \gg m$, which is for example the case for a large number of nonlinear controlled sources modeling distributed sources.

Methods of the description of PWL-functions of several variables, used in the modeling of distributed sources, are presented. A reduction of the dimension of the function space of the sources can be obtained by applying these methods. The reduced dimension of the function space of the distributed sources can be subsequently used in the port reduction presented in this work.

4.3.1.2.5 Further PWL-representations Beside the explicit representations there is a large investigation in the field of implicit PWL representations. For example, Chua's representation [150] presented above is also capable of describing unicursal multivalued functions. Nevertheless, for the method presented in this work an explicit function description of the distributed sources' models is necessary, which excludes the usage of the decomposition for the implicit description of unicursal functions.

Another type of PWL approximations is the lattice PWL function, where a finite set of local linear functions is used as basis functions. The general form contains min- and max-functions.

Construction methods are for example presented in [156, 157]. While these PWL approximations can be used to efficiently model one $f(x)$ function, it is untypical that several functions share the same basis functions. Thus this PWL representation can only be used in a few hypothetical cases to obtain a decomposition as in Eqn. 4.33 with a lowered dimension of the function space of distributed sources.

4.3.1.3 Polynomial Basis Functions

The series expansion is another method for the reduction of the dimension of the function space of the distributed sources. All sources' functions are expanded into polynomials up to a predefined order. For example, Newton polynomials, trigonometric polynomials, Bernstein polynomials or Lagrange polynomials can be used in the series expansion. The polynomials are the basis functions in a reduced dimension function space. By using this method, an approximation of the original function space is created, if the order of the polynomials is finite. Two typical series expansions, the Taylor series expansion as well as the Fourier series expansion are presented below. Their conditions are given for the use in the port reduction method of this work, to enable a higher efficiency of a model reduction.

4.3.1.3.1 Taylor Series Expansion That every continuous real function in a range $x_{low} \leq x \leq x_{high}$ can be approximated by algebraic polynomials as power series

$$P_n(x) = \sum_{k=0}^n w_k x^k \quad (4.70)$$

is stated in the Weierstrass approximation theorem [158].

This approximation is only valid in a defined range. An example for elements, where the domain space, which corresponds to the definition space of the describing function, is defined in the modeling process, are for example nonlinear controlled sources, modeling the behavior of distributed sources in a predefined range. For these elements the behavior is given with q nonlinear functions, valid in the defined domain space.

With the Taylor series expansion in a given point x_0 the basis functions for Eqn. 4.33 are defined with

$$g_i(x) = (x - x_0)^i, \quad 0 \leq i \leq r \quad (4.71)$$

and the weights $w_{j,i}$ can be calculated with the i th derivatives of the elements functions

$$w_{j,i} = \frac{1}{i!} f_j^{(i)}(x_0), \quad 0 \leq i \leq r. \quad (4.72)$$

These basis functions can be used for an r th order approximation. The order of approximation is set according to a specified accuracy. The decomposed functions of the nonlinear elements only differ in the coefficients. This decomposition method is feasible for the port reduction of this work, if the number of elements q is larger than the order of the power series approximation

r . Thereby $q \gg r$ has to hold for a significant reduction of the dimension of the function space of the distributed sources. If the sources' functions are defined in k different definition regions, the sources have to be grouped according to nearby definition regions. The approximation has to be done in way that all sources' functions are well approximated in the definition domain. In this case the overall number of basis functions has to be lower than the number of sources $\sum_{i=1}^k r_i \ll q$ to enable a significant decrease in the dimension of the function space of the sources.

With the power series expansion a reduction of the dimension of the function space of distributed sources is enabled. This reduction can be subsequently used for the port reduction method of this work.

4.3.1.3.2 Fourier Series Expansion A method for the decomposition of periodic non-linear functions of distributed sources is the decomposition into trigonometric polynomials. Typical models of distributed sources with periodic functions are independent sources, modeling a behavior that is periodic in time. Also for nonlinear elements with a predefined definition range an efficient modeling is enabled with trigonometric polynomials [159].

With the help of trigonometric polynomials the functions of all elements are decomposed into

$$f_j(x) \approx w_{j,0}g_0(x) + \sum_{i=1}^r w_{j,c,i}g_{c,i}(x) + \sum_{i=1}^r w_{j,s,i}g_{s,i}(x); \quad 1 \leq j \leq q. \quad (4.73)$$

For example, with the well-known method for the decomposition into trigonometric polynomials with Fourier series expansion the basis functions of Eqn. 4.33 are given with

$$\begin{aligned} g_0(x) &= 1 \\ g_{c,i}(x) &= \cos\left(i \frac{2\pi}{X} \cdot x\right) \\ g_{s,i}(x) &= \sin\left(i \frac{2\pi}{X} \cdot x\right) \\ 1 &\leq i \leq r \end{aligned} \quad (4.74)$$

where the functions have a period of X . The coefficients of the linear combination of Eqn. 4.73 can be calculated with

$$\begin{aligned} w_{j,0} &= \frac{1}{X} \int_0^X f_j(x) dx \\ w_{j,c,i} &= \frac{2}{X} \int_0^X f_j(x) \cos\left(i \frac{2\pi}{X} \cdot x\right) dx \\ w_{j,s,i} &= \frac{2}{X} \int_0^X f_j(x) \sin\left(i \frac{2\pi}{X} \cdot x\right) dx \\ 1 &\leq i \leq r \\ 1 &\leq j \leq q \end{aligned} \quad (4.75)$$

and used for the weights in Eqn. 4.33.

For a reduction of the dimension of the function space of the distributed sources, the condition that the number of elements q is larger than $2r + 1$ has to hold, where r is the order of approximation. The overall number of trigonometric polynomials has to be lower than the number of distributed sources, $\sum_{i=1}^k 2r_i \ll q$, for a significant reduction of the dimension of the function space of the sources. With the Fourier series expansion a reduction of the dimension of the function space of distributed sources is enabled. This allows for the port reduction method of this work, especially if the distributed sources are modeled with periodic functions.

4.3.1.4 Basis Functions in Neural Network Modeling

In this section the so-called neural network modeling approach is presented as a method for the reduction of the dimension of the function space of distributed sources.

The neural network modeling is inspired by biological systems [160, 161]. Despite its name this modeling approach is not yet capable of building intelligent systems comparable to the nature. Nevertheless, it has become a widely used method as universal approximator [161]. In the field of black box modeling of dynamical systems the neural network modeling approach has become an important method [162–166]. Neural networks are mainly used in the field of modeling, if the physical properties of the underlying model are unknown and only measured data of the input-output-behavior is accessible. This leads to the use of basis functions, which can emulate nearly all nonlinear functions, so-called universal approximators.

A neural network is built by an input layer, several hidden layers and an output layer. Each layer consist of a number of so-called neurons which generate a linear or nonlinear function of its inputs. In the class of feed-forward networks each neuron uses several or all outputs of the former layer as input. The output of each layer is used as input for the next layer. Neurons in the same layer are not connected with each other. Typically the input layer neurons realize linear functions, the hidden layer neurons realizing nonlinear functions and the output layer is linear. The structure of a feed-forward neural network with one hidden layer is shown in Fig. 4.26. As structure of the neural network only feed forward networks with one hidden layer are considered below. The input layer connects all variables with the hidden layer. The hidden layer corresponds to the basis functions $\mathbf{g}(x)$. The output layer is assumed to be linear.

The overall function of one output $f_j(x)$ of a neural network with inputs \mathbf{x} and r hidden layer neurons is described by

$$f_j(x) = \sum_{i=1}^r w_{j,i} g_i(\mathbf{x}, \mathbf{k}) \quad (4.76)$$

where $g_i(\mathbf{x}, \mathbf{k}_i)$ describes the nonlinear function of the i th hidden layer neuron with the parameters \mathbf{k}_i and $w_{j,i}$ is the weighting of the neuron of the output layer. For a system with m inputs and q outputs the starting point for the black-box modeling is a set of observed inputs $\mathbf{u} \in \mathbb{R}^m$

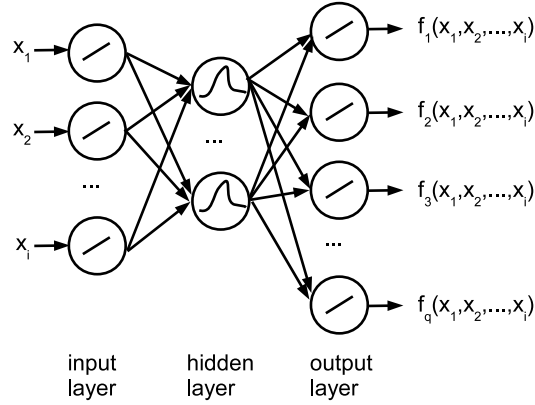


Figure 4.26: Schematic of a feed forward neural network with inputs \mathbf{x} and outputs $\mathbf{f}(\mathbf{x})$ with linear input and output layers and one nonlinear hidden layer

and outputs $\mathbf{y} \in \mathbb{R}^q$ of a system

$$\begin{aligned} \mathbf{u}^T &= [\mathbf{u}_1, \mathbf{u}_2, \dots, \mathbf{u}_m] \\ \mathbf{y}^T &= [\mathbf{y}_1, \mathbf{y}_2, \dots, \mathbf{y}_q] \end{aligned} \quad (4.77)$$

where a relation $\mathbf{g}(\mathbf{u}, \mathbf{y})$, which can estimate further outputs, is searched for. This relation is parameterized in $\mathbf{g}(\mathbf{x}, \theta)$ with a finite dimensional parameter vector θ and a so-called regression vector \mathbf{x} , containing the former observations. Several possibilities for the regression vector are given in [163, 167, 168]. Independently on the choice of the regression vector the relation $\mathbf{g}(x, \theta)$ is typically described by a parameterized family of functions, which can be written as function expansion

$$\mathbf{g}(x, \theta) = \sum w_i g_i(x) \quad (4.78)$$

where $g_i(x)$ are the basis functions [166]. Note that this structure for feed forward neural networks with one hidden layer is similar to the linear combination of the reduced dimension function space in Eqn. 4.33.

In neural network models as basis functions $g_i(x)$, which describe the nonlinear functions of the hidden neurons in the neural network sense, several classes of functions are used. Most model structures are composed of a so-called *mother basis function* $\kappa(x, \mathbf{k})$ and the basis functions $g_i(x)$ are obtained by varying the parameters \mathbf{k} . Typical properties used as parameters of the mother basis function are scaling $k_1 \cdot x$ and translation $x - k_2$ of the function.

If the nonlinear functions which are to be modeled depend on more than one variable, the input vector \mathbf{x} is used as variable instead of x . The three most often used methods for composing the multi-variable basis functions are, according to [166]: Firstly the product $g_i(\mathbf{x}) = g_{i,1}(x_1) \cdot \dots \cdot g_{i,m}(x_m)$ where the basis functions are generated by multiplication of single-variable basis functions. Secondly the radial construction $g_i(\mathbf{x}) = g_i(\|\mathbf{x} - \sigma_i\|)$ where the basis function is a function of a chosen norm of the variables and a so-called center σ_i are

used. And third the ridge function $g_i(\mathbf{x}) = g_i(\beta_i^T \mathbf{x})$, $\beta \in \mathbb{R}^m$ where all variables are weighted according to a chosen vector β_i .

Several groups of the most widely used basis functions are presented as follows.

A group of basis functions are the wavelets. The name wavelet comes from the fact, that the function integrates to zero and *waves* above and below the x-axis. Wavelets are mainly used in the signals and data processing area. In the signal processing area the wavelet transform is used instead of the Fourier transform, though the fact that wavelets are not only localized in the frequency, but also in the time, which for example gives an advantage in analyzing signals. In the data processing area the wavelet transform can handle discontinuities and sharp spikes more compact than for example sine-cosine-functions, and thus allow for higher reduction rates of data. This is used for example in compressing data of images or sounds. In addition the wavelet transform is computationally much cheaper than the Fourier transform. A wavelet is described by a function in the following form

$$g_{k,l}(x) = 2^{k/2} g(2^k x - l). \quad (4.79)$$

Famous *mother wavelet* functions are the Haar-wavelet, Daubechies wavelets and the so-called Mexican hat, where the basis functions necessary for the decomposition in this work are generated by translating and scaling the mother wavelets. After transformation of the function with the wavelet transform, the inverse wavelet transformation is in the form of Eqn. 4.33, where each wavelet forms a basis of the reduced dimension function space. As wavelet functions are functions of only one variable, the multi-variable basis functions can be generated in the ways presented in a former paragraph. Mostly the (tensor) product is used for generation of the multi-variable wavelet basis functions. The basis functions are generated in a constructive way, which makes them advantageous for the approximation used in this work.

Another widely used class are the radial basis functions (RBF). An RBF network consists of basis functions $g(x)$ in the form

$$g\left(\frac{x - z_i}{\sigma_i}\right) \quad (4.80)$$

where the location of the centers z_i are distributed over an specified range and σ_i defines the width of the i th neuron functions. In [164] and [162] it is independently proven that a neural network with one hidden layer of Gaussian type radial basis functions is capable of universal approximation. This enables a wide usage in nonlinear modeling of systems [162]. The parameters of the radial basis functions, namely the centers and the width of the hidden neurons and the weights of the output neurons have to be determined. This is done by estimation methods, whereas typical challenges are local maxima of the accuracy of the model and the so-called overtraining, where with an increasing number of iteration steps the accuracy of the model deteriorates [166]. As stated in [165] a sufficient number of RBF neurons with fixed centers is sufficient to approximate every function by adjusting only the values of the output layer neurons. This corresponds to the decomposition of Eqn. 4.33, whereas for all nonlinear element functions the same subset of basis functions has to be found and by only changing the weights w all nonlinear element functions can be reconstructed.

Further basis functions are the sigmoid functions, which are *almost always* capable of universal approximation [169], the nearest neighbors, kernel estimators, hinging hyperplanes, partial least squares and fuzzy functions [166].

The dimension of the function space of distributed sources can be reduced with neural network modeling methods into the form of Eqn. 4.33. The input of the neural network model is defined by the time, in the case of independent sources used as model for the distributed sources, or by the controlling variables of the nonlinear controlled sources. The output of the neural network is the behavior of the distributed sources. Several preliminary steps are necessary using the neural network modeling approach for the reduction of the dimension of the function space of the sources in this work. Firstly the data for the modeling process in Eqn. 4.77 has to be generated from the original functions. For this, calculating a number of functional values for given variables is necessary. This corresponds to a sampling of the behavior of the distributed sources. Based on the sampled data a neural network can be built. The neural network structure as well as the type of nonlinear basis functions has to be chosen in the second step. This can be a quite complicated process, as shown in the field of black box modeling. For the approach in this work the definition of the structure of the network is supported by the knowledge of the function of the sources. For example, the validity range of the functions of the sources and the smoothness are known a priori. In black-box modeling the inputs and outputs are also related to a time, where their values are observed. As we are dealing with static nonlinear functions of distributed sources only, the dynamic behavior and thereby the time when the signals are observed plays no role. After sampling the behavior of the distributed sources and the definition of the structure of the neural network, the modeling process can be started. By using iterative or direct methods of the neural network modeling, a model of the distributed sources' functions is obtained. As this model is in the form shown in Fig. 4.26, the reduced dimension function space is obtained directly by using the functions of the hidden layer neurons as basis functions in Eqn. 4.33. The weights for Eqn. 4.33 are obtained directly by the weights of the output layer neurons.

For a reduction of the dimension of the function space of the distributed sources the number of neurons in the hidden layer has to be smaller than the number of output neurons. This is different from the use of the neural network approach in modeling. In modeling, the number of hidden neurons is typically not limited nor correlated with the number of output neurons. In addition, for the method of this work the number of outputs is typically very large, while in system identification the number of outputs is relatively small, in many cases only one output is considered.

With the methods of neural network modeling nonlinear models can be built. If in the network model the number of hidden neurons is lower than the number of distributed sources, a reduction of the dimension of the function space is achieved. If this condition is fulfilled, the methods of neural networking can be used for the reduction of the dimension of the function space of the sources, used in the network models under consideration in this work. The advantage of the neural network methods is in their universal ability of modeling nonlinear functions. A large variety of nonlinear functions of distributed sources can be modeled with the neural network approach. Due to the large amount of modeling methods in neural networking, a low-dimensional function space of a large class of distributed sources' functions can be found.

Subsequently this function space is used for the port reduction method presented in this work.

4.3.2 Embedding of Reduced Function Space into the Network

In the former section methods for reducing the dimension of the function space of distributed sources in a network model are presented. As these methods result in mathematical formulae, more exact in a set of basis functions, the realization of the lowered dimension function space in the network model is shown in this section. At the end of this section a network will be given, where with the help of the lowered dimension of the function space a reducible network with a lowered number of ports is created.

For illustration purpose only the case of q independent current sources, with the waveforms described by the functions $f(t)$ in the model, is considered. A reduction of the q -dimensional function space of the current sources into an r -dimensional function space with the basis functions $g(t)$ is assumed by using one of the methods of the former section. At the end of this section necessary changes are given for networks with distributed sources modeled by voltage sources or nonlinear controlled sources.

The realization of the reduced dimension function space in the network model is shown in Fig. 4.27. The method for generating the network with a lowered number of ports (lower right part in Fig. 4.27), compared to the extraction of the distributed sources (upper right part in Fig. 4.27), is divided into the following steps. In the first step, independently of the method

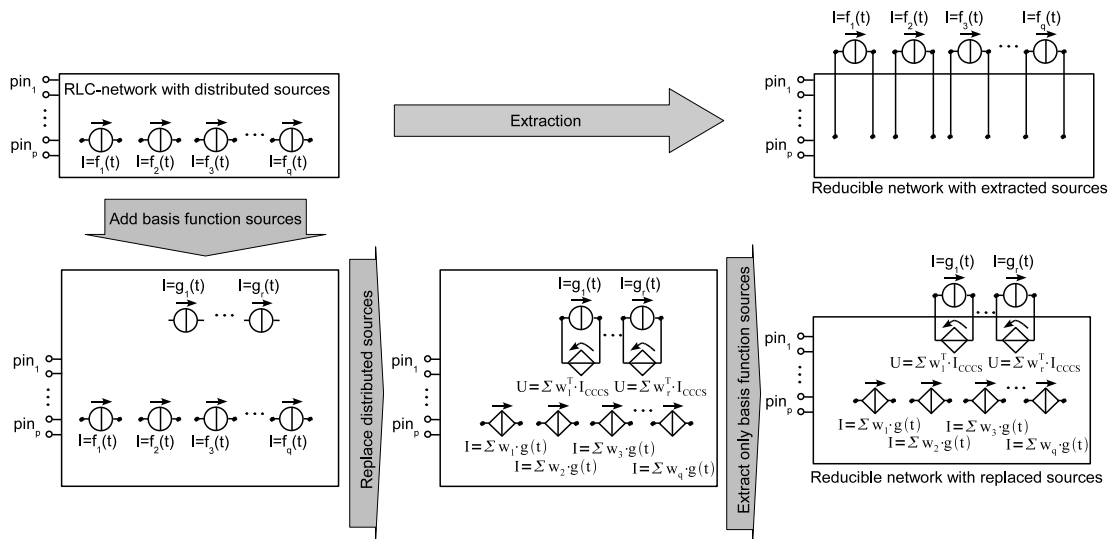


Figure 4.27: Illustration of the realization of the reduced dimension function space into the network model by replacing of the distributed sources

for the reduction of the dimension of the function space, for every basis function $g(t)$ an independent current source, generating a current corresponding to the basis function, is added. This results in r additional independent current sources, as many as basis functions are used in

the reduced dimension function space. In the second step, all q original independent current sources are replaced by linear current controlled current sources (CCCS). These controlled sources are controlled by the additional independent sources. The gains of these controlled sources are given by the columns of the weights matrix \mathbf{W} , which maps the reduced dimension function space to the distributed sources function space (Eqn. 4.33). In the second step voltage controlled voltage sources (VCVS) are connected with the additional independent sources. The gains are chosen according to the lines of the weights matrix \mathbf{W} of Eqn. 4.33. With these gains the preservation of passivity and reciprocity of the reducible network is preserved, as will be shown in the next sections. In the next step the extraction of only the additional r independent sources leads to a reducible linear network. Only the r additional independent current sources are extracted and connected through ports with the reducible part of the network, requiring only r ports. As the resulting network contains a lower number of independent sources as the original network, in this way a reducible network with a reduced number of ports is generated. With these steps the behavior at the pins of the network is exactly the same if the reduction of the dimension of the function space of the distributed sources is exact. If the reduction is approximative, the behavior at the pins is approximated as well, because the behavior of the distributed sources is approximated. The linear RLC-part of the network remains the same as only changes in the distributed sources' models are made. The resulting reducible linear network also contains linear controlled sources in addition to the RLC-elements, which can be included in a model reduction process due to their linearity and time-invariance. The resulting network is called network with replaced sources in the following.

The generation of the network with replaced sources is similar for the case of independent voltage sources modeling the distributed sources' behavior. For voltage sources the dual electrical elements have to be used. The r additional elements are voltage sources that have the basis functions $g(t)$ as waveforms. The original voltage sources in the model are replaced by VCVS, instead of CCCS in the current sources case. In the same way, connected to the additional voltage sources, CCCS have to be used instead of VCVS. The gains of the controlled sources are given by the weights \mathbf{W} of the mapping of the reduced dimension function space to the distributed sources function space (Eqn. 4.33). The resulting network now contains a lower number of independent voltage sources. By extracting these voltage sources the reducible part of the network contains a lower number of ports compared to the extraction of the voltage sources in the original model.

For network models containing nonlinear controlled sources, belonging to the class of elements described by one explicit nonlinear current or voltage function $f(\mathbf{x}, t)$ the generation of the network with replaced sources is quite similar. For every basis function $g(\mathbf{x}, t)$ of the reduced dimension function space a nonlinear element is created. The original nonlinear elements modeling the distributed sources are replaced by linear controlled sources, controlled by the additional elements currents or voltages. Linear controlled sources are connected with the additional nonlinear elements. The gains of all linear controlled sources are again chosen corresponding to the weights \mathbf{W} of the mapping of the reduced dimension function space to the distributed sources function space (Eqn. 4.33). As only the lowered number of r nonlinear sources has to be extracted from the reducible network part, the number of ports lowered.

By using the proposed method for every model with q models of distributed sources the re-

sulting network contains only a lower number r of elements, which cannot be included in the model reduction. By extracting these r elements and connecting them with the reducible part of the network by ports, a lower number of ports is necessary. The resulting network contains only r ports for the distributed sources instead of q . The number of ports thereby depends not on the number of distributed sources, but on the dimension of the reduced dimension function space of the sources. As the dimension of the function space is lowered, compared to the number of distributed sources, this enhances the following model reduction as shown in the next sections. Notably, the number of ports for the pins is not reduced by using the proposed method. The preservation of all relevant properties of systems describing networks in the port reduced model is shown in the following sections.

4.3.2.1 Preservation of System Properties

In this section, it is shown that the port reduced system of the network with replaced sources can be described in the form

$$\begin{aligned} (s\mathbf{C} + \mathbf{G}) \cdot \mathbf{x} &= \mathbf{B} \cdot \mathbf{u} \\ \mathbf{y} &= \mathbf{L}^T \cdot \mathbf{x} \end{aligned} \quad (4.81)$$

with the relevant properties of systems describing RLC-networks. It will be shown that properties of the system matrices, such as (J-)symmetry, (semi-)definiteness and block structure, are preserved in the port-reduced system. For sake of simplicity we will concentrate on networks with only resistors, capacitors and inductors, pins described as impedance ports, as well as current sources modeling the distributed sources' behavior. However, an expansion to networks with other distributed sources' models and admittance ports is possible, and the necessary changes are presented at the end of this section.

An RLC-network model with p pins and q current sources is assumed. The currents at the pins are denoted by \mathbf{i}_{pin} and the voltages by \mathbf{u}_{pin} . The waveforms \mathbf{i}_f of the current sources are assumed to be described with a lowered dimension function space with the r basis functions \mathbf{i}_g . The q current sources are replaced by linear controlled sources, controlled by the r additional current sources which generate the basis functions \mathbf{i}_g . The weights of the linear combination (Eqn. 4.33) of the basis waveforms are given with $\mathbf{W} \in \mathbb{R}^{q \times r}$. The coefficients of the weights matrix \mathbf{W} are used as the parameters of the gains of the CCCS, while the gains of the VCVS are given with \mathbf{W}^T as described in Sec. 4.3.2. For the generation of the system matrices of this network with replaced sources the incidence matrices $\mathbf{K}_C, \mathbf{K}_R, \mathbf{K}_L, \mathbf{K}_{pin}$ for capacitors, resistors, inductors and pins are used. As every original current source is replaced by a CCCS, the incidence matrices of the original distributed sources' models and the CCCS are equal

$\mathbf{K}_{CS} = \mathbf{K}_{CCCS}$. The branch constitutive relations are given as

$$\begin{aligned}
 \mathbf{i}_C &= s\hat{\mathbf{C}}\mathbf{u}_C \\
 \mathbf{i}_R &= \hat{\mathbf{G}}\mathbf{u}_R \\
 \mathbf{u}_L &= s\hat{\mathbf{L}}\mathbf{i}_L \\
 \mathbf{i}_{f,CCCS} &= \mathbf{W}\mathbf{i}_g \\
 \mathbf{u}_{VCVS} &= \mathbf{W}^T\mathbf{u}_{CCCS}.
 \end{aligned} \tag{4.82}$$

In the standard modified nodal analysis the stamps of the linear controlled sources appear in the system matrix \mathbf{G} . In addition, several additional currents or voltages may be added in \mathbf{x} for the inclusion of controlling variables. As for this method the properties of the matrices \mathbf{C} and \mathbf{G} are not preserved in the general case, a slightly modified way describing the network with replaced sources is presented in the following. With Kirchoff's Current Law $\mathbf{K}\mathbf{i} = 0$ we get

$$\begin{pmatrix} \mathbf{K}_C & \mathbf{K}_R & \mathbf{K}_L & -\mathbf{K}_{CCCS} & -\mathbf{K}_{pin} & \mathbf{0} & \mathbf{0} \\ \mathbf{0} & \mathbf{0} & \mathbf{0} & \mathbf{0} & \mathbf{0} & -\mathbf{I} & \mathbf{I} \end{pmatrix} \begin{pmatrix} \mathbf{i}_C \\ \mathbf{i}_R \\ \mathbf{i}_L \\ \mathbf{i}_{f,CCCS} \\ \mathbf{i}_{pin} \\ \mathbf{i}_{VCVS} \\ \mathbf{i}_g \end{pmatrix} = \mathbf{0} \tag{4.83}$$

with \mathbf{I} as the identity matrix. Notably, the modification of MNA is based on the fact that the network is divided into two parts, which are not interchanging charges. These two parts can be seen in the network with replaced sources in Fig. 4.27. The first part contains the RLC-elements, the pins and the CCCSs replacing the original current sources. The second part contains the VCVS and the additional sources having the basis functions as waveforms. The voltages are accordingly defined with

$$\begin{pmatrix} \mathbf{u}_C \\ \mathbf{u}_R \\ \mathbf{u}_L \\ \mathbf{u}_{CCCS} \\ \mathbf{u}_{pin} \\ \mathbf{u}_{VCVS} \end{pmatrix} = \begin{pmatrix} \mathbf{K}_C^T & \mathbf{0} \\ \mathbf{K}_R^T & \mathbf{0} \\ \mathbf{K}_L^T & \mathbf{0} \\ \mathbf{K}_{CCCS}^T & \mathbf{0} \\ \mathbf{K}_{pin}^T & \mathbf{0} \\ \mathbf{0} & \mathbf{I} \end{pmatrix} \begin{pmatrix} \mathbf{u}^\phi \\ \mathbf{u}_{VCVS}^\phi \end{pmatrix}. \tag{4.84}$$

Again, the fact that both network parts have no nodes in common is used for dividing the node potentials into two groups. Two groups of potentials are defined, where \mathbf{u}^ϕ contains the potentials of the first part of the network and \mathbf{u}_{VCVS}^ϕ contains the potentials of the second part of the network. With Eqn. 4.82 and Eqn. 4.84 in Eqn. 4.83 a system of circuit equations is

defined with

$$\begin{aligned}
 \underbrace{\begin{pmatrix} s\mathbf{K}_C\widehat{\mathbf{C}}\mathbf{K}_C^T + \mathbf{K}_R\widehat{\mathbf{G}}\mathbf{K}_R^T & \mathbf{K}_L \\ -\mathbf{K}_L^T & s\widehat{\mathbf{L}} \end{pmatrix}}_{(s\mathbf{C}+\mathbf{G})} \underbrace{\begin{pmatrix} \mathbf{u}^\phi \\ \mathbf{i}_L \end{pmatrix}}_{\mathbf{x}} &= \underbrace{\begin{pmatrix} \mathbf{K}_{CCCS}\mathbf{W} & \mathbf{K}_{pin} \\ \mathbf{0} & \mathbf{0} \end{pmatrix}}_{\mathbf{B}} \underbrace{\begin{pmatrix} \mathbf{i}_g \\ \mathbf{i}_{pin} \end{pmatrix}}_{\mathbf{u}} \\
 \underbrace{\begin{pmatrix} \mathbf{u}_{VCVS} \\ \mathbf{u}_{pin} \end{pmatrix}}_{\mathbf{y}} &= \underbrace{\begin{pmatrix} \mathbf{W}^T\mathbf{K}_{CCCS}^T & \mathbf{0} \\ \mathbf{K}_{pin}^T & \mathbf{0} \end{pmatrix}}_{\mathbf{L}^T} \underbrace{\begin{pmatrix} \mathbf{u}^\phi \\ \mathbf{i}_L \end{pmatrix}}_{\mathbf{x}}.
 \end{aligned} \tag{4.85}$$

The currents \mathbf{i}_g and \mathbf{i}_{pin} are the inputs \mathbf{u} of the system. The voltages \mathbf{u}^ϕ and the inductor currents \mathbf{i}_L form the system vector \mathbf{x} . The voltages \mathbf{u}_{VCVS} across the additional basis function sources and at the pins \mathbf{u}_{pin} are the outputs \mathbf{y} . Therewith the system has the form of Eqn. 4.81 with \mathbf{C} , \mathbf{G} having the system matrix properties of pure RLC-networks without controlled sources (Eqn. 2.16). The controlled sources of the network with replaced sources only appear in the matrices \mathbf{B} and \mathbf{L} . As described in Sec. 4.3.2, the gains of the VCVS are the transposed gains of the CCCS. Thus the condition $\mathbf{B} = \mathbf{L}$ still holds, as in the original system.

For distributed sources modeled with voltage sources, the description is similar. Based on the division of the network into two separate network parts, having no nodes in common and are not interchanging charges, the system can be described with MNA.

With this description it is shown that the controlled sources which normally influence the matrix \mathbf{G} , can be described in a way where only \mathbf{B} , \mathbf{L} are changed. The difference is that the matrices \mathbf{B} , \mathbf{L} are not incidence matrices anymore and thereby their structural properties are lost. In addition \mathbf{B} , \mathbf{L} are typically less sparse, but have a lower number of columns because of the reduction of the number of ports. Properties of \mathbf{C} , \mathbf{G} , such as (semi-)definiteness, (J-)symmetry and block structure of pure RLC-networks, are preserved, enhancing the model reduction and the following synthesis (Sec. 3.1 and 3.2). In addition the order N of the system, namely the number of equations, is not changed.

4.3.2.2 Preservation of Network Properties

As shown in the former sections, the system of the network with replaced sources now has only r ports for the models of the distributed sources. This is less than the number of ports q , if all distributed sources are extracted. In the following, it is shown that this reducible network is passive, and thereby stable, and reciprocal. For the proofs only currents as inputs of the system and voltages as outputs are used, which results in an impedance description. Nevertheless, the extension to admittance or hybrid descriptions is possible and explained at the end of this section.

As every passive system is also stable, a proof of stability is not necessary, as the following proofs show the passivity of the network with replaced sources. Nevertheless, as the system matrices \mathbf{C} , \mathbf{G} are not changed, the poles of the system remains the same. If in the transfer function of the network with extracted sources all poles are stable, the poles of the transfer function of the network with replaced sources are as well stable.

In the following paragraph, a mathematically based proof of the passivity of the network with replaced sources is shown. For the proof of passivity, the conditions for passivity have to be considered. The necessary and sufficient condition for the passivity of the impedance transfer function $\mathbf{Z}(s)$ of the model is positive-realness [34]:

1. $\mathbf{Z}(s^*) = \mathbf{Z}^*(s)$ where $*$ is the conjugate complex operator
2. $\mathbf{Z}(s)$ is positive, that means $\mathbf{a}^h (\mathbf{Z}(s) + \mathbf{Z}^h(s)) \mathbf{a} \geq 0$, with h as Hermitian operator is satisfied for all complex s with $\text{Re}(s) \geq 0$ and for all finite complex vectors \mathbf{a}
3. $\mathbf{Z}(s)$ is analytical

Since the system matrices stay real while replacing the independent current sources, the first condition is still fulfilled. The second condition of positive-realness can be written as

$$\mathbf{a}^h (\mathbf{Z}(s) + \mathbf{Z}^h(s)) \mathbf{a} = \mathbf{a}^h \mathbf{L}^T [(s\mathbf{C} + \mathbf{G})^{-1} + (s\mathbf{C} + \mathbf{G})^{-h}] \mathbf{B} \mathbf{a}. \quad (4.86)$$

With $\mathbf{B} = \mathbf{L}$ (Sec. 4.3.2.1) a finite complex vector $\mathbf{b} = \mathbf{B} \mathbf{a} = \mathbf{L} \mathbf{a}$ is defined and the transfer function of the network with replaced sources is positive for

$$\mathbf{b}^h [(s\mathbf{C} + \mathbf{G})^{-1} + (s\mathbf{C} + \mathbf{G})^{-h}] \mathbf{b} \geq 0. \quad (4.87)$$

Since the controlled sources are described in a way that does not influence the system matrices \mathbf{C} , \mathbf{G} , they are still positive (semi-)definite and real (Sec. 4.3.2.1). This means that the passivity of the network is conserved, as long as $\mathbf{B} = \mathbf{L}$ holds, which is guaranteed as shown in Sec. 4.3.2.1. The third condition, the analyticity of the transfer function, is fulfilled if the second condition is fulfilled [34] and is not additionally discussed. With this proof it is shown that the network with replaced sources is passive if the RLC-part is passive.

In this paragraph another proof of passivity, based on considerations of energy generation and dissipation is given. A physical interpretation of the passivity of the network with replaced sources is not obvious. Controlled sources, such as independent sources, are able to generate energy. Thereby networks with controlled sources are not passive in the general case. For the circuitry used in the network with replaced sources, the physical interpretation of energy generation and energy dissipation is as follows. The energy generated (dissipated) by the CCCS is defined with

$$E_{CCCS} = \sum_{k=1}^q i_{k_{CCCS}} \cdot u_{k_{CCCS}} \quad (4.88)$$

and the energy dissipated (generated) by the VCVS is

$$E_{VCVS} = \sum_{l=1}^r i_{l_{VCVS}} \cdot u_{l_{VCVS}}. \quad (4.89)$$

By using the branch constitutive relations of the controlled sources with the gains defined in

\mathbf{W} of the linear combination (Eqn. 4.33) the relations are given by

$$\begin{aligned} i_{kCCCS} &= \sum_{l=1}^r w_{k,l} i_{lVCVS} \\ u_{lVCVS} &= \sum_{k=1}^q w_{k,l} u_{kCCCS}. \end{aligned} \quad (4.90)$$

Inserting these relations into the energy generated or dissipated by the controlled sources leads to

$$\begin{aligned} E_{CCCS} &= \sum_{k=1}^q \sum_{l=1}^r w_{k,l} i_{lVCVS} \cdot u_{kCCCS} \\ E_{VCVS} &= \sum_{k=1}^q \sum_{l=1}^r i_{lVCVS} \cdot w_{k,l} u_{kCCCS} \end{aligned} \quad (4.91)$$

It can be seen that $E_{CCCS} = E_{VCVS}$ holds. This shows that the energy generated (dissipated) by the CCCS is equal to the energy dissipated (generated) by the VCVS. Thereby the overall generated (dissipated) energy of all controlled sources sums to zero. The network of controlled sources is lossless. As the network containing the RLC-elements is assumed to be passive, the overall network including the controlled sources is still passive. The amount of dissipated energy is not changed by replacing the sources and the network with replaced sources is always passive for a passive RLC-part.

In the following the proof of the reciprocity of the network with replaced sources is shown. For the proof of reciprocity, the condition for reciprocity has to be considered. The condition for a model to be reciprocal is that the impedance transfer function is symmetric [12, 34]:

$$\mathbf{Z}(s) = \mathbf{Z}^T(s). \quad (4.92)$$

By inserting the transfer function, using the system matrices form, this condition can be written as

$$\mathbf{L}^T (s\mathbf{C} + \mathbf{G})^{-1} \mathbf{B} = \mathbf{B}^T (s\mathbf{C} + \mathbf{G})^{-T} \mathbf{L}. \quad (4.93)$$

The system matrices \mathbf{C} and \mathbf{G} are still J-symmetric after replacing the independent current sources (Sec. 4.3.2.1). By left-multiplying the system of the network with replaced sources with a diagonal matrix

$$\mathbf{J} = \begin{pmatrix} \mathbf{I} & 0 \\ 0 & -\mathbf{I} \end{pmatrix} \quad (4.94)$$

$\mathbf{J}\mathbf{C}$, $\mathbf{J}\mathbf{G}$ are symmetric. The condition for reciprocity can be written with

$$\mathbf{L}^T (s\mathbf{J}\mathbf{C} + \mathbf{J}\mathbf{G})^{-1} \mathbf{J}\mathbf{B} = \mathbf{B}^T \mathbf{J}^T (s\mathbf{J}\mathbf{C} + \mathbf{J}\mathbf{G})^{-T} \mathbf{L}. \quad (4.95)$$

With $\mathbf{JB} = \mathbf{B}$, as the lower block of \mathbf{B} is zero and with $\mathbf{B} = \mathbf{L}$ (Sec. 4.3.2.1) the condition of reciprocity holds for every network with replaced sources. With this proof it is shown that the network with replaced sources is reciprocal if the RLC-part is reciprocal.

For distributed sources modeled as voltage sources the proofs are similar. The mathematical proof of passivity is the same, as positive realness of the transfer function as a condition for passivity is also necessary in the admittance case. As \mathbf{C} , \mathbf{G} stay real and positive (semi-)definite and $\mathbf{B} = \mathbf{L}$ holds the conditions of passivity are also fulfilled. The proof of passivity based on energy balance is equal, only the terms CCCS and VCVS have to be interchanged. For the proof of reciprocity the slight extension of the \mathbf{J} matrix in three sub-blocks is necessary (Eqn. 2.20), as the inclusion of voltages sources extends the system matrices by one block. The condition $\mathbf{B} = \mathbf{L}$ has to be replaced by $\mathbf{JB} = \mathbf{L}$ and the proof is still valid for voltage sources modeling the distributed sources' behavior.

With the proofs in this section it is shown that important network properties are preserved in the reducible part of the network with replaced sources. The reducible part contains a lowered number of ports and is still stable, passive and reciprocal.

4.3.2.3 Illustrative Numerical Example

In this section the network with replaced sources of the numerical example (Sec. 4.1.2.1), which is used throughout this work for illustration purpose, is built. It is assumed that the waveforms of the two independent sources of the example network, spanning a two-dimensional function space, can be described by one basis function $g(t)$. Thus it is assumed that the two waveforms can be grouped into one group, and thus are proportional. The linear combination for the distributed sources' behavior calculated by the basis functions (Eqn. 4.33) is given with

$$\begin{pmatrix} I_1(t) \\ I_2(t) \end{pmatrix} = \begin{pmatrix} f_1(t) \\ f_2(t) \end{pmatrix} = \begin{pmatrix} w_1 \\ w_2 \end{pmatrix} \cdot g(t) = \begin{pmatrix} w_1 \\ w_2 \end{pmatrix} \cdot i_g(t) \quad (4.96)$$

The weights of the superposition are assumed to be

$$\mathbf{W} = \begin{pmatrix} w_1 \\ w_2 \end{pmatrix} = \begin{pmatrix} 1 \\ 2 \end{pmatrix}. \quad (4.97)$$

By using the method of generating the network with replaced sources in Sec. 4.3.2 a network as shown in Fig. 4.28 is created. The network now contains one additional independent current

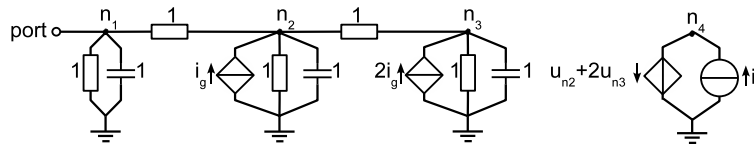


Figure 4.28: Realization of the reduced dimension function space into the illustrative example network by replacing of the two independent sources

source, having $i_g = g(t)$ as waveform. Both original independent current sources are replaced

by CCCS, controlled by the additional independent current source. The gains correspond to the weights \mathbf{W} of Eqn. 4.97. A VCVS is connected with the additional current source. The VCVS is controlled by the voltages across the CCCS replacing the original independent current sources. The gain of the VCVS is chosen with \mathbf{W}^T , resulting in

$$\begin{aligned}
 u_{VCVS} &= \mathbf{W}^T \mathbf{u}_{CCCS} \\
 &= \begin{pmatrix} w_1 & w_2 \end{pmatrix} \cdot \begin{pmatrix} u_{n2} \\ u_{n3} \end{pmatrix} \\
 &= u_{n2} + 2u_{n3} \\
 &= \phi_{n2} + 2\phi_{n3}.
 \end{aligned} \tag{4.98}$$

The network with replaced sources of the illustrative example is now described as a system of equations with the help of the MNA, using the slight extension of Sec. 4.3.2.1. The coefficients for the branch constitutive relations are given as shown in Sec. 2.4. In addition, the gains of the controlled sources are given with \mathbf{W} (Eqn. 4.97). The resulting system is now

$$\begin{aligned}
 \left[s \begin{pmatrix} \mathbf{C} \\ \begin{pmatrix} 1 & 0 & 0 \\ 0 & 1 & 0 \\ 0 & 0 & 1 \end{pmatrix} \end{pmatrix} + \begin{pmatrix} \mathbf{G} \\ \begin{pmatrix} 2 & -1 & 0 \\ -1 & 3 & -1 \\ 0 & -1 & 2 \end{pmatrix} \end{pmatrix} \right] \begin{pmatrix} \mathbf{x} \\ \begin{pmatrix} \phi_{n1} \\ \phi_{n2} \\ \phi_{n3} \end{pmatrix} \end{pmatrix} &= \begin{pmatrix} \mathbf{B} \\ \begin{pmatrix} 1 & 0 \\ 0 & 1 \\ 0 & 2 \end{pmatrix} \end{pmatrix} \begin{pmatrix} \mathbf{u} \\ \begin{pmatrix} i_{pin} \\ i_g \end{pmatrix} \end{pmatrix} \\
 \begin{pmatrix} u_{pin} \\ u_{I_g} \end{pmatrix} &= \begin{pmatrix} \mathbf{L}^T \\ \begin{pmatrix} 1 & 0 & 0 \\ 0 & 1 & 2 \end{pmatrix} \end{pmatrix} \begin{pmatrix} \mathbf{x} \\ \begin{pmatrix} \phi_{n1} \\ \phi_{n2} \\ \phi_{n3} \end{pmatrix} \end{pmatrix}.
 \end{aligned} \tag{4.99}$$

As can be seen, the matrices \mathbf{C} , \mathbf{G} are the same as for the network with extracted distributed sources in Sec. 2.4. The property of (J-)symmetry and (semi-)definiteness of \mathbf{C} , \mathbf{G} is preserved, as no change to these system matrices is made. It can be seen as well that the incidence structure of \mathbf{B} , \mathbf{L} is lost. The behavior at the pin, namely the voltages and currents i_{pin} , u_{pin} are equal to the original network. Nevertheless, the system of the network with replaced sources now has only two ports, one for the pin and one for the additional current source representing the basis function of the reduced dimension function space of the two distributed sources. Thereby the matrices \mathbf{B} , \mathbf{L} have one column or line less than the system of the original network (Eqn. 4.1). The resulting two-port impedance transfer function of the network with replaced sources is now given with

$$\mathbf{Z}(s) = \begin{pmatrix} 1/3 & 1 \\ 1 & 3 \end{pmatrix} \frac{1}{s+1} + \begin{pmatrix} 1/2 & -1 \\ -1 & 2 \end{pmatrix} \frac{1}{s+2} + \begin{pmatrix} 1/6 & 0 \\ 0 & 0 \end{pmatrix} \frac{1}{s+4}. \tag{4.100}$$

The poles of the transfer function are not affected by replacing of the distributed sources. The poles are equal to the original networks transfer function in Sec. 2.4, and thus the system is still stable. Positive realness of the transfer function is still given, which shows the preserved

passivity. In addition, the transfer function is still symmetric, showing the preserved reciprocity of the network.

It is noticeable that, for the special case in the illustrative example of independent sources having proportional waveforms and thus being able to be grouped into one group, the port reduced transfer function can be obtained directly from the original transfer function. For the illustrative example, with port one for the connection with other networks and two independent current sources modeling the distributed sources' behavior with proportional waveforms, the following transformation

$$\mathbf{Z}_{orig}(s) = \begin{bmatrix} Z_{1,1} & Z_{1,2} & Z_{1,3} \\ Z_{2,1} & Z_{2,2} & Z_{2,3} \\ Z_{3,1} & Z_{3,2} & Z_{3,3} \end{bmatrix} \quad (4.101)$$

$$\mathbf{Z}_{port-reduced}(s) = \begin{bmatrix} Z_{1,1} & \sum_{i=2}^3 w_{i-1} Z_{1,i} \\ \sum_{i=2}^3 w_{i-1} Z_{i,1} & \sum_{i=2}^3 \sum_{j=2}^3 w_{i-1} w_{j-1} Z_{i,j} \end{bmatrix} \quad (4.102)$$

leads to a transfer function with a lower number of ports. For the weights of the illustrative example (Eqn. 4.97), the reduced port transfer function is

$$\mathbf{Z}_{port-reduced}(s) = \begin{bmatrix} Z_{1,1} & Z_{1,2} + 2Z_{1,3} \\ Z_{2,1} + 2Z_{3,1} & Z_{2,2} + 2Z_{2,3} + 2Z_{3,2} + 4Z_{3,3} \end{bmatrix}. \quad (4.103)$$

In the more general case, where the functions of the distributed sources are not proportional, and the dimension of the function space is lowered by the methods presented in Sec. 4.3.1, this transformation is not possible.

With this illustrative network the generation of the system with a lowered number of ports is shown by using the network with replaced sources. Properties of the system matrices as well as of the transfer function are preserved, as shown with this illustrative example. The behavior at the nodes of interest, here at the pin, is preserved. The system with a reduced number of ports can be reduced more efficiently in the following model reduction step.

4.3.3 Implementation of Port Reduction

Methods for an efficient implementation of the presented port reduction method into an existing model reduction flow are given in this section. Three implementation hints are presented. Firstly the construction of the system of the network with replaced sources, without explicitly building the network, is shown. In the second part special attention is paid to the nonlinear sources used for the modeling of distributed sources. In the third part an extension to the network synthesis step after order reduction of a port reduced model is presented, which results in a more robust reduced model.

4.3.3.1 Implementation into Model Reduction Flows

In this section the implementation of the port reduction method in an existing model reduction flow is presented. The explicit construction of the network with replaced sources is avoided by dealing directly with the reducible system description.

In a few cases the explicit construction of the network with replaced sources is necessary. If for example the reduction of the dimension of the function space of the sources is approximative, the network with replaced sources is built for comparing the accuracy with the original network by simulations. Explicitly constructing the network with replaced sources is not necessary, if for example an exact decomposition is used. If the accuracy of the approximation is determined without simulation, the construction of the network with replaced sources can be avoided, too.

If the explicit construction of the network with replaced sources is not necessary, the system equations can be determined in a simple way, as described in the following. Assuming the original sources' functions $\mathbf{f}(\mathbf{x}, t)$ are described by the basis function $\mathbf{g}(\mathbf{x}, t)$ with a method described in Sec. 4.3.1 all weights \mathbf{W} for the linear combination of all distributed sources' models

$$\mathbf{f}(\mathbf{x}, t) \approx \mathbf{W} \cdot \mathbf{g}(\mathbf{x}, t) \quad (4.104)$$

are given. Inserting this in the system equations where the ports for the pins as well as the ports for the sources are divided

$$\begin{aligned} (s\mathbf{C} + \mathbf{G}) \cdot \mathbf{x} &= [\mathbf{B}_{pins} \quad \mathbf{B}_{sources}] \cdot [\mathbf{u}_{pins} \quad \mathbf{f}(\mathbf{x}, t)]^T \\ \mathbf{y} &= \begin{bmatrix} \mathbf{L}_{pins} \\ \mathbf{L}_{sources} \end{bmatrix} \cdot \mathbf{x} \end{aligned} \quad (4.105)$$

gives for the right-hand-side

$$\begin{aligned} &= [\mathbf{B}_{pins} \quad \mathbf{B}_{sources}] \cdot [\mathbf{u}_{pins} \quad \mathbf{f}(\mathbf{x}, t)]^T \\ &\approx [\mathbf{B}_{pins} \quad \mathbf{B}_{sources}] \cdot [\mathbf{u}_{pins} \quad \mathbf{W} \cdot \mathbf{g}(\mathbf{x}, t)]^T. \end{aligned} \quad (4.106)$$

By expanding with a block-diagonal matrix of proper size, using the pseudo-inverse \mathbf{W}^{-1} , the right-hand-side is now given with

$$\begin{aligned} &= [\mathbf{B}_{pins} \quad \mathbf{B}_{sources}] \cdot \begin{bmatrix} \mathbf{1} & \mathbf{0} \\ \mathbf{0} & \mathbf{W} \end{bmatrix} \cdot \begin{bmatrix} \mathbf{1} & \mathbf{0} \\ \mathbf{0} & \mathbf{W}^{-1} \end{bmatrix} \cdot [\mathbf{u}_{pins} \quad \mathbf{W} \cdot \mathbf{g}(\mathbf{x}, t)]^T \\ &= [\mathbf{B}_{pins} \quad \mathbf{B}_{sources} \cdot \mathbf{W}] \cdot [\mathbf{u}_{pins} \quad \mathbf{g}(\mathbf{x}, t)]^T \end{aligned} \quad (4.107)$$

where $\mathbf{g}(\mathbf{x}, t)$ is used as input. Note that the pseudo-inverse \mathbf{W}^{-1} does not have to be calculated for this operation and is only used as temporary variable. In the systems of networks often $\mathbf{B} = \mathbf{L}$ holds, as the dual electrical values of the inputs are used as outputs. As in the case for the system of the network with replaced sources \mathbf{L} is set equal to \mathbf{B} avoiding the explicit generation of the network with replaced sources. If the condition $\mathbf{B} = \mathbf{L}$ does not hold in the original network, for example further electrical values are to be observed, a similar method for generating \mathbf{L} can be used, resulting in

$$\mathbf{y} \approx \begin{bmatrix} \mathbf{L}_{pins}^T \\ \mathbf{W}^T \cdot \mathbf{L}_{sources}^T \end{bmatrix} \cdot \mathbf{x}$$

for the right-hand-side of the output definitions in the system equations. The system of the network with replaced sources

$$\begin{aligned} (s\mathbf{C} + \mathbf{G}) \cdot \mathbf{x} &= \begin{bmatrix} \mathbf{B}_{pins} & \widehat{\mathbf{B}}_{sources} \end{bmatrix} \cdot [\mathbf{u}_{pins} \quad \mathbf{g}(\mathbf{x}, t)]^T \\ \mathbf{y} &= \begin{bmatrix} \mathbf{L}_{pins}^T \\ \widehat{\mathbf{L}}_{sources}^T \end{bmatrix} \cdot \mathbf{x} \end{aligned} \quad (4.108)$$

can thereby directly created by multiplying the matrices \mathbf{B} , \mathbf{L} with the weights matrix \mathbf{W} . This leads to the changed system matrices

$$\begin{aligned} \widehat{\mathbf{B}} &= \mathbf{B}_{sources} \cdot \mathbf{W} \\ \widehat{\mathbf{L}}^T &= \mathbf{W}^T \cdot \mathbf{L}_{sources}^T. \end{aligned} \quad (4.109)$$

With this method the construction of the network with replaced sources is avoided. The port reduced system of the network with replaced sources is generated directly from the system of the network with extracted sources by applying a multiplication with the weights matrix. The resulting system can be reduced with model order reduction techniques. Alternatively the transfer function can be calculated from the system description for the reduction with order reduction techniques based on the transfer function. In each case, the system with a reduced number of ports can be obtained directly by simple calculations, and the explicit construction of the network with replaced sources can be avoided.

4.3.3.2 Nonlinear Controlled Sources

In this section special attention is paid to the handling of distributed sources modeled with nonlinear controlled sources.

For the reduction of network models with nonlinear controlled sources, the proposed port reduction is used for the reduction of the number of nonlinear elements. After the reduction of the dimension of the function space of the sources, as described in Sec. 4.3.1, the nonlinear elements for the basis functions realize the functions $\mathbf{g}(\mathbf{x}, t)$.

Typically, the nonlinear elements functions, the original as well as the basis functions, only depend on a few system variables, for example special controlling variables inside the network. Order reduction methods based on elimination of internal nodes can only be used, if the preservation of the controlling electrical values is guaranteed. In this case no changes of the nonlinear elements in the reduced network are necessary. For the order reduction methods based on the transfer function no reassignment is possible, due to the lack of internal variables by only considering the transfer behavior. Reduction methods based on the system description use a projection with a matrix \mathbf{T} . The projection space is based on the Gramians, a Krylov subspace or other suitable subspaces as shown in Sec. 3.1.4 and Sec. 3.1.5. In the order reduction the system variables in \mathbf{x} are changed to $\tilde{\mathbf{x}}$. The nonlinear elements functions have to be adapted to the new system variables. For these methods the reassignment of the original electrical values controlling the nonlinear elements to the reduced order system variables in $\tilde{\mathbf{x}}$

is possible by the transformation $\mathbf{x} = \mathbf{T}\tilde{\mathbf{x}}$, using the projection matrix \mathbf{T} of the order reduction process. For the nonlinear elements this results in approximated functions given by

$$\mathbf{g}(\mathbf{x}, t) \approx \mathbf{g}(\mathbf{T}\tilde{\mathbf{x}}, t). \quad (4.110)$$

These nonlinear elements functions approximate the behavior of the nonlinear elements before the model reduction. As the internal controlling variables do not exist anymore in the order reduced model, the approximation given by projection is used for the nonlinear elements in the reduced system. Note that this approximation is also necessary, if the port reduction method proposed in this work is not used. The nonlinear elements are given by

$$\mathbf{f}(\mathbf{x}, t) \approx \mathbf{f}(\mathbf{T}\tilde{\mathbf{x}}, t) \quad (4.111)$$

in the reduced model in this case. For both methods, extracting the nonlinear elements or using the network with replaced sources, after order reduction the functions typically depend on all system variables of the reduced linear model, as the projection matrix \mathbf{T} is typically dense. This leads to a higher complexity of the nonlinear elements functions, requiring a higher effort in simulations. Nevertheless, in most cases the reduction of the linear part overcompensates this disadvantage in simulation effort. The nonlinear controlled sources in a reduced model are taken into account in this section. As was shown, the nonlinear controlled sources can be handled efficiently in the model reduction process.

4.3.3.3 Robust Network Synthesis

A method to enhance the network synthesis, used for the generation of a network after applying port reduction and model reduction algorithms, is presented in this section. Especially a method is shown, which avoids a large number of controlled sources that make the model less robust.

If filter synthesis methods are used, the synthesized networks do not contain any controlled sources by construction, but the size of the network depends strongly on the number of ports. After order reduction by using a method based on the system description, the system matrices are typically dense. For a synthesis step from this reduced order matrices, a network having a large number of controlled sources is created by using direct stamping methods. By using a synthesis method based on the system description, as for example GC-Synthesis (Sec. 3.2.2) or RLCSYN [77], a lower number of controlled sources is necessary. The resulting synthesized network still has a quite a large number of controlled sources, as for example shown for a section of a network synthesized with the GC-synthesis in Fig. 4.29. The RLCSYN method is able to generate synthesized networks without any controlled sources, as described in Sec. 3.2.2, under the assumption of (J-)symmetric reduced system matrices $\tilde{\mathbf{C}}$, $\tilde{\mathbf{G}}$ and that $\tilde{\mathbf{B}}$, $\tilde{\mathbf{L}}$ are incidence matrices. The cost for this is a higher order of the reduced system. As \mathbf{C} , \mathbf{G} are not changed with the port reduction method, this condition is still fulfilled for $\tilde{\mathbf{C}}$, $\tilde{\mathbf{G}}$ after order reduction using adapted methods. However, as $\hat{\mathbf{B}}$, $\hat{\mathbf{L}}$ are not in incidence form after applying port reduction (Sec. 4.3.3.1), the order reduced matrices $\tilde{\hat{\mathbf{B}}}$, $\tilde{\hat{\mathbf{L}}}$ are not in incidence form as well.

A method for generating a network without controlled sources with RLCSYN, or a network with a reduced number of controlled sources with GC-Synthesis or other network synthesis

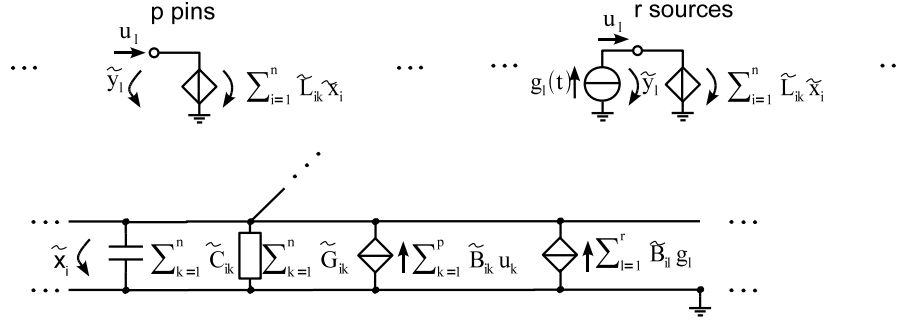


Figure 4.29: Synthesized network using GC-synthesis and a large number of controlled sources

methods based on the reduced system, is enabled by the following additional synthesis step. Assuming the order reduced system generated by projection

$$\begin{aligned} (s\tilde{\mathbf{C}} + \tilde{\mathbf{G}}) \cdot \tilde{\mathbf{x}} &= \begin{bmatrix} \tilde{\mathbf{B}}_{pins} & \tilde{\mathbf{B}}_{sources} \end{bmatrix} \cdot [\mathbf{u}_{pins} \quad \mathbf{g}(\tilde{\mathbf{x}}, t)]^T \\ \tilde{\mathbf{y}} &= \begin{bmatrix} \tilde{\mathbf{L}}_{pins}^T \\ \tilde{\mathbf{L}}_{sources}^T \end{bmatrix} \cdot \tilde{\mathbf{x}} \end{aligned} \quad (4.112)$$

where $\tilde{\mathbf{B}}_{sources}$ is a full matrix and $\tilde{\mathbf{L}}_{sources}^T = \tilde{\mathbf{B}}_{sources}$ holds. By expanding the right-hand-side of the system with matrices of proper size

$$\begin{aligned} &= \begin{bmatrix} \tilde{\mathbf{B}}_{pins} & \tilde{\mathbf{B}}_{sources} \end{bmatrix} \cdot [\mathbf{u}_{pins} \quad \mathbf{g}(\tilde{\mathbf{x}}, t)]^T \\ &= \begin{bmatrix} \tilde{\mathbf{B}}_{pins} & \tilde{\mathbf{B}}_{sources} \end{bmatrix} \cdot \begin{bmatrix} \mathbf{I} & \mathbf{0} \\ \mathbf{0} & \tilde{\mathbf{B}}_{sources}^{-1} \end{bmatrix} \cdot \begin{bmatrix} \mathbf{I} & \mathbf{0} \\ \mathbf{0} & \tilde{\mathbf{B}}_{sources} \end{bmatrix} \cdot [\mathbf{u}_{pins} \quad \mathbf{g}(\tilde{\mathbf{x}}, t)]^T \\ &= \begin{bmatrix} \tilde{\mathbf{B}}_{pins} & \mathbf{I} \end{bmatrix} \cdot [\mathbf{u}_{pins} \quad \tilde{\mathbf{B}}_{sources} \cdot \mathbf{g}(\tilde{\mathbf{x}}, t)]^T \end{aligned} \quad (4.113)$$

where the calculation of the pseudo-inverse $\tilde{\mathbf{B}}_{sources}^{-1}$ is not necessary. With this step the number of ports for the sources is increased at most to the order n of the reduced system, which is not critical, as the system is already order reduced and the number of ports is not a limitation anymore. At each node an independent source or nonlinear controlled source is connected, realizing the superposition

$$h_k(\tilde{\mathbf{x}}, t) = \sum_{l=1}^r \tilde{\mathbf{B}}_{k,l,sources} \cdot g_l(\tilde{\mathbf{x}}, t) \quad 1 \leq k \leq n \quad (4.114)$$

With this step a synthesized network without controlled sources for $\tilde{\mathbf{B}}_{sources}$ is generated. The dual electrical values at the elements realizing $\mathbf{h}(\tilde{\mathbf{x}}, t)$ are used as outputs, avoiding the use of

controlled sources for synthesizing $\tilde{\mathbf{L}}_{sources}$. Only for the connection of the pins by synthesizing $\tilde{\mathbf{B}}_{pins}, \tilde{\mathbf{L}}_{pins}$, linear controlled sources are necessary. The resulting synthesized networks has a lowered number of controlled sources. As an example a section of a network synthesized with the GC-synthesis is shown in Fig. 4.30, which has a lowered number of controlled sources compared to Fig. 4.29. The behavior at the nodes of interest, typically the nodes of the pins, is

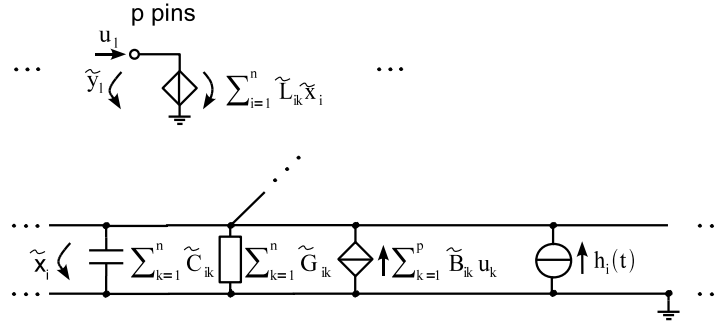


Figure 4.30: Synthesized network using GC-synthesis and a reduced number of controlled sources

exactly the same for both synthesis methods. By additionally utilizing RLCSYN the controlled sources for the pins are avoided and the synthesized network does not contain any controlled sources at all. With this method, the disadvantage of the lost incidence structure in the port reduced systems matrices $\tilde{\mathbf{B}}, \tilde{\mathbf{L}}$ of the network with replaced sources, what is passed through into the reduced system matrices $\tilde{\tilde{\mathbf{B}}}, \tilde{\tilde{\mathbf{L}}}$, can be compensated. With this method the incidence structure of the system matrices is rebuilt after order reduction. This allows for using a synthesis based on the reduced system matrices, where a lowered number of controlled sources is necessary, making the reduced network more robust in simulations.

4.3.4 Reduction Efficiency

This section shows the higher efficiency of the model reduction of models, whose number of ports is reduced with the port reduction method of this work. The illustrative example used throughout this work, as well as the RCI-grid of Sec. 4.1.2.2, are used for illustration purpose.

4.3.4.1 Illustrative Numerical Example

The system of the network with replaced sources of the illustrative example network used throughout this work (Fig. 2.2 and Fig. 4.2) is reduced in this section. The system is of order three, as shown in Sec. 4.3.2.3, and has only two ports. This is one port less compared to the three ports of the system of the network with extracted sources in Sec. 4.1.2.1. For the system of the network with extracted sources it was shown in Sec. 4.1.2.1 that no feasible model reduction is possible. Thus in this section, if the proposed port reduction method is utilized, the higher efficiency of the model reduction will be presented.

Firstly, in Fig. 4.31 the approximated HSV of the system of the network with replaced sources are compared with the approximated HSV of the system of the network with extracted sources. Note that the decay is much higher for the system of the network with replaced sources. For the system of the network with extracted sources with three ports the HSV are mainly in the same order of magnitude. With the proposed port reduction method the magnitude of the HSV decays more than two orders of magnitude, comparing the largest and smallest HSV. As the decay of the magnitude of the HSV gives an insight into the reducibility of a system, better model reduction results of the port reduced system can be assumed.

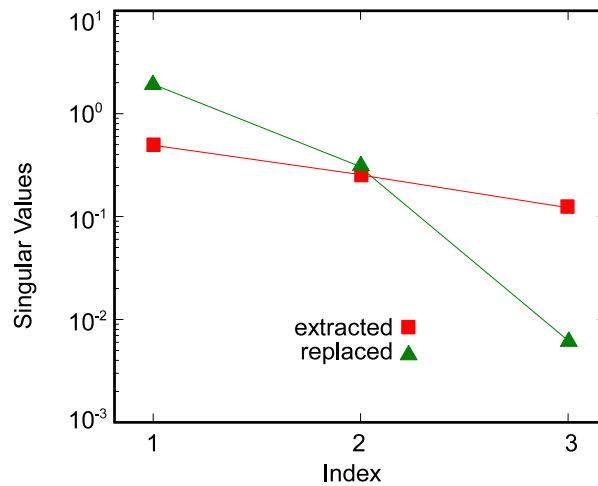


Figure 4.31: HSV for the system of the illustrative network with extracted and with replaced sources

For the model reduction a moment matching as well as a Gramian-based method are used, as for the reduction of the system of the network with extracted sources in Sec. 4.1.2.1. The frequency range of interest, where the behavior at the pin is to be approximated, is set from 10^{-5}Hz to 10^5Hz as in Sec. 3.1.8 and Sec. 4.1.2.1. At first, the system is reduced from order $N = 3$ down to $n = 2$ with both methods. The resulting reduced systems and corresponding transfer functions are presented in the following, whereas all values are rounded for readability. The moment matching based reduced system of order $n = 2$ is built using a first order Krylov

subspace \mathcal{K} in one real expansion point $s_p = 10^2$, which leads to

$$\left[s \underbrace{\begin{pmatrix} 1 & 0 \\ 0 & 1 \end{pmatrix}}_{\tilde{\mathbf{C}}} + \underbrace{\begin{pmatrix} 1.998 & -0.448 \\ -0.448 & 1.4003 \end{pmatrix}}_{\tilde{\mathbf{G}}} \right] \underbrace{\begin{pmatrix} \tilde{\mathbf{x}} \\ \tilde{\phi}_{n1} \\ \tilde{\phi}_{n2} \end{pmatrix}}_{\tilde{\mathbf{x}}} = \underbrace{\begin{pmatrix} -1 & -1 \cdot 10^{-3} \\ 4.47 \cdot 10^{-4} & -2.2361 \end{pmatrix}}_{\tilde{\mathbf{B}}} \underbrace{\begin{pmatrix} i_p \\ I1 \end{pmatrix}}_{\mathbf{u}}$$

$$\underbrace{\begin{pmatrix} u_p \\ u_{I1} \end{pmatrix}}_{\tilde{\mathbf{y}}} = \underbrace{\begin{pmatrix} -1 & 4.47 \cdot 10^{-4} \\ -1 \cdot 10^{-3} & -2.2361 \end{pmatrix}}_{\tilde{\mathbf{L}}^T} \underbrace{\begin{pmatrix} \tilde{\phi}_{n1} \\ \tilde{\phi}_{n2} \end{pmatrix}}_{\tilde{\mathbf{x}}}$$
(4.115)

The transfer function is given with two real poles by

$$\mathbf{Z}_{n=2}(s) \approx \begin{pmatrix} 0.2221 & 0.9294 \\ 0.9294 & 3.8895 \end{pmatrix} \frac{1}{s + 1.1608} + \begin{pmatrix} 0.7779 & -0.9294 \\ -0.9294 & 1.1105 \end{pmatrix} \frac{1}{s + 2.2376}.$$
(4.116)

Using the Gramian-based order reduction, the reduced system of order $n = 2$ is given with

$$\left[s \underbrace{\begin{pmatrix} 1 & 0 \\ 0 & 1 \end{pmatrix}}_{\tilde{\mathbf{C}}} + \underbrace{\begin{pmatrix} 1.3999 & 0.4472 \\ 0.4472 & 1.9999 \end{pmatrix}}_{\tilde{\mathbf{G}}} \right] \underbrace{\begin{pmatrix} \tilde{\mathbf{x}} \\ \tilde{\phi}_{n1} \\ \tilde{\phi}_{n2} \end{pmatrix}}_{\tilde{\mathbf{x}}} = \underbrace{\begin{pmatrix} 6.65 \cdot 10^{-5} & -2.2361 \\ 1 & -1.49 \cdot 10^{-4} \end{pmatrix}}_{\tilde{\mathbf{B}}} \underbrace{\begin{pmatrix} i_p \\ I1 \end{pmatrix}}_{\mathbf{u}}$$

$$\underbrace{\begin{pmatrix} u_p \\ u_{I1} \end{pmatrix}}_{\tilde{\mathbf{y}}} = \underbrace{\begin{pmatrix} 6.65 \cdot 10^{-5} & 1 \\ -2.2361 & -1.49 \cdot 10^{-4} \end{pmatrix}}_{\tilde{\mathbf{L}}^T} \underbrace{\begin{pmatrix} \tilde{\phi}_{n1} \\ \tilde{\phi}_{n2} \end{pmatrix}}_{\tilde{\mathbf{x}}}$$
(4.117)

with the transfer function with two real poles

$$\mathbf{Z}_{n=2}(s) \approx \begin{pmatrix} 0.2215 & 0.9286 \\ 0.9286 & 3.8924 \end{pmatrix} \frac{1}{s + 1.1614} + \begin{pmatrix} 0.7785 & -0.9286 \\ -0.9286 & 1.1076 \end{pmatrix} \frac{1}{s + 2.2384}.$$
(4.118)

Note that the transfer functions of both reduced systems are quite similar, differing only in decimal places. This is due the low complexity of the illustrative example. For systems larger than this illustrative example, the differences in the coefficients of the reduced models will be higher.

The size of the reduced system, reduced with the moment matching method, depends directly on the number of ports. The lower bound of the reduced size is the number of ports. As the system has two ports, no reduction below $n = 2$ is possible. With the Gramian-based method the number of ports is an indirect limitation in the reduction process, and no lower bound exists.

By model reduction down to an order of $n = 1$, the Gramian-based reduced system is given with

$$\begin{aligned} \left[s \underbrace{\tilde{\mathbf{C}}}_{(1)} + \underbrace{\tilde{\mathbf{G}}}_{(1.3999)} \right] \underbrace{\tilde{\mathbf{x}}}_{\left(\tilde{\phi}_{n1} \right)} &= \underbrace{\tilde{\mathbf{B}}}_{\left(\begin{array}{cc} -6.65 \cdot 10^{-5} & -2.2361 \end{array} \right)} \underbrace{\mathbf{u}}_{\left(\begin{array}{c} i_p \\ I1 \end{array} \right)} \\ \underbrace{\left(\begin{array}{c} u_p \\ u_{I1} \end{array} \right)}_{\tilde{\mathbf{y}}} &= \underbrace{\left(\begin{array}{c} -6.65 \cdot 10^{-5} \\ -2.2361 \end{array} \right)}_{\tilde{\mathbf{L}}^T} \underbrace{\left(\tilde{\phi}_{n1} \right)}_{\tilde{\mathbf{x}}} \end{aligned} \quad (4.119)$$

The transfer function of the reduced system now has only one real pole and is given with

$$\mathbf{Z}_{n=1}(s) \approx \left(\begin{array}{cc} 4.4184 \cdot 10^{-9} & 1.4863 \cdot 10^{-4} \\ 1.4863 \cdot 10^{-4} & 5 \end{array} \right) \frac{1}{s + 1.3999}. \quad (4.120)$$

The pole of the reduced system is now situated between the poles of the $n = 2$ reduced systems.

A comparison of the reduced systems transfer function with the unreduced systems transfer function is given in Figs. 4.32-4.35. Both models with a reduced order of $n = 2$ show a good agreement with the unreduced model. The relative approximation error in the frequency range of interest stays below 10% for the magnitude and below 20% for the phase. The reduced model with the order of $n = 1$ has a higher approximation error, especially in the magnitude behavior. The reduced model with only one pole cannot approximate the magnitude slope of the unreduced model for the $Z_{2,1}$ impedance as well as the phase change of 180 degree. This shows that the port reduced system cannot be approximated by a reduced system of order one, but with a reduced system of order two.

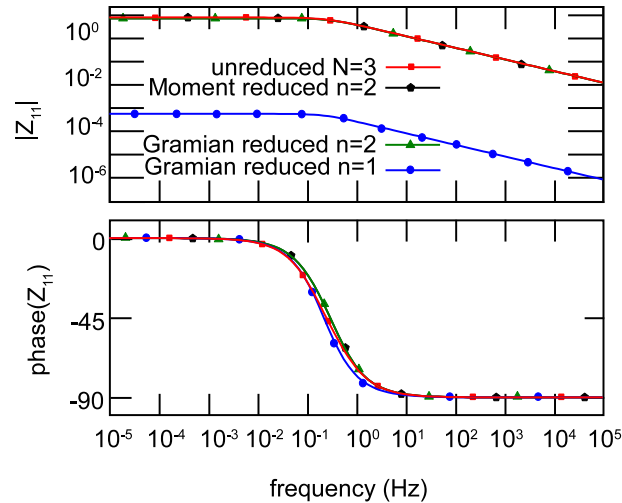


Figure 4.32: Illustrative example transfer function $Z_{1,1}$ of the original and the reduced models with replaced sources

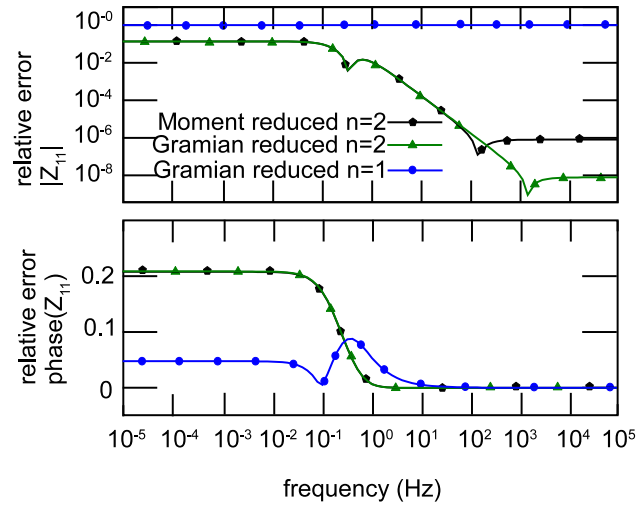


Figure 4.33: Relative approximation error of the illustrative example transfer function $Z_{1,1}$ of the reduced models with replaced sources

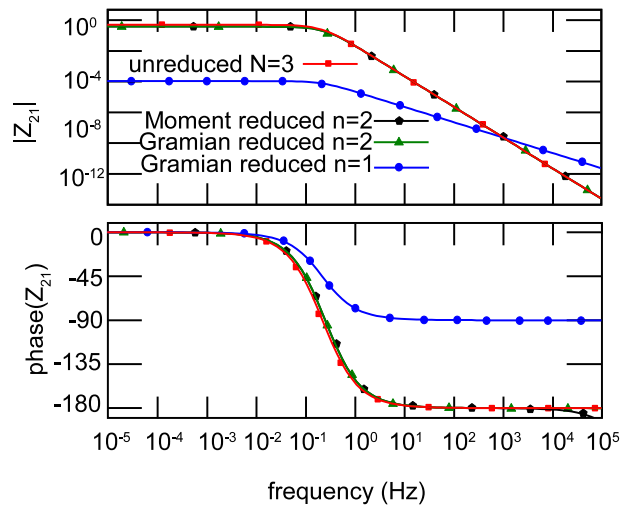


Figure 4.34: Illustrative example transfer function $Z_{2,1}$ of the original and the reduced models with replaced sources

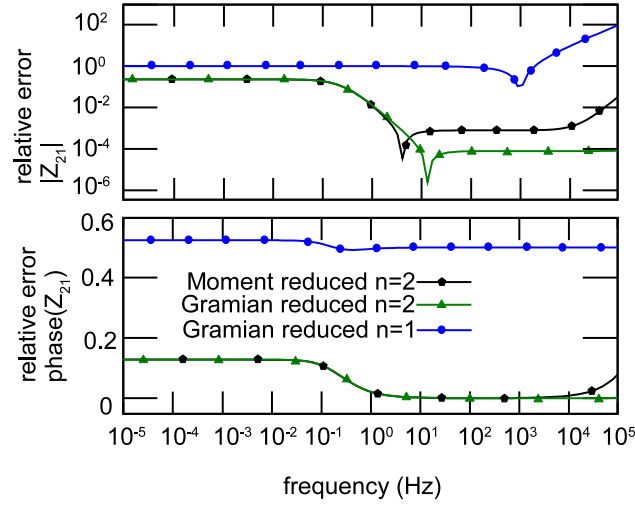


Figure 4.35: Relative approximation error of the illustrative example transfer function $Z_{2,1}$ of the reduced models with replaced sources

In Sec. 4.1.2.1 it was shown that the system of the network with extracted sources, which has three ports, is not reducible at all. With the port reduction method proposed in this work, the number of ports is lowered down to two and a model reduction of the illustrative example is enabled. Both models with a reduced order of $n = 2$ are good approximations to the model of order $N = 3$. The order one model is unfeasible, due to the high approximation error. With this illustrative example it is shown that using the proposed port reduction enables a more efficient model reduction of networks with distributed sources.

4.3.4.2 Illustrative RC-Grid

In this section the efficiency increase is further investigated by using the preceding port reduction method in model reduction of networks with distributed sources.

For the illustration of the efficiency of the port reduction, the RCI-grid of Sec. 4.1.2.2 is used. A large number of sources generates, by extraction of these sources, a large number of ports of the reducible system. As shown in Sec. 4.1.2.2, this large number of ports results in a lower efficiency of the model reduction. This was shown in Sec. 4.1.2.2 by observing the HSV of systems with a varying number of sources. In this section it will be shown that, for the port reduction method proposed in this work, the efficiency of the model reduction is higher. It will be shown that the limitation of the efficiency of the model reduction by the number of sources in the RCI-grid is eliminated by the port reduction. Only the number of the necessary basis functions of the reduced dimension function space, necessary for the approximation of the functions of the sources, limits the model reduction efficiency.

For the investigations of the reducibility of the RCI-Grid in Sec. 4.1.2.2, the waveforms of the distributed independent current sources are not considered. For the port reduction of this work the waveforms are now taken into account. It is assumed that all q waveforms of the

independent sources can be sufficiently well approximated by r basis waveforms by using the methods of Sec. 4.3.1. The independent sources are replaced and a network as shown in Sec. 4.3.2 is built. The corresponding system is created by using the method of Sec. 4.3.2.1.

Firstly, the reducibility of the network is compared for a given number of independent sources and a varying number of basis functions necessary to describe the functions of all sources. The reduced network has 900 nodes ($d = 30$) and a fixed number of 200 independent current sources. In Fig. 4.36 the approximated HSV calculated with the Gramian-based PMTBR algorithm are shown for a varying number r of basis functions. It can be seen that with the port reduction method the approximated HSV of the system of the network decay faster than for the system of the network with extracted sources. Also it can be seen that, for a lower number of basis functions, the approximated HSV decay faster. For a larger network with 10000 nodes

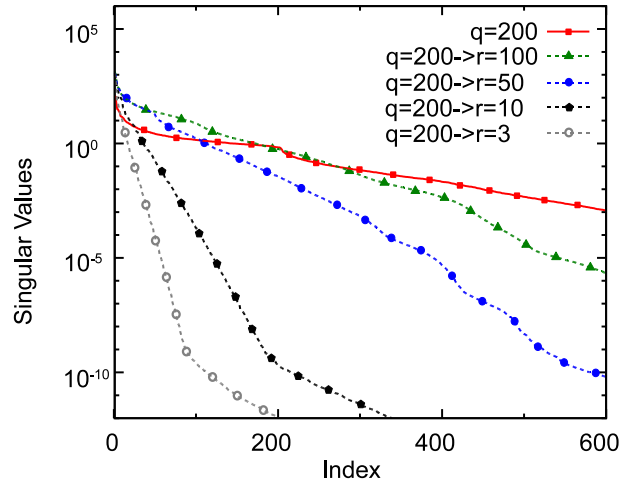


Figure 4.36: HSV for the $d = 30$ RCI-grid networks with $q = 200$ extracted sources and replaced sources with a varying dimension r of the approximating function space

($d = 100$) and 250 independent current sources the same trend of the approximated HSV can be observed, as shown in Fig. 4.37. With these two examples it is shown that, according to the decay rate of the approximated HSV, the model reduction is more efficient for a given approximation error of the reduced system by using the proposed port reduction as preceding step. Alternatively, for a given size of the reduced model the approximation error will be lower by using the port reduction method of this work.

Secondly, the reducibility is compared for a fixed number of basis functions suitable to describe a varying number of sources in the network. For the network with 900 nodes ($d = 30$) a differing number of independent sources ($5 \leq q \leq 200$) is connected. It is assumed that all waveforms of the independent sources can be approximated by $r = 3$ basis functions. In Fig. 4.38 the approximated HSV of the systems differing by the number of ports are shown. It can be seen that the approximated HSV decay slower with a lower number of sources q , as already shown in Sec. 4.1.2.2. If the port reduction method is applied, using $r = 3$ basis waveforms, the HSV decay faster. For every port reduced system the HSV decay is quite

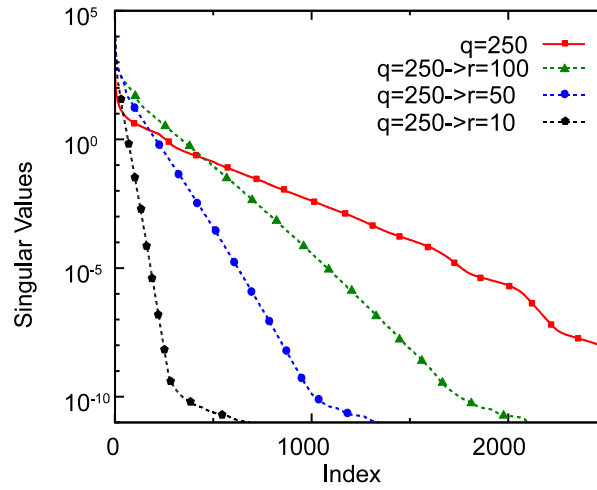


Figure 4.37: HSV for the $d = 100$ RCI-grid networks with $q = 250$ extracted sources and replaced sources with a varying dimension r of the approximating function space

similar, independently on the number q of functions that are described by the r basis functions. A similar trend is observed for the network with 10000 nodes ($d=100$) and a varying number of independent sources ($20 \leq q \leq 250$) in Fig. 4.39, where it is assumed that all sources' functions can be approximation by $r = 10$ basis functions. The first conclusion is that, for networks with a low number of independent sources, the gain achievable in model reduction by using the port reduction is quite low. If for example $q = 5$ sources are replaced by models of $r = 3$ basis functions (black solid and dotted lines in Fig. 4.38), the decay of the HSV differs only slightly. For networks with a large number of independent sources and $r \ll q$ the port reduction is more effective, as for example shown for $q = 200$ waveforms replaced by $r = 3$ basis functions (red solid and dotted lines in Fig. 4.38). The second conclusion from this investigation is that, independently on the number of sources in the original network, the HSV decay of every system with the same reduced number of ports is similar, as can be seen in Fig. 4.38. Thus the number of basis functions used for the approximation of the sources' functions is responsible for the efficiency of the model reduction. By using the proposed port reduction, the number of distributed sources used in the model is not a limiting factor of the reduction, as in the standard extraction of all sources. By using the port reduction, the number of basis functions used in the reduced dimension function space is the limiting factor of the reduction efficiency, which is a weaker limitation.

In this section the efficiency increase of model reduction by using the port reduction presented in this work as preceding step, is investigated. The higher efficiency in model reduction was demonstrated with several example networks with distributed sources

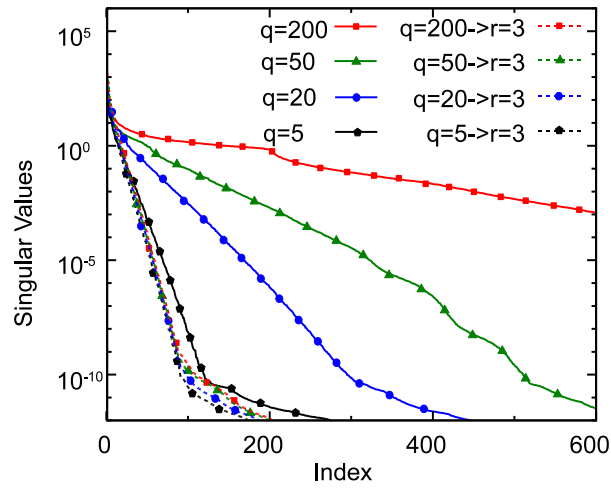


Figure 4.38: HSV for the $d = 30$ RCI-grid networks with a varying number of extracted sources q and replaced sources with a dimension of $r = 3$ of the approximating function space

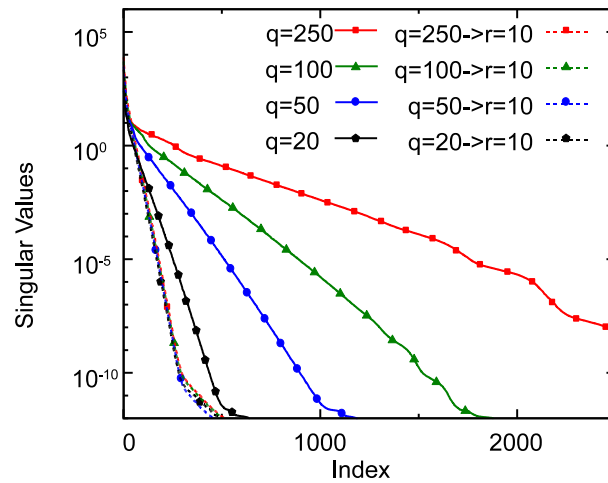


Figure 4.39: HSV for the $d = 100$ RCI-grid networks with a varying number of extracted sources q and replaced sources with a dimension of $r = 10$ of the approximating function space

4.4 Comparison and Classification

In this section the port reduction method presented in this work (Sec. 4.3) is compared to existing methods (Sec. 4.2) dealing with the reduction of systems with a large number of ports. The capabilities of the methods in reducing networks with a large number of sources are compared. Advantages and disadvantages of the methods are highlighted.

Several methods based on partitioning of the network or the system (Sec. 4.2.1) rely on the internal structure of the network to be efficient. Mainly these methods can be applied to networks having a block structure. Methods based on the correlation (Sec. 4.2.2) of ports also rely on the internal structure in the network, allowing for the reduction of the number of ports. These methods are mainly applied if the network is regularly structured. For systems that cannot be partitioned into subsystems with a small number of ports, or systems with a small correlation of the ports, these methods fail. The advantage of the presented method, compared to the partitioning and port correlation methods, is the complete independence on the internal structure. Independently on the network structure the proposed port reduction method can be applied.

Another disadvantage of the methods based on partitioning of the model (Sec. 4.2.1) is that the problem of the reduction of a system with a large number of ports is shifted to the problem dealing with a large number of systems. Each system has only a small number of ports, but the number of systems can be very large. Thus an advantage of the presented port reduction method in this work is the creation of only one system, having a small number of ports.

In the methods, compared in the former paragraphs with the method presented in this work, no information about the elements connected with the ports is needed nor taken into account. Several reduction methods exploit information of the connected models at the ports in model reduction (Sec. 4.2.3).

The methods of Sec. 4.2.3.2 are including the input information in the reduction process, requiring all inputs to be determined. Thereby these methods cannot handle pins where arbitrary (nonlinear) elements are connected after model reduction. Thus, these methods are more in the simulation field. The advantage of the proposed method, compared to these simulation methods, is the generation of a reduced model, which can be connected with other models in a simulation environment.

Methods based on predetermined loads (Sec. 4.2.3.3) shifting the problem of a large number of ports to the problem of a large number of parameters, and are only able of dealing with simple parameterized linear network elements connected to the ports. The port reduction method in this work allows for a reduced model, where arbitrary elements can be connected to the pins.

The method based on correlated input signals (Sec. 4.2.3.1) has a wide applicability for the reduction of networks with distributed sources. This method can handle ports with arbitrary connected network models, like the method presented in this work. Also, like the presented method, it is possible to efficiently handle ports where the input information is determined. Advantageous of method based on correlated input signals, compared to the method presented in this work, is the fact that the inputs do not have to be determined exactly. The allowed variation of the inputs allows for a wide field of application in reducing networks with distributed sources. Nevertheless, the rigorous use of the a priori defined knowledge of the distributed

sources in the models under consideration allows for a higher efficiency of the method developed in this work. However, another advantage of the presented method is the inclusion of not only functions of time but also nonlinear controlled sources' functions. In addition, the presented method does not rely on a single model reduction algorithm. The presented method can be used as a preceding step to almost all model reduction methods, contrary to the method based on correlated input signals.

The preservation of properties of the system, as well as properties of the network, is another advantage of the method proposed in this work. Properties of the system matrices such as (J-)symmetry, (semi-)definiteness and block structure can be preserved. Passivity, stability and reciprocity are preserved in the port reduced model and can be further preserved during the model reduction by using appropriated reduction algorithms. Most of the existing algorithms dealing with a large number of ports are as well able to preserve some of these properties. Nevertheless, most state-of-the-art methods cannot preserve all properties. For example, several methods create reduced systems, which are not realizable as electrical networks. For example, the reduced models of methods using predefined loads and using parametric model reduction (Sec. 4.2.3.3) are parameterized and hence not realizable as an electrical network. The methods using partitioning of the complete system (Sec. 4.2.1) generate reduced models that have a differing number of inputs and outputs and lose properties like reciprocity and passivity of the original model. The presented method in this work has, compared to these methods, the advantage of preserving all relevant properties of networks.

The main advantage of the presented method is the inclusion of the knowledge of the functions of the inputs at the ports to improve efficiency. For the networks under consideration, having a large number of distributed sources, this information is known a priori. Nevertheless, the disadvantage is that only the number of ports for the connection with distributed sources can be lowered and the number of ports for the connection with other network models remains the same.

The main limitation of the efficiency of the proposed method is in the complexity of the distributed sources' functions. If the distributed sources' functions are quite simple, the function space can be approximated with a very low dimensional function space. If the distributed sources functions are complex, a large number of basis functions is necessary and the dimension of the reduced function space may be quite high. Nevertheless, as the dimension of the reduced function space equals the number of necessary ports of the reducible network, even a low reduction results in a reduced number of ports and allows for a higher model reduction efficiency. Also, as a large variety of methods exist that are capable of reducing the dimension of a function space, the method presented in this work can be applied to a large class of distributed sources' models.

Another advantage of the proposed port reduction method is the fact that, as the method is a preceding step, it allows for the usage of almost all reduction algorithms. In addition, the reduced model of the presented method can be synthesized as an electrical network. Due to the preservation of all relevant properties of systems describing a network, the network synthesis can be carried out by using practically all network synthesis methods.

Concluding, the existing methods are capable in reducing networks with a large number of

distributed sources, but are limited in efficiency. Several boundary conditions, not always fulfilled in a reducible model, are necessary for using existing methods. The method presented in this work is very flexible, as arbitrary RLC-networks can be handled. The rigorous inclusion of the knowledge of the distributed sources' behavior in a preceding port reduction step enables a high efficiency of the model reduction. The class of distributed sources that can be handled in the port reduction is quite high, due to the possible use of several approximation methods for the reduction of function spaces. Additionally, in the port reduced model all relevant properties of networks are preserved. The properties can furthermore be preserved in a reduced model by using appropriate model reduction methods.

5 Examples

In this chapter several networks modeling distributed systems with distributed sources are reduced. With the help of the port reduction presented in Sec. 4.3 and a subsequent model reduction as presented in Sec. 3 a reduced network is generated. Several aspects of the port reduction as well as the model reduction are highlighted. It is shown that by using the state-of-the-art model reduction methods directly (Sec. 3), as well as with the methods developed for the reduction of system with a large number of ports (Sec. 4.2), no or only a slight reduction of networks with a large number of sources is possible. The higher efficiency of the model reduction by using the port reduction proposed in this work as preceding step is illustrated. Two actual computers¹ are used to determine the speed-up of the reduced systems in simulations.

Three examples of networks modeling distributed systems with a large number of distributed sources are presented. An RC-grid with independent sources (Sec. 5.1), an RC-grid with non-linear controlled sources (Sec. 5.2) and an industrial emission model used in the IC design (Sec. 5.3) are to be reduced.

5.1 RC-Grid with Independent Sources

As an example, the RCI-grid, presented in Sec. 4.1.2.2 and shown in Fig. 4.8 is used. The example RCI-grid in this section contains 2500 nodes ($d = 50$) and $q = 55$ independent current sources. The element values for the 4900 resistors and 2500 capacitors are chosen randomly with $1 \pm 0.5\Omega$ and $0.1 \pm 0.05F$ as described in Sec. 4.1.2.2. All 55 waveforms of the independent current sources are piece-wise linear functions $f(t)$, described by six sections, which are periodically repeated. Examples of one period of the current sources waveforms $I_{f,i} = f_i(t); 1 \leq i \leq 55$ are shown in Fig. 5.1.

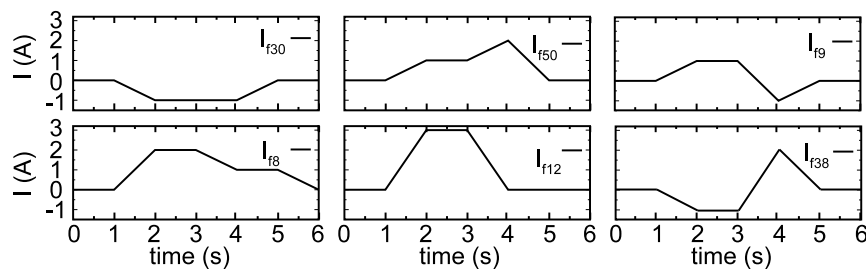


Figure 5.1: Example waveforms of the independent current sources in the RCI-grid

The network has the structure of a power grid, used in the modeling of the power distribution in the IC design flow [10, 11]. It is well-known that such networks are hardly reducible with model reduction techniques [125], which was also illustrated in this work in Sec. 4.1.2.2.

¹Intel Harwich 8 Dual Core Xeon (Tulsa) 16GB RAM and Intel Core 2 Duo 8400 4GB RAM

The network is described with the help of MNA, leading to a system of order $N = 2500$. With the method of extracting all independent current sources, and connecting them through ports with the system, a number of 55 ports for the independent sources and two ports for the pins are created, leading to overall 57 ports. The number of ports is quite large compared to the order of the system.

Several state-of-the-art approaches dealing with the reduction of systems with a large number of ports with respect to the size of the network (Sec. 4.2) are reviewed for applicability on this example. The coupling of the network does not allow for partitioning of the network into sub-blocks (Sec. 4.2.1) with a lower number of ports. Each sub-block of a partitioned network would contain at least the nodes at the boundaries of the sub-block as ports, which is quite high due to the coupling of all adjacent nodes. The transfer function partitioning methods (Sec. 4.2.1) cannot be applied, as the reduced model has to be synthesized as a passive and reciprocal electrical network. In addition the generation of a large number of reduced models, describing the complete model, is inefficient for this model as the behavior of the overall model is of interest. The example network is regularly structured, which allows for the usage of the methods based on port correlation (Sec. 4.2.2). Nevertheless, the distribution of all ports across the complete model results in only a small correlation of all ports. Thus still a large number of representative ports would be necessary. The reduced order simulation method (Sec. 4.2.3.2) assuming all inputs to be determined cannot be applied, as the driver models at the two pins are not a priori defined. As can be seen in Fig. 5.1 the correlation of the waveforms is quite low, which also limits the applicability of the methods based on input signal correlation (Sec. 4.2.3.1).

The state-of-the-art methods are not capable of efficiently reducing this example network. Thereby the port reduction method of this work is applied to illustrate the possibility of a high efficiency reduction. The waveforms of the distributed sources' models are taken into account in the port reduction step prior to the model reduction in the following.

5.1.1 Port Reduction

For the port reduction method of this work the waveforms of the sources are taken into account. The PWL-functions of the 55 independent current sources span a $q = 55$ dimensional function space. A function space with a lower dimension, which is capable to describe all 55 waveforms is searched for the port reduction. As there are six sections for the description of the waveform in one period by decomposition into ramp functions six basis periodic functions can be found. In Fig. 5.2 the six basis functions $I_{g,i} = g_i(t); 1 \leq i \leq 6$ are graphically shown. The six basis functions span a reduced dimension function space of the distributed sources behavior. Also a decomposition into the three basis functions shown in Fig. 5.3 is possible, resulting in only three basis waveforms $I_{g,i} = g_i(t); 1 \leq i \leq 3$. Thereby the dimension of the reduced function space is only three. As the number of basis waveforms is the limiting factor of the efficiency of the following model reduction, the lower number of basis waveforms with $r = 3$ is used.

The network with replaced sources as presented in Sec. 4.3.2 and a reduced number of ports is built. For the network with replaced sources only three ports for the independent sources

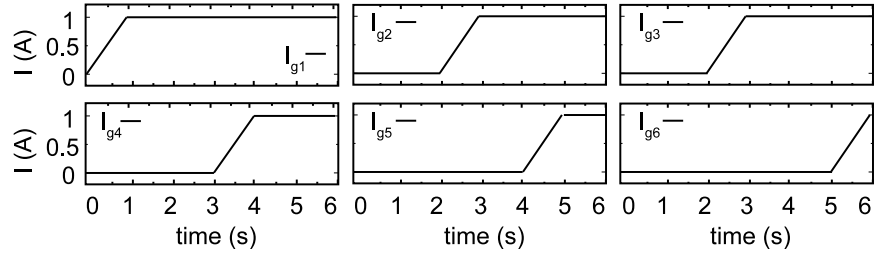


Figure 5.2: Ramp basis functions for the independent current sources in the RCI-grid

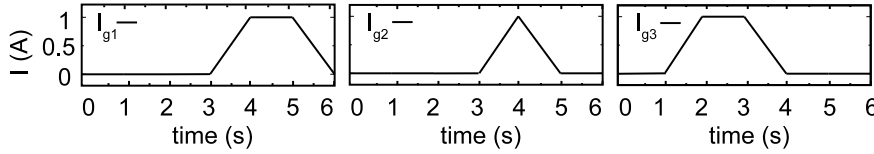


Figure 5.3: Another set of basis functions for the independent current sources in the RCI-grid

with the $r = 3$ basis waveforms and two ports for the pins are created, leading to overall 5 ports. With this it is shown that the port reduction enables significant reduction of the number of ports, compared to the standard method of extracting the distributed sources. The number of ports is lowered from 57 down to 5, which allows for a higher efficiency of the following model reduction, as will be shown in the next sections.

5.1.2 Model Reduction

With the help of order reduction both system descriptions, the system of the network with extracted as well as the system of the network with replaced sources, are to be reduced. The frequency behavior is chosen to be approximated, according to the values of the resistors and capacitors, in the range from 10^{-5}Hz to 10^5Hz . Two order reduction methods, based on moment matching and based on the Gramians are used for the reduction of the models.

5.1.2.1 Moment Matching based Order Reduction

As first order reduction algorithm an implicit moment matching method is used. A projection on a multipoint Krylov subspace as described in Sec. 3.1.4 is used.

Firstly, both systems are reduced to a comparable accuracy by implicit moment matching. For the reduction of the network with extracted sources two expansion points ($s_1 = 10^{-3}$, $s_2 = 1$) and two Krylov subspace iterations are used. The resulting reduced system has an order of $n_{extr.} = 228$. For a comparable accuracy of the reduced model after port reduction, the model reduction is performed with three expansion points ($s_1 = 10^{-3}$, $s_2 = 1$, $s_3 = 10^3$) and three Krylov subspace iterations. This larger number of expansion points and Krylov subspace iterations is necessary for comparable accuracy. Nevertheless, due to the lower number of ports, the reduced system of the network with replaced sources has a lower order of $n_{repl.} = 45$. For

accuracy comparison the transfer function $Z_{1,1}(s)$ is used in the following, which describes the impedance behavior at the first pin of the network. For all other transfer functions the results are comparable. The results of the model reduction are shown in Fig. 5.4 and the approximation error is shown in Fig. 5.5. The approximation error of both reduced models is comparable, but the reduced model of the port reduced network with replaced sources is much smaller, $n_{repl.} = 45$ compared to $n_{extr.} = 228$.

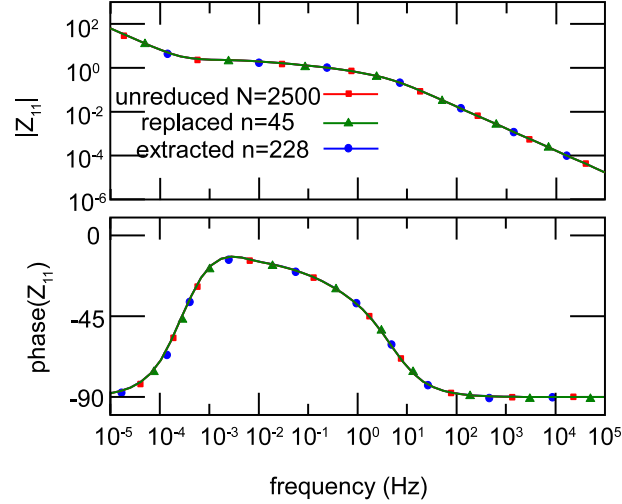


Figure 5.4: RCI-grid transfer function $Z_{1,1}$ of the original and the moment matching reduced models with comparable approximation error

Secondly, both system are reduced by moment matching to a comparable size. For the reduction of the port reduced network with replaced sources the same three expansion points as before and three Krylov subspace iterations are used, resulting in the reduced order $n_{repl.} = 45$ model. For a comparable size for the reduction of the network with extracted sources, only one expansion point ($s_1 = 1$) and one Krylov subspace iteration can be used, resulting in an order of $n_{extr.} = 57$ for the system of the network with extracted sources. For a similar size of the reduced models, the accuracy of the reduced model of the network with replaced sources is better than of the reduced model of the network with extracted sources (Figs. 5.6 and 5.7).

5.1.2.2 Gramian-based Order Reduction

As second order reduction algorithm a Gramian-based reduction with PMTBR as described in Sec. 3.1.5 is used.

For this order reduction algorithm an approximation to the HSV is calculated. The largest approximated HSV for the system of the network with extracted sources as well as for the system of the network with replaced sources are shown in Fig. 5.8. The HSV of the replaced sources network decay much faster than for the extracted sources network. As the HSV give an estimation of the approximation error of the reduced model depending on the reduced order, it can be seen that for equal reduced order the approximation error of the reduced system for

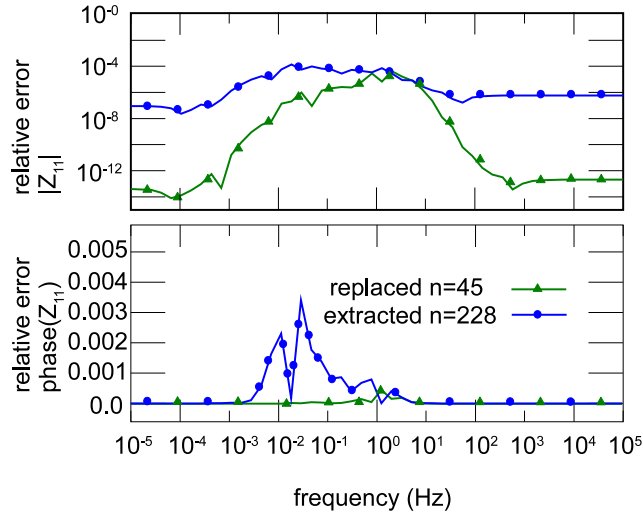


Figure 5.5: Relative error of the RCI-grid transfer function $Z_{1,1}$ of the moment matching reduced models with comparable approximation error

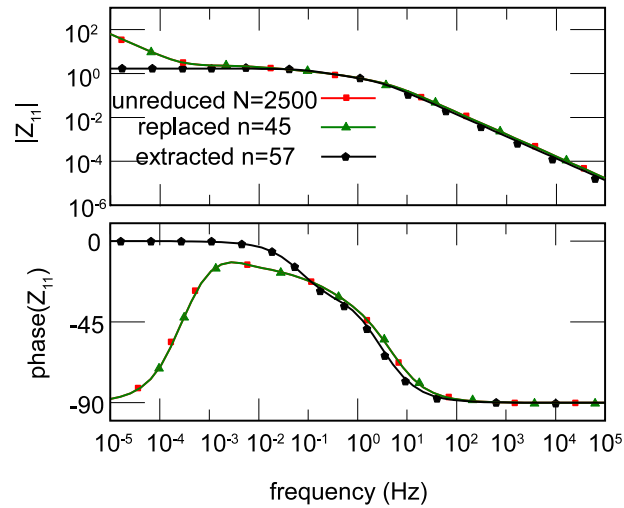


Figure 5.6: RCI-grid transfer function $Z_{1,1}$ of the original and the moment matching reduced models with comparable size

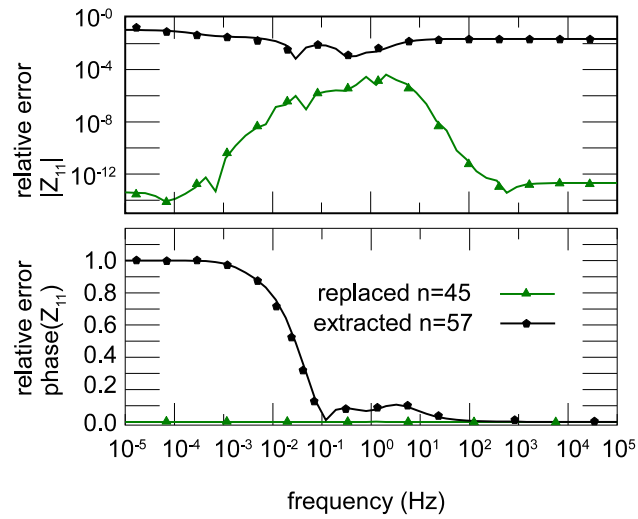


Figure 5.7: Relative approximation error of the RCI-grid transfer function $Z_{1,1}$ of the moment matching reduced models with comparable size

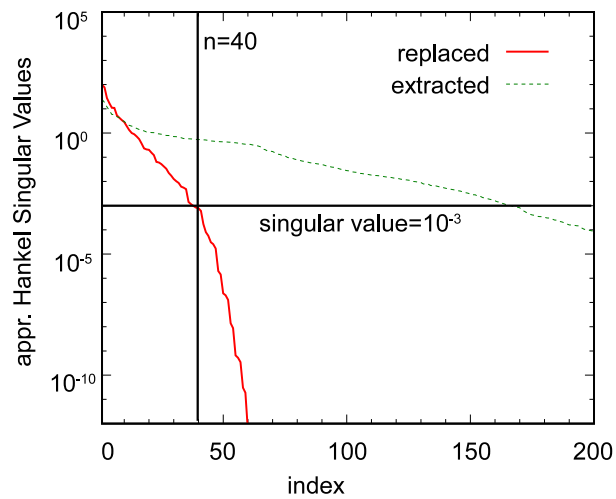


Figure 5.8: HSV of the RCI-grid networks with extracted and replaced sources

the replaced sources network will be lower than for the reduced system of the network with extracted sources. Vice versa it can be expected that for an equal approximation error of the reduced systems, the reduced system of the network with replaced sources is smaller.

Firstly, both system are reduced to the same highest preserved HSV of 10^{-3} . With that the orders of the reduced systems are set to $n_{repl} = 40$ and $n_{extr} = 165$ according to Fig. 5.8, for the system of the network with replaced and extracted sources, respectively. In Fig. 5.9 the results of magnitude and phase for the transfer function $Z_{1,1}$ for the original as well as both reduced systems is shown. Both transfer functions of the reduced systems are indistinguishable from the original transfer function, which shows the high accuracy of the model reduction. In Fig. 5.10 the relative errors of both reduced transfer functions are shown. Over the whole

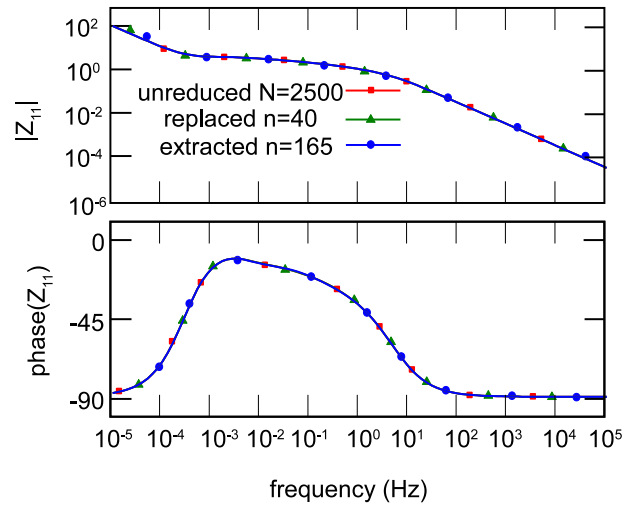


Figure 5.9: RCI-grid transfer function $Z_{1,1}$ of the original and the Gramian-based reduced models with comparable approximation error

frequency range of interest the error is below two percent in magnitude as well as in phase for both reduced models. This shows that if a low estimated error, according to the approximated HSV, is chosen, the resulting reduced systems are very accurate for both networks with extracted or replaced sources. Nevertheless, the order of the reduced system of the network with replaced sources is much lower than for the network with extracted sources, $n_{repl} = 45$ compared to $n_{extr} = 165$. As both reduced systems are very accurate, the system of the network with replaced sources is much smaller and can be henceforth much faster simulated. This shows that if the reduction is carried out according to an estimated approximation error of the reduced model, the proposed port reduction enables a stronger model reduction.

Secondly, both system are reduced to the same order of $n_{repl} = n_{extr} = 40$. In Fig. 5.11 the simulation results of magnitude and phase of the transfer function $Z_{1,1}$ for the original as well as both reduced systems is shown. In Fig. 5.12 the relative errors of both reduced transfer functions are shown. As can be seen the reduced system of the network with replaced sources is well approximated while the system of the network with extracted sources shows inaccuracies in the complete frequency range of interest. The reduction of both networks to the

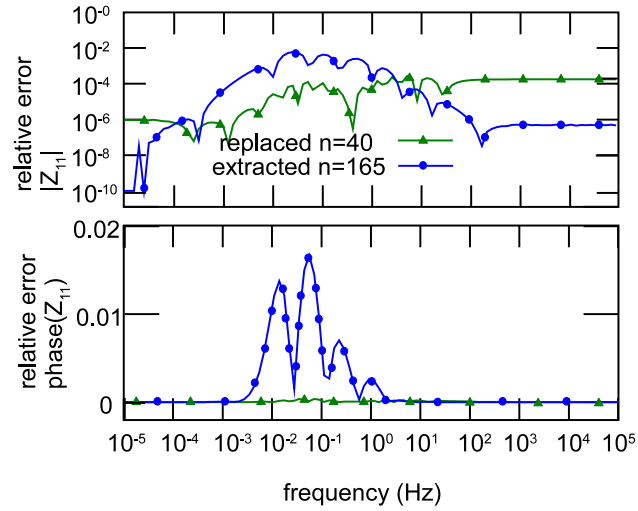


Figure 5.10: Relative approximation error of the RCI-grid transfer function $Z_{1,1}$ of the Gramian-based reduced models with comparable approximation error

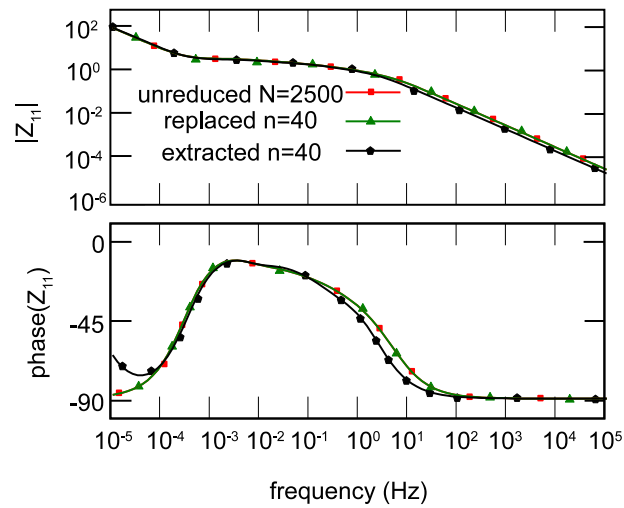


Figure 5.11: RCI-grid transfer function $Z_{1,1}$ of the original and the Gramian-based reduced models of the same size

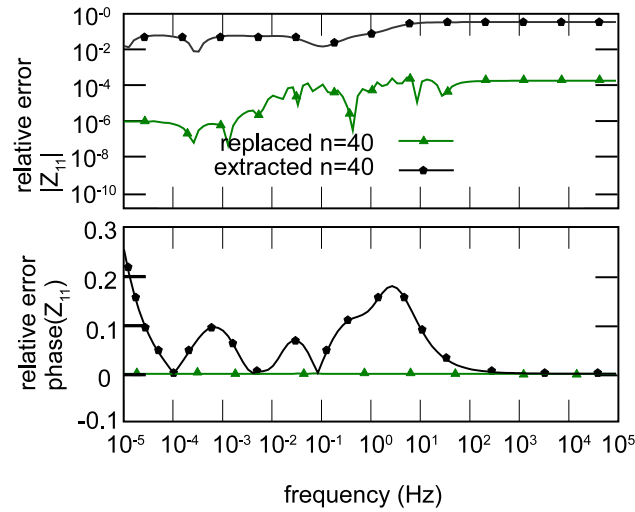


Figure 5.12: Relative approximation error of the RCI-grid transfer function $Z_{1,1}$ of the Gramian-based reduced models of the same size

same order shows that the system of the network with replaced sources is more accurate than the reduced system of the network with extracted sources. Thus the proposed port reduction method, creating a network with replaced sources, enables a higher accuracy of the reduced model.

5.1.2.3 Order Reduction Results

The results of the order reduction are summarized in Tab. 5.1. For the measurement of the speed-up, MATLAB calculations of the transfer function of the reduced systems in several frequency points are used. On different computers slightly different speed-ups are achieved and the corresponding ranges are given in the table. It can be seen that for the reduction of the network with extracted sources only a speed-up of 16 can be achieved with an acceptable accuracy of the reduced model. For the proposed port reduction method, using replacing of the sources, the possible speed-up is much higher, in the range of up to 200. For the same size of the reduced systems the speed-up is comparable for the systems of the networks with extracted and replaced sources. Nevertheless, the accuracy of the reduced system of the network with extracted sources is unacceptable as described in the former sections. Note that the transfer function of the unreduced system of the network with replaced sources can be calculated 3-4 times faster than the transfer function of the system of the network with extracted sources as the number of port-port-relations is lower due to the lower number of ports.

5.1.2.4 Network Synthesis

With the algorithms described in Sec. 3.2 the reduced systems can be synthesized as an electrical network. Several preliminary considerations are necessary for choosing the synthesis

Table 5.1: Comparison of order reduction results for the RCI-grid network

| Original Order $N = 2500$ | Ports p | Reduced Order n (Reduction) | MATLAB Speed-up | Accuracy |
|---|---------------------|---|------------------------|-------------------|
| Extracted sources | 57 | 2500 - | 1x | Exact at the pins |
| Extracted sources Moment matching reduction | 57 | 228 (90.9%) | 7x-8x | Very Good |
| Extracted sources Moment matching reduction | 57 | 57 (97.7%) | 45x-55x | Bad |
| Extracted sources Gramian-based reduction | 57 | 165 (93.4%) | 11x-16x | Very Good |
| Extracted reduced with Gramian-based reduction | 57 | 40 (98.4%) | 60x-120x | Bad |
| Replaced sources | 5 | 2500 - | 3x-4x | Exact at the pins |
| Replaced sources Moment matching reduction | 5 | 45 (98.2%) | 80x-180x | Very Good |
| Replaced sources Gramian-based reduction | 5 | 40 (98.4%) | 90x-200x | Very Good |

method. As the simulation environment is not to be changed for the simulation of the reduced model, time-variant models cannot be taken into account. Due to the quite high order of the reduced systems, the calculation of the poles is numerically crucial. Thus an efficient synthesis method, which does not need to calculate the poles of the system, is preferable, avoiding the use of filter synthesis methods. In the simulation environment HSPICE polynomial controlled sources (Eqn. 3.97) are available. Unfortunately, no dynamic elements are available, which avoids the use of direct stamping methods, as the size of the network will be quite large. The reduced matrices $\tilde{\mathbf{B}}$, $\tilde{\mathbf{L}}$ do not have an incidence structure, ruling out the use of synthesis methods based on the reduced system without using controlled sources. The remaining synthesis method, the GC-synthesis method presented in this work, can be used due to preserved (J-)symmetry in the reduced system matrices $\tilde{\mathbf{C}}$, $\tilde{\mathbf{G}}$. By using the GC-synthesis, a network with a small number of nodes and a low number of controlled sources is built, which can be investigated in the simulation environment.

With the method of extracting the sources, the corresponding reduced systems are larger in size or inaccurate for similar sizes than with the proposed method of replacing the sources. Thereby the synthesized network will be larger in size and the simulation effort is higher. For a similar size of the reduced models, the synthesized network of the reduced system with extracted sources will lead to inaccurate simulation results, as the transfer functions are bad approximations to the original network. Hence only the smallest and still most accurate reduced order system, the Gramian-based reduced system of the port reduced network with replaced sources of order $n_{repl} = 40$ is synthesized. The resulting network consists of 1685 elements, including resistors, capacitors and controlled sources, connecting 45 nodes and is exported as SPICE netlist.

5.1.3 Simulation Results

The netlist containing the reduced network is simulated with HSPICE. On both pins of the network 1V DC voltage sources in series with an 1Ω resistor are connected. An overview of the network size and the simulation effort with HSPICE is given in Tab. 5.2. For the simulation

Table 5.2: Comparison of model reduction results for the RCI-grid network

| | Original Network | Reduced Network |
|-----------------------|-------------------------|------------------------|
| Network elements | 7450 | 1685 |
| Network nodes | 2500 | 45 |
| SPICE parsing time | 18s | 0.9s |
| SPICE simulation time | 27s | 2.6s |
| SPICE memory | 16.7mbytes | 2.1mbytes |

of the original network, around 45 seconds are necessary on an actual computer. In this simulation, 27 seconds for the transient analysis and 18 seconds for reading the netlist, calculation of the operation point and other overhead calculations like error check are used. The reduced network is simulated on the same computer and the overall simulation time is only 3.5 seconds.

The transient analysis takes 2.6 seconds while the rest is used for the other calculations. This shows that the reduced network is around ten times faster in transient simulations than the original network. In addition the reduced model needs only 13% of the memory resources. This proves the efficiency of the reduction method. The speed-up is not as high as in the MATLAB calculation of the transfer behavior of the system, but nevertheless still high for this example.

Results for the simulation of the reduced network in comparison to the original network are shown in Figs. 5.13 and 5.14. Due to the distributed sources in the network, current and

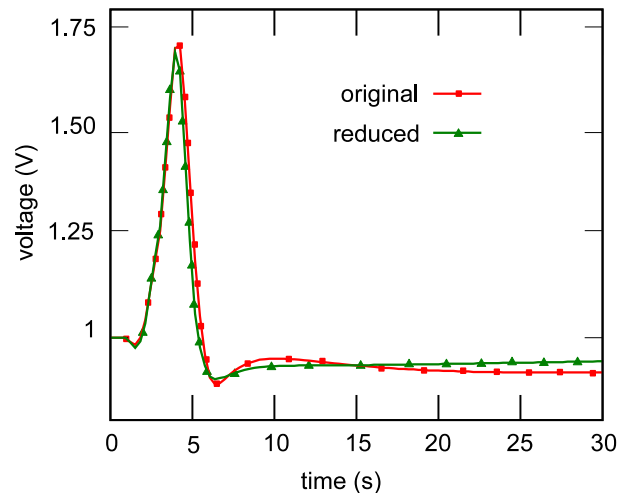


Figure 5.13: RCI-grid voltage fluctuation at pin1 of the original and the Gramian-based reduced model with replaced sources

voltage fluctuations are generated at the pins. In Fig. 5.13 the voltage waveform at pin1 is shown. Good agreement between the behavior at the pin of the original as well as the reduced network can be seen. Also for the current fluctuation at pin1 (Fig. 5.14) only small derivations, due to the approximation error of the model reduction, are observed. Noticeably, the differences in simulation are only due to the model reduction approximation, as the port reduction is exact for this example by using an exact reduction of the dimension of the function space of the distributed sources.

5.1.4 Conclusion of RC-Grid Reduction

In this section an example network of a system with distributed sources was reduced. Due to the large number of distributed sources in the network, the existing model reduction methods are limited in efficiency. By using state-of-the-art methods for the reduction of the example network either quite large reduced models are generated or the reduced models have large approximation errors. Methods for the reduction of systems with a large number of ports cannot be efficiently applied for the reduction of the example, due to their limitations regarding network structure or input signals. It is shown that the port reduction method presented in this work is capable of efficiently reducing the example network. By incorporating the knowledge

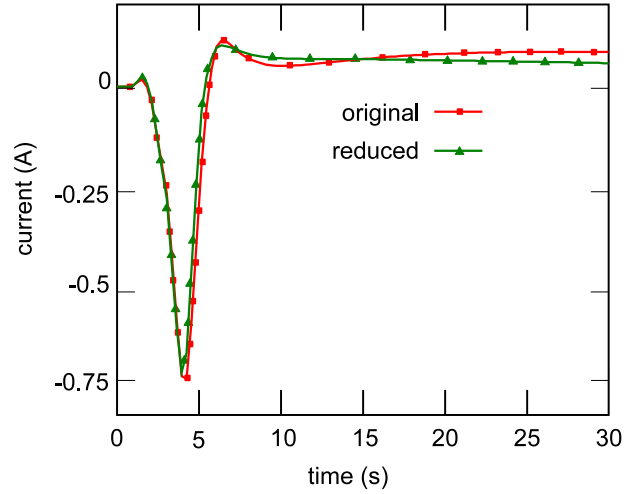


Figure 5.14: RCI-grid current flow at pin1 of the original and the Gramian-based reduced model with replaced sources

of the distributed sources' behavior, a system with a lowered number of ports is generated. This port reduced system can be more efficiently reduced by using existing model reduction methods. With the example in this section the method proposed in this work is validated. It is shown that the proposed method enables an efficient model reduction.

5.2 RC-Grid with Nonlinear Controlled Sources

As an example for a network with distributed sources, modeled by nonlinear elements, an RC-network as shown in Fig. 5.15 is used. The network contains 10×10 nodes, 180 resistors, 100 capacitors, 12 nonlinear elements and two pins for the connection with other networks. The order of the system describing the linear part is $N = 100$. The behavior at the pins should be approximated in a frequency range of 10^{-5} Hz to 10^5 Hz during model reduction, while the size of the network is to be reduced.

The values of the linear RC-elements are randomly chosen in the ranges $1 \pm 0.5\Omega$ and $0.1 \pm 0.05\text{F}$ for the resistors and capacitors, respectively. Between arbitrarily chosen nodes in the network nonlinear elements are connected, modeling the distributed sources' behavior. The nonlinear elements are functions of the voltage V_{45} , defined between a node in the middle of the linear RC-part of the network and ground. The nonlinear elements are described with $q = 12$ functions

$$I_j = f_j(\mathbf{x}) = \frac{a_{0,j} + V_{45}(a_{1,j} + a_{2,j}V_{45})}{1 - 2V_{45}^2 + V_{45}^4} \quad 1 \leq j \leq 12; \quad a_{0,j}, a_{1,j}, a_{2,j} \in \mathbb{R}. \quad (5.1)$$

The extraction of all nonlinear controlled sources elements would lead to 12 ports. The number

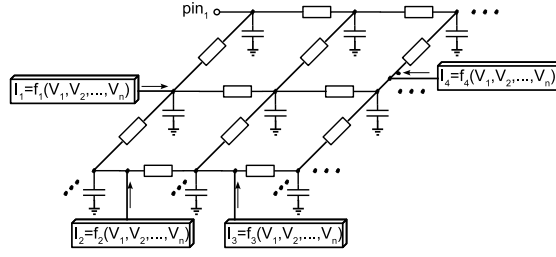


Figure 5.15: Section of the RCNL-grid with nonlinear elements modeling distributed sources

of ports is quite high with respect to the order of $N = 100$ of the model, which limits the model reduction of this example.

The state-of-the-art approaches dealing with the reduction of systems with a large number of ports (Sec. 4.2) are reviewed for the reduction of this example model. For the partitioning (Sec. 4.2.1) and port correlation methods (Sec. 4.2.2) the same applies as for the RC-Grid with independent sources in Sec. 5.1. The reduced order simulation method (Sec. 4.2.3.2) cannot be applied as only independent sources can be handled. The nonlinear controlled sources of this example model cannot be included in this reduction method. The methods based on input signal correlation (Sec. 4.2.3.1) are also not capable of dealing with nonlinear controlled sources, which rules out the use of these methods.

In the following it is shown that, despite the state-of-the-art methods, with the port reduction method presented in this work as preceding step a significant model reduction of the example is possible. As the extraction of these 12 nonlinear elements would lead to a large number of 12 ports, the port reduction method of this work is applied as preceding step to the model reduction. To enable the port reduction, a reduced dimension function space for the nonlinear elements functions is searched for. Although the numerator of the distributed sources equations can be expanded, resulting in $r = 3$ basis functions, a partial-fraction-decomposition of the equations is used for illustration purposes resulting in $r = 4$ basis functions

$$\begin{aligned}
 g_1(\mathbf{x}) &= 1/(V_{45} + 1) \\
 g_2(\mathbf{x}) &= 1/(V_{45} + 1)^2 \\
 g_3(\mathbf{x}) &= 1/(V_{45} - 1) \\
 g_4(\mathbf{x}) &= 1/(V_{45} - 1)^2.
 \end{aligned} \tag{5.2}$$

The 12 nonlinear functions can now be calculated by linear combination of the four basis functions with the corresponding weighting factors w

$$\begin{aligned}
 I_j &= w_{1,j}g_1 + w_{2,j}g_2 + w_{3,j}g_3 + w_{4,j}g_4 \\
 w_{1,j}, w_{2,j}, w_{3,j}, w_{4,j} &\in \mathbb{R}.
 \end{aligned} \tag{5.3}$$

The network with replaced sources as presented in Sec. 4.3.2 is built, and the weighting factors w are used as gains of the controlled sources. The system of the network with replaced sources

now has a smaller number of six ports (4 for $g(x)$ + 2 pins) compared to the system with extracted sources having 14 ports (12 for $f(x)$ + 2 pins) and can thus be reduced more efficiently as will be shown in the following.

For the model reduction of the linear part the Gramian-based PMTBR algorithm is used. The approximated HSV during the reduction are shown in Fig. 5.16. The HSV of the system of the linear part of the network, where the nonlinear elements are replaced by the lower dimensional function space $g(x)$ elements, decay much faster than for the linear system of the network where the nonlinear elements $f(x)$ are extracted, which promises a better reduction. For com-

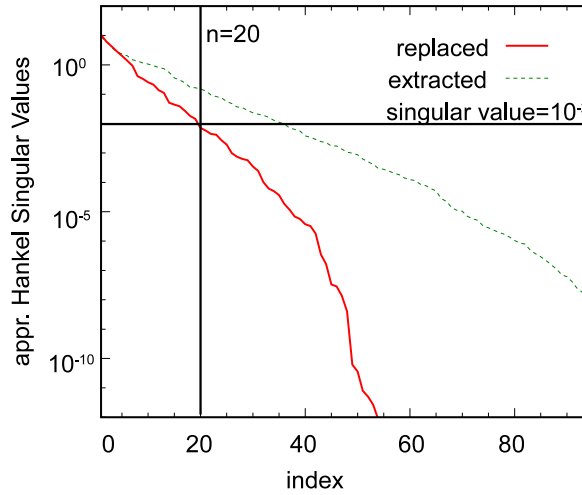


Figure 5.16: HSV of the RCNL-grid networks with extracted and replaced sources

parison both systems are reduced to the same order ($n_{repl} = n_{extr} = 20$) and to the same maximum HSV (10^{-2}), resulting in an order of $n_{repl} = 20$ and $n_{extr} = 36$. Magnitude and phase of the impedance behavior $Z_{1,1}$ at the first pin of the original as well as the reduced systems are shown in Fig. 5.17. The errors of approximation with model reduction are shown in Fig. 5.18. The reduced linear systems of the network with replaced sources ($n_{repl} = 20$) as well as of the network with extracted sources ($n_{extr} = 36$) show a good agreement with the unreduced system with respect to the transfer behavior at the pins. The transfer function of the reduced system of low order ($n_{extr} = 20$) of the network with extracted sources deviates from the original transfer function.

The reduced systems are investigated in time domain with MATLAB by numerical integration. For the time-domain simulation on the first pin a sinusoidal current source $I = 0.1 \cdot \sin(t) + 1$ and on the second pin a DC current source with one ampere are connected and the voltage at the pins is observed. Simulation results of the reduced linear systems connected with the nonlinear parts are shown in Figs. 5.19 and 5.20 for the voltage at the first pin.

The MATLAB simulation speed-up for the order $n_{repl} = n_{extr} = 20$ models is 2x and 1.1x for the order $n_{extr} = 36$ model in comparison to the original model. It can be seen that all reduced models show a good agreement with the original one. Nevertheless, the reduced system of the network with replaced sources ($n_{repl} = 20$) is more accurate than the reduced system of

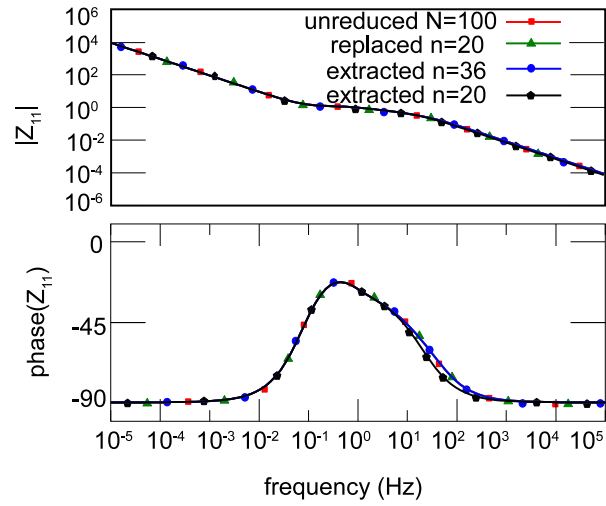


Figure 5.17: RCNL-grid transfer function $Z_{1,1}$ of the original and the Gramian-based reduced models

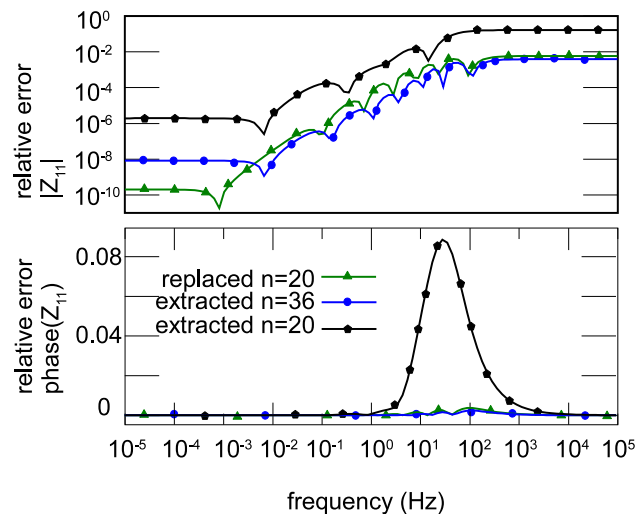


Figure 5.18: Relative approximation error of the RCNL-grid transfer function $Z_{1,1}$ of the Gramian-based reduced models

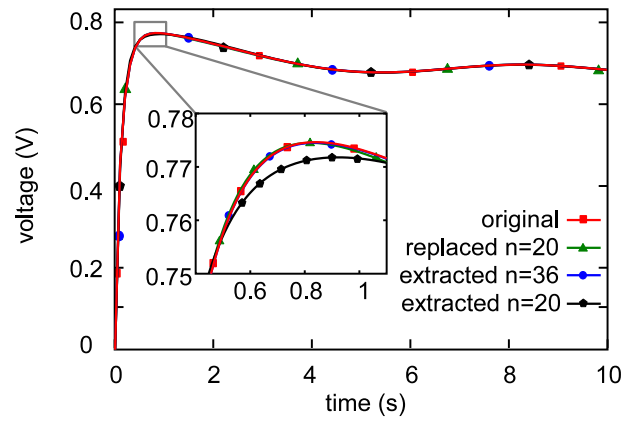


Figure 5.19: RCNL-grid voltage fluctuation at pin1 of the original and the Gramian-based reduced models

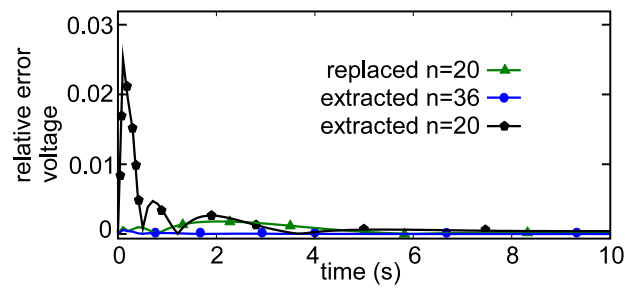


Figure 5.20: Relative approximation error of the RCNL-grid voltage fluctuation at pin1 for the Gramian-based reduced models

the network with extracted sources of the same size ($n_{extr} = 20$). Furthermore, for similar accuracy, the reduced system of the network with replaced sources ($n_{repl} = 20$) is smaller than the reduced system of the network with extracted sources ($n_{extr} = 36$). Therefore the computational effort in simulations is lower.

For illustration of the port reduction of a network, where the distributed sources' models are in addition time varying, the network is slightly changed. A time variance in the models of the distributed sources is introduced. The $q = 12$ nonlinear elements additionally depend periodically on the time with

$$I_k = f_k(\mathbf{x}) = \sin(t) \frac{a_{0,k} + V_{45}(a_{1,k} + a_{2,k}V_{45})}{1 - 2V_{45}^2 + V_{45}^4}$$

$$1 \leq k \leq 12; \quad a_{0,k}, a_{1,k}, a_{2,k} \in \mathbb{R}. \quad (5.4)$$

where the $r = 4$ basis functions of the reduced dimension function space are again calculated by partial fraction decomposition

$$\begin{aligned} g_1(\mathbf{x}) &= \sin(t)/(V_{45} + 1) \\ g_2(\mathbf{x}) &= \sin(t)/(V_{45} + 1)^2 \\ g_3(\mathbf{x}) &= \sin(t)/(V_{45} - 1) \\ g_4(\mathbf{x}) &= \sin(t)/(V_{45} - 1)^2. \end{aligned} \quad (5.5)$$

The basis functions can be mapped to the distributed sources' functions with the corresponding weights. This shows that the time-variance of the nonlinear elements can be included easily in the port reduction flow. The basis functions spanning the reduced dimension function space of the distributed sources' behavior are now also functions of the time. The time is handled as just another variable, which has to be included in the algorithm for reducing the dimension of the function space of the distributed sources. As the linear part of the network is equal to the former example, the reduction results of the linear network are the same. The resulting time simulations for 1A DC current sources connected to the pins of the original as well as the reduced networks are shown in Fig. 5.21 for the voltage at the first pin.

With this illustrative examples it is shown that the port reduction method proposed in this work can lead to smaller and more accurate reduced models in comparison to the standard approach. Instead of extracting the models of the distributed sources, a lowered dimension function space for the sources' behavior is found. By replacing the time-variant nonlinear models of the distributed sources, the number of ports of the reducible part is lowered. With the proposed method a significant model reduction is enabled while with the existing methods no or only a slight reduction is possible with acceptable accuracy.

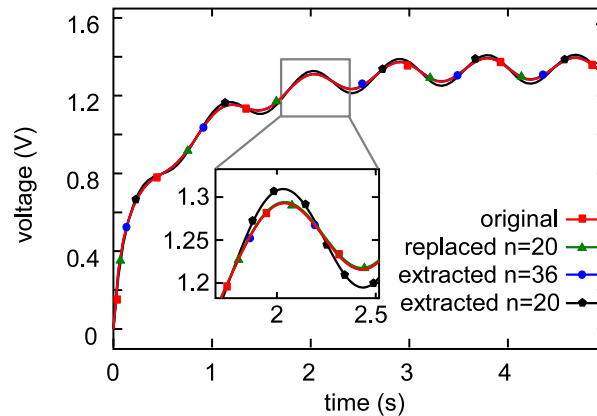


Figure 5.21: Further RCNL-grid voltage fluctuation at pin1 of the original and the Gramian-based reduced models

5.3 Emission Model of an IC

In this section an industrial network model of a distributed system with distributed sources, an emission model of an IC, is to be reduced. With decreasing feature sizes in microelectronic applications, electromagnetic compatibility (EMC) and reliability (EMR) have to be considered early in the design phase [7, 170–172]. Macromodels of the electromagnetic behavior of chips are created to help semiconductor manufacturers to take EMC/EMR effects into account during the design process. With these models the most appropriate placement and routing configurations for chip and package can be found. One part of the EMC/EMR effects is the electromagnetic emission of integrated circuits (ICs). The electromagnetic emission of an IC is determined by the operation activity plus the propagation paths through the power network of the IC, the package and the printed circuit board traces.

The emission behavior of an IC can be modeled with an IC conducted emission model (ICEM) [170, 171]. For modeling, the IC is divided into sections, whereas each section is modeled by a so-called supply line model. The supply line models consist of a model of the passive power distribution network and a model for the internal sources [170]. A supply line model contains RLC-elements modeling the electric behavior of the power distribution network of this section and an independent current source modeling the current due to switching of the transistors inside the IC. The whole ICEM is built with up to tens of thousands of supply line models for the complete IC [173, 174]. The pins of the IC are modeled at the corresponding nodes of the ICEM as ports for the connection with other EMC/EMR models. A section of the ICEM can be seen in Fig. 5.22. The parameters of the ICEM can be obtained by several methods. The RLC-parameters of the IC supply line models can be determined either during the IC design phase by taking into account material parameters or by taking measurements on an existing chip [170, 174]. The independent sources representing the simultaneous switching of the transistors [170] are obtained by simulations of a predefined state of the IC. The waveforms of the current sources are generated with the help of standard parameters for rise-/fall-times, switching period and amplitude, by taking measurements or by netlist-based emission modeling [175]. The

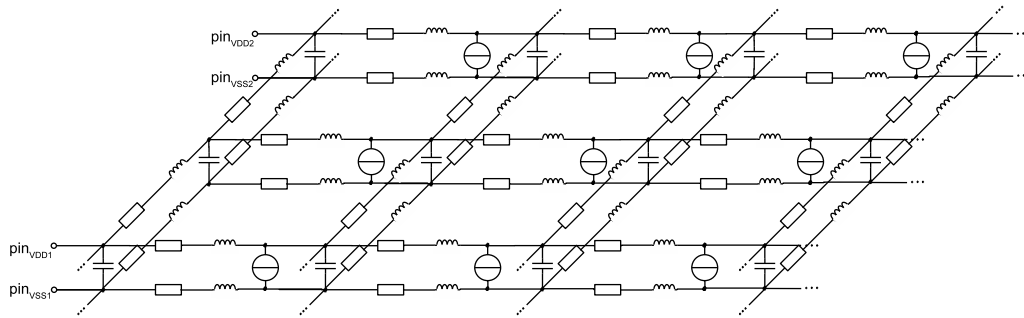


Figure 5.22: Section of the network of the ICEM

complete IC is divided into blocks, corresponding to the functional block, for example digital logic or memory, where each block contains a large number of supply line models. Within every block of the IC, the supply line model parameters for the passive elements are the same as well as the prescribed waveforms of the independent sources [173, 174]. In addition to the supply line models, several other parts of the IC are included in the modeling process. For modeling the substrate coupling a resistive network is used. The model of the package of the IC also consists of passive RLC-elements. For the network model of the pads passive RLC-elements, as well as independent current sources for the activated pads due to switching of the inputs/outputs of the IC, are used.

The resulting ICEM network models the IC as well as the distributed sources in the IC. Overall the ICEM can contain thousands of passive RLC-elements and independent sources as well as a large number of pins [173, 174]. The high complexity leads to long simulation times, in the range of days for typical investigations. Due to the large number of elements this model requires a high computational effort in simulations, which will be reduced with model reduction. Since only the behavior at the pins of the IC is of interest, the electrical values of the internal nodes of the ICEM can be disregarded. A smaller model however, which engulfs the main properties and enables faster simulations can be obtained by model reduction. The use of the reduced model instead of the original one speeds up time- and frequency-domain simulations.

The large number of independent sources used in the ICEM modeling is a limitation for the order reduction algorithms (Sec. 4.1). In the following sections two ICEM examples are reduced and it will be shown that the proposed port reduction enhances the reduction efficiency, and thereby overcomes the limitations by the large number of sources in model reduction.

5.3.1 Supply Voltage Domain Related Model

As first example the supply voltage domain related ICEM of the Infineon TriCore1796, a 32 Bit automotive microcontroller with 30 million transistors, is used. The supply pins of the microcontroller are grouped with respect to their voltage domain in this model. Every voltage domain pin is used as a pin of the network model. The resulting model is an ICEM, which can be investigated at each voltage domain block. The reduced model should be valid in frequencies ranging from DC to one GHz.

The electrical network contains around 30000 passive RLC-elements and $q = 567$ independent current sources with a piece-wise linear waveform [173]. The order of the system for the example network is $N = 24967$. As the model contains four voltage domains, four supply pin ports are necessary.

Due to the large number of independent current sources 571 ports, 567 for the sources and four for the pins are necessary, if all sources are extracted. This number is quite high and limits the model reduction efficiency. The state-of-the-art approaches dealing with the reduction of systems with a large number of ports (Sec. 4.2) are reviewed for applicability of the reduction of the ICEM. The coupling of the network does not allow for a partitioning into sub-blocks (Sec. 4.2.1) with a lower number of ports. An obvious partitioning would be to divide into package model, substrate, supply domain model and so on. Each sub-block would contain at least the nodes at the boundaries of the sub-block as ports, which is in the range of several hundred nodes for this example and is still too high for an efficient model reduction. In addition, a partitioning of the supply line model part, where most of the sources are connected, is not possible, due to the high coupling like in the RC-grid with independent sources (Sec. 5.1). The transfer function partitioning methods (Sec. 4.2.1) cannot be applied, as the resulting reduced model has to be synthesized as an electrical network. The generation of a large number of reduced models, describing the complete model, leads to a high overhead in the reduced network for coupling the subsystems. The example network is not regularly structured, as the package, pad and substrate models are included with the supply domain model in the network, which does not allow for the usage of the methods based on port correlation (Sec. 4.2.2). The reduced order simulation method (Sec. 4.2.3.2) assumes all inputs to be determined and cannot be applied, as the models, which are connected with the supply pins are not known. The correlation of the waveforms is quite high, which allows for the application of the methods based on input signal correlation (Sec. 4.2.3.1). Nevertheless, this method is restricted to the use of a Gramian-based model reduction method using Lyapunov equations. The high order of the system does not allow for the Gramian-based reduction using Lyapunov equations due to the high numerical effort. In addition the block structure for the RLC-elements in the system matrices of the system of the ICEM has to be preserved during reduction, which is not possible by using the reduction method based on input signal correlation.

The state-of-the-art methods are not capable of efficiently reducing this example network. Thus the port reduction method of this work is applied to illustrate the possibility of a high efficiency reduction. The waveforms of the distributed sources' models are taken into account in a preceding port reduction step (Sec. 4.3). For every modeled block of the IC the prescribed waveforms of the independent sources are the same [173]. For finding the basis function of the reduced dimension function space this property is used. The independent current sources waveforms can be divided up into $r = 2$ proportional waveform characteristics, one for 31 current sources and one for 536 current sources. Realizing the network with replaced sources by adding $r = 2$ additional independent current sources having the two basis function waveforms and replacing the 567 independent sources by CCCS leads to a reduced number of independent sources (Sec. 4.3). As only two independent sources are used in the network with replaced sources, only two ports for the sources are necessary. Overall, the port reduced system consists of a mere six ports, two for the basis functions of the sources waveforms and four for the supply

pins. As the waveforms of the distributed sources can be exactly determined from the lowered dimension function space the behavior at the four supply pins of the network with replaced sources is exactly the same as in the network with extracted sources.

Both systems, the system of the network with extracted sources and 571 ports, and the system of the network with replaced sources and six ports, are reduced. As order reduction method the implicit moment matching is used. In two expansion points (1Hz and 1MHz) four moments are to be matched in a reduced order model. A comparison of the results of the model reduction of the original system and the port reduced system is given in Table 5.3.

Table 5.3: Comparison of model reduction results of the voltage-domain-related ICEM network

| | Extracted sources | Replaced sources |
|----------------------------------|---------------------------------|---------------------------------|
| Original elements / nodes | $\approx 29000 / \approx 16500$ | $\approx 29000 / \approx 16500$ |
| Order N | 24967 | 24967 |
| Ports in circuit equations | 571 | 6 |
| Reduced order n | 4568 | 48 |
| MATLAB speed-up factor | no savings | 1080 |
| Reduced network elements / nodes | $\approx 14 \cdot 10^6 / 5139$ | 1650 / 54 |
| HSPICE speed-up factor | no savings | 800 |

By order reduction the order of the system of the network with extracted sources can only be reduced by 80% to an order of $n_{extr} = 4568$. This results in MATLAB simulations of the transfer function being not faster than the unreduced system, since the reduced matrices are smaller but dense, in contrast to the sparse unreduced system matrices. With the same parameters for the model reduction the order of the circuit equations of the network with replaced sources are reduced by 99.8% to an order of $n_{repl} = 48$. With this reduced model the MATLAB simulation of the transfer functions has a speed-up factor of around one thousand. The reduced system of the port reduced system shows a close consistency with the unreduced system in the frequency range of interest up to 1GHz. As an example a transfer function of an arbitrarily chosen supply pin is shown in Figs. 5.23,5.24.

The reduced system is synthesized as a network with the GC-synthesis (Sec. 3.2.2). The reduced system of the network with extracted sources has a lot more elements than the original network and therefore is not feasible. A network with 1650 elements and only 54 nodes is generated from the $n_{repl} = 48$ reduced system, which is much smaller than the original network. The model is embedded in the surrounding network containing supply voltage sources. As this model is used for early estimations in the design process, the desired accuracy is not as high as for other applications [173]. The results of the time domain simulations in the HSPICE simulation environment show an acceptable accuracy, as can be seen in Figs. 5.25 and 5.26 for a supply voltage pin of the ICEM. A speed up of around 800 is achieved in simulations. If further improvements are necessary, the parameters for model reduction can be adjusted, which leads to bigger and slower, but more accurate reduced models. In any case, the reduced model of the port reduced network is always much smaller than the reduced model of the network with extracted sources, which proves the efficiency of the proposed method.

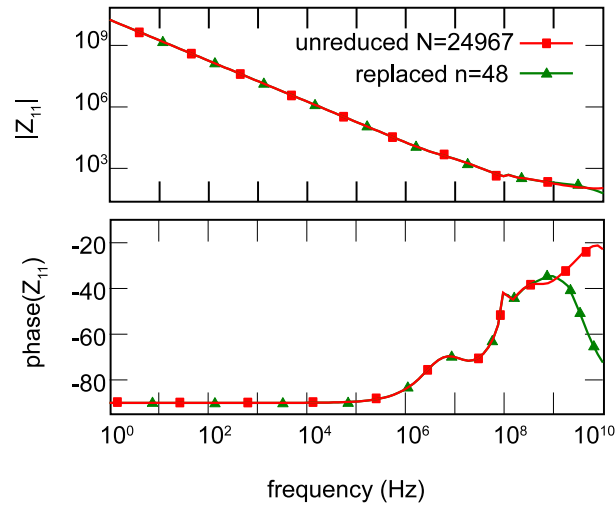


Figure 5.23: ICEM transfer function $Z_{1,1}$ of the original and the reduced model

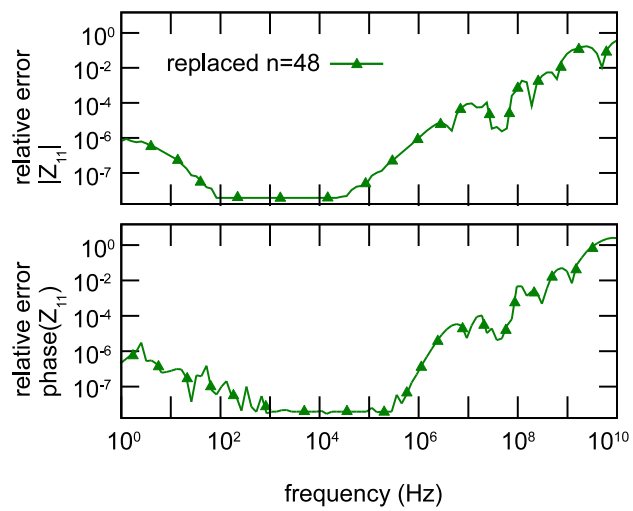


Figure 5.24: Relative approximation error of the ICEM transfer function $Z_{1,1}$ of the reduced model

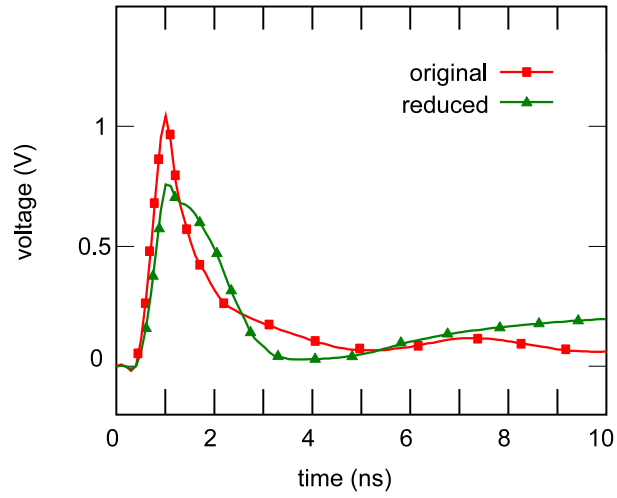


Figure 5.25: ICEM voltage fluctuation at pin1 of the original and the reduced model

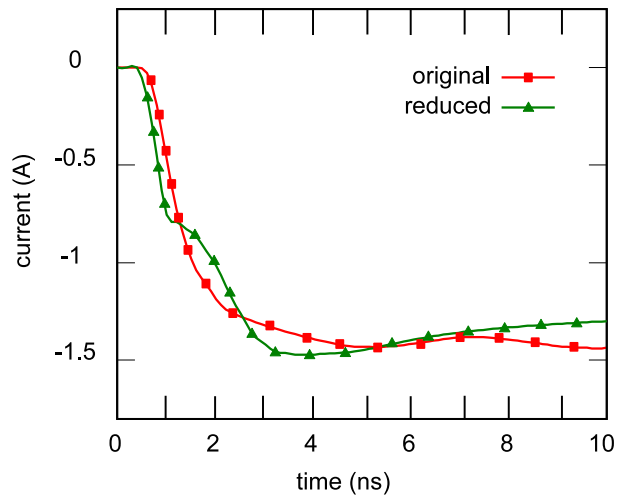


Figure 5.26: ICEM current flow at pin1 of the original and the reduced model

5.3.2 Supply Voltage Pin Related Model

As a further ICEM example the pin related model of the Infineon TriCore1796 used. The example differs from that in the former section, in the sense that the voltage pins are not grouped with respect to their voltage domain. Every supply voltage pin is used as a pin of the ICEM network.

The whole model of the microcontroller contains now 61 supply pins. The number of passive elements is around 35000. For modeling the internal activity overall $q = 328$ independent current sources, 316 sources for the ICEM as well as 12 sources for the pads are included in the model. The circuit equations of the complete model have an order of 25062. The model is to be reduced, and the reduced model should be valid in frequencies ranging from DC to one GHz.

With the standard method, where every independent source of the network model is extracted and connected through a port with the reducible system, the system has 389 ports including the pins. For this example the same review of the applicability of the state-of-the-art model reduction methods dealing with a large number of ports of the supply voltage domain related model applies (Sec. 5.3.1). As existing approaches are not capable of efficiently reducing the ICEM network, the port reduction method presented in this work is employed. With respect to their prescribed waveforms the current sources of the network can be grouped in eight groups. Two groups of proportional waveforms for the supply line models, one representing 300 and one representing 16 waveforms, and six groups for the pad sources, concluding in $r = 8$ basis functions, are found. The network with replaced sources as shown in Sec. 4.3.2 is built. Note that, as the waveforms of the model can be exactly determined from the lowered dimension function space, the behavior at the 61 pins of the network with replaced sources is exactly the same as in the network with extracted sources. Together with the pins of the model the resulting systems has 69 ports, which is much less than in the system of the network with extracted sources having 389 ports.

For comparison both systems are reduced with an implicit moment matching method based on Krylov subspaces (Sec. 3.1.4) and with the Gramian-based order reduction method PMTBR (Sec. 3.1.5). The results for the order reduction are presented in Table 5.4.

Table 5.4: Comparison of model reduction results of the supply-pin-related ICEM network

| | Order N | Ports p | Reduced Order n | Reduction | Speed-up |
|---|---------------------|---------------------|------------------------------------|------------------|-----------------|
| Extracted sources and Gramian-based reduction | 25062 | 389 | 590 | 97.6% | 33x |
| Replaced sources and Gramian-based reduction | 25062 | 69 | 201 | 99.2% | 188x |
| Extracted sources and moment matching reduction | 25062 | 389 | 1556 | 93.8% | 2.8x |
| Replaced sources and moment matching reduction | 25062 | 69 | 276 | 98.9% | 132x |

For the implicit moment matching the number of expansion points is set to two (1kHz and

1GHz) and two moments in each expansion point are to be matched. As there is a direct dependency of the order of the reduced model on the number of ports, there is a significant difference in the reduced order for the extracted and replaced sources networks system. Since the system of the network with extracted sources has more than five times as many ports as the system of the network with replaced sources, the reduced model is over five times larger.

For the Gramian-based order reduction, where the reduced order does only indirectly depend on the number of ports, the approximation to the HSV, which represent the error depending on the order of the reduced model, is shown in Fig. 5.27. It can be seen that the approximated

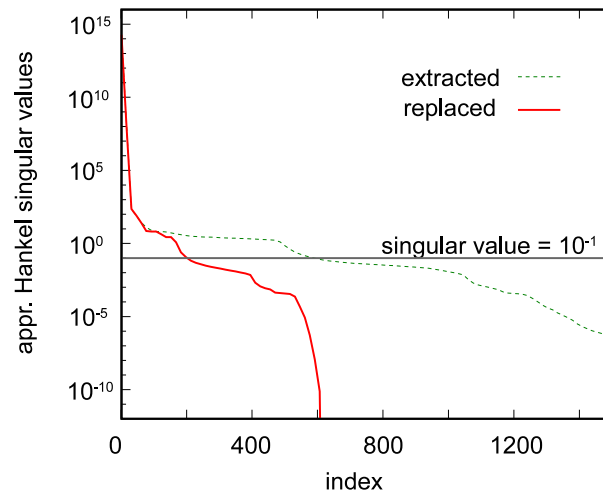


Figure 5.27: HSV of the ICEM networks with extracted and replaced sources

HSV of the port reduced system decay faster than the approximated HSV of the system of the network with extracted sources. This means that, for a given maximum error, the system of the network with replaced sources can be more efficiently reduced. Likewise for a given reduced order the reduced model of the system of the network with replaced sources is more exact than the reduced model of the network with extracted sources. For our model the maximum HSV is set to 10^{-1} , which results in a reduced order of 201 and 590 for the port reduced and standard system, respectively. With this model reduction algorithm the reduced model of the system of the network with replaced sources is three times smaller than the reduced model of the system with extracted sources.

All models show a close alignment in the frequency-domain and can be investigated with mathematical simulators. The close agreement of the reduced models with the unreduced model, in the frequency range of interest up to a few GHz, for the transfer function $Z_{3,3}$ of a supply pin, is shown in Fig. 5.28. The error between the original and the reduced models is plotted in Fig. 5.29.

The speed up in frequency-domain simulations, which is achieved with the reduction of the model is shown in Tab. 5.4. For the implicit moment matching based reduction of the system of the network with extracted sources, although the order is reduced by more than 93%, the speed up factor is below three. The reason for this is that the reduced matrices are dense

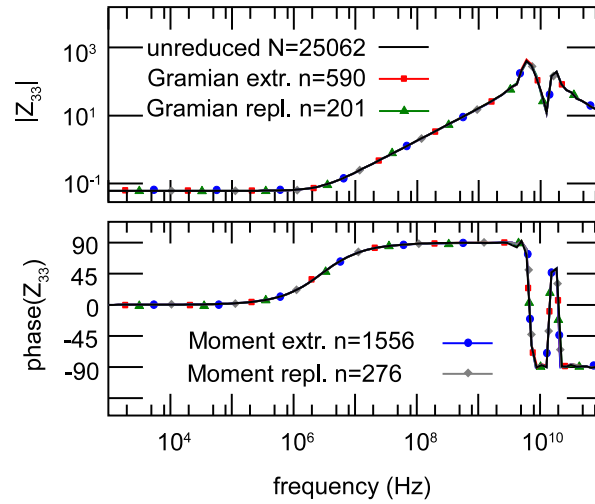


Figure 5.28: ICEM transfer function $Z_{3,3}$ of the original and the reduced models

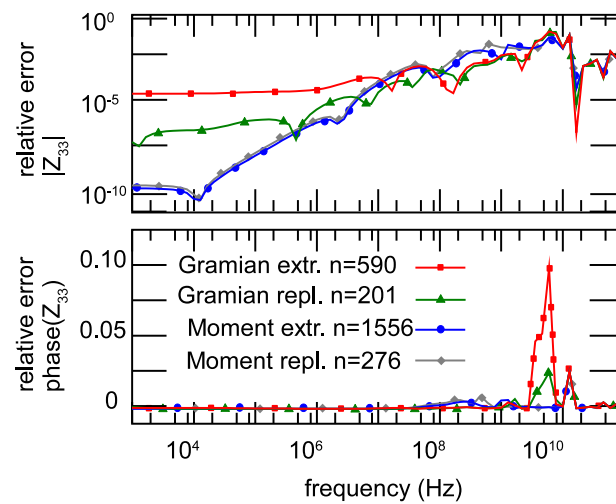


Figure 5.29: Relative approximation error of the ICEM transfer function $Z_{3,3}$ of the reduced models

while the original matrices are sparse and therefore require more computational effort for solving. If the system of the network with extracted sources is reduced with the more efficient Gramian-based order reduction method, the speed up is higher, approximately in the range of 30. Nevertheless, much faster simulations, more than 100 times faster than the original model, can only be achieved with the port reduction as preceding step, which proves the efficiency of the proposed method. Both model order reduction algorithms enable stronger reductions and therewith faster simulations, if the port reduced network with replaced sources is used.

For investigations with electrical simulators, the reduced models can be synthesized with well-known network-synthesis algorithms as described in Sec. 3.2, which allows for simulations with circuit simulators.

5.3.3 Conclusion of ICEM Reduction

In this section the reduction of industrial example networks, two ICEM models, is presented. Due to the large number of distributed sources modeling the internal switching currents, the efficiency of existing model reduction methods is limited. The model reduction of the example network either leads to quite large reduced models or the reduced models have large approximation errors. The existing approaches dealing with systems with a large number of ports, as generated by extracting the distributed sources, are not capable of reducing the ICEM efficiently. The port reduction method presented in this work is capable of reducing the ICEM model. A system with a lowered number of ports is generated by introducing the knowledge of the behavior of the distributed sources in a preceding port reduction step. The examples can be more efficiently reduced by using the port reduction method presented in this work as preceding step for a model reduction. The increase in efficiency of the model reduction was shown by exemplary reducing two industrial ICEM models.

6 Conclusions and Future Work

In the first part of this conclusion a summary of the methods investigated and the developed methods in this work is given. Open problems of the presented methods and ideas for further steps are presented in the second part.

6.1 Conclusion

Physical distributed systems are modeled by large electrical networks to enable fast and efficient investigations. In this work methods for reducing the size of network models of distributed systems with distributed sources are presented. While reducing the size of the network, in the sense of lowering the number of nodes and elements, the behavior at several specified nodes should be preserved or at least approximated. Examples for nodes where the behavior should be preserved or approximated are nodes for the connection with other network models and observed nodes. Properties of networks and mathematical descriptions of networks are highlighted and the necessity of their preservation in a reduced model is motivated.

In the first part of this work algorithms based on circuit theory, control theory and system identification are examined in a common framework for the applicability to the reduction of electrical networks and their mathematical models. Synthesis methods, realizing reduced mathematical models as electrical network, are investigated. A synthesis method is presented, called GC-synthesis, which is capable of efficiently realizing reduced order systems of networks as an electrical network. If existing methods are used, the need for controlled dynamic elements in the simulation environment, for creating small and efficient networks, is a disadvantage. By using the proposed GC-synthesis this disadvantage vanishes. Based on preserved system properties, a small and efficient network can be built, which does not need controlled dynamic elements.

The second part of this work concerns the reduction of a class of networks, having in addition to a large number of linear resistive, capacitive and inductive elements, also a large number of sources. The sources can be independent sources, or in the more general case, nonlinear controlled sources. In existing methods the sources' models are extracted from the linear part of the network. The linear part and the extracted sources are connected by ports, resulting in a large number of ports for a large number of sources. The model reduction methods are capable of reducing the linear part of the network while the behavior at the ports is approximated in the reduced network. Nevertheless, the standard model reduction methods suffer from low efficiency for a large number of ports. Extended methods, especially dealing with the reduction of systems with a large number of ports, are investigated. The advantages as well as the disadvantages and limitations of the existing methods in reducing networks with a large number of sources are highlighted. Mainly, existing methods are either not able to preserve network relevant properties, are limited to special classes of networks, or are limited in efficiency.

A new method is presented in this work, especially dealing with the model reduction of net-

works with a large number of sources. In the presented method not all sources are extracted, avoiding the generation a large number of ports in this way. Instead, based on the a priori defined functions of the sources, a function space is spanned by the sources' functions. With methods from approximation theory a function space with a lower dimension is found, representing the function space of the sources' functions. This lower dimension function space is realized with additional electrical elements in the network model. The sources in the network model are replaced by linear controlled sources, mapping the reduced dimension function space to the function space of the distributed sources. The overall network model now contains a lowered number of elements, which cannot be included in the model reduction process. By extracting this lowered number of elements, a reducible system with a lowered number of ports, compared to the extraction of all sources as in the standard method, is created. This system with a smaller number of ports can be reduced more efficiently with model reduction methods. In this work the complete flow for creating the port reduced system is presented. Several applicable methods for the reduction of the dimension of the function space of the sources are given, able to handle a large variety of distributed sources' models. The realization of the reduced dimension function space in the network is shown, while relevant network properties are preserved in the reducible system. Implementation hints are given, to enable the extension of existing model reduction flows to the capability of reducing systems with a large number of sources.

The increase in efficiency of the reduction of network models with a large number of sources by using the port reduction proposed in this work is shown. By reducing illustrative examples as well as industrial examples with a large number of sources, the improved accuracy of the reduced models and the higher efficiency of the model reduction is demonstrated.

6.2 Future Work

Several ideas for further development of the methods presented in this work will be specified in the following.

Firstly, the model reduction of networks still faces several open issues. Due to the mathematically based reduction of systems of networks, the resulting reduced model typically is not based on physical parameters anymore. Despite the fact that the model of the distributed system contains only physically based element values, the reduced network, synthesized from the reduced mathematical model, contains non-physical element values. The element values of the reduced models can be quite small or quite large, compared to the range of elements created by modeling. Even negative element values can arise, having no physical basis. Due to the investigation of the reduced network in simulation environments, normally dealing with physical models, numerical problems can occur. Other numerical issues occur during the reduction of the models. For example, though the preservation of passivity is guaranteed by the algorithm, the reduced model may be active, due to finite precision of the numerical calculations.

Secondly, future work for the port reduction presented in this work remains open. The presented methods for the reduction of the dimension of the function space of the sources are only a small prospect. Several other methods exist, and for every model an applicable method has

to be found. Due to the large variety of possible functions of the distributed sources, no general method exists. Especially in the case of nonlinear controlled sources, used for modeling distributed sources' behavior, a large number of controlling variables can lead to only small or even no possible reduction of the dimension of the function space of the sources.

The realization of the reduced dimension function space basis functions as additional network elements is another relevant point. Typically the basis functions belong to the same class as the functions of the sources. For example, if the sources' functions are piece-wise linear functions, the basis functions of a reduced dimension function space are as well piece-wise linear. Thus, if the distributed sources' models are implemented in the simulation environment, the basis functions of a reduced dimension function space can be most likely implemented in a similar way. Nevertheless, due to limitations of the simulation environment, in a few cases the realization of the basis functions may be complicated or even impossible, which has to be further investigated.

Another open issue, especially by approximating the function space of the sources, is the accuracy. The effect of a small accuracy derivation, during the reduction of the function space of the distributed sources, on the behavior at the network nodes of interest has to be investigated properly. In fact, the behavior at the nodes of interest is approximated in up to three different steps. The first step is the approximation of the behavior of the distributed sources with a lower dimension function space. If the function space of the distributed sources can only be obtained approximatively and not exactly from the reduced dimension function space, deviations of the behavior at the nodes of interest occur. The second approximation is introduced by applying model reduction to the linear network part. A possible third approximation is by converting the nonlinear controlled sources' models to be controlled from the reduced networks values. Overall, all of these approximations have to be handled with care, and the corresponding influence on the behavior at the nodes of interest has to be monitored.

In the actual implementation of the proposed port reduction a few manual steps are necessary. Especially in the field of lowering the dimension of the function space of the sources, knowledge has to be included for finding an appropriate approximation method. The presented port reduction method can be further fully automated for several classes of functions describing distributed sources. The definition of these classes, and the implementation of a fully automated process of the port reduction for several classes of distributed sources' models, remains open for future work.

Bibliography

- [1] CIARLET, P. G.: *The finite element method for elliptic problems*. North-Holland, 2002.
- [2] ZIENKIEWICZ, O.C. and R.L. TAYLOR: *The finite element method for solid and structural mechanics*. Elsevier, 2005.
- [3] JIN, J.: *The Finite Element Method in Electromagnetics*. Wiley, 2002.
- [4] RUEHLI, A.E.: *Equivalent circuit models for three-dimensional multiconductor Systems*. IEEE Transactions on Microwave Theory and Techniques, MTT-22:216 – 221, 1974.
- [5] DAVIS, J. A. and J. D. MEINDL: *Compact Distributed RLC Interconnect Models Part I*. IEEE Transactions on Electron Devices, 47:2068 – 2077, 2000.
- [6] NITSCH, J., F. GRONWALD and G. WOLLENBERG: *Radiating Nonuniform Transmission-Line Systems and the Partial Element Equivalent Circuit Method*. Wiley, 2009.
- [7] STEINECKE, THOMAS: *Analog Circuit Design*, chapter Modeling and verification techniques to ensure system-wide electromagnetic reliability, pages 129 – 150. Springer Netherlands, 2006.
- [8] BECHTHOLD, T., E.B. RUDNYI and J.G. KORVINK: *Dynamic electro-thermal simulation of microsystems - a review*. Journal of Micromechanics and Microengineering, 15:R17– R31, 2005.
- [9] YANG, Y.-J., S.-Y. CHENG and K.-Y. SHEN: *Macromodeling of coupled-domain MEMS devices with electrostatic and electrothermal effects*. Journal of micromechanics and microengineering, 14:1190 – 1196, 2004.
- [10] NASSIF, S.R. and J.N. JOZHAYA: *Fast Power Grid Simulation*. In *ACM/IEEE Design Automation Conference*, 2000.
- [11] CHAUDHRY, R., R.V. PANDA, S.S SAPATNEKAR, T. EDWARDS, D. BLAAUW and M. ZHAO: *Hierarchical analysis of power distribution networks*. In *ACM/IEEE Design Automation Conference*, 2000.
- [12] BELEVITCH, V.: *Classical network theory*. Holden Day, 1968.
- [13] HO, C.-W., A.E. RUEHLI and P.A. BRENNAN: *The Modified Nodal Approach to Network Analysis*. IEEE Transactions on Circuits and Systems, CAS-22:504 – 509, 1975.
- [14] HACHTEL, G., R. BRAYTON and F. GUSTAVSON: *The Sparse Tableau Approach to Network Analysis and Design*. IEEE Transactions on Circuit Theory, 18:101 – 113, 1971.

- [15] REINSCHKE, K. and P. SCHWARZ: *Verfahren zur Rechnergestützten Analyse Linearer Netzwerke*. Akademie Verlag Berlin, 1976.
- [16] VLACH, J. and K. SINGHAL: *Computer Methods for Circuit Analysis and Design*. van Nostrand Reinhold, 1994.
- [17] CHUA, L.O. and P.-M. LIN: *Computer-Aided Analysis of Electronic Circuits*. Prentice Hall, 1975.
- [18] GANTMACHER, F.R.: *The theory of matrices, Volume 2*. AMS Chelsea Publishing, 1998.
- [19] MATHIS, W.: *Zur Theorie und Numerik verallgemeinerter Zustandsgleichungen im Frequenzbereich und deren Anwendung bei der Netzwerkanalyse*. PhD thesis, University of Technology Braunschweig, 1984.
- [20] MATHIS, W.: *Mathematical Modelling and Simulation of Electrical Circuits and Semiconductor Devices*, chapter Analysis of Linear Time-invariant Networks in the Frequency Domain, pages 83 – 90. Birkhäuser, 1994.
- [21] DAVISON, E.J.: *A Method for Simplifying Linear Dynamic Systems*. IEEE Transactions on Automatic Control, AC-11:93 – 101, 1966.
- [22] AGUIRRE, L.A.: *Quantitative measure of modal dominance for continuous systems*. In *IEEE Conference on Decision and Control*, 1993.
- [23] GREEN, M. and D.J.N. LIMEBEER: *Linear Robust Control*. Prentice Hall, 1994.
- [24] ROMMES, J.: *Model Order Reduction: Theory, Research Aspects and Applications*, chapter Modal Approximation and Computation of Dominant Poles, pages 177 – 193. Springer, 2008.
- [25] MARTINS, N., L.T.G. LIMA and H.J.C.P. PINTO: *Computing dominant poles of power system transfer functions*. IEEE Transactions on Power Systems, 11:162 – 170, 1996.
- [26] VARGA, A.: *Enhanced Modal Approach for Model Reduction*. Mathematical Modelling of Systems, 1:91–105, 1995.
- [27] CAUER, W.: *Die Verwirklichung von Wechselstromwiderständen vorgeschriebener Frequenzabhängigkeit*. PhD thesis, Technische Hochschule zu Berlin, 1926.
- [28] BRUNE, O.: *Synthesis of a finite two-terminal network whose driving-point impedance is a prescribed function of frequency*. PhD thesis, Massachusetts Institute of Technology, 1931.
- [29] ELMORE, W.C.: *The Transient Response of Linear Networks with Particular Regard to Wideband Amplifiers*. Journal of Applied Physics, 19:55 – 63, 1948.
- [30] BROGAN, W.L.: *Modern Control Theory*. Englewood Cliffs, Prentice Hall, 1991.

- [31] LU, K. and K.-S. LUDWIG: *Controllability and observability of RLC networks over $F(z)$* . In *IEEE International Symposium on Circuits and Systems*, 1999.
- [32] LU, K.-S. and K. LU: *Controllability and observability criteria of RLC networks over $F(z)$* . *International Journal of Circuit Theory and Applications*, 29:337 – 341, 2001.
- [33] LU, K.-S., X.-Y. FENG and G.-Z.-GAO: *The separability, reducibility and controllability of RLCM networks over $F(z)$* . In *IEEE International Symposium on Circuits and Systems*, 2005.
- [34] KUH, E. S. and R. A. ROHRER: *Theory of Linear Active Networks*. Holden Day, 1967.
- [35] KUO, B.C.: *Automatic Control Systems*. Prentice Hall, 1962.
- [36] ATABEKOV, G.I.: *Linear Network Theory*. Pergamon Press Ltd., 1965.
- [37] SU, S.-L., V.B. RAO and T.N. TRICK: *A Simple and Accurate Node Reduction Technique for Interconnect Modeling in Circuit Extraction*. In *IEEE/ACM International Conference on Computer Aided Design*, 1986.
- [38] SU, S.-L., V.B. RAO and T.N. TRICK: *HPEX: A hierarchical parasitic circuit extractor*. In *ACM/IEEE Design Automation Conference*, 1987.
- [39] KOZHAYA, J.N., S.R. NASSIF and F.N. NAJM: *A Multigrid-Like Technique for Power Grid Analysis*. *IEEE Transactions on Computer Aided Design of Integrated Circuits and Systems*, 21:1148–1160, 2002.
- [40] KOZHAYA, J.N., S.R. NASSIF and F.N. NAJM: *A Multigrid-Like Technique for Power Grid Analysis*. In *IEEE/ACM International Conference on Computer Aided Design*, 2001.
- [41] KLEIN, W.: *Mehrtortheorie*. Akademie Verlag Berlin, 1976.
- [42] JOHNSON, T.A.: *Resistive Network Simplification Technique*. Technical Report, IBM Technical Disclosure Bulletin, 1981.
- [43] MEIJS, N.P. VAN DER: *Model Order Reduction: Theory, Research Aspects and Applications*, chapter Model Order Reduction of Large RC Circuits, pages 421 – 446. Springer, 2008.
- [44] PONG, T.-S. and M.A. BROOKE: *A parasitics extraction and network reduction algorithm for VLSI*. In *IEEE Midwest Symposium on Circuits and Systems*, 1989.
- [45] GENDEREN, A.J. VAN and N.P. VAN DER MEIJS: *Extracting Simple but Accurate RC Models for VLSI Interconnect*. In *IEEE International Symposium on Circuits and Systems*, 1988.
- [46] GENDEREN, A.J. VAN and N.P. VAN DER MEIJS: *Reduced RC models for IC interconnections with couplingcapacitances*. In *European Conference on Design Automation*, 1992.

- [47] HARBOUR, M.G. and J.M. DRAKE: *Calculation of Signal Delay in Integrated Interconnection*. IEEE Transactions on Circuits and Systems, 36:272 – 276, 1989.
- [48] HARBOUR, M.G. and J.M. DRAKE: *Simple RC model for integrated multiterminal interconnections*. IEE Proceedings Electronic Circuits and Systems, 135:19 – 23, 1988.
- [49] ELIAS, P.J.H.: *Efficient moments extraction from VLSI interconnections*. In *ProRISC/IEEE Conference on Circuits, Systems and Signal Processing*, 1995.
- [50] ELIAS, P. J. H. and N. P. VAN DER MEIJS: *Including Higher-Order Moments of RC Interconnections in Layout-to-Circuit Extraction*. In *European Conference on Design and Test*, 1996.
- [51] ENNS, M.K and J.J. QUADA: *Sparsity-Enhanced Network Reduction for Fault Studies*. IEEE Transactions on Power Systems, 6:613 – 621, 1991.
- [52] TINNEY, W., W. POWELL and N. PETERSPM: *Sparsity-oriented network reduction*. In *Power Industry Computer Applications Conference*, 1973.
- [53] ROMMES, J. and W.H.A. SCHILDERS: *Efficient Methods for Large Resistor Networks*. IEEE Transactions on Computer-Aided Design of Integrated Circuits and Systems, 29:28 – 39, 2010.
- [54] ELIAS, P. J. H. and N. P. VAN DER MEIJS: *Extracting Circuit Models for Large RC Interconnections that are Accurate up to a Predefined Signal Frequency*. In *ACM/IEEE Design Automation Conference*, 1996.
- [55] RAO, V.B., J.P. SOREFF, R. LEDALLA and F.L. YANG: *Aggressive Crunching of Extracted RC Netlists*. In *ACM/IEEE International Workshop on Timing Issues in the Specification and Synthesis of Digital Systems*, 2002.
- [56] SHEEHAN, B.N.: *TICER: Realizable reduction of extracted RC circuits*. In *IEEE/ACM International Conference on Computer Aided Design*, 1999.
- [57] ROMMES, J. and N. MARTINS: *Efficient computation of transfer function dominant poles using subspace acceleration*. IEEE Transactions on Power Systems, 21:1218 – 1226, 2006.
- [58] MARTINS, N.: *The dominant pole spectrum eigensolver*. IEEE Transactions on Power Systems, 12:245 – 254, 1997.
- [59] RADIC-WEISSENFELD, L.J.: *Model Order Reduction of Linear Systems with Applications to Signal Processing and EMC*. PhD thesis, University of Hannover, 2008.
- [60] MARTINS, N. and P.E.M. QUINTAO: *Computing Dominant Poles of Power System Multivariable Transfer Functions*. IEEE Transactions on Power Systems, 18:152 – 159, 2003.

- [61] ROMMES, J. and N. MARTINS: *Efficient Computation of Multivariable Transfer Function Dominant Poles Using Subspace Acceleration*. IEEE Transactions on Power Systems, 21:1471 – 1483, 2006.
- [62] PILLAGE, L. T. and R. A. ROHRER: *Asymptotic waveform evaluation for timing analysis*. IEEE Transactions on Computer-Aided Design of Integrated Circuits and Systems, 9:352–366, 1990.
- [63] LIN, S. and E.S. KUH: *Transient simulation of lossy interconnects based on the recursive convolution formulation*. IEEE Transactions on Circuits and Systems, 39:879 – 892, 1992.
- [64] BRACKEN, J. E., V. RAGHAVAN and R. A. ROHRER: *Interconnect simulation with asymptotic waveform evaluation (AWE)*. IEEE Transactions on Circuits and Systems I: Fundamental Theory and Applications, 39:869–878, 1992.
- [65] XU, G. L. and A. BULTHEEL: *Matrix Pade Approximation: Definitions and Properties*. Linear Algebra and its Application, 137-138:67–136, 1990.
- [66] XU, G. and A. BULTHEEL: *Approximation, Optimization and Computing: Theory and Applications*, chapter The problem of matrix Padé approximation, pages 217–220. Elsevier Science Publishers, 1990.
- [67] FELDMANN, P. and R. W. FREUND: *Reduced-order modeling of large linear subcircuits via a block Lanczos algorithm*. In *ACM/IEEE Design Automation Conference*, 1995.
- [68] FELDMANN, P. and R. W. FREUND: *Efficient linear circuit analysis by Pade approximation via the Lanczos process*. IEEE Transactions on Computer-Aided Design of Integrated Circuits and Systems, 14:639–649, 1995.
- [69] SILVEIRA, L. M., M. KAMON and J. WHITE: *Efficient reduced-order modeling of frequency-dependent coupling inductances associated with 3-D interconnect structures*. In *IEEE/ACM Design Automation Conference*, 1995.
- [70] SILVEIRA, L.M., M. KAMON, I. ELFADEL and J. WHITE: *A Coordinate-Transformed Arnoldi Algorithm for Generating Guaranteed Stable Reduced-Order Models of RLC Circuits*. In *IEEE/ACM International Conference on Computer Aided Design*, 1997.
- [71] ODABASIOGLU, A., M. CELIK and L. T. PILEGGI: *PRIMA: passive reduced-order interconnect macromodeling algorithm*. In *IEEE/ACM International Conference on Computer Aided Design*, 1997.
- [72] ODABASIOGLU, A., M. CELIK and L. T. PILEGGI: *PRIMA: passive reduced-order interconnect macromodeling algorithm*. IEEE Transactions on Computer-Aided Design of Integrated Circuits and Systems, 17:645–654, 1998.
- [73] GRIMME, E.J.: *Krylov Projection Methods For Model Reduction*. PhD thesis, University of Illinois at Urbana-Champaign, 1997.

- [74] ELFADEL, I. M. and D. D. LING: *A block rational Arnoldi algorithm for multipoint passivemodel-order reduction of multiport RLC networks*. In *IEEE/ACM International Conference on Computer Aided Design*, 1997.
- [75] FREUND, R. W.: *SPRIM: structure-preserving reduced-order interconnect macromodeling*. In *IEEE/ACM International Conference on Computer Aided Design*, 2004.
- [76] FREUND, R. W.: *Model Order Reduction: Theory, Research Aspects and Applications*, chapter Structure-Preserving Model Order Reduction of RCL Circuit Equations, pages 49 – 74. Springer, 2008.
- [77] YANG, F., X. ZENG, Y. SU and D. ZHOU: *RLCSYN: RLC Equivalent Circuit Synthesis for Structure-Preserved Reduced-order Model of Interconnect*. In *IEEE International Symposium on Circuits and Systems*, 2007.
- [78] SHEEHAN, B.N.: *ENOR: Model Order Reduction of RLC Circuits Using Nodal Equations for Efficient Factorization*. In *ACM/IEEE Design Automation Conference*, 1999.
- [79] BAI, Z. and Y. SU: *Dimension Reduction of Large-Scale Second-Order Dynamical Systems via a Second-Order Arnoldi Method*. *SIAM Journal on Scientific Computing*, 26:1692 – 1709, 2005.
- [80] SALIMBAHRAMI, B. and B. LOHMANN: *Order reduction of large scale second-order systems using Krylov subspace methods*. *Linear Algebra and its Applications*, 415:385 – 405, 2005.
- [81] BOND, B.N. and L. DANIEL: *Guaranteed Stable Projection-Based Model Reduction for Indefinite and Unstable Linear Systems*. In *IEEE/ACM International Conference on Computer Aided Design*, 2008.
- [82] MOORE, B.: *Principal component analysis in linear systems: Controllability, observability, and model reduction*. *IEEE Transactions on Automatic Control*, 26:17 – 32, 1981.
- [83] GLOVER, K.: *All optimal Hankel-norm approximations of linear multivariable systems and their L^∞ -error bounds*. *International Journal of Control*, 39:1115 – 1193, 1984.
- [84] ENNS, D.F.: *Model reduction with balanced realizations: An error bound and a frequency weighted generalization*. In *IEEE Conference on Decision and Control*, 1984.
- [85] STYKEL, T.: *Numerical solution and perturbation theory for generalized Lyapunov equations*. *Linear Algebra and its Applications*, 349:155 – 185, 2002.
- [86] MEHRMANN, V. and T. STYKEL: *Dimension Reduction of Large-Scale Systems*, chapter Balanced truncation model reduction for large-scale systems in descriptor form, pages 93 – 115. Springer, 2005.
- [87] SORENSEN, D.C. and A.C. ANTOULAS: *Projection methods for balanced model reduction*. Technical Report, Rice University, 2001.

- [88] LIU, Y. and B.D.O. ANDERSON: *Singular Perturbation Approximation of Balanced Systems*. In *IEEE Conference on Decision and Control*, 1989.
- [89] LIU, Y. and B.D.O. ANDERSON: *Singular Perturbation Approximation of Balanced Systems*. *International Journal of Control*, 50:1379 – 1405, 1989.
- [90] STYKEL, T. and T. REIS: *Scientific Computing in Electrical Engineering SCEE 2008*, chapter Passivity-preserving balanced truncation model reduction of circuit equations. Springer, 2010.
- [91] PHILLIPS, J. R. and L. M. SILVEIRA: *Poor man's TBR: a simple model reduction scheme*. *IEEE Transactions on Computer-Aided Design of Integrated Circuits and Systems*, 24:43–55, 2005.
- [92] LEVY, E.C.: *Complex Curve Fitting*. *IRE Transactions on Automatic Control*, 4:37 – 44, 1959.
- [93] SANATHANAN, C.K. and J. KOERNER: *Transfer function synthesis as a ratio of two complex polynomials*. *IEEE Transactions on Automatic Control*, AC-8:56 – 58, 1963.
- [94] WARD, J.B.: *Equivalent Circuits for Power-Flow Studies*. *Transactions of the American Institute of Electrical Engineers*, 68:373 – 382, 1949.
- [95] GUSTAVSEN, B. and A. SEMLYEN: *Rational Approximation of Frequency Domain Responses by Vector Fitting*. *IEEE Transactions on Power Delivery*, 14:1052 – 1061, 1999.
- [96] D. DESCHRIJVER, T. DHAENE: *Model Order Reduction: Theory, Research Aspects and Applications*, chapter Data-driven Model Order Reduction using Orthonormal Vector Fitting, pages 341 – 359. Springer, 2008.
- [97] D. DESCHRIJVER, T. DHAENE, D. DE ZUTTER: *Robust Parametric Macromodeling using Multivariate Orthonormal Vector Fitting*. *IEEE Transactions on Microwave Theory and Techniques*, 56:1661 – 1667, 2008.
- [98] RICHARDSON, M.H. and D.L. FORMENTI: *Parameter Estimation from Frequency Response Measurements using Rational Fraction Polynomials*. In *International Modal Analysis Conference*, 1982.
- [99] LEVENBERG, K.: *A method for the solution of certain nonlinear problems in least squares*. *Quarterly Applied Mathematics*, 2:164 – 168, 1944.
- [100] MARQUARDT, D.W.: *An Algorithm for Least-Squares Estimation of Nonlinear Parameters*. *Journal of the Society for Industrial and Applied Mathematics SIAM*, 11:431 – 441, 1963.
- [101] LIN, P.L. and Y.C. WU: *Identification of Multi-Input Multi-Output Linear Systems From Frequency Response Data*. *Journal of Dynamic Systems, Measurement, and Control*, 104:58 – 64, 1982.

Bibliography

- [102] DAILEY, R.L. and M.S. LUKICH: *MIMO transfer function curve fitting using Chebyshev polynomials*. In *SIAM 35th Anniversary Meeting*, 1987.
- [103] GU, G. and P.P. KHARGONEKAR: *A class of algorithms for identification in H_∞* . *Automatica*, 28:299 – 312, 1992.
- [104] BAYARD, D.S.: *High-order multivariable transfer function curve fitting: algorithms, sparse matrix methods and experimental results*. *Automatica*, 30:1439 – 1444, 1994.
- [105] ANTOULAS, A.C., C.A. BEATTIE and S. GUGERCIN: *Interpolatory Model Reduction of Large-scale Dynamical Systems*. <http://www.win.tue.nl/casa/meetings/special/mor09/antoulaspaper.pdf>, 2009.
- [106] GUSTAVSEN, B. and A. SEMLYEN: *Enforcing passivity for admittance matrices approximated by rational functions*. *IEEE Transactions on Power Systems*, 16:97 – 104, 2001.
- [107] GRIVET-TALOCIA, S.: *Passivity enforcement via perturbation of Hamiltonian matrices*. *IEEE Transactions on Circuits and Systems I*, 51:1755–1769, 2004.
- [108] GRIVET-TALOCIA, S.: *Fast passivity enforcement for large and sparse macromodels*. In *IEEE Topical Meeting on Electrical Performance of Electronic Packaging*, 2004.
- [109] SCHROEDER, C. and T. STYKEL: *Passivation of LTI systems*. Technical Report, Math-eon, 2007.
- [110] ANTOULAS, A.C.: *On the Construction of Passive Models from Frequency Response Data*. *at - Automatisierungstechnik*, 56:447 – 452, 2008.
- [111] ANDERSON, B.D.O. and A.C. ANTOULAS: *Rational Interpolation and State Variable Realizations*. In *IEEE Conference on Decision and Control*, 1990.
- [112] LEFTERIU, S. and A.C. ANTOULAS: *A New Approach to Modeling Multiport Systems From Frequency-Domain Data*. *IEEE Transactions on Computer-Aided Design of Integrated Circuits and Systems*, 29:14 – 27, 2010.
- [113] ANTOULAS, A.C. and B.D.Q. ANDERSON: *On the Scalar Rational Interpolation Problem*. *Journal of Mathematical Control and Information*, 3:61 – 88, 1986.
- [114] MAYO, A.J. and A.C. ANTOULAS: *A framework for the solution of the generalized realization problem*. *Linear Algebra and its Application*, 425:634 – 662, 2007.
- [115] FOSTER, R. M.: *A Reactance Theorem*. Technical Report, The Bell System Technical Journal, 1924.
- [116] E. GUILLEMIN, R. FOSTER, L. WEINBERG I. CEDERBAUM and G. BIORCI: *The realization of n -port networks without transformers - a panel discussion: Statements by discussants*. *IRE Transactions Circuit Theory*, CT-9:202 – 208, 1962.

- [117] P. STEPIAN, S. HAKIMI, R. NEWCOMB Y. TOKAD and W. KIM: *The realization of n-port networks without transformers - a panel discussion: Evaluation and Questions*. IRE Transactions Circuit Theory, CT-9:208 – 211, 1962.
- [118] G. BIORCI, R. FOSTER and I. CEDERBAUM: *The realization of n-port networks without transformers - a panel discussion: Rebuttals*. IRE Transactions Circuit Theory, CT-9:212 – 214, 1962.
- [119] S. LUDWIG, L.J. RADIC-WEISSENFELD, W. MATHIS and W. JOHN: *Efficient Model Reduction of Passive Electrical Networks with a Large Number of Independent Sources*. In *IEEE International Symposium on Circuits and Systems*, 2008.
- [120] MATSUMOTO, Y., Y. TANJI and M. TANAKA: *Efficient SPICE-Netlist Representation of Reduced-Order Interconnect Model*. In *European Conference on Circuit Theory and Design*, 2001.
- [121] PALENIUS, T. and J. ROOS: *Comparison of Reduced-Order Interconnect Macromodels for Time-Domain Simulation*. IEEE Transactions on Microwave Theory and Techniques, 52:2240 – 2250, 2004.
- [122] KUBOTA, H., A. KAMO, T. WATANABE and H. ASAI: *Noise analysis of power/ground planes on PCB by SPICE-like simulator with model order reduction technique*. In *IEEE International Symposium on Circuits and Systems*, 2002.
- [123] PALENIUS, T. and J. ROOS: *An efficient reduced-order interconnect macromodel for time-domain simulation*. In *IEEE International Symposium on Circuits and Systems*, 2003.
- [124] LIU, YING, L. T. PILEGGI and A. J. STROJWAS: *Ftd: frequency to time domain conversion for reduced-order interconnect simulation*. IEEE Transactions on Circuits and Systems I: Fundamental Theory and Applications, 48:500–506, 2001.
- [125] SILVA, J. M. S. and L. M. SILVEIRA: *Issues in Model Reduction of Power Grids*. VLSI-SOC: From Systems To Silicon, 240:127–144, 2007.
- [126] YAN, B., S.X.-D. TAN, G. CHEN and L. WU: *Modeling and simulation for on-chip power grid networks by locally dominant Krylov subspace method*. In *IEEE/ACM International Conference on Computer Aided Design*, 2008.
- [127] SILVEIRA, L.M. and J.R. PHILLIPS: *Exploiting input information in a model reduction algorithm for massively coupled parasitic networks*. In *ACM/IEEE Design Automation Conference*, 2004.
- [128] LIAO, H. and W. W.-M. DAI: *Partitioning and reduction of RC interconnect networks based on scattering parameter macromodels*. In *IEEE/ACM International Conference on Computer Aided Design*, 1995.
- [129] KARYPIS, G. and V. KUMAR: *A fast and high quality multilevel scheme for partitioning irregular graphs*. SIAM Journal on Scientific Computing, 20:359 – 392, 1999.

- [130] MIETTINEN, P., M. HONKALA and J. ROOS: *Using metis and hmetis algorithms in circuit partitioning*. Technical Report, Circuit Theory Laboratory, Helsinki University of Technology, 2006.
- [131] BENNER, P., L. FENG and E.B. RUDNYI: *Using the Superposition Property for Model Reduction of Linear Systems with a Large Number of Inputs*. In *International Symposium on Mathematical Theory of Networks and Systems*, 2008.
- [132] RADIC-WEISSENFELD, LJ., S. LUDWIG, W. MATHIS and W. JOHN: *Two-step order reduction of IC conducted emission models*. In *Asia-Pacific Symposium on Electromagnetic Compatibility and International Zurich Symposium on Electromagnetic Compatibility*, 2008.
- [133] YAN, B., L. ZHOU, S.X.-D. TAN, J. CHEN and B. MCGAUGHY: *DeMOR: Decentralized model order reduction of linear networks with massive ports*. In *ACM/IEEE Design Automation Conference*, 2008.
- [134] BRISTOL, E.: *On a new measure of interaction for multivariable process control*. *IEEE Transactions on Automatic Control*, 11:133–134, 1966.
- [135] FELDMANN, P.: *Model order reduction techniques for linear systems with large numbers of terminals*. In *Design, Automation and Test in Europe*, 2004.
- [136] FELDMANN, P. and F. LIU: *Sparse and efficient reduced order modeling of linear sub-circuits with large number of terminals*. In *IEEE/ACM International Conference on Computer Aided Design*, 2004.
- [137] LI, P. and W. SHI: *Model Order Reduction of Linear Networks With Massive Ports via Frequency-Dependent Port Packing*. In *ACM/IEEE Design Automation Conference*, 2006.
- [138] LIU, P., S. X. D. TAN, B. MCGAUGHY, L. WU and L. HE: *TermMerg: An Efficient Terminal-Reduction Method for Interconnect Circuits*. *IEEE Transactions on Computer-Aided Design of Integrated Circuits and Systems*, 26:1382–1392, 2007.
- [139] LIU, P., S. X. D. TAN, B. YAN and B. MCGAUGHY: *An efficient terminal and model order reduction algorithm*. *Integration, the VLSI Journal*, 41:210 – 218, 2008.
- [140] WANG, J.M. and T.V. NGUYEN: *Extended Krylov Subspace Method for reduced Order Analysis of Linear Circuits with Multiple Sources*. In *ACM/IEEE Design Automation Conference*, 2000.
- [141] LEE, Y.-M., Y. CAO, T.-H. CHEN, J.M. WANG and C.C.-P. CHEN: *HiPRIME: hierarchical and passivity preserved interconnect macromodeling engine for RLKC power delivery*. *IEEE Transactions on Computer-Aided Design of Integrated Circuits and Systems*, 24:797–806, 2005.

- [142] LI, D., S. X.-D. TAN and B. MCGAUGHY: *ETBR: Extended Truncated Balanced Realization Method for on-Chip Power Grid Network Analysis*. In *Design, Automation and Test in Europe*, 2008.
- [143] MA, M. and R. KHAZAKA: *Model Order Reduction With Parametric Port Formulation*. IEEE Transactions on Advanced Packaging, 30:763–775, 2007.
- [144] WEILE, D. S., E. MICHELSEN, E. GRIMME and K. GALLIVAN: *A method for generating rational interpolant reduced order models of two-parameter linear systems*. Applied Mathematics Letters, 12:93 – 102, 1999.
- [145] DANIEL, L., O. SIONG, L. CHAY, K. LEE and J. WHITE: *Multiparameter Moment Matching Model Reduction Approach for Generating Geometrically Parameterized Interconnect Performance Models*. IEEE Transactions on Computer Aided Design of Integrated Circuits, 23:678 – 693, 2004.
- [146] FENG, L.: *Parameter independent model order reduction*. Mathematics and Computers in Simulation, 68:221 – 234, 2005.
- [147] FENG, L. and P. BENNER: *A robust algorithm for parametric model order reduction based on implicit moment matching*. Proceedings in Applied Mathematics and Mechanics, 7:1021501 – 1021502, 2008.
- [148] BAUR, U. and P. BENNER: *Model Reduction for Parametric Systems Using Balanced Truncation and Interpolation*. at-Automatisierungstechnik, 57:411 – 420, 2009.
- [149] LOHMANN, B. and R. EID: *Efficient Order Reduction of Parametric and Nonlinear Models by Superposition of Locally Reduced Models*. In *Methoden und Anwendungen der Regelungstechnik. Erlangen-Münchener Workshops 2007 und 2008*, 2009.
- [150] CHUA, L.O. and S.M. KANG: *Section-Wise Piecewise-Linear Functions: Canonical Representation, Properties, and Applications*. Proceedings of the IEEE, 65:915 – 929, 1977.
- [151] KANG, S.M. and L.O. CHUA: *A Global Representation of Multidimensional Piecewise-Linear Functions with Linear Partitions*. IEEE Transactions on Circuits and Systems, CAS-25:938 – 940, 1978.
- [152] KEVENAAR, T.A.M., D.M.W. LEENARTS and W.M.G. VAN BOKHOVEN: *Extensions to Chua's Explicit Piecewise-Linear Function Descriptions*. IEEE Transactions on Circuits and Systems - I: Fundamental Theory and Applications, 41:308 – 314, 1994.
- [153] LEENARTS, D.M.W.: *Further Extensions to Chua's Explicit Piecewise Linear Function Descriptions*. International Journal of Circuit Theory and Applications, 24:621 – 633, 1996.
- [154] CHUA, L.O. and A.-C. DENG: *Canonical Piecewise-Linear Representation*. IEEE Transactions on Circuits and Systems, 35:101 – 111, 1988.

- [155] CHUA, L.O. and A-C. DENG: *Canonical Piecewise-Linear Modeling*. IEEE Transactions on Circuits and Systems, CAS-33:511 – 525, 1986.
- [156] WANG, S.: *General Constructive Representations for Continuous Piecewise-Linear Functions*. IEEE Transactions on Circuits and Systems I, 51:1889 – 1896, 2004.
- [157] WEN, C., S. WANG, F. LI and M.J. KHAN: *A Compact f-f Model of High-Dimensional Piecewise-Linear Function Over a Degenerate Intersection*. IEEE Transactions on Circuits and Systems I, 52:815 – 821, 2005.
- [158] WEIERSTRASS, K.: *Über die analytische Darstellbarkeit sogenannter willkürlicher Functionen einer reellen Veränderlichen*. In *Sitzungsberichte der Königlich Preussischen Akademie der Wissenschaften zu Berlin*, pages 633 – 639, 789 – 805, 1885.
- [159] CONDON, M. and G.G. GRAHOVSKI: *A Parametric Macromodelling Technique*. In *European Conference on Circuit Theory and Design*, 2009.
- [160] GROSSBERG, S.: *Nonlinear Neural Networks: Principles, Mechanisms, and Architectures*. Neural Networks, 1:17 – 61, 1988.
- [161] ARBIB, M.A. (editor): *Handbook of Brain Theory and Neural Networks*. MIT Press, 1995.
- [162] PARK, J. and I.W. SANDBERG: *Universal Approximation Using Radial-Basis-Function Networks*. Neural Computation, 3:246 – 257, 1991.
- [163] CHEN, S., S.A. BILLINGS and P.M. GRANT: *Non-Linear system identification using neural networks*. International Journal of Control, 51:1191 – 1214, 1990.
- [164] HARTMAN, E.J., J.D. KEELER and J.M. KOWALSKI: *Layered Neural Networks with Gaussian Hidden Units as Universal Approximations*. Neural Computation, 2:210 – 215, 1990.
- [165] SCARSELLI, F. and A.C. TSOI: *Universal Approximation Using Feedforward Neural Networks: A Survey of Some Existing Methods, and Some New Results*. Neural Networks, 11:15 – 37, 1998.
- [166] SJOBERG, J., Q. ZHANG, L. LJUNG, A. BENVENISTE, B. DEYLON, P.-Y. GLORENEC, H. HJALMARSSON and A. JUDITSKY: *Nonlinear Black-Box Modeling in System Identification: a Unified Overview*. Automatica, 31:1691 – 1724, 1995.
- [167] LEONTARITIS, I.J. and S.A. BILLINGS: *Input-output parametric models for non-linear systems*. International Journal of Control, 41:303 – 341, 1985.
- [168] CHEN, S. and S.A. BILLINGS: *Neural networks for nonlinear dynamic system modelling and identification*. International Journal of Control, 56:319 – 346, 1992.
- [169] HORNIK, K., M. STINCHCOMBE and H. WHITE: *Multilayer feedforward networks are universal approximators*. Neural Networks, 2:359 – 366, 1989.

- [170] DHIA, S.B., M. RAMDANI and E. SICARD: *Electromagnetic Compatibility of Integrated Circuits*. Springer USA, 2006.
- [171] SICARD, E., S.B. DHIA, M. RAMDANI, J. CATRYSSSE and M. COENEN: *Towards an EMC Roadmap for Integrated Circuit*. In *International Workshop on Electromagnetic Compatibility of Integrated Circuits*, 2007.
- [172] JOHN, W.: *Improved EMC Design for Microelectronic Applications*. In *International Wrocław Symposium and Exhibition on EMC*, 2004.
- [173] STEINECKE, T., M. GOEKCEN, D. HESIDENZ and A. GSTOETTNER: *High-Accuracy Emission Simulation Models for VLSI Chips including Package and Printed Circuit Board*. In *IEEE International Symposium on Electromagnetic Compatibility*, 2007.
- [174] HESIDENZ, D. and T. STEINECKE: *Chip-Package EMI Modeling and Simulation Tool 'EXPO'*. In *International Workshop on Electromagnetic Compatibility of Integrated Circuits*, 2005.
- [175] GSTOTTNER, A., T. STEINECKE and M. HUEMER: *Activity based high level modeling of dynamic switching currents in digital IC modules*. In *International Zurich Symposium on Electromagnetic Compatibility*, 2006.

Publications - Stefan Ludwig

Bookchapters

Ludwig, S. and W. Mathis: *Model Reduction Methods for Linear Network Models of Distributed Systems with Sources*. Book: *Model Reduction for Circuit Simulation*, ISBN 978-94-007-0088-8, Chapter 13, pp. 215-230, Springer, February 2011.

Freibothe, M., J. Doege, T. Coym, **S. Ludwig**, E. Fordran, B. Straube and E. Kock: *Verification-Oriented Behavioral Modeling of Non-Linear Analog Parts of Mixed-Signal Circuits*. Book: *Advances in Design and Specification Languages for Embedded Systems*, ISBN 978-1-4020-6147-9 (Print) 978-1-4020-6149-3 (Online), Chapter 3, pp. 37–51, Springer, July 2007.

Journal Articles

Ludwig, S. and W. Mathis: *Reduction of Network Models of Parasitic Effects in Mixed-Signal VLSI Circuits*. *International Journal for Computation and Mathematics in Electrical and Electronic Engineering*, 2010 (accepted).

Ludwig, S. and W. Mathis: *Transformation of Passive Electrical Networks with Distributed PWL Sources using a Model Order Reduction*. *Advances in Radio Science*, ISSN 1684-9965 (print) 1684-9973 (online), Vol. 7, pp. 113-118, 2009.

Radic-Weissenfeld, Lj., **S. Ludwig** and W. Mathis: *Comparison of Order Reduction Algorithms for Application to Electrical Networks*. *Advances in Radio Science*, ISSN 1684-9965 (print) 1684-9973 (online), Vol. 7, pp. 119-122, 2009.

Kazemzadeh, R., **S. Ludwig**, Lj. Radic-Weissenfeld and W. Mathis: *Efficient Modelling of IC Conducted Emission for Power Integrity Analysis*. *Advances in Radio Science*, ISSN 1684-9965 (print) 1684-9973 (online), Vol. 7, pp. 123-126, 2009.

Ludwig, S., Lj. Radic-Weissenfeld, W. Mathis and W. John: *Efficient Passive Network Description of IC Conducted Emission Models for Model Reduction*. *Advances in Radio Science*, ISSN 1684-9965 (print) 1684-9973 (online), Vol. 6, pp. 133-137, 2008.

Radic-Weissenfeld, Lj., **S. Ludwig**, W. Mathis and W. John: *Model order reduction of linear time invariant systems*. *Advances in Radio Science*, ISSN 1684-9965 (print) 1684-9973 (online), Vol. 6, pp. 129-132, 2008.

Hellebrand, S., C. G. Zoellin, H.-J. Wunderlich, **S. Ludwig**, T. Coym and B. Straube: *Testing and Monitoring Nanoscale Systems - Challenges and Strategies for Advanced Quality Assurance*, *Informacije MIDEM Journal of Microelectronics, Electronic Components and Materials*, ISSN 0352-9045, Vol. 37, No. 4(124), pp. 212-219, 2007

Peer-Reviewed Conference Papers

W. Mathis, **S. Ludwig** and J. Xiong: *Network Modelling of Electromagnetic Field Distributions using a Statistical Mechanical Approach*. *International Conference on Electromagnetics in Advanced Applications - ICEAA*, Torino, Italy, September 2009.

Ludwig, S. and W. Mathis: *Model Reduction of Linear Networks with Nonlinear Elements*. *European Conference on Circuit Theory and Design - ECCTD*, Antalya, Turkey, August 2009.

Ludwig, S. and W. Mathis: *Reduction of Network Models of Parasitic Coupling Effects in Mixed-Signal VLSI Circuits*. *XV. International Symposium on Theoretical Electrical Engineering - ISTET*, pp. 231-235, Luebeck, Germany, June 2009.

Ludwig, S., Lj. Radic-Weissenfeld, W. Mathis and W. John: *Passive and Reciprocal Network Description of Independent Sources for Efficient Model Reduction*. International Conference on Signals and Electronic Systems - ICSES, pp. 253-256, Krakow, Poland, September 2008.

Ludwig, S., Lj. Radic-Weissenfeld, W. Mathis and W. John: *Efficient Description of RLC Macromodels with a Large Number of Independent Sources for Model Order Reduction*. International Symposium on Electromagnetic Compatibility - EMC Europe 2008, Hamburg, Germany, September 2008.

Ludwig, S., Lj. Radic-Weissenfeld, W. Mathis and W. John: *Efficient Description and Implementation of Electrical Networks of EMC-Macromodels for Model Order Reduction*. 19th Wroclaw International Symposium and Exhibition on Electromagnetic Compatibility, Wroclaw, Poland, June 2008.

Radic -Weissenfeld, Lj., **S. Ludwig**, W. Mathis and W. John: *Comparison of Order Reduction Algorithms for IC Emission Models*. 19th Wroclaw International Symposium and Exhibition on Electromagnetic Compatibility, Wroclaw, Poland, June 2008.

Ludwig, S., Lj. Radic -Weissenfeld, W. Mathis und W. John: *Efficient Model Reduction of Passive Electrical Networks with a Large Number of Independent Sources*. IEEE International Symposium on Circuits and Systems ISCAS, pp. 1280-1283, Seattle, USA, May 2008.

Radic -Weissenfeld, Lj., **S. Ludwig**, W. Mathis and W. John: *Two-step Order Reduction of IC Conducted Emission Models*. 2008 Asia-Pacific Symposium on Electromagnetic Compatibility, 19th Intern. Zurich Symposium on Electromagnetic Compatibility – Asia-Pacific EMC Week, pp. 200-203, Singapur, May 2008.

Coym, T., S. Hellebrand, **S. Ludwig**, H.-J. Straube, B. Wunderlich and C. G. Zoellin: *Ein verfeinertes elektrisches Modell für Teilchentreffer und dessen Auswirkung auf die Bewertung der Schaltungsempfindlichkeit*. 20th ITG/GI/GMM Workshop Testmethoden und Zuverlaessigkeit von Schaltungen und Systemen, pp. 153-157, Wien, Austria, February 2008.

Ludwig, S., Lj. Radic-Weissenfeld, W. Mathis und W. John: *Model Order Reduction of Integrated Circuit Conducted Emission Models*. 6th International Workshop on Electromagnetic Compatibility of Integrated Circuits - EMC Compo, pp. 215-219, Torino, Italy, November 2007.

Hellebrand, S., C. G. Zoellin, H.-J. Wunderlich, **S. Ludwig**, T. Coym and B. Straube: *Testing and Monitoring Nanoscale Systems - Challenges and Strategies for Advanced Quality Assurance*. 43rd International Conference on Microelectronics, Devices and Material with the Workshop on Electronic Testing - MIDEM'07, pp. 3-10, Bled, Slovenia, September 2007 (invited).

Hellebrand, S., C. G. Zoellin, H.-J. Wunderlich, **S. Ludwig**, T. Coym and B. Straube: *A Refined Electrical Model for Particle Strikes and its Impact on SEU Prediction*. 22nd IEEE International Symposium on Defect and Fault Tolerance in VLSI Systems - DFT'07, pp. 50-58, Rome, Italy, September 2007.

Freibothe, M., J. Doege, T. Coym, **S. Ludwig**, E. Fordran, B. Straube and E. Kock: *Verification-Oriented Behavioral Modeling of Non-Linear Analog Parts of Mixed-Signal Circuits*. Proceedings of the Forum on Specification & Design Languages - FDL'06, Darmstadt, pp. 53-59, Germany, September 2006.

Freibothe, M., J. Doege, T. Coym, **S. Ludwig**, E. Fordran, B. Straube and E. Kock: *Simulatorgestützte Verhaltensmodellierung nichtlinearer analoger Komponenten für die semiformale Mixed-Signal-Verifikation*. 9. ITG/GMM-Fachtagung Entwicklung von Anlogschaltungen mit CAE-Methoden - ANALOG'06, pp. 69-74, Dresden, Germany, September 2006.

Freibothe, M., J. Doege, T. Coym, **S. Ludwig**, E. Fordran, B. Straube and E. Kock: *Ein Ansatz für die semi-formale Verifikation von Mixed-Signal-Schaltungen mit Hilfe von Bounded Model Checking*. Tagungsband Dresdener Arbeitstagung Schaltungs- und Systementwurf - DASS, pp. 143–145, Dresden, Germany, May 2006.

Freibothe, M., J. Doege, T. Coym, B. Straube, **S. Ludwig** and E. Kock: *Modellierung des dynamischen Verhaltens nichtlinearer analoger Komponenten für die semiformale Mixed-Signal-Verifikation*. Tagungsband 9.ITG/GI/GMM Workshop Methoden und Beschreibungssprachen zur Modellierung und Verifikation von Schaltungen und Systemen, pp. 95–105, Dresden, Germany, Februar 2006.

Theses

Ludwig, S.: *Untersuchung der Wirkung von Strahlungsteilchen auf digitale CMOS-Schaltungen. (Investigation of the effect of radiation particles on digital CMOS-circuits)*, Diplomarbeit, Technische Universität Dresden, December 2006.

Ludwig, S.: *Modellierung des dynamischen Verhaltens nichtlinearer analoger Komponenten von Mixed-Signal-Schaltungen für die semi-formale Verifikation. (Modelling of the dynamical behaviour of nonlinear analog components of mixed-signal-circuits for semi-formal verification)*, Technical Report, Technische Universität Dresden, February 2006.

Ludwig, S.: *Entwicklung eines Microcontroller IP-Cores. (Design of a Microcontroller IP-Core)*, Studienarbeit, Technische Universität Dresden, September 2005.

Selected Talks and Workshop Contributions

Ludwig, S. and W. Mathis: *Model Reduction of Linear Networks with Embedded Nonlinear Time variant Elements*. COMSON Autumn School Future Developments in Model Order Reduction, Terschelling, Netherlands, September 2009.

Ludwig, S. and W. Mathis: *Effiziente Reduktion von parasitären Koppelnetzwerken in Mixed-Signal VLSI-Schaltungen*. 11. Workshop 'Integrierte Analogschaltungen', Hannover, Germany, March 2009.

Ludwig, S. and W. Mathis: *Application of Order Reduction to Emission Models of Automotive Controllers*. Topical Forum: EMC Design, Optimization and Modelling of Automotive Components, 20th Zurich International Symposium on Electromagnetic Compatibility, Zurich, Switzerland, January 2009.

Ludwig, S. and W. Mathis: *Efficient Reduction of Electrical Network Models with Internal Sources*. SyreNe Workshop - Model Reduction for Circuit Simulation, Hamburg, Germany, October 2008.

Ludwig, S., Lj. Radic-Weissenfeld, W. Mathis and W. John: *Similarity Transformation of Passive Electrical Networks using a Model Order Reduction*. Kleinheubacher Tagung, Miltenberg, Germany, September 2008.

Ludwig, S., Lj. Radic-Weissenfeld, W. Mathis, R. Kazemzadeh and W. John: *Modellreduktion von elektrischen Netzwerken für die Untersuchung der elektromagnetischen Zuverlässigkeit von integrierten Schaltungen*. 10. Workshop 'Integrierte Analogschaltungen', Berlin, Germany, March 2008.

Ludwig, S., Lj. Radic-Weissenfeld, W. Mathis and W. John: *Modellordnungsreduktion von Integrated Circuit Conducted Emission Modellen*. Kleinheubacher Tagung, Miltenberg, Germany, September 2007.

Curriculum Vitae

Personal Data

Name Stefan Ludwig
Date and Place of Birth 13.10.1981, Mühlhausen (Thüringen), Germany

Work Experience

Since 07/2010 **BMW AG, München**

04/2009 – 06/2010 **Gottfried Wilhelm Leibniz Universität Hannover, Hannover**
Institut für Theoretische Elektrotechnik
Research Engineer

04/2007 – 03/2009 **Gottfried Wilhelm Leibniz Universität Hannover, Hannover**
Institut für Theoretische Elektrotechnik
Research Engineer
Work place:
Fraunhofer Research Institution for Electronic Nano Systems, Paderborn
Department Advanced System Engineering
Research Engineer

09/2005 – 03/2007 **Fraunhofer Institute for Integrated Circuits, Dresden**
Division Design Automation
Research Engineer

11/2000 – 09/2001 **Military Service**

Education

04/2007 – 09/2010 **Gottfried Wilhelm Leibniz Universität Hannover**
Faculty of Electrical Engineering and Computer Science
Ph.D. Student

10/2001 – 12/2006 **Technische Universität Dresden**
Faculty of Electrical Engineering and Information Technology
Degree: Diplom-Ingenieur

07/1988 – 07/2000 **Friedrich Schiller Gymnasium Bautzen**
Degree: Abitur